

**A WIDE AREA SYSTEM FOR POWER
TRANSMISSION SECURITY ENHANCEMENT USING A
PROCESS SYSTEMS APPROACH**

Jegatheeswaran Thambirajah

Department of Chemical Engineering and Chemical Technology

Imperial College of Science, Technology and Medicine

London SW7 2AZ

A Thesis submitted for the degree of
Doctor of Philosophy of the University of London
And for the Diploma of Imperial College

Declaration of Authorship

I declare that the thesis I am submitting is entirely my own work except otherwise indicated, in which case I have clearly referenced the sources and acknowledged appropriately any assistance provided to me.

For God and My Family

Abstract

Inter-area oscillations are inherent in large interconnected power systems and are typically created when groups of synchronous machines in one part of the system oscillate with respect to groups in another part of the system at a frequency ranging between 0.2 to 1.0 Hz. These oscillations, or modes as they are more commonly referred to, are usually stable but typically have small damping ratios. Even though oscillations are characteristic of the post-fault response of a system, they can also be excited by random events such as the normal variation of load demand. These poorly damped oscillations can pose various problems such as limiting transfer capacities and in more severe cases can lead to system instability causing a wide-scale blackout.

This thesis presents a novel approach to monitoring the frequency and damping of inter-area oscillations during ambient operation of electrical power transmission networks. It uses multivariate analysis techniques, with the aim of providing increased situational awareness to power transmission system operators. A three-step method is presented (i) the Teager Operator for the distinction between ambient and transient operation of the power system, (ii) Independent Component Analysis for the detection of inter-area modes and estimation of their frequencies, and (iii) Random Decrement for the estimation of mode damping. The steps of the method are described in detail and thereafter demonstrated using various examples including simulated and real measurements taken in Finland within the Nordic Power System. These measurements are used to monitor the evolution of the critical inter-area mode frequency (in Finland) and its damping using the proposed method. The developed method is finally packaged in a user-operated tool to demonstrate how it can be deployed at a transmission operation centre. The thesis concludes with a discussion of the novelty of the developed approach and presents ideas for future work.

Acknowledgements

I would to thank, first and foremost, my supervisor, Professor Nina Thornhill, for her unending advice and support right from my undergraduate days till present. I thank her for having given me the opportunity to undertake such a wonderful research project despite my inexperience in the field and for having taken a personal stake in bringing me to this moment of time at the end of this chapter of my studies. I also have Dr. Bikash Pal to thank for his invaluable advice regarding matters of my research as well as the hours of teaching he undertook to make sure that I was fully equipped to tackle the problems in this field.

I would like to thank ABB and National Grid for the commitment, time and expertise given to make this research industrially relevant. The direction of Dr. Mats Larsson at ABB, and Dr. Alex Carter and Dr. William Hung at National Grid, through numerous discussions, shaped this research. I would also like to thank National Grid specifically for providing me with the opportunity to experience firsthand the challenges my research has been aimed at addressing through the three month internship I undertook at the UK Electricity National Control Centre (ENCC) at the beginning of 2009. The expertise and outlook I was exposed to at the ENCC was unparalleled.

I would also like to thank Fingrid for providing enough data for my research. Without this data, all the methods I researched would have been unproved and in vain. Special thanks go to Jukka Turunen and Professor Liisa Haarla at Aalto University School of Science and Technology who forged the relationship between Fingrid, Imperial College, ABB and National Grid. Their support by providing parallel research to validate my research is greatly appreciated.

I would like to thank Imperial College London, EPSRC and ABB for the dedicated funding that was provided for my three years of study. I acknowledge the critical funding that was provided by ABB during the first year of my research and the Overseas Research Scholarship provided by Imperial College London that continued this critical funding that I would have otherwise not be able to obtain.

I would also like to thank all my friends, both in Imperial College London and elsewhere, who continued to support me through my years of study and for making my time as a PhD student more

enjoyable that I could ever have imagined. My special thanks go to the gang in my office, both present and past - Alex, Ali, Colin, Inés, Mahdi, May, Nick, Sarah, Tope and Waqas. Thank you for making our office an enjoyable and friendly place to work in; I will not forget all the deep conversations, pointless arguments and twisted humour anytime soon. Many thanks to my network of friends outside the office Gabriel, Globy, Meza, Rohit and Roshni; you always believed in me even through the days when my research seemed to be going nowhere. I would also like to thank my friends at Hope Church who were always my spiritual support during the critical times when I was down; Anita, Eldos, Jon, Kelly, Ita, Thomas, Vincent and Yanti, it is a pleasure serving the LORD with you.

Finally and most importantly, I would like to thank my family for all they have done and still do for me. My thanks to my dad and mum, Sinnathamby and Vijayamalar, who were ready to encourage me to fulfil my potential and who, through their hard work, gave me the opportunity to come to London to study. I cannot fully express my thanks for everything they sacrificed for my brother, sister and I. Thank you for standing by me during my life. Many thanks to my brother Hareeswaran who has had to put up with me all this while and for supporting me especially through the busy days of my life. My dear sister Shamanthi, thank you for teaching me patience and love, and for showing me that despite any circumstances in our lives, we have the capacity to do our best. To my uncle and aunty, Sathyaseelan and Jegamalar, thank you for putting me up for three years without any grudges; you were my family away from home.

Table of Contents

List of Figures	11
List of Acronyms	15
1. Introduction	20
1.1. Introduction to the Research Problem	20
1.1.1. Electrical Power Systems – A Snapshot.....	20
1.1.2. Power Transmission Security	21
1.1.3. Inter-Area Oscillations	22
1.2. Motivation for Research	24
1.2.1. The Need for Oscillation Monitoring	24
1.2.2. Advances in Power System Monitoring	30
1.2.3. Summary.....	36
1.3. Aim, Objectives, Challenges and Requirements.....	37
1.3.1. Aim.....	37
1.3.2. Objectives.....	37
1.3.3. Challenges	40
1.3.4. Requirements for Solution.....	44
1.4. Introduction to the Thesis	44
1.5. Novelty of Research	45
1.6. Summary.....	46
2. Review of Literature.....	49
2.1. Methods for Power System Stability Estimation	49
2.1.1. Overview	49
2.1.2. Ambient Operation	50
2.1.3. Transient Operation.....	64
2.1.4. Summary.....	69
2.2. Methods for Stability Estimation in Vibration Analysis.....	70
2.2.1. Overview	70

2.2.2. Stationary methods	71
2.2.3. Non-Stationary methods	78
2.2.4. Summary	82
2.3. Methods for Process Systems Fault/Oscillation Diagnosis and Detection	83
2.3.1. Process Systems - Overview	83
2.3.2. Process History-Based Methods	85
2.3.3. Summary	93
2.4. Summary	94
3. Overview of Proposed Solution and Case Study	96
3.1. Outline of Requirements and Selected Methods	96
3.1.1. Ambient and Transient Operation	97
3.1.2. Detection of Modes and Sources (Modal Observability)	97
3.1.3. Damping Estimation	98
3.1.4. Alerting System Operators	99
3.2. Structure of Solution	99
3.3. Case Study System – The Nordic Power System	101
3.3.1. Scenario Matching	102
3.3.2. Measured Scenario	103
3.3.3. Simulated Scenario	103
3.4. Summary	104
4. Ambient and Transient Detection	105
4.1. Overview	105
4.2. Signal Selection	107
4.3. Mexican Case Study Signal	107
4.4. Schemes for Detection of Transient Behaviour using Teager operator	109
4.4.1. Threshold Detection	109
4.4.2. Integrated Absolute Teager Energy (IATE)	111
4.5. Results from Case Study System	115
4.5.1. Simulated Scenario	118

4.5.2. Measured Scenario	118
4.6. Summary.....	119
5. Mode Detection and Source Identification	120
5.1. Overview	120
5.2. Method Development	128
5.2.1. Parameter Selection	128
5.2.2. Effect of Noise on Estimate.....	131
5.3. Results from Case Study System.....	132
5.3.1. Simulated Scenario	132
5.3.2. Measured Scenario	135
5.3.3. Discussion of Results.....	138
5.4. Summary.....	139
6. Damping Estimation.....	141
6.1. Overview	141
6.1.1. Estimation of Impulse Response	142
6.1.2. Estimation of Damping.....	144
6.2. Method Development	145
6.2.1. Multivariate Damping Estimation	146
6.2.2. Parameter Selection for RD method.....	147
6.3. Results from Case Study System.....	153
6.3.1. Simulated Scenario	155
6.3.2. Measured Scenario	159
6.3.3. Discussion of Average Damping Results	163
6.4. Summary.....	164
7. Integrated Tool	166
7.1. Requirements	166
7.1.1. Functional Requirements.....	166
7.1.2. Non-functional Requirements.....	167
7.2. Implemented Algorithm.....	167

7.3. Constraints Imposed by Implemented Algorithm.....	169
7.4. System Design	169
7.4.1. C# .NET.....	170
7.4.2. Integration of MATLAB Algorithms	171
7.4.3. Settings	172
7.4.4. Implementation of sliding window.....	174
7.4.5. Storage of Results.....	176
7.4.6. Display.....	176
7.5. Summary.....	179
8. Summary & Future Research Opportunities.....	181
8.1. Summary.....	181
8.1.1. Motivation and Aim.....	181
8.1.2. Selection of Methods	182
8.1.3. Structural Methodology.....	183
8.1.4. Case Study System	185
8.1.5. Transient Detection Algorithm.....	185
8.1.6. Mode Detection and Source Identification.....	186
8.1.7. Damping Estimation	187
8.1.8. Integrated Tool	188
8.1.9. Conclusion.....	189
8.2. Future Research Opportunities	189
8.2.1. Opportunities to Build This Strand of Research.....	190
8.2.2. Opportunities for Strategic Research.....	192
9. References	193

List of Figures

Figure 1: The process of generation.....	21
Figure 2: Illustration of an inter-area oscillation	23
Figure 3: Map showing major system blackouts since 2003. After Skok(2010)	24
Figure 4A - Dominant inter-area oscillations detectable in Finland: 0.3-0.4 Hz (blue arrow) and 0.5 Hz (green arrow).....	25
Figure 5: Changes in generation mix between 2010 and 2020. After Carter (2010)	27
Figure 6: Changes in system inertia and inertia constant between 2010 and 2020. After Carter (2010)	28
Figure 7: Utilisation of wind and nuclear energy to meet summer minimum demand in A - 2010 and B - 2020. After Carter (2010)	29
Figure 8: The current and future grids; A - Current wind generation and interconnectors; B - Wind generation and interconnectors in 2020	29
Figure 9: Timescales and localities of monitoring technology	30
Figure 10: An illustration of a Wide Area Measurement System (WAMS).....	32
Figure 11: Phasors. After Phadke (1993).....	32
Figure 12: Block diagram of a PMU. After Phadke (1993).....	34
Figure 13: Positive, zero and negative damping	39
Figure 14: Exponentially decaying sinusoid.....	39
Figure 15: A - Example of ambient response	41
Figure 16: Modal observability.....	41
Figure 17: Frequency spectrum of data from ambient operation	42
Figure 18: Input-output demonstration	43
Figure 19: Hierarchical tree showing classification of methods for power systems engineering	50
Figure 20: Hierarchical tree showing classification of methods for ambient operation of power systems.....	52
Figure 21: Hierarchical tree showing classification of methods for system identification with known input.	53
Figure 22: Hierarchical tree showing classification of methods for transient operation of power systems.....	63

Figure 23: Hierarchical tree showing classification of methods for vibration analysis	71
Figure 24: Hierarchical tree showing classification of stationary methods for vibration analysis	72
Figure 25: Stationary and non-stationary response in vibration analysis. After http://www.owlnet.rice.edu/~elec532/PROJECTS00/earthquake/earthquakes.htm , accessed December 2009	73
Figure 26: Hierarchical tree showing classification of non-stationary methods for vibration analysis	77
Figure 27: Classification of diagnostic algorithms. After Venkatasubramanian <i>et al.</i> (2003a)	84
Figure 28: Classification of process history based methods. After Venkatasubramanian <i>et al.</i> (2003c)	86
Figure 29: Data-driven methods of fault detection. After Thornhill and Horch (2007), with additions of recent work	88
Figure 30: Structural methodology for determining power system stability	100
Figure 31: Map of the Nordic power system showing locations of points where measurements were made in the measured and simulated scenarios.	102
Figure 32: Case study Mexican frequency signal for the demonstration of the Teager Operator....	108
Figure 33: Teager energy signal of Mexican frequency signal calculated using the Teager Operator	109
Figure 34: Absolute Teager energy signal of Mexican frequency signal	110
Figure 35: Ambient and transient operation using Absolute Teager energy signal for Mexican frequency signal	111
Figure 36: Integrated Absolute Teager Energy (IATE) signal of Mexican frequency signal	112
Figure 37: Ambient and transient operation using Integrated Absolute Teager Energy (IATE) signal for Mexican frequency signal	113
Figure 38: Demonstration of calculation of IATE directly from Teager energy calculations and indirectly from output measurements	114
Figure 39: Flowchart demonstrating the use of the TO-IATE method	115
Figure 40: Integrated Absolute Teager Energy (IATE) signal of simulated case study frequency deviation signal	116
Figure 41: Ambient and transient operation using Integrated Absolute Teager Energy (IATE) signal for simulated case study frequency deviation signal.....	116
Figure 42: Plot of frequency measurements for measured scenario	117
Figure 43: Integrated Absolute Teager Energy (IATE) signal of measured case study frequency signal.....	117

Figure 44: Ambient and transient operation detection using Integrated Absolute Teager Energy (IATE) signal for measured case study frequency signal	118
Figure 45: Flowchart demonstrating Independent Component Analysis (ICA)	125
Figure 46: A - Synthetic signals, B - Independent components from application of ICA on synthesized signals.....	126
Figure 47: Demonstration of sliding window	129
Figure 48: Variation of mean of frequency estimate with window length.....	129
Figure 49: Variation of standard deviation of frequency estimate with window length.....	130
Figure 50: Variation of mean of frequency estimate with SNR using voltage angle difference data	131
Figure 51: Plot of bus frequency deviation measurements from simulated scenario.....	133
Figure 52: Contour plot of SIs for the 0.31 Hz mode at different times for bus frequency deviations	134
Figure 53: Plot of df/dt measurements from measured scenario.....	135
Figure 54: Unfiltered variation of frequency estimate over time.....	136
Figure 55: Filtered variation of frequency estimate over time.....	137
Figure 56: Contour plot of SIs for the 0.35 Hz mode at different times for frequency derivative measurements	137
Figure 57: Fulcrum of 0.3 Hz oscillation relative to oscillation path	138
Figure 58: A - Example of an ambient response, B - Example of a second order decay function...	142
Figure 59: Demonstration of triggering mechanism of the Random Decrement method	143
Figure 60: Flowchart demonstrating the Random Decrement method	145
Figure 61: Implementation of RD-ICA.....	147
Figure 62: SIMULINK model used to obtain robust threshold value. ω_n is the natural frequency and ζ is the damping value	149
Figure 63: RD damping estimates using different threshold values for 0% actual damping	149
Figure 64: RD damping estimates using different threshold values for 20% actual damping	150
Figure 65: Variation of mean of damping estimate with window length.....	151
Figure 66: Variation of standard deviation of damping estimate with window length.....	152
Figure 67: Mode damping estimates using different number of cycles in RD for 0.3 Hz oscillation	154

Figure 68: Estimated RD signature for the 0.3 Hz oscillation obtained using 6 cycles (* points) and second order decay curve fitted using MATLAB optimization toolbox (solid line)	154
Figure 69: 0.31 Hz critical mode damping estimates using voltage angle differences	156
Figure 70: Contour plot of <i>SIs</i> at different times for voltage angle differences.....	157
Figure 71: Variation of mean of damping estimate with SNR using voltage angle difference data	158
Figure 72: Unfiltered variation of damping estimate over time.....	161
Figure 73: Filtered variation of damping estimate over time.....	162
Figure 74: 0.35 Hz critical mode damping estimates using derivatives of frequency measurements	163
Figure 75: Implemented algorithm – sequential processing	168
Figure 76: Map settings tab.....	173
Figure 77: Parameters settings tab	173
Figure 78: Data source settings tab	174
Figure 79: Flowchart showing implementation of sliding window	175
Figure 80: Main window of GUI showing system overview and dynamic markers.....	177
Figure 81: Signals view window of GUI showing measurements, modes and frequency vs. damping over 1 hr time horizon.....	178
Figure 82: Filtered damping window of GUI allowing operators to focus on damping of modes in a customisable frequency range over 1 hr time horizon	179
Figure 83: Structural methodology for determining power system stability	184

List of Acronyms

Acronym	Meaning
2SLS	Two-Stage Least Squares
ACF	Autocorrelation Function
ANN	Artificial Neural Network
AR	Autoregressive
ARMA	Autoregressive Moving Average
ARMAX	Autoregressive Moving Average with External inputs
BR	Balanced Realization
CA	Correlation Approach
CI	Confidence Interval
CLI	Common Language Infrastructure
CLR	Common Language Runtime
CMIF	Complex Mode Identification Function
CVA	Canonical Variate Analysis
DCT	Discrete Cosine Transform
DLL	Dynamic-Link Library
DoD	Department of Defence
EMD	Empirical Mode Decomposition
EMS	Energy Management Systems
ERA	Eigenvalue Realisation Algorithm
ES	Evolutionary Spectra
ETFE	Empirical Transfer Function Estimation
FCL	Framework Class Library
FDD	Frequency Domain Decomposition

FDPR	Frequency Domain Pattern Recognition
FFT	Fast Fourier Transform
FS-TAR	Functional Series Time-varying State Space
FS-TARMA	Time-varying Autoregressive Moving Average
GB	Great Britain
GT	Gabor Transform
GUI	Graphical User Interface
HHT	Hilbert huang Transform
HOS	Higher Order Speactral
HTLS	Hankel Total Least Squares
HVDC	High Voltage Direct Current
IAE	Integrated Absolute Error
IATE	Integrated Absolute Teager Energy
ICA	Independent Component Analysis
ICA	Independent Component
ICA-RD	Independent Component Analysis - Random Decrement
IDE	Integrated Development Environment
IEEE	Institution of Electrical and Electronic Engineers
IMF	Intrinsic Mode Function
IP	Interleaved Prony
ITD	Ibrahim Time Domain
IV	Instrumental Variable
JIT	Just-in-Time
KF	Kalman Filter
LMS	Least Means Squares

LPM	Linear Prediction Model
LS	Least Squares
LSCE	Least Squares Complex Exponential
LSE	Least Square Error
MA	Moving Average
MBHSRE	Matrix Block Hankel Stochastic Realization Algorithm
ML	Maximum Likelihood
MOESP	Multivariate Output Error State Space
MP	Matrix-Pencil
MSIL	Microsoft Intermediate Language
N4SID	Numerical Algorithm for State-Space System Identification
NMF	Non-negative Matrix Factorisation
OCI	Oscillation Contribution Index
PA	Polynomial-Algebraic
PCA	Principal Component Analysis
PCA	Principal Component
PDC	Phasor Data Concentrator
PDF	Probability Density Function
PEM	Prediction-Error identification Method
PMU	Phasor Measurement Unit
PP	Peak Picking
PSD	Power Spectral Density
QR	Rayleigh Quotient
R3LS	Recursive Regularized Least Squares
RD	Random Decrement

RELS	Recursive Extended Least Squares
RML-TARMA	Recursive Maximum Likelihood Time-varying Autoregressive Moving Average
R-TSS	Recursive Time-varying Subspace
RTU	Remote Terminal Unit
SCADA	Supervisory Control And Data Acquisition
SHETL	Scottish Hydro Electricity Transmission Limited
SI	Significance Index
SNR	Signal-to-Noise Ratio
SoC	Second-of_Century
SOFR	Second Order Frequency Regression
SP-TARMA	Smoothness Priors Time-varying Autoregressive Moving Average
SPTL	Scottish Power Transmission Limited
SSI	Subspace Identification
SSI-COV	Covariance-driven Subspace Identification
SSI-DAT	Data-driven Subspace Identification
ST-ARMA	Short Time Autoregressive Moving Average
STFT	Short Time Frequency Transform
ST-TSS	Short Time Time-varying Subspace
SVD	Singular Value Decomposition
TARMA	Time-varying Autoregressive Moving Average
TE	Teager Energy
TKEO	Teager Kaiser Energy Operator
TO-IATE	Teager Operator- Integrated Absolute Teager Energy
TSS	Tme-varying State Space
UK	United Kingdom

US	United States
UTC	Universal Time Coordinated
WAMS	Wide Area Measurement Systems
WT	Wavelet Transform
YW	Yule Walker
YWS	Yule Walker Spectrum

1. Introduction

This chapter presents an overall description of the research problem addressed in this thesis, the motivation for the research and the aims and objectives of the research. It starts by placing the research problem in the appropriate area of power system engineering and goes on to elaborate on the reasons for the research. It also presents the drivers that are facilitating this project and which set it in motion, and therefore the aim, objectives, challenges and requirements for the solution of the research. It finally introduces the layout of the rest of the thesis. The ultimate aim of this chapter is to define the research problem and provide specifications for the development of a solution.

1.1. Introduction to the Research Problem

This section places the research problem in the context of the full view of electrical power systems. It begins with a description of the general processes involved in electrical power systems and then provides a detailed explanation of power transmission security, which is the area of research in this project. The section goes on to introduce inter-area oscillations which are the subject of research within power transmission security.

1.1.1. Electrical Power Systems – A Snapshot

Electrical power systems can be broadly separated into three main components of operation: generation, transmission and distribution. *Generation* refers to the process that involves the conversion of mechanical energy to electrical energy. The mechanical energy is usually obtained from steam that is obtained by heating water (with a furnace and boiler) using the energy captured from burning a suitable fuel source such as coal, gas or nuclear fuel. This steam is used to drive a turbine which produces torque that is converted by a generator into electrical energy or electricity. By varying the level of fuel being combusted, the generated power can be varied. Figure 1 shows the progression of the process of generation.

A transformer is then used to step up the voltage (to 115 kV and above) at the end of the generator in order to prepare the electricity for transport over long distances. This transport is done using the *transmission network/grid* which connects the generators (sources of electricity) to the loads

(consumers of electricity). At various ends of the transmission networks, the voltage of the electricity is stepped down again using transformers for distribution to consumers via the electricity *distribution network*. Transformers to perform step-up and step-down of voltages are typically located in *substations* that are operated as part of the transmission network.

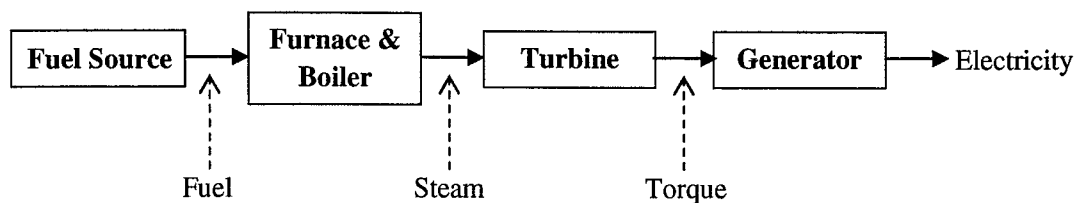


Figure 1: The process of generation

At any point in time, the generation of electricity needs to match the demand or the electricity consumed by loads because storage options are very limited. This demand generally fluctuates over time leading to cyclic variations in the level of electricity produced and transmitted. The *transmission operator* is in charge of the transmission network and fulfils the role of ensuring that generation always matches demand; this process is known as *balancing*. In the UK, the transmission operator is National Grid plc. The focus of this project is on problems encountered in the process of electricity transmission.

1.1.2. Power Transmission Security

Power transmission security refers to the ability of the power transmission system to provide a continuous supply of electricity to the consumers all year round. It is usually divided into *stability* and *reliability* where stability generally refers to the ability of the system to maintain operation in the presence of power oscillations while reliability generally refers to the ability of the system to maintain delivery of electricity regardless of system faults. Due to the large dependence of nations on secure power networks to drive industry, power system security is a main concern for power transmission operators. This project focuses on power system stability and therefore the problem of oscillations that can cause failure of the system.

Due to the great number of mechanisms in operation in an electrical power system, there are typically a high number of oscillations that are present during normal operation of the system. These oscillations are superimposed onto the nominal system frequency and therefore appear as low

frequency variations that modulate the nominal system frequency. They are classified according to the frequency range of the oscillations; they can be intraplant oscillations, local plant oscillations, inter-area oscillations, control oscillations and torsional oscillations (Pal and Chaudhuri, 2005). Intraplant oscillations take place between machines at the same site and are typically in the frequency range of 2.0 – 3.0 Hz. They can be measured at local substations but do not affect the rest of the system in general. Local plant oscillations occur when one machine swings against the rest of the system and they are in the frequency range of 1.0 – 2.0 Hz. These oscillations only localised to the affected generator and the line connecting it to the power transmission grid. Inter-area oscillations take place in large networks and occur when a group of generators in one part of the system oscillates against another group in another part of the system. They are typically in the frequency range of 0.2 – 1.0 Hz and are observable in a greater part of the transmission grid. Control oscillations are associated with control equipment in a power system and usually manifest as voltage oscillations. Finally, torsional oscillations are associated with moving parts in the turbine of a generator. These modes have typically high frequencies in the range of 10 – 46 Hz.

Of all these oscillations, inter-area oscillations pose a significant threat to power transmission security for various reasons mentioned in the next subsection which describes inter-area oscillations in greater detail.

1.1.3. Inter-Area Oscillations

Synchronous operation of electrical power systems requires that generators connected to a fixed voltage bus operate at a constant speed. Each machine additionally has a limit to the power it can deliver to the system or the torque that can be applied to it when working as a motor. Taking the voltage output of each machine to be constant, the power output and torque can be increased by increasing the excitation voltage and hence the field current in the generator. In order to maintain synchronism, the torque of the machine can be adjusted by adjusting the field current. The power output and torque of each machine therefore depends on an angle known as a power angle which is the angle of the induced voltage in the machine.

In an interconnected network, generators will produce a torque proportional to the relative angular displacement of their rotors in order to maintain synchronism (in order to stay at the nominal grid

frequency). When there is a small disturbance in the system, the synchronizing torque of each generator is used to bring it back to synchronism. The synchronizing torque is usually sufficient when small disturbances, such as nominal changes in load and generation (Kundur, 1994), are introduced into the system. However, due to this synchronizing action, the relative rotor angles of the generators oscillate creating a local oscillation or mode. In the modern power system, various areas are connected together using interconnections. These interconnections are weak compared to the connections within each area and the synchronizing torque across the interconnection is therefore low. This low synchronizing torque, coupled with the electrical inertia of each of the interconnected areas, leads to a low-frequency inter-area oscillation or mode. Electrical inertia refers to the resistance of generators to change their speed. An analogy can be made with reference to a system that consists of two individual sets of blocks that are connected within themselves by small springs, and then the two sets connected together by one long spring. The small springs have high spring constants while the long spring has a low spring constant. The blocks within one set can oscillate relative to one another (local mode), while each set of blocks can oscillate relative to the other via the long spring, such that the relative frequency of oscillation is affected by the oscillation on the other end of the spring (inter-area mode). To summarize, inter-area oscillations arise from one group of generators oscillating against another group due to a weak interconnecting tie line (Kundur, 1994).

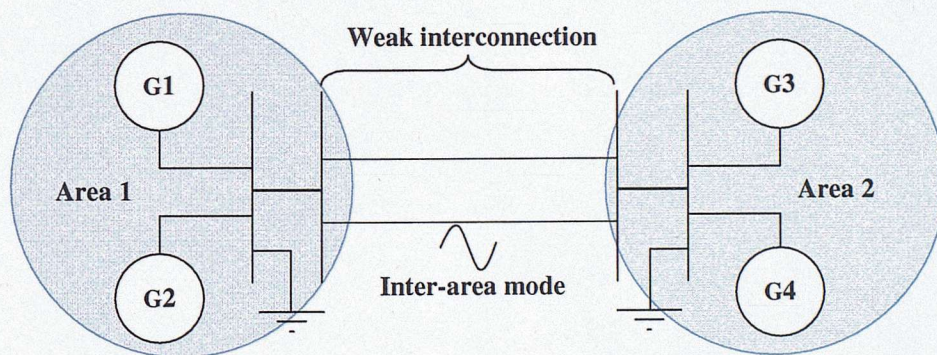


Figure 2: Illustration of an inter-area oscillation

Figure 2 illustrates this (G1, G2, G3 and G4 are generators). These inter-area oscillations place restrictions on system operability, for example, limiting the power transfer across the interconnection because the peaks of the oscillation drive against the maximum power transferrable across the interconnection. They can, in the most adverse cases, even lead to a widespread system disturbance

that can eventually lead to a blackout (Breulmann *et al.*, 2000). The following subsection provides more examples for the motivation for monitoring such oscillations. In normal operation, the oscillations are properly damped and decay with time, but in an overstressed system, they may be unstable and increase in amplitude.

1.2. Motivation for Research

This section presents the motivation for the research project which is two-way: an increasing requirement for monitoring of power systems and an increasing sophistication in equipment for monitoring. This section presents an overview of these drivers and how, combined together, they provide a motivating case for the research.

1.2.1. The Need for Oscillation Monitoring

Historical context: One of the main dangers of poorly damped oscillations was mentioned in the previous section: the risk of system-wide blackouts.

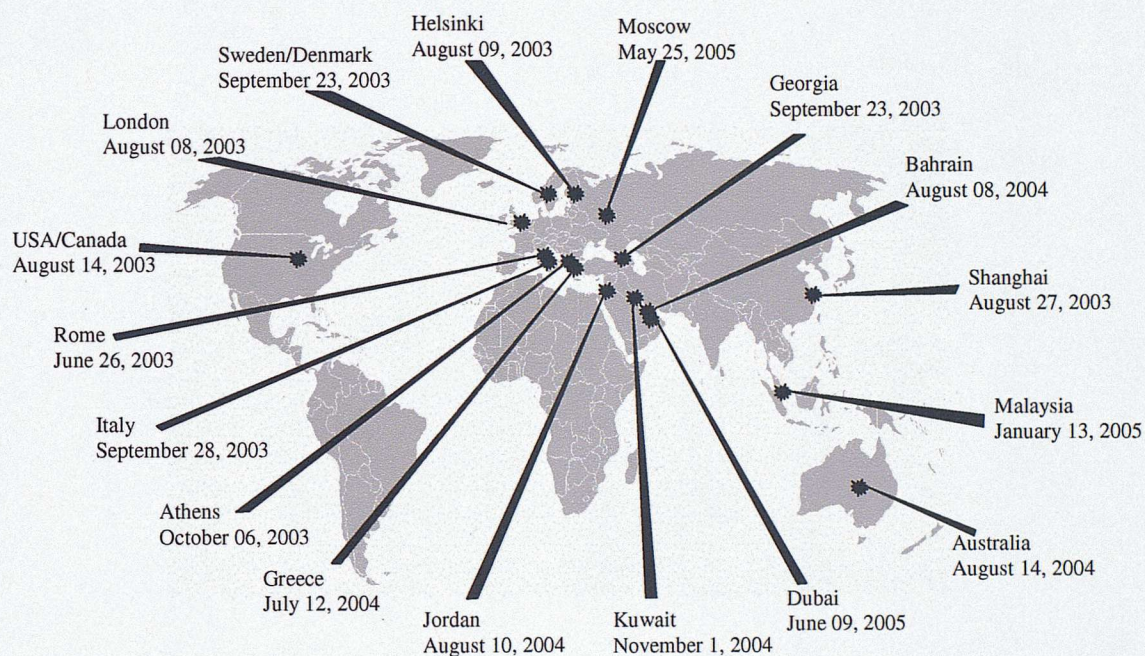


Figure 3: Map showing major system blackouts since 2003. After Skok(2010)

Figure 3 shows a map of major power blackouts in the world since 2003 (Skok, 2010). These blackouts were caused by sustained negatively damped oscillations cascading through the system, tripping generators and hence shutting down the power grids. The most severe of these blackouts

was the August 2003 blackout on the East Coast of Canada and the United States of America which affected most of the mid-East states including New York, Massachusetts and Ohio. Power was not restored in some states until up to four days after the incident and a loss of \$ 4-10 billion was estimated as a result of looting and the loss of work hours in the US alone. As a result of these incidents, various taskforces were set up by governments to investigate the events leading to these incidents and to outline a roadmap for tackling future occurrences.

One of the recommendations made by the taskforce investigating the August 2003 blackout in the US was to “evaluate and adopt better real-time tools for operators and reliability coordinators.” These tools would need to provide operators with a system-wide view of the power grid as close to real-time as possible and also enhance situational awareness by providing indicators of system behaviour and condition.

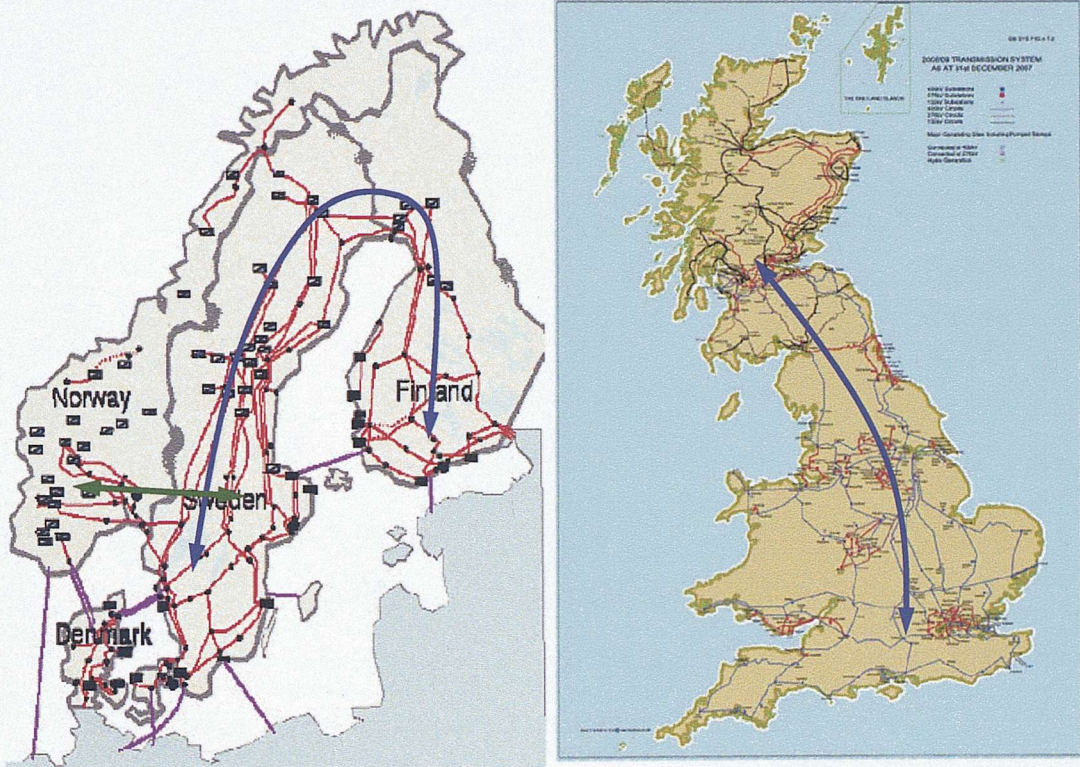


Figure 4A - Dominant inter-area oscillations detectable in Finland: 0.3-0.4 Hz (blue arrow) and 0.5 Hz (green arrow)

B - Dominant inter-area oscillation in the Great Britain Transmission System: 0.5 Hz (blue arrow)

Present context: In a more present context, the case for oscillation monitoring is made by the constraints placed by inter-area oscillations in the operation of an interconnected system, for

example the Nordic interconnected power system. The Nordic interconnected power system comprises the Denmark-Norway-Sweden interconnected transmission network, with a peak load of about 63 GW and the main load centres being located in the south of the system (Turunen, 2008). Within the different countries are different transmission voltage systems for example the 400 kV level exists in all countries but a 300 kV system exists in Norway and 220 kV systems in Denmark, Finland and Sweden. In addition, parts of the 110-150 kV systems belong to the transmission grid in Denmark, Finland and northern Norway. [4] Figure 4A shows an overview of this system demonstrating only the 400 kV system (red lines) and High Voltage Direct Current (HVDC) lines (pink lines).

This thesis will use the Nordic Power grid as an example throughout and a more detailed view of the system is hence presented in Chapter 3, later in this thesis. The reasons for choosing the Nordic system were that data from the system was readily available through a project partner, there are many interesting problems related to inter-area oscillations that affect the Nordic grid and because there was scope for collaboration with other research and industrial groups that were initially not involved in the project.

There are two main inter-area modes that can be detected in Finland. The first dominant mode is in the frequency range of 0.3-0.4 Hz and is due to the oscillation of generators in southern Finland against those in Southern Sweden and Norway. The second dominant mode is around 0.5 Hz and is due to the oscillation of generators in Southern Norway against those in Southern Sweden (Turunen, 2008). The critical inter-area mode in the system is the 0.3-0.4 Hz mode. The significance of this mode is that its level of damping limits the power that can be exported from Finland to Sweden in the winter seasons when power is exported from Finland to Sweden. This is a similar situation encountered by transmission operators in most electrically large networks. Given the increasingly economically driven business strategies being adopted by transmission operators, there is a need to maximise power exports for increased revenues while minimising the risks of blackouts that can be caused by unstable inter-area oscillations. The present need is therefore the ability to track the damping of known inter-area modes in the Nordic and other transmission systems and to provide this information to the control room engineers.

Future context: The case for oscillation monitoring can be further made by considering problems that are expected to be encountered during daily operation in future expanded power systems. This can be explained by considering the interconnected network of Great Britain (GB) which was also examined in the research leading to this thesis. The GB interconnected grid comprises the English and Scottish transmission networks. The infrastructure in each transmission network is owned and maintained by the system operator in the respective country; National Grid Electricity Transmission maintains the infrastructure in the English system while Scottish Power Transmission Ltd (SPTL) maintains the transmission network in the south of Scotland and Scottish Hydro Electricity Transmission Ltd (SHETL) maintains the transmission network in the north of Scotland. The critical inter-area oscillation in the system is a 0.5 Hz oscillation between Scotland and England. This oscillation is most observable in North England at the locations of the interconnectors between Scotland and England as demonstrated in Figure 4B. There are various changes anticipated to take place in the structure of the grid over the next few years and the impact of these changes on the GB system were discussed in depth during a three month internship with National Grid. The following sub-sections are referenced from Carter (2010).

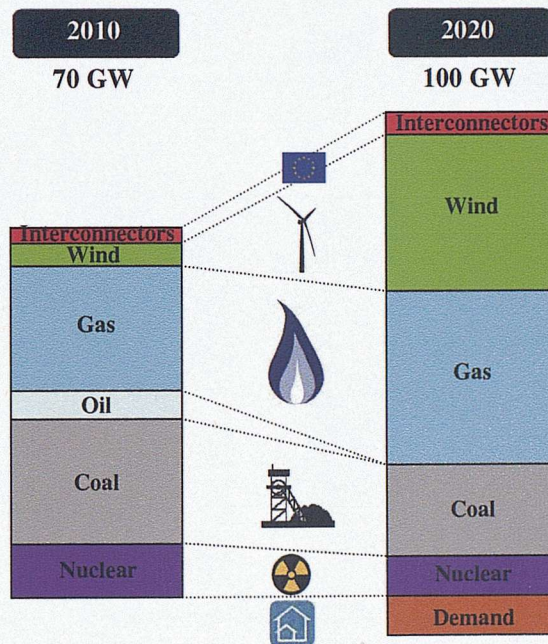


Figure 5: Changes in generation mix between 2010 and 2020. After Carter (2010)

Diversity of Generation and Renewable Energy: The current mix of electricity generation sources contributing to the 70 GW capacity available in the GB system is skewed towards coal and gas (each

accounting for a third of total capacity). However, an emphasis on climate change and reduction of CO₂ emissions around the world is driving an increase in renewable energy and a decrease in coal and gas. In GB, the greenhouse gas target is to reduce CO₂ emissions to 80% below 1990 levels by 2050 while the Scottish renewables target is to derive 50% of gross electricity consumption from renewable sources. The result of this is that the mix of electricity generation sources is expected to become more skewed towards wind energy with an expected increase of 30 GW in wind energy capacity (BBC, 2010) but only a small increase in peak demand. Figure 5 demonstrates this change. Wind energy, however, is intermittent depending on the season and therefore the system operator is aiming to be able to meet the peak summer demand using wind energy by majority. This is a system security constraint because wind energy is less during summer than winter and therefore enough wind energy needs to be produced to ensure that the peak summer demand is met despite the low level of wind. Additionally, as a result of the intermittency, there is expected to be an increased variation in power flows across the system.

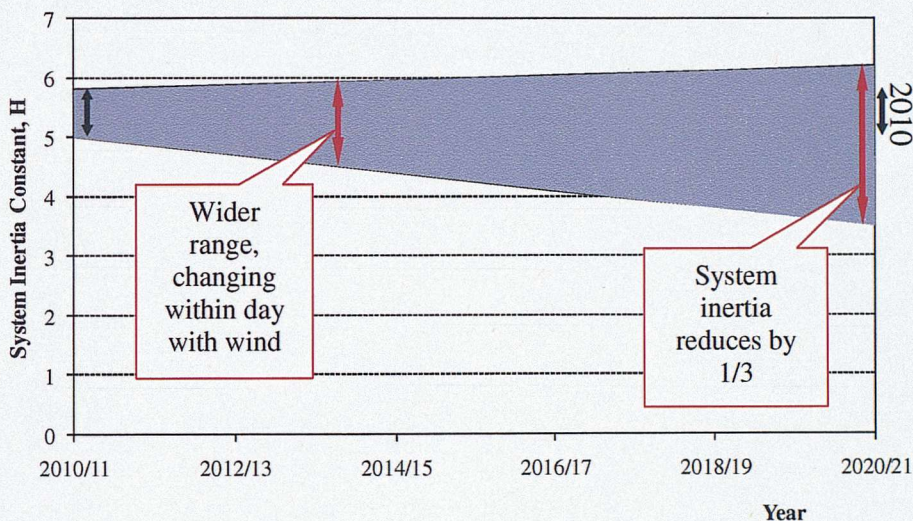


Figure 6: Changes in system inertia and inertia constant between 2010 and 2020. After Carter

(2010)

Another significant effect of the change in the generation mix will be on the system inertia. The system inertia is a characteristic of the generators in the system and relates to the ability of the power system to cope with major faults as well as to be able to limit oscillations. The current system inertia constant is bounded in a narrow range; however, by 2020, it is anticipated that the range of the

inertia constant will increase because wind farms have small amounts of natural inertia, changing within the day with the level of wind generation, such that the system inertia reduces by approximately a third. Figure 6 demonstrates this change graphically. This greater variability in system inertia will lead to a decrease in power system security especially with respect to oscillations.

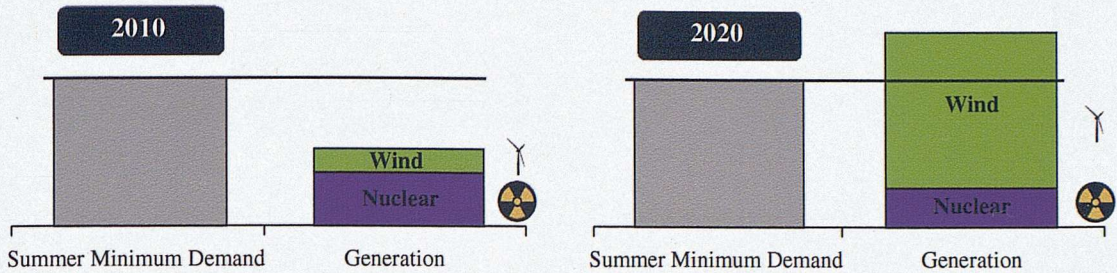


Figure 7: Utilisation of wind and nuclear energy to meet summer minimum demand in A - 2010 and B - 2020. After Carter (2010)

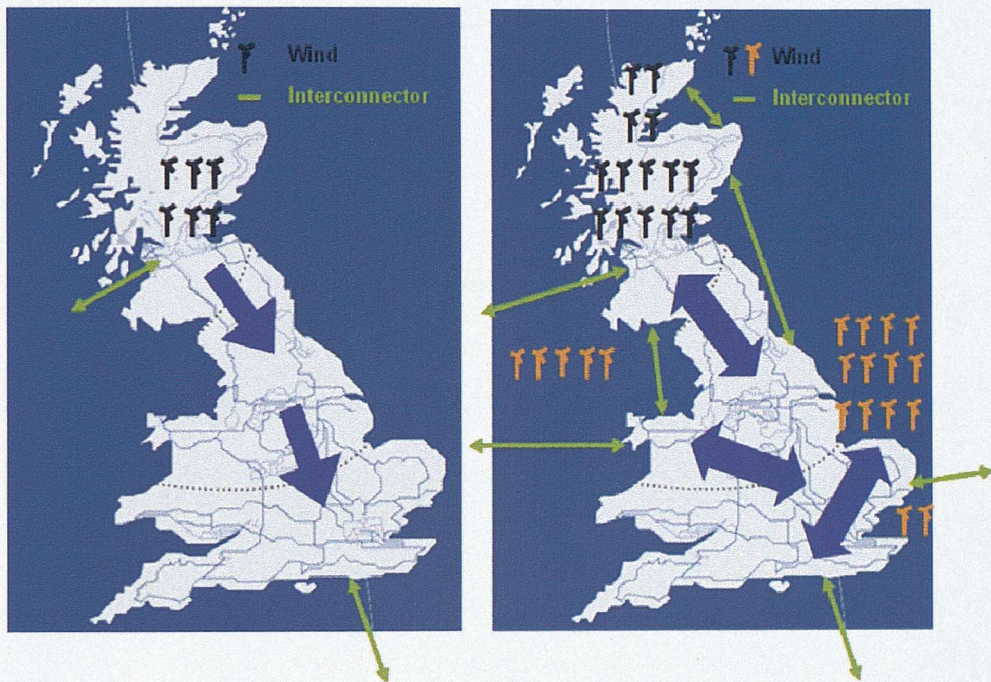


Figure 8: The current and future grids; A - Current wind generation and interconnectors; B - Wind generation and interconnectors in 2020

Interconnections: Figure 7 shows the expected changes in nuclear and wind energy contributing to the current and the 2020 projected summer minimum demand respectively (Carter, 2010). Due to the surplus wind energy that will be available in the summer season, there will be a need to build storage facilities or more interconnectors to export this energy to neighbouring countries. There is currently one High Voltage Direct Current (HVDC) connection between England and France. However, by

2020, there are plans to increase the number of interconnections within the system as well as with the surrounding countries. Figure 8A shows the wind generation connected to the system and interconnections at present while Figure 8B demonstrates those that will be in place by 2020.

The result of these changes will be that the current transmission flows, which are at present generally unidirectional and reasonably predictable, will become variable in direction, time-varying and difficult to predict. The change in direction of flows is indicated by the blue arrows in the figures. The operators will not be completely aware of all the oscillations in the system and therefore the need will be to determine which oscillations are in the system, where they are and the damping levels of these oscillations.

There is therefore motivation for research right now to underpin the tools that the transmission operator will need in the future.

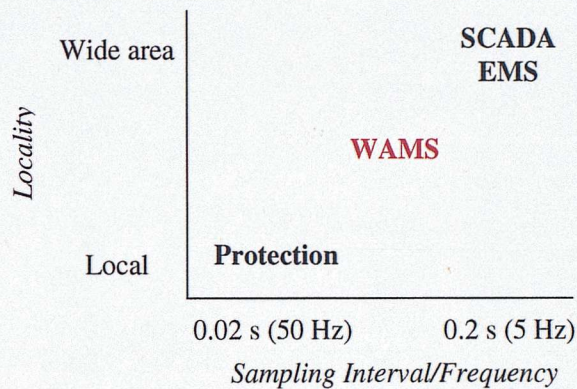


Figure 9: Timescales and localities of monitoring technology

1.2.2. Advances in Power System Monitoring

As a result of increased awareness of the need for oscillation monitoring, there has been an increased amount of research into hardware for power system monitoring. Recent developments have made the work of this thesis possible because technologies with higher sampling rates are now available. Sampling rate refers to the interval between measurements. For instance, if 10 measurements are made per second then the sampling interval is 0.1 sec and the sampling rate is 10 Hz. Technologies for monitoring have been driven by the rate of detection required whereby very high sampling rates (for example, 50 Hz) are required to detect high frequency (dynamic) oscillations such as torsional modes which are local in nature whereas low sampling rates (for example, 5 Hz) are adequate to

detect low frequency modes such as inter-area modes. The latter are called *static* modes by power system engineers. However technology to detect inter-area modes needs to be scalable in order to fulfil the network-wide requirements that are a result of these oscillations being more wide-spread, where *scalable* means it has to be deployed over a wide area. Examples of such technologies are shown in Figure 9 whereby protection systems deal with local dynamic events while SCADA (Supervisory Control and Data Acquisition) systems and EMS (Energy Management Systems) deal with static wide-area events (Larsson, 2010). A more recent development that is advancing power system monitoring is the development of Wide Area Measurement Systems (WAMS) which sit in between the two timescales and localities of deployment as shown in the figure.

WAMS Systems: WAMS is the generic name for a “modular solution using phasor measurement information from different collection points in a power system, located mainly in substations or at the critical nodes of a grid” (Larsson, 2010). In essence, WAMS are systems that collect data from various critical points on the grid, and then make this data available altogether for analysis. They are commonly implemented using Phasor Measurement Units (PMUs). PMUs are data-acquisition units that provide the additional functionality of synchronising measurements made from a system to a common GPS time signal. PMUs and their GPS time-stamping capability are discussed in greater detail in the following section. Figure 10 illustrates the use of PMUs as part of a WAMS. The use of WAMS is beginning to take over the use of SCADA systems for the purposes of monitoring of stability of system voltages, power flow and frequency. SCADA systems also allow real-time monitoring of processes using Remote Terminal Units (RTUs), which are the counterparts of PMUs. However, unlike PMUs, RTU data is not GPS synchronized, but RTUs can be reconfigured to provide data similar to that from PMUs.

The development of PMUs arose from the need for an improvement of methods for monitoring, protection, operation and control that use sampled data to facilitate the calculation of voltage and current phasors; simultaneous measurement sets with a common time base were needed in order to obtain a synchronously sampled system-wide view.

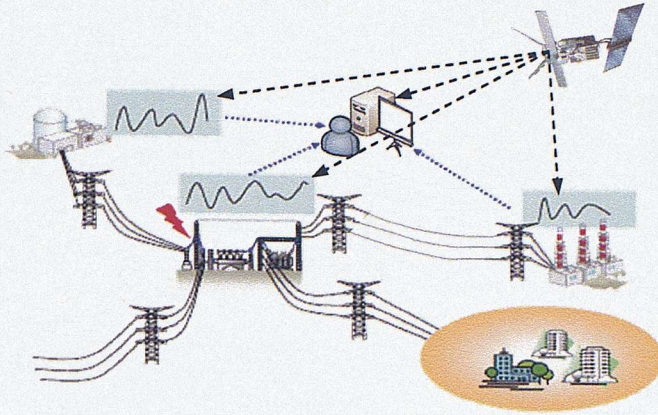


Figure 10: An illustration of a Wide Area Measurement System (WAMS)

Phasors: A phasor is a mathematical representation of a sinusoidal wave used for the purpose of simplifying mathematical analysis of the wave. In electrical systems, phasors are typically used to represent voltage and current measurements sampled from both steady-state (ambient) and dynamic (transient) system behaviour. Ambient and transient behaviour of a power system is described later in this chapter. The general form of a phasor comprises a magnitude (usually the root mean square (r.m.s) value) followed by an exponent which contains the phase angle of the measurement. These useful mathematical representations of waveforms provide a simple way to manipulate electrical quantities both in analysis and also in data-logging since techniques to measure the required parameters exist. Consider the time waveform shown in Figure 11A. The peak of the waveform leads by an angle ϕ , whereas the waveform has an r.m.s value of r . Figure 11B shows the corresponding phasor representation of the time waveform.

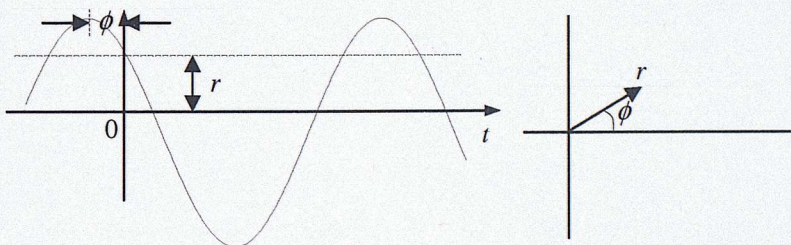


Figure 11: Phasors. After Phadke (1993)

The PMU emerged from the requirement for better data to facilitate development of better monitoring algorithms (IEEE Working Group H-8, 1998). PMUs were initially highly priced which limited their deployment. However, they are becoming more accessible and affordable to system

operators making quantitative analysis of data to infer system stability more viable. An example of an industrially available PMU is the *RES 521*1.0* that has been developed by ABB as part of its range of wide area solutions. It can be deployed as part of the “*Inform^{IT} Wide Area Monitoring PSG830*” solution from ABB. The *PSG830* solution is a Wide Area Monitoring System (WAMS) that collects and analyzes real-time data throughout the power grid. An incorporated communication system provides data transmission links between individual PMUs located in substations to the wide area monitoring system (Larsson, 2010).

Principles of operation of a PMU: The PMU consists of four major parts each of which plays a specific important role in its operation. These parts are illustrated in Figure 12 which shows a general block diagram illustrating the parts of a simple PMU: the filter, the analogue to digital converter, the GPS receiver and finally the microprocessor (IEEE Working Group H-8, 1998). The processes that occur in a PMU can be described as follows.

Signal sampling: The analogue to digital filter samples analogue voltages and currents at a constant rate and converts them to digital phasor signals. This is done using a moving time window. The phasor is calculated using the Discrete Fourier Transform (DFT) as shown in Equation 1, where N is the total number of samples in one period of the sampling, X is the phasor and x_k are the waveform samples.

$$X = \frac{\sqrt{2}}{N} \sum_{k=1}^N x_k e^{-j2k\pi / N}$$

Equation 1

X is complex and, when written in polar form, is expressed as $X = |X|e^{j\varphi}$ where $|X|$ is the magnitude of the phasor and φ is the phase angle. The RMS value, if the waveform is sinusoidal, is $|X|/\sqrt{2}$.

This representation of the phasor is used irrespective of whether or not the signal contains other transient components. The input signal (sampled data) is further filtered to eliminate aliasing errors by ensuring that it contains only frequencies up to one half of the sampling rate. The reason for this is the Nyquist sampling theorem which states that an oscillation requires at least two samples per cycle for accurate analysis.

The sampling process is time-continuous and hence a new phasor is calculated for a new segment of signal that is sampled. Phasors are measured and calculated for each of the three phases in a three phase system, and the positive phase sequence set values are calculated by the microprocessor using a pre-programmed algorithm (Phadke, 1993). The positive phase sequence is one of three vectors of equal magnitude but symmetrically spaced at 120° in time-phase that fully represent a three-phase network. The PMU reports the phasor quantities at every sampling instant (for example 10 times per second), and they can therefore be plotted as a time trend.

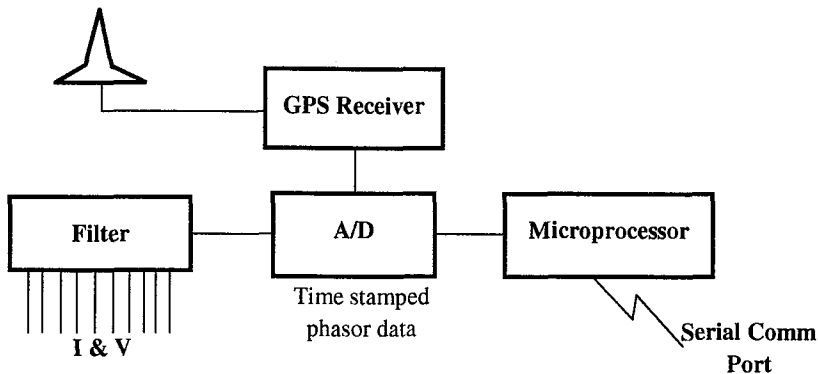


Figure 12: Block diagram of a PMU. After Phadke (1993)

A PMU can monitor the positive phase sequence current and voltage whereby the phasor representations of the measurements are in the polar form that was introduced previously and the RMS values are derived from $|X_r|$, or the corresponding quantity $|X_v|$ if voltage is being monitored. The positive sequence phasor calculated using the recursive DFT method rotates in the complex plane with an angular frequency equal to the difference between the nominal power system frequency and the prevailing actual power system frequency (Phadke, 1993). The deviations from the nominal system frequency can therefore be detected by numerical differentiation of the time trend of the phase angle. Hence, given the positive voltage or current sequence phasor in Equation 2, the prevailing angular power system frequency ω can hence be calculated using the nominal angular system frequency, ω_0 , and the deviation in angular frequency obtained from differentiating the phase angle ϕ as shown in Equation 3. This angular frequency can be converted to Hz using the relationship $f = \omega/2\pi$.

$$X = |X|e^{j\phi} \quad \text{Equation 2}$$

$$\omega = \omega_0 + \frac{d\phi}{dt} \quad \text{Equation 3}$$

For example, if the phasor is rotating at one revolution per second in a counter-clockwise direction (positive), then the prevailing system frequency becomes 61 Hz while if the rotation is in the opposite direction (clockwise), the prevailing system frequency is 59 Hz. This method of frequency determination has been practically proven to produce very accurate results with deviations as small as ± 0.001 Hz being measured.

Time Stamping: In order to achieve measurements based on a common reference, sampling of power system measurements needs to be done at the same instant. The reason for needing a common reference is that power system stability is time dependent and characteristics of the power system that can be inferred from these measurements are only correct at the precise time of measurements. The measurements on the other hand are dynamic and rapidly changing hence time stamping achieves the aim of enabling ordering of measurements in the order of sampling as well as ensuring that correct decisions are made with respect to the time of occurrence of incidents.

Synchronous phasor measurements hence help achieve this aim. An IEEE standard defining the acceptable capabilities of PMUs is available at present and it details the time stamping requirements for any single unit manufactured by any company (IEEE Working Group H-8, 1998). The standard specifies that each measurement of a synchrophasor needs to be tagged with the UTC (Universal Time Coordinated) time at which the particular measurement was made, and this time tag should consist of three numbers: a second-of-century (SoC) count, a fraction-of-second count and a time status value, whereby the SOC count refers to a four byte binary count in seconds from midnight of January 1, 1970 to the current second. The time synchronization should also have sufficient accuracy to minimize errors in the phase hence time lag.

Various techniques for achieving accurate time-stamping were investigated during the development of PMUs, for example the use of fibre optics and Geostationary Operational Environment Satellite (GOES) systems. However, the technique that was eventually implemented uses Global Position System (GPS) satellite transmissions. GPS based systems rely on transmissions from a constellation of satellites that are in non-stationary orbit above the surface of the earth. These satellites consist the GPS, a United States Department of Defence (DoD) satellite based radio broadcast system that

consists of 24 satellites continuously orbiting the earth in six different orbital planes such that even restricted sites have coverage of a minimum of four satellites, hence making reliability of the signal at such sites quite good. GPS signals were designed for the primary use of navigation and consist of a common-access timing pulse that is accurate to about 1 μ s. This corresponds to a phase error of 0.022° for a 60 Hz system and 0.018° for a 50 Hz system, both well within the range of the accuracy required (IEEE Working Group H-8, 1998). Additionally, in order to achieve accurate time-stamping, only one satellite needs to be in the field of the receiving antenna, which itself is quite small. GPS systems have been proven to be very reliable over the years that they have been utilised (Phadke, 1993).

Communication - Synchrophasor Message Format: Having sampled the voltages and currents from an electrical system, derived the positive sequence phasors and time-stamped the measurements, the PMU then formulates a message containing all the relevant information about the measurement made for real-time communication. In order to facilitate this process, IEEE Working Group H-8 (1998) sets guidelines for the format of the messages that are sent to and from the PMU. The communication protocol used in the PMU is very similar to Internet Protocol. Data is sent in packets to another unit and each unit has a unique ID code which is used to identify the unit.

Data Concentrator: A secondary system could be used to receive measurements from various PMUs, and this secondary system is known as a Data Concentrator or a Phasor Data Concentrator (PDC); the PDC has its own unique ID code, as do the other PMUs. The PDC can be used to maintain a database of measurements collected from various substations.

1.2.3. Summary

Advances in power system measurement technology coupled with an increasing need for power system monitoring are driving new research in electrical power systems. On one hand, new technology such as WAMS makes time-synchronised measurements from various points in the grid available to users at a central location via a PDC. On the other hand, there is an increasing need for system monitoring because of the problems expected in the future grid.

The next section outlines the aim and objectives of this research in line with the driving motivation covered in this section.

1.3. Aim, Objectives, Challenges and Requirements

This section presents the aim and objectives of the research. It starts with an explanation of how the issues discussed in the previous section have contributed to the aims of the research. It also presents a list of the objectives of the research and explains the concepts of frequency, damping, ambient operation and transient operation. Since the research concerns ambient operation, the challenges of estimating mode hence system stability under ambient operation are discussed. Based on all these considerations, the requirements of a solution are outlined followed by a brief discussion of the cross-disciplinary nature of the research. Other areas of engineering research which could benefit this strand of research are also briefly explained.

1.3.1. Aim

The previous sections presented the main drivers for the research presented in this thesis. The main driver is a greater need for monitoring of oscillations taking advantage of recent developments in hardware technology for monitoring. Inter-area oscillations have historically posed stability issues in power systems and are expected to become less predictable as electrical transmission networks become more dependent on intermittent renewable energy sources. On the other hand, methods for data gathering are becoming more widely deployed in power systems hence increasing the potential to monitor the systems in real-time. The aim of the research is therefore,

*“To create tools to monitor, in **real-time**, the **stability** of electrical power transmission systems during **ambient** operation by making use of the increased **quantitative information** that is becoming available.”*

1.3.2. Objectives

The key words in the aim of the research are *real-time*, *stability*, *ambient* and *quantitative information*. *Real-time* implies that the created algorithms must produce a result in the time-scale required for an operator to make a decision. *Stability* refers to the main metric that needs to be determined and is inferred from the damping ratio of the oscillatory mode. *Ambient operation* refers to the normal operation of power systems which is in contrast to transient operation which refers to post-fault operation. This section discusses the differences in observed measurements during

episodes of ambient and transient operations and section 1.3.3 further explains the challenges faced in achieving the aim of the research during ambient operation. It is important to monitor the damping in ambient operation because it is critical to detect critical changes in damping before they happen and prior to a system collapse – this can only be achieved when the system is in normal operation. *Quantitative information* refers to the nature of the available observations that will be used by the algorithm.

The aim of the research can therefore be broken up into a number of objectives:

- Differentiate between ambient and transient operation.
- Detect the existence of inter-area oscillations during ambient operation using data measurements.
- Determine the frequency of the oscillations.
- Detect the areas participating in the oscillations.
- Estimate the damping factors of the oscillations.
- Alert operators to critical changes in damping.

The research aims to address these objectives by creating algorithms that can be used to effectively and robustly address these requirements. First however, some of the terminology that has been introduced in the objectives, that is frequency and damping, and ambient and transient operation, needs to be introduced.

Frequency and Damping: Frequency refers to the number of cycles of an oscillation that occur in one second. It is the reciprocal of the period which is the time taken by an oscillation to complete one cycle. For example, an oscillation with a period of 0.5 s completes one cycle in 0.5 s and therefore the frequency of the oscillation is 2 Hz (2 cycles/second).

The damping of the oscillation refers to the rate of decay of the oscillation. This is related to the change in the peak amplitude of the oscillation with time. For example, Figure 13A, B and C show three oscillations. In the Figure 13A, the peak amplitude of the oscillation is decreasing over time hence the oscillation is said to be positively damped. In Figure 13B, the peak amplitude of the oscillation remains the same over time and therefore the oscillation is said to be zero-damped. In Figure 13C, the peak amplitude of the oscillation increases over time and therefore the oscillation is

said to be negatively damped. A negatively damped oscillation is hard to control and is therefore continuously growing. In power systems, this is dangerous because it can lead to generators shutting down in order to protect their rotating parts and hence can lead to a grid collapse.

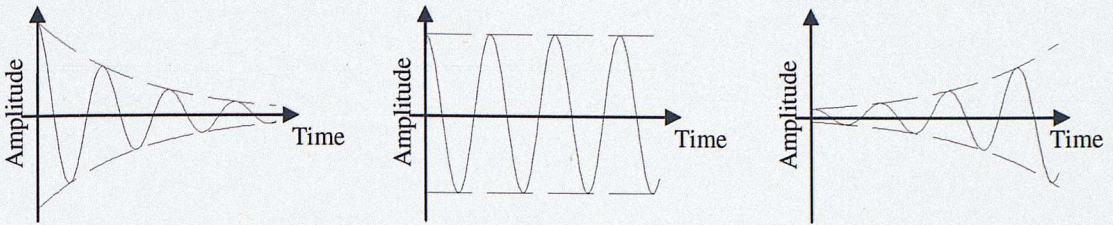


Figure 13: Positive, zero and negative damping

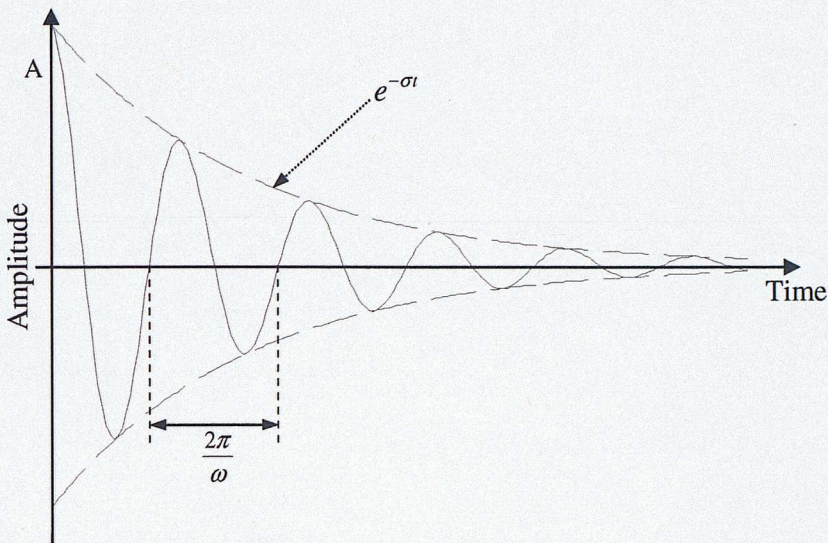


Figure 14: Exponentially decaying sinusoid

$$y = Ae^{-\sigma t} \cos(\omega t + \phi) \quad \text{Equation 4}$$

$$\zeta = \frac{-\sigma}{\sqrt{\sigma^2 + \omega^2}} \quad \text{Equation 5}$$

$$\omega_n = \omega \sqrt{1 - \zeta^2} \quad \text{Equation 6}$$

Inter-area oscillations are typically positively damped though the level of damping is generally low. This makes it critical to determine the changes in damping with time. A damped oscillation can be modelled as an exponentially decaying sinusoid as shown in Figure 14. By fitting such a sinusoid (Equation 4) to data, the rate of decay and oscillatory period can be determined. Using these parameters the natural frequency of oscillation and the damping ratio can be obtained through the equations in equations 5 and 6, where y is the measured quantity, A the amplitude of the oscillation, σ the decay rate, ω the measured oscillation frequency, ω_n the natural frequency of oscillation, ϕ the

phase delay, and ζ the damping ratio. The natural frequency of oscillation refers to the frequency of the zero-damped oscillation.

Ambient vs. Transient Operation: *Ambient operation*, as previously explained, refers to the normal operation of the power system. During ambient operation, the system characteristics can be assumed to be linear and measurements from the system have a random nature. This can be assumed to be due to random or stochastic excitation. Figure 15A shows an example of a set of measurements of the acceleration of a generator rotor made during ambient operation of a power system. It can be noted that distinct oscillations are harder to visually observe and that the signal has continuous episodes of both positive and negative damping. This signal damping is not the same as the system damping as explained later in the next section. *Transient response* on the other hand refers to the response of the system after a fault or major disturbance has occurred. A typical example of a transient response is shown in Figure 15B. The figure shows the frequency of the grid prior to and following a system event. It is possible to observe the form an exponentially decaying sinusoid in one part of the measured system response (from 8.5 to 9 s), and therefore damping of the oscillation can easily be inferred using the relationships given in Equation 5. This might not be the case when the transient is strongly non-linear and contains coupled frequencies, but in the case of simple post-fault transients for example following a line trip, this simple exponentially decaying sinusoid is a good approximation.

1.3.3. Challenges

The research of this thesis concerns the estimation of the damping of inter-area modes during ambient operation of a power system. This subsection outlines the main challenges involved with working with measurements from ambient operation. The challenges are split into challenges to mode detection and challenges to damping estimation, both of which are objectives of the research.

Challenges to Mode Detection: The main challenges to the detection of the inter-area modes and subsequent estimation of their frequencies are the observability of the mode at the measurement locations and the level of noise relative to the signal in each measurement.

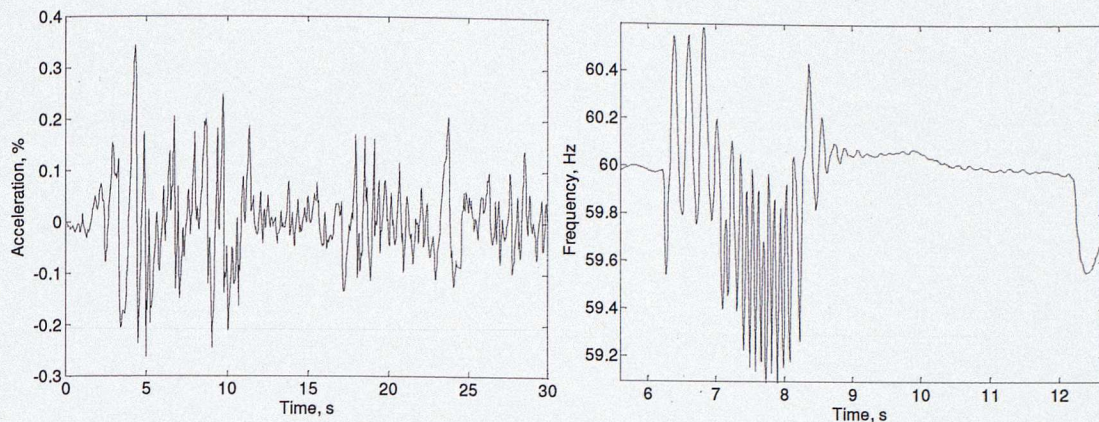


Figure 15: A - Example of ambient response

B - Example of transient response

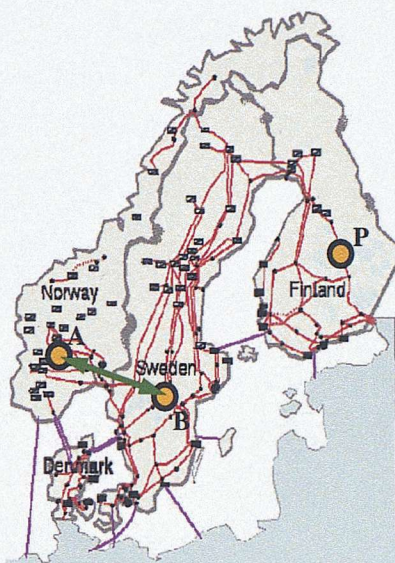


Figure 16: Modal observability

Modal Observability: The *observability* of a mode refers to the amplitude of the mode in measurements at a particular location relative to all other locations. Observability of a mode at a location is related to the location's relative position to the areas participating in the oscillation and the direction of the oscillation, for example in Figure 16, an oscillation between generators in Southern Sweden and Southern Norway will not be clearly observable in measurements from point P in Finland, but will be most clearly visible in measurements from the areas participating in the oscillation which are A and B. In a full power system model, linearization can be carried out in order to determine a modal observability matrix – a matrix that gives the relative observability of a mode at different locations in the model. However, in practice, measurements from a power system, unless carefully chosen, can come from numerous locations. Therefore, observability of a mode is critical to detecting it. It is expected that there will be unknown inter-area modes in the system in the future

and therefore any algorithm to detect these modes from data should not be constrained to certain known modes but must be capable of identifying new modes in measurements.

Noise: Measurements from ambient operation have a great deal of noise present in them. This noise is both system and measurement noise. System noise is noise that is introduced by components in a system whereas measurement noise is noise that is introduced by the equipment making measurements from the system. System noise is predominant during ambient operation of power systems because the components of the power system are coupled. Therefore network events such as line switching and other load-change dynamics are present in the measured data. These events corrupt the modes of interest which are buried in the data. Figure 17 shows an example of the frequency spectra of measurements from a power system in ambient operation (sampled at 10 Hz). The spectrum is generally flat with magnitude around 0.15 VA. The individual spikes around 3.3 Hz, 0.8 Hz and 4.1 Hz may represent spurious random effects, while the broader peak at around 0.3 Hz is an inter-area mode, and the feature on the extreme left close to 0 Hz represents very slow variations in the system such as hourly or daily variations. Any algorithm processing ambient data should be capable of filtering out most of the unwanted noise and identify the inter-area modes that are of interest to the operator.

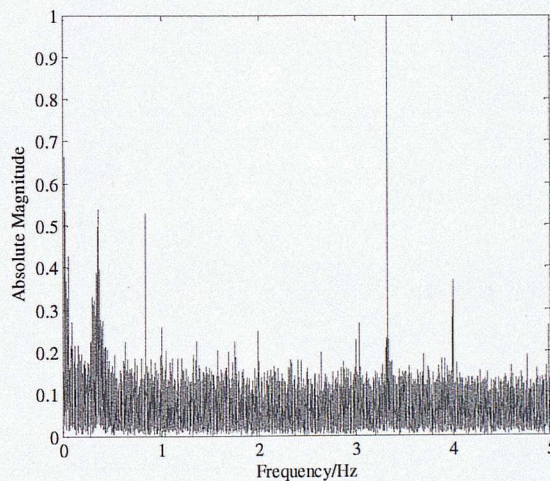


Figure 17: Frequency spectrum of data from ambient operation

Challenges to Damping Estimation: Output measurements from a system are the response of the system to certain inputs. This relationship is illustrated in Figure 18 whereby inputs excite a system and the result of the excitation is the measured outputs. The system output, $y(t)$, is therefore a convolution (*) of the system input, $x(t)$, and the system impulse response function, $g(t)$. Hence, in

order to determine any of the quantities in this relationship, the other two quantities must be known. Since damping is a property of $g(t)$, this implies the need to know something about $x(t)$ as well as the measurements $y(t)$.

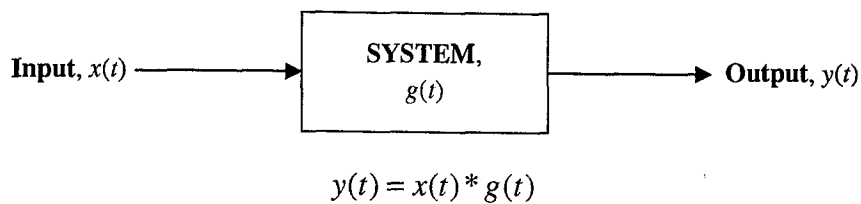


Figure 18: Input-output demonstration

The main challenges to the estimation of damping are the unknown nature of the power system inputs and the presumed unavailability of knowledge about the system structure. The following subsections discuss these challenges.

Unknown Inputs: A system impulse response can be obtained by exciting the system with a known output, measuring the output and therefore deducing the required impulse response using standard input-output relationships. This impulse response is then analysed to obtain the damping of critical modes of the system. In power systems, outputs can be measured at substations and other places but the inputs to the system are immeasurable because all the components are coupled to a certain degree and also because measurements cannot be made at all possible sources of excitation. The inputs are therefore unknown. However, certain assumptions can be made regarding the inputs during ambient operation, for example that the input excitation is stochastic white noise.

Unknown Structure of System: Also similarly, the structure of the power system is assumed to be unknown. Until recently, it was possible for the system operator to use a model of the system to determine system states. However, it is a time consuming task to run a model to determine system damping, and it also relies on the accuracy of the model. Model-based methods are likely to become problematical and are not future-proof because network topologies could constantly change with the expected use of smart grids and distribution level generation. There is therefore an urgent need for a method which can determine the system impulse response directly from data.

1.3.4. Requirements for Solution

Given the objectives and challenges discussed in the previous sections, the main requirements for a solution to determine the frequency and damping of inter-area modes during ambient operation of a power system are algorithms to:

- Detect ambient and transient operation
- Detect modes and the frequencies of the modes
- Determine the sources of modes or the participating areas
- Determine the damping ratios of the modes

There are many possible ways to address these research requirements. However, this thesis being undertaken in the Centre for Process Systems Engineering allows for the use of a cross-disciplinary approach which utilises expertise from various different fields of research.

Cross-Disciplinary Approach: Signal processing has found wide application in many other industries, such as chemical process systems engineering, structural engineering and vibration analysis. In these fields, various applications of signal processing exist for the purpose of monitoring and offline diagnosis of oscillations (abnormal event management in chemical process systems), determining the stability of structures in continuous use (structural engineering), as well as for the detection of transient events such as earthquakes (vibration analysis). It was envisioned at the beginning of this research project that some of these methods might be applicable to the problem of stability monitoring in power systems. The following chapter therefore reviews some of the literature in these fields that might be applicable to the research project, starting with an overview of methods in literature for estimation of power system stability.

1.4. Introduction to the Thesis

The focus of this thesis is on the use of the large amount of data available from WAMS for power transmission security enhancement, particularly for the detection of inter-area oscillation and estimation of modal damping in ambient operation, in order to fulfil the requirements for monitoring that have been highlighted by past events in power transmission systems, situations currently encountered and constraints to be placed on systems as they expand in the future. The research also

recognises similar research problems in other engineering disciplines, particularly in process systems engineering, and therefore aims to present a cross-disciplinary approach towards addressing the current research problem. The thesis is therefore organised as below:

- Chapter 2 presents a review of the literature available in power systems engineering for the determination of stability of power systems using data measurements. It goes on to present methods for stability estimation in the fields of structural engineering and vibrational analysis, two fields that were found to have similar stability estimation research problems as power system engineering. Finally a review of the expertise in process systems engineering literature for the identification of oscillations in chemical processes which can have applications in power systems engineering is presented.
- Chapter 3 collates the information collected from all the literature reviews to identify specific methods to fulfil the research objectives set out in this chapter.
- Chapters 4, 5 and 6 present the theoretical basis of the chosen methods as well as the novel research carried out to apply them to the research problem, including examples of application of the methods to both simulated and measured case study scenarios.
- Chapter 7 presents the integration of the developed methods into a demo tool that can be deployed at electricity operation centres for stability monitoring to illustrate the feasibility of the research for industrial technology transfer.
- Finally, Chapter 8 concludes the thesis with a summary of the work presented and a discussion of opportunities for future research related to this problem.

1.5. Novelty of Research

The output of this research is a novel approach to the problem of determination of power system stability during ambient operation of power transmission networks. As described in the rest of the thesis, this approach makes use of multivariate techniques that have their roots in various fields of engineering to provide an integrated solution addressing the research aim. The benefits to the research community are substantiated by two research papers that have been published, one paper in review and one further paper being worked on which compares the method developed here to two

other methods developed by collaborating researchers. The research papers that have currently been accepted or submitted for publication are:

- Thambirajah, J., Barocio, E., and Thornhill, N.F., “A Comparative Review of Methods for Stability Monitoring in Electrical Power Systems and Vibrating Structures,” Special Issue on Wide Area Monitoring and Control, IET Journal on Generation, Transmission and Distribution, doi: 10.1049/iet-gtd.2009.0485, 2010.
- Thambirajah, J., Thornhill, N.F., and Pal, B.C., “A Multivariate Approach Towards Inter-Area Oscillation Damping Estimation Under Ambient Conditions Via Independent Component Analysis and Random Decrement,” IEEE Transactions on Power Systems, Accepted for publication, 2010, doi: 10.1109/TPWRS.2010.2050607.
- Turunen, J., Liisa, H., Tuomas, R., and Thambirajah, J., “A Wavelet-Based Method for Oscillation Damping Estimation Under Ambient Conditions,” Submitted to IEEE Transactions on Power Systems, 2010.

The main benefit to the industrial community is the design of a tool incorporating the developed algorithms that allows the researched methodology to be implemented in real-time. The PhD programme included a three month internship spent with the UK Electricity National Control Centre of National Grid plc. During this placement, the methods were used to diagnose oscillation problems encountered by UK transmission grid operators. The results of these studies are not published in this thesis in the interest of confidentiality but have been presented to managers at National Grid plc.

1.6. Summary

This chapter has presented an overview of the research project and has introduced the research objective, being the monitoring of electrical power transmission systems. The factors driving the research were presented; these are the increasing threat of inter-area oscillations to power transmission security and the evolution of monitoring technology providing large amounts of data containing key information about system stability.

The wide-scale power system blackouts especially in 2003 opened the eyes of industry to the risks posed by such oscillations resulting in research activity into development of tools towards improving

awareness of operators. However, even in the current grid, the damping of the known inter-area oscillations limit power transfers (export and import) in various grids and therefore need to be continuously monitored. In the future, as the generation capacity of power systems increase and become skewed towards intermittent renewable energy such as wind, the power flows are expected to become more varied and less predictable. The inter-area oscillations in the system will become less predictable and hence system operators will have to depend on tools to provide them with a clearer picture of the condition of the grids.

On the other hand, Wide Area Monitoring Systems (WAMS) provide the capability for determination of system stability because of the synchronised view of the whole power network that they provide through Phasor Measurement Unit (PMU) technology. They allow tracking of both static and dynamic events in both a local zone as well as in a wide area. This research uses data from the ever-increasing deployment of PMUs to provide a solution for monitoring of inter-area oscillations.

The aim of the research is therefore “to create tools to monitor, in real-time, the stability of electrical power transmission systems during ambient operation by making use of the increased quantitative information that is becoming available.” Hence, the objectives are to create algorithms that can detect the on-set of transient events, detect inter-area modes in ambient operation, the participating areas in the oscillations and the damping of the oscillations.

The chapter went on to explain the concepts of frequency and damping, as well as ambient and transient operation. Since this project is focused on ambient operation, the challenges for estimation of inter-area mode frequencies and damping in ambient operation were outlined. The main challenges to frequency estimation are the observability of modes at different locations and the presence of a large amount of noise, while the main challenges to damping estimation are the unknown nature of the system inputs and the system structure.

The chapter continued to identify the main algorithms needed for the research and also introduced some fields in which similar applicable research have been carried out. Finally, the outline of the rest of the thesis was presented and a statement of the novelty of the research was described with evidence from both academia and the industry. The following chapter presents three reviews of

different methods in literature that are applicable to this research. The first section of this chapter presents methods for determination of system stability from power system literature, the second section reviews methods for detection of transients and determination of stability in structural engineering and vibration analysis, and the final of section reviews methods for detection and diagnosis of oscillations in chemical process systems literature. The aim of the reviews is to identify suitable approaches to this research problem and therefore implement a cross-disciplinary solution tailored for this application.

2. Review of Literature

This chapter presents a review of literature available in three different engineering fields that are related to the research problem addressed in this thesis. The first section reviews methods for stability estimation in electrical power systems and comments on the short-comings of the methods currently available as well as currently missing avenues of research that can be addressed in this thesis. The second section reviews methods from vibration analysis, a strand of structural engineering in which the scope of research has relevance to power systems. A review of methods is once again presented but additionally a discussion of the similarities between the methods in this field and those in electrical power systems. A discussion of methods with the potential of application to electrical power systems and the problems they can address is also presented. Finally a review of methods from process systems is presented. Methods for oscillation detection have been widely researched in process systems engineering and therefore the research problem addressed in this thesis can benefit from advances in that field.

2.1. Methods for Power System Stability Estimation

This section presents a review of the literature on methods used for determination of system stability in electrical power systems. This review has been published in Thambirajah *et al.* (2010). The methods are divided into methods applicable to ambient operation and methods applicable to transient operation. This project concerns the determination of system stability during only ambient operation of power systems; however, a review of methods applicable to transient operation is beneficial in identifying requirements and methods that may be suitable for the automated detection of ambient and transient operation regimes. All the methods are classified in hierarchical trees in order to show distinct classes of methods.

2.1.1. Overview

A survey of the methods available for analysis of signals from electrical power systems is presented in Messina *et al.* (2009) which provides a classification of the methods and examples of methods that fall within the respective classifications. The same classification augmented by tree diagrams is

used in this section, including more recent applications. Greater detail of the methods that fall within the classifications is also presented.

The top-level classification of methods refers to the system response during which they are applicable, and a distinction is made between methods for ambient operation and those for transient operation, as shown in Figure 19.

As explained in the previous chapter, an *ambient response* describes measurements from the system during ambient operation when the system can be assumed to be reasonably linear (around the operating point) and the excitation (load variation) can be approximated as being random and Gaussian; the outputs from the system are stochastic in nature. A *transient response* describes measurements from the system during transient operation which is initiated after a disturbance has been applied or a fault has occurred. This fault-induced response is usually characterised by a large deviation in system frequency or other system measurements, for example power flow in a transmission line. In Messina *et al.* (2009), the methods applicable to these operation types are referred to as mode-meter and ring-down methods respectively. *Mode-meter* methods are called so because they give mode frequency estimations more readily than damping estimations while *ring-down* methods are called so because they work on signals that characterize the damped oscillatory behaviour of the system. The first of the following sections describes the classification of methods for ambient operation while the second describes the classification of methods for transient operation.

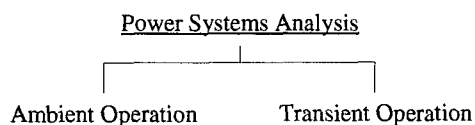


Figure 19: Hierarchical tree showing classification of methods for power systems engineering

2.1.2. Ambient Operation

Signals measured during ambient operation are stochastic in nature and are dominated by broadband noise which originates in the load demand. Additionally, since the load cannot be measured everywhere in the system, the input is assumed to be unknown. The aim of analysis is to determine the damping of the system using measurements of the system output such as power flows, voltage

measurements and frequency deviations. It can be difficult to obtain information about the system damping of modes from outputs only. In order to make such estimations easier, probing might be applied. In the cases that probing is applied, a power signal that can be measured is injected into the system. However, care is taken to ensure that the injected signal does not cause a disturbance in the power system. Methods for ambient operation can therefore be sub-divided into methods that require probing and methods that do not require probing. Figure 20 shows the classification of methods for ambient operation.

Methods that require probing: *Probing* refers to the injection of an external disturbance into a system (through a large load or an interconnector) and measurement of the response of the system. For example, Fingrid imposed a 50 MW (peak-to-peak) signal onto the High Voltage Direct Current (HVDC) link between Finland and Sweden in 2007 in an experiment designed to excite the inter-area mode between Sweden and Finland and hence determine the damping of the mode (Turunen *et al.*, 2008). The probing signal is taken as a system input and the measurements the system outputs. The system response is then calculated from standard input-output system theory. These methods are standard methods for system identification and are reviewed in depth in Ljung (1987). The hierarchical tree in Figure 21 classifies these methods. They are initially divided into parametric and non-parametric methods. *Parametric* methods refer to those approaches that aim to determine transfer functions of systems by first selecting and confining the search to a set of possible models while *non-parametric* methods are those that aim to determine the transfer functions by direct techniques (Ljung, 1987). Non-parametric methods tend to work on data to estimate characteristics of the data itself whereas parametric methods tend to work on data to make inferences about the system generating the data.

Non-parametric methods: Non-parametric methods are further divided into time-domain methods and frequency-domain methods. *Time-domain* methods use the measured time series directly while *frequency-domain* methods use the spectra of the measurements in analysis.

Of the time-domain methods described in Ljung (1987), the only one applicable to ambient measurements (without any impulse or step excitation) is Correlation Analysis. A system output is

obtained by convolution of the measured system input and system impulse response and hence the cross-correlation of the system input and output $R_{yu}(\tau)$ is equivalent to the convolution of the estimate of the system impulse response $g(k)$ and the input autocorrelation function $R_u(\tau)$. The system frequency and damping of a mode can then be obtained by analyzing the estimated impulse response given in Equation 7, where $\hat{\cdot}$ represents estimated quantities.

$$\hat{R}_{yu}^N(\tau) = \sum_{k=1}^M \hat{g}(k) \hat{R}_u^N(k-\tau) \quad \text{Equation 7}$$

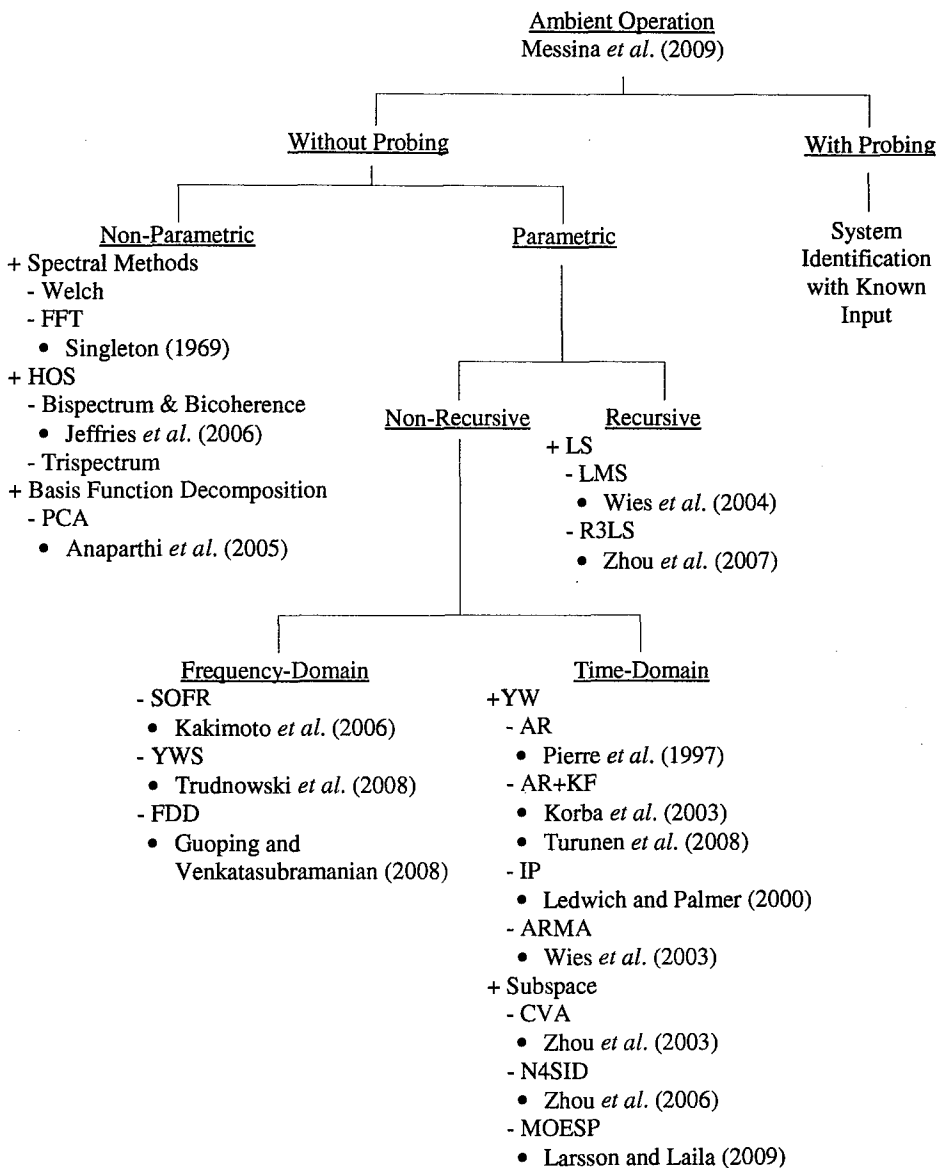


Figure 20: Hierarchical tree showing classification of methods for ambient operation of power systems

If the input were a noise sequence, an estimation of the output autocorrelation would hence be an

estimate of the system impulse response. This is the assumption used to obtain the system response prior to the application of the parametric method in Ledwich and Palmer (2000).

The other applicable methods shown in Figure 21 are frequency domain methods: Empirical Transfer Function Estimation (ETFE) and Spectral Analysis. ETFE makes use of the relationship between the system input and output in a frequency transfer function. Since convolution corresponds to multiplication in the frequency domain, the system output spectrum $Y(j\omega)$ is simply the product of the spectrum of the system response $G(j\omega)$ and that of the input $U(j\omega)$. Hence, using this relationship, the system frequency response can be estimated as shown in Equation 8.

$$\hat{G}(j\omega) = \frac{Y(j\omega)}{U(j\omega)} \quad \text{Equation 8}$$

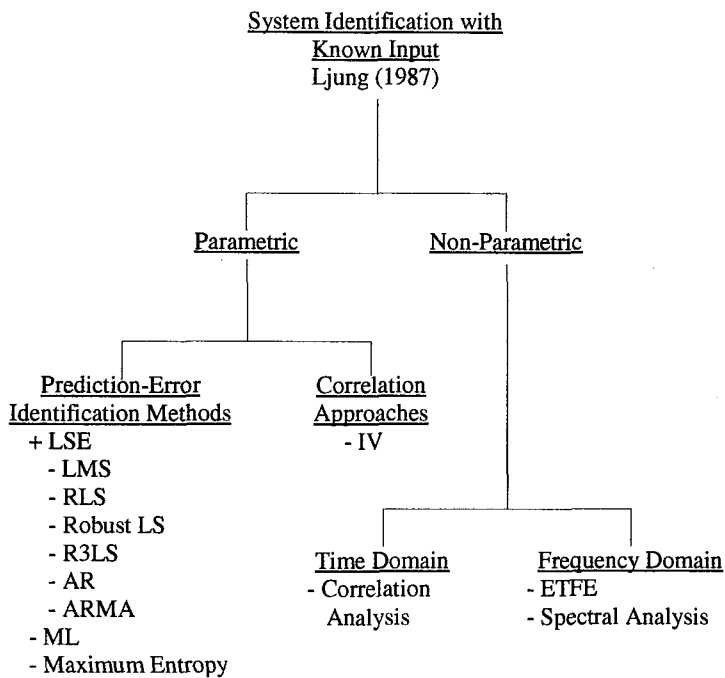


Figure 21: Hierarchical tree showing classification of methods for system identification with known input.

Ljung (1987) however remarks that the system response estimated in this way is very crude and that the variance of the estimate does not decrease with the length of the sampled signals. This is because the method stipulates that the estimates at different frequencies are uncorrelated and hence collecting a signal for a longer length of time simply increases the number of frequencies at which the frequency response is to be estimated. In order to improve the estimates, it is assumed that the values

of the true frequency response function at various frequencies are related. This is the basis of spectral analysis methods which aim to smooth the ETFE estimate using a weighting function or window in the vicinity of the system frequencies, for example the Blackman-Tukey periodogram.

Parametric methods: The second branch of methods that require probing in the hierarchical tree are parametric methods. Parametric approaches are divided into Prediction-Error Identification Methods (PEMs) and Correlation Approaches (CAs).

A. Prediction-Error Identification Methods (PEMs):

PEMs aim to minimize the prediction error which is a function of the error between the outputs of the constructed model and the measured system outputs. In PEMs, the prediction error is usually represented as a function of the actual error, in most cases a quadratic norm which is the sum of the square of the errors. A norm is a function that assigns a positive value to a measure. Two examples of such methods are Least Square Error (LSE) methods and Likelihood Estimators for example the Maximum Likelihood (ML) method.

LSE models try to minimize the error obtained by applying a linear regression to data. A linear regression model employs a linear predictor which is in the form shown in Equation 9 where $\hat{y}(t, \theta)$ is the modelled output which is a function of the vector of linear regressors $\varphi(t)$, the parameter vector θ and noise $\mu(t)$ at time t . The prediction error is therefore as shown in Equation 10.

$$\hat{y}(t, \theta) = \varphi^T(t)\theta + \mu(t) \quad \text{Equation 9}$$

$$\varepsilon(t, \theta) = y(t) - \varphi^T(t)\theta \quad \text{Equation 10}$$

The aim is then to minimize the quadratic norm of this error. Examples of variants of these methods are Least Squares (LS), Recursive Least Squares (RLS), Robust LS, Recursive Regularized Least Squares (R3LS), Auto-Regressive (AR) and Auto-Regressive Moving Average (ARMA) methods which are described later under the heading of parametric methods that do not require probing. Another PEM is the ML estimator which is a statistical approach that aims to recreate the probability density function (PDF) of the observations. It however requires the user to know the form of the PDF of the observations. The maximum entropy approach is a method that searches for a PDF model that minimizes the information distance to the true system. Details of these methods are available in

Ljung (1987).

B. Correlation Approaches (CAs)

CAs aim to minimize the correlation between the prediction error and past data because an ideal model should have an error completely independent of past data (Ljung, 1987). The best known CAs are Instrumental Variable (IV) methods. IV methods try to estimate the parameters of a model that minimize the correlation between the prediction errors and a finite-dimensional vector sequence derived from the past data whose elements are termed instrumental variables. In IV methods, a linear regression is performed on data with the conditions that the IVs $\zeta(t)$ are correlated to the regression variables $\varphi(t)$ but uncorrelated with the noise (hence the residuals) $v_0(t)$. These conditions can be expressed as expectation equations, $E\{\}$, as shown in equations 11 and 12.

$$E\{\zeta(t)\varphi^T(t)\} \text{ is non-singular} \quad \text{Equation 11}$$

$$E\{\zeta(t)v_0(t)\} = 0 \quad \text{Equation 12}$$

The IVs are usually then obtained from the past inputs by applying linear filtering; criteria for selection of the IVs are presented in detail in Ljung (1987).

Methods that do not require probing: Following Messina *et al.* (2009), the methods for ambient operation which do not use a probing signal can be further divided into non-parametric and parametric methods. The definitions of the two are the same as those discussed in the previous section. Non-parametric methods are mainly spectral methods and can be used to estimate mode frequencies in data; they however cannot provide system damping information.

Non-parametric methods: The hierarchical classification tree in Figure 20 shows that the well-known Fast Fourier Transform (FFT) (Singleton, 1969) and Welch Periodogram methods fall into the category of non-parametric methods. These methods transform a time-domain signal into a frequency-domain function where the signal is decomposed into a set of oscillatory components with a magnitude and phase.

Other non-parametric methods in the same branch of the tree are higher order spectral (HOS) methods and basis function decomposition methods. HOS methods such as the bispectrum and

trispectrum provide information about the magnitude and phase relationships between frequencies in a signal and can be used for mode detection as well as fault monitoring. An example is demonstrated in Jeffries *et al.* (2006) where bicoherence (the normalized bispectrum) is used for condition monitoring of turbine blades by making use of the phase-coupling characteristics of fault signals.

Basis function decomposition methods are multivariate analysis techniques that transform an input matrix of data into a different dimensional space where relationships between the different sets of data are more easily observable. An example of such a method is Principal Component Analysis (PCA) which decomposes a set of inputs into a set of weighted uncorrelated orthonormal functions called principal components (PCs); these PCs describe all the variability in the data (Wold *et al.*, 1987). Spectral methods have also been used for mode shape and coherency estimation for example in Trudnowski (2008) where the mode shapes are estimated using synchrophasor measurements from cross-spectral densities derived from the FFTs of the signals, and in Anaparthi *et al.* (2005) where PCA is used to obtain coherent groups of generators by clustering the weightings of the PCs obtained using simulated speed measurements at the rotors of generators.

Parametric methods: The other branch of the hierarchical tree under the probing signal classification contains parametric methods. Parametric methods usually make assumptions of the nature of the system inputs that result in the measured outputs by assuming a functional form for the probability distribution functions of the observations [1]. If the nature of the input-generating mechanism is unknown, it is usually assumed to be a random and Gaussian varying-load process hence methods based on this assumption are applicable to estimate the system characteristics that produce the observed output measurements.

Parametric methods can be further classified as recursive or non-recursive methods. This classification refers to the nature of the estimation involved. *Recursive* methods are those that converge to a solution for the model parameters with respect to time where new data is used to update a previously calculated solution, whereas *non-recursive* methods are those that re-calculate a new solution for every set of new data. Therefore, there is a further branching in the tree distinguishing between recursive and non-recursive methods.

A. Recursive Methods

The most used recursive methods are adaptive filter techniques of which least squares (LS) algorithms are the ones that have been applied to power systems (Zhou *et al.*, 2007, Wies *et al.*, 2004). LS algorithms estimate a model for a set of data by assuming a functional form of the input probability density function and minimizing a penalty or cost function which is the sum of the square of the differences between the observed values and the ones obtained from the model. They can be described as optimization algorithms in this sense. The general adaptive linear filter algorithm is of the form of equations 13-15.

$$y_{fil}(k) = X^T(k)W(k) \quad \text{Equation 13}$$

$$e(k) = y_{obs}(k) - y_{fil}(k) \quad \text{Equation 14}$$

$$\Delta W(k) = f[e(k)] \quad \text{Equation 15}$$

The modelled uncorrelated system outputs y_{fil} are a weighted function (W) of the system inputs X (white noise), where e is a vector of errors between the modelled outputs and the measured outputs y_{obs} at instant k . The weighting function (W) is then adjusted (by ΔW) as a function of the cost function (error). The adjustment to the weights is carried out using an optimization algorithm to iteratively search the space of the previous solution, for example using the method of steepest descent, Newton's method or the Gauss-Newton Method. The Least Means Squares (LMS) method uses the Gauss-Newton method and an error-squared cost function in the estimation of the filter weights (Kamel, 2009). The error e associated with the previous estimation can also be used as an estimate of the unknown system input. The LMS algorithm is usually stable and simple to code, but is slow to converge.

An evolution of the LMS algorithm is the Recursive Regularized Least Squares (R3LS) algorithm in which an initial state of the filter coefficients is specified and included in the cost function such that the deviation from the initial state is also minimized as shown in Equation 16 where q is a function representing the confidence in the deviation from the initial guess of filter estimates \hat{W} .

$$\Delta W(k) = q[W(k) - \hat{W}] + \lambda f[e(k)] \quad \text{Equation 16}$$

Additionally, a forgetting factor, λ , which reduces the influence of large prediction errors is used to weight the error cost function (Zhou *et al.*, 2007). The reason for including a forgetting factor is to

make the filter less sensitive to small departures from the assumed functional form of the input probability distribution. This algorithm can therefore be applied to a collection of other similar distributions [1]. Such departures can be caused by missing or erroneous data. However, there can be large estimation errors if the initial filter states are wrongly specified. These described techniques are generally well known from system identification (Ljung, 1987). The algorithms are used to estimate autoregressive (AR) model parameters in Zhou *et al.* (2007) and Wies *et al.* (2004). The structure of AR models is introduced in the following description of non-recursive methods, including the procedure for obtaining the system mode frequencies and damping values from the model parameters.

B. Non-Recursive Methods

Non-recursive methods, as previously defined, calculate a new estimate for every new set of data and discard the previous estimate entirely. The hierarchical tree in Figure 20 shows that these methods can be further sub-divided into time-domain methods and frequency-domain methods. The hierarchical tree shows that there are two main types of time domain non-recursive methods implemented in literature for the analysis of ambient measurements from power systems: methods based on the Yule Walker (YW) algorithms and Subspace Identification (SSI) methods.

▪ Time domain methods – YW

It is reported in Messina *et al.* (2009) that the earliest implementation of a non-recursive method for power systems analysis is the YW implementation of an Auto-Regressive (AR) model in Pierre *et al.* (1997). The YW algorithm is further extended to estimate an Auto-Regressive Moving Average (ARMA) model in Wies *et al.* (2003). The authors proposed the application of these methods to determine the modal characteristics of electromechanical modes in power systems from measured responses only. These models represent the most common implementations of the YW algorithm in system identification literature. The AR and ARMA models are linear input-output models used to describe stationary data. An ARMA model is formed by combining an AR model and a Moving Average (MA) model; it represents a generic form of representing an input-output relationship. An AR model represents the present output measurement as a weighted sum of previous outputs and an uncorrelated noise term, whereas a MA model represents the present output measurement as a

weighted sum of present and previous inputs. The inputs are usually assumed to be white noise sequences. Equation 17 represents an ARMA model [2].

$$y(k) = -\sum_{i=1}^m a_i y(k-i) + \sum_{i=1}^n b_i x(k-i) + \varepsilon(k) \quad \text{Equation 17}$$

a_1, a_2, \dots, a_m are the coefficients of the m -order AR-part of the model, b_0, b_1, \dots, b_n are the coefficients of the n -order MA-part of the model, $x(k)$ are the elements of the input, $y(k)$ are the elements of the observed output and the $\varepsilon(k)$ represents the uncorrelated noise in the output. The AR model is therefore an ARMA model where all the coefficients of the MA model are zero. The AR model is also referred to as an all-pole or infinite impulse response filter. The system poles are obtained by solving the z -polynomial characteristic equation comprising the a coefficients of the model as shown in Equation 18.

$$1 + a_1 z^{-1} + a_2 z^{-2} + \dots + a_m z^{-m} = 0 \quad \text{Equation 18}$$

These poles correspond to the eigenvalues of the power system and hence provide the system mode frequencies and damping values. The coefficients of the model are not easily obtained by least squares estimation; instead, the YW algorithm determines the coefficients by expressing the estimation problem as a matrix equation using the estimated autocorrelations of the signals which can easily be solved. However, a main drawback of these methods is that the order of the models (m and n) needs to be chosen. These values need to be chosen to be high enough to capture all the dynamics of interest as well as noise (Wies *et al.*, 2003), while ensuring that they are not too large to be computationally inefficient.

A similar YW method is reported in Ledwich and Palmer (2000), where the authors use ambient measurements from a power system to estimate the autocorrelation functions (ACFs) of the measured system outputs and use an AR algorithm to estimate the system modes. They observed that there is an error introduced from the use of a standard one-step predictor model in the presence of signal noise, and therefore extend the analysis to a multi-step predictor solution which they called the interleaved Prony (IP) method.

In Korba *et al.* (2003), an AR algorithm is implemented in conjunction with a Kalman filter (KF) to recursively determine the AR model parameters (AR + KF method in the hierarchical tree). The

Kalman filter is a recursive linear filter that can be used to estimate the state of a linear process in the presence of noise (Welch and Bishop, 2006). It is however shown in Turunen *et al.* (2008) that the estimation of modal damping by this method is only reliable when a large excitation is applied to the power system.

- Time domain methods – SSI

The second set of commonly used methods shown in the hierarchical tree in Figure 20 consists of methods for Subspace Identification (SSI). SSI methods make use of linear subspaces which are ways of representing data in different planes of reduced dimensionality. It is reported in Lobos *et al.* (2006) that in these subspaces, the eigenvectors resulting from noise added to a signal are separated from those of the signals themselves hence making its resolution theoretically independent of the signal-to-noise ratio. SSI is a method used to estimate the state-space model of a system. A discrete state-space model of a system is of the form shown in equations 19 and 20.

$$\mathbf{x}(k+1) = \mathbf{A}\mathbf{x}(k) + \mathbf{B}\mathbf{u}(k) + \mathbf{w}(k) \quad \text{Equation 19}$$

$$\mathbf{y}(k) = \mathbf{C}\mathbf{x}(k) + \mathbf{D}\mathbf{u}(k) + \mathbf{v}(k) \quad \text{Equation 20}$$

At time k , $\mathbf{x}(k)$ represents the system states, $\mathbf{y}(k)$ the measurable system outputs, $\mathbf{u}(k)$ the system inputs, $\mathbf{w}(k)$ the process noise, $\mathbf{v}(k)$ the measurement noise, \mathbf{A} the state transition matrix, \mathbf{B} the input matrix, \mathbf{C} the output matrix, and \mathbf{D} the feed-through matrix. The system dynamics are contained in the state transition matrix \mathbf{A} , hence the eigenvalues of the system are obtained by eigenvalue analysis of \mathbf{A} . SSI aims to estimate the \mathbf{A} , \mathbf{B} , \mathbf{C} and \mathbf{D} matrices by estimating the state vector $\mathbf{x}(k)$ first, using regression analysis to determine the state-space model and finally determining the transfer matrix which is the overall relationship between \mathbf{x} and \mathbf{y} .

This contrasts to the classical methods of system identification that use regression analysis to estimate the transfer matrix, realizing it as a state-space model and finally calculating or predicting the state-vector. The state vector is estimated using reliable numerical algorithms such as Rayleigh Quotient (QR) methods and Singular Value Decomposition (SVD) (Katayama, 2005). It is however assumed that the eigenvalues of the \mathbf{A} matrix lie within the unit circle, and that the measurement noise, $\mathbf{v}(k)$ is stationary, zero-mean white noise (Qin, 2006). Some of the SSI algorithms that have been applied to the problem of mode identification under ambient conditions are Canonical Variate

Analysis (CVA) (Zhou *et al.*, 2003), the Numerical Algorithm for Subspace State-Space System Identification (N4SID) (Zhou *et al.*, 2006) and the Multivariate Output Error State Space (MOESP) algorithm (Larsson and Laila, 2009).

▪ Frequency-Domain Methods - SOFR

The right-hand branch of non-recursive methods in the hierarchical tree in Figure 20 shows frequency-domain methods. The first method under this group is Second Order Frequency Regression (SOFR) that was applied in Kakimoto *et al.* (2006). A least-squares algorithm based on the Newton-Raphson method is applied to estimate the mode frequency and damping utilizing the frequency spectrum of the derivative of the phase angle difference between two phasor measurements. The authors propose that the derivative of the angle difference between the measurements (y) during ambient operation can be modelled using a second order equation which is equivalent to the representation of the signal computed via a finite Fourier series as shown in Equation 21 where ζ is the damping ratio and ω_n is the undamped natural angular frequency of the inter-area mode.

$$\frac{d^2y}{dt^2} + 2\zeta\omega_n \frac{dy}{dt} + \omega_n^2 y = \sum_{i=0}^{m/2} A_i \cos(\omega_i t + \phi_i) \quad \text{Equation 21}$$

The second order decomposition can be compared to the frequency spectrum of the signal via the magnitude A_i and phase ϕ_i of the i th mode obtained from the FFT. By establishing the relationships between the known values from the FFT, hence finite Fourier series, and the unknown parameters ζ and ω_n from the second order model, a least-squares optimization can be carried out. The demonstrated method however requires a large amount of data (spanning almost an hour with an inter-sampling time of 0.1 s) and the estimated quantities have a large variance when implemented with actual measured data. The authors propose that this variation can be removed by averaging the estimates obtained over a long time scale (for example 3 hours).

▪ Frequency-Domain Methods – YWS and FDD

Two other recent frequency-domain methods shown in the hierarchical tree in Figure 20 that have been applied for mode identification without probing under ambient conditions are reported in

Messina *et al.* (2009): the Yule-Walker with Spectral Analysis (YWS) algorithm, and Frequency Domain Decomposition (FDD). The YWS method is introduced in Trudnowski *et al.* (2008) and is very similar to the YW method described previously from Pierre *et al.* (1997), the only difference being that the autocorrelation functions of the signals are estimated from the spectra of the signals whereby the autocorrelation functions (at lag λ), $R(\lambda)$, are the inverse Fourier transforms, $\mathfrak{S}^{-1}\{\}$, of the power spectra, $P(\omega)$, which are the squares of the frequency spectra, $X(\omega)$; these relationships are shown in equations 22 and 23. The drawback of the YWS algorithm is the same as that of the YW algorithm: the order of the model needs to be pre-determined.

$$R(\lambda) = \mathfrak{S}^{-1}\{P(\omega)\} \quad \text{Equation 22}$$

$$P(\omega) = X(\omega)X^*(\omega) \quad \text{Equation 23}$$

Unlike YWS, FDD is a purely frequency domain method which involves SVD of the matrix of spectra of the output measurements. SVD is a way of factorizing a matrix into a set of linear approximations using basis vectors which expose the underlying structure of the matrix [3]. FDD is described as the process of decomposing a matrix of spectra of outputs into a function of the spectra of the unknown inputs in Brincker, Zhang and Andersen (2001).

$$G_{yy}(j\omega) = H^*(j\omega)G_{xx}(j\omega)H(j\omega)^T \quad \text{Equation 24}$$

Equation 24 demonstrates SVD where $G_{xx}(j\omega)$ is the estimated power spectral density (PSD) matrix of the r unknown inputs given the PSD matrix $G_{yy}(j\omega)$ of the m responses, where $H(j\omega)$ is the $m \times r$ matrix of frequency response functions (FRFs) which map the estimated inputs to the measured outputs. $H(j\omega)^T$ and $H^*(j\omega)$ represent the transpose and complex conjugate of $H(j\omega)$ respectively. The FRFs consist of singular vectors whose corresponding singular values are the power spectral densities of the equivalent single degree of freedom systems. The power spectral densities are then taken back to the time domain via an inverse Fourier transform which are analyzed using the logarithmic decrement method to obtain the mode natural frequencies and damping values (Brincker, Ventura and Andersen, 2001). This method is applied to ambient measurements from a power system in Guoping and Venkatasubramanian (2008). The FDD is an efficient and reliable technique. However, the number of singular values formed during SVD can be large and a threshold is required

to determine the dominant values. This can be difficult to automate. Additionally, there are some errors introduced by (i) truncation of the Fourier series and (ii) the phenomenon of spectral leakage due to the use of finite data lengths which respectively cause the damping to be over-estimated and under-estimated (Brincker, Ventura and Andersen, 2001).

Observations and Comments: The above overview of the methods that have currently been applied to the problem of system identification without probing shows that parametric methods are dominant. The key steps in applying parametric methods are:

- Estimation of the probability density function (PDF) or nature of the input excitation, which is assumed to be random and Gaussian.
- Choice of a system model that can be represented as a stochastic process.
- Estimation of system model parameters.
- Inferring the system eigenvalues hence mode frequencies and damping.

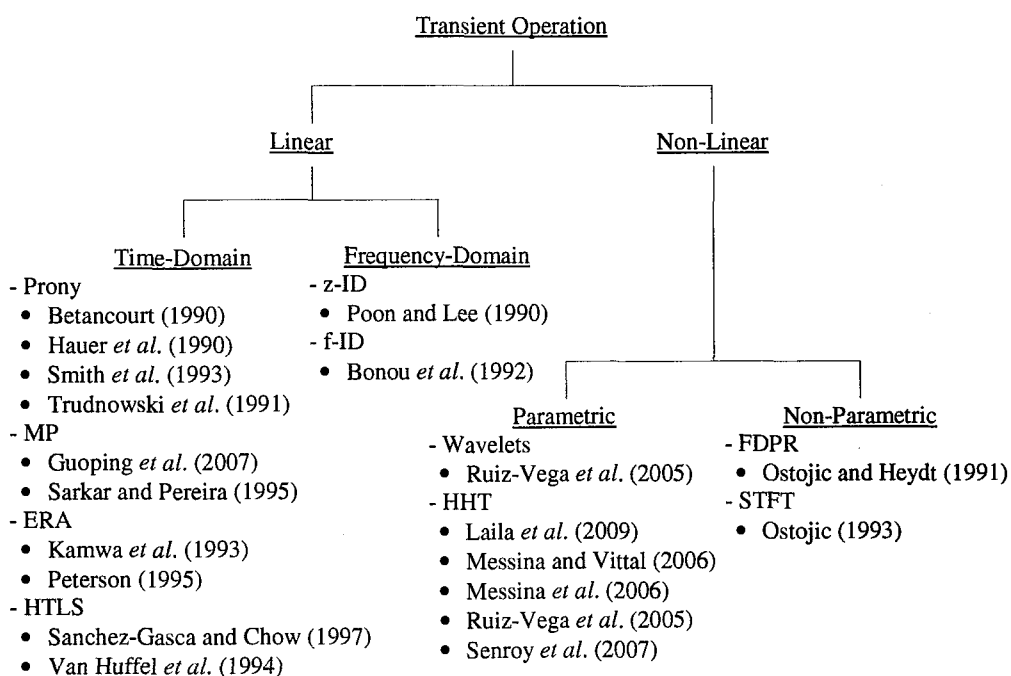


Figure 22: Hierarchical tree showing classification of methods for transient operation of power systems

Of the methods described in this section, the time-domain parametric methods have the advantage that they are able to use models which relate more directly to the underlying system structure. However, an important observation to note in all the described implementations of parametric

methods is that the underpinning assumption is that the system is driven by white noise. However, there is no concrete practical evidence in the literature to establish this theoretical assumption. Most of the reviewed parametric methods which do not require probing also give the same weighting to all measured data: all the measurements are assumed to contain an equal amount of information about the system damping of a mode. In the cases where this assumption is not valid, a suitable signal is chosen for analysis through experience of the person implementing it. There is therefore a need to automate the selection of a suitable signal or to automate the assignment of weights to different measurements in order to ensure that the best signals for analysis are used in the model estimation.

2.1.3. Transient Operation

Transient operation as previously defined refers to the response of a power system after a fault has occurred or a large disturbance has been initiated. This operation is characterised by large deviations in measurable system parameters such as system frequency. It is assumed that the post-fault/post-disturbance transient represents the true impulse response of the system hence the aim of transient analysis is to measure the stability of the system by determining the oscillatory frequency and damping of the transient. This project concerns the determination of system stability during ambient operation of power systems. However, a review of methods applicable to transient operation is beneficial in highlighting the need for methods that may be suitable for the automated detection of ambient and transient operation regimes. Methods in the literature are sub-divided according to the assumption of linearity of the system during such excursions. The hierarchical tree in Figure 22 therefore branches into linear and non-linear methods.

Linear Methods: *Linear methods* assume that the system maintains linearity after the fault or disturbance and they aim to fit a model of a sum of decaying sinusoids to the transient data. The measured output $y(t)$ is composed of a weighted sum of n decaying sinusoids λ_i (with weights B_i) as shown in Equation 25, where λ_i can be decomposed into a frequency component ω_i and an exponential decay component σ_i , such that $\lambda_i = j\omega_i + \sigma_i$.

$$y(t) = \sum_{i=1}^n B_i e^{\lambda_i t} \quad \text{Equation 25}$$

The differences between the methods result from the approach taken to fit this model. The hierarchical tree in Figure 22 is further subdivided into time-domain methods and frequency-domain methods.

Time-Domain Methods: These methods fit a linear model to data by analysing the time-series of the data. The hierarchical tree shows four different time-domain methods: Prony methods, the Matrix-Pencil (MP) method, the Eigenvalue Realisation Algorithm (ERA) and the Hankel Total Least Squares (HTLS) method. All these methods are univariate and several of them make use of a Hankel matrix, a square matrix which includes the signal and time-shifted versions of the signal giving the form below where k is the sampling time and ℓ is a delay.

$$\begin{pmatrix} y(k) & y(k+\ell) & y(k+2\ell) & y(k+3\ell) \\ y(k+\ell) & y(k+2\ell) & y(k+3\ell) & y(k+4\ell) \\ y(k+2\ell) & y(k+3\ell) & y(k+4\ell) & y(k+5\ell) \\ y(k+3\ell) & y(k+4\ell) & y(k+5\ell) & y(k+6\ell) \end{pmatrix} \quad \text{Equation 26}$$

A. Prony Methods

Prony methods are those that utilise Prony analysis to determine the linear model described previously. Prony analysis is a two-step process that involves creating a linear prediction model (LPM) of the data and having obtained the coefficients of the model, determining the eigenvalues of the system by evaluating the roots of the least-squares polynomial created by the LPM. This is quite similar to the AR model introduced in the previous section for ambient methods. Prony methods suffer from problems evaluating damping of closely-spaced modes. Despite this, they are widely used for transient analysis in power systems. Examples are available in Hauer *et al.* (1990), Trudnowski *et al.* (1991), Smith *et al.* (1993) and Betancourt (1990).

B. MP

The Matrix-Pencil method makes use of functions known as pencil functions. Pencil functions represent the system matrix as a function of two known matrices (\mathbf{Y}_1 and \mathbf{Y}_2) such that the system eigenvalues λ are the same as the eigenvalues of the function $\mathbf{Y}_2 - \lambda\mathbf{Y}_1$. This special decomposition achieves the purpose of reducing the sensitivity of the method to noise in the measurements. It is introduced in Sarkar and Pereira (1995) as a one-step process to obtain system modes and damping

and as an alternative to Prony analysis. The MP method involves the SVD of a matrix of time-shifted output measurements where the length of the rows and columns of the matrix depends on the length of the time-shift which is itself dependent on the number of dominant modes to be estimated and a parameter termed the pencil parameter. After SVD, the resulting singular matrices are truncated to the number of dominant modes required, and by carrying out two different inverse SVD operations on these truncated matrices, the pencil functions Y_1 and Y_2 can be obtained, and hence the system eigenvalues. The MP method has the advantage of being more robust to noise than Prony methods and is demonstrated in Guoping *et al.* (2007).

C. ERA

The Eigenvalue Realisation Algorithm was introduced in Kamwa *et al.* (1993) and involves the singular value decomposition (SVD) of the Hankel matrix of measured outputs to obtain the reduced state-space model of the system. The state-transition matrix is then analysed to obtain the system modes and damping. Variants of this method are applied to power systems in Juang and Pappa (1985), Peterson (1995) and Sanchez-Gasca and Chow (1997). In Peterson (1995), the numerical characteristics of the method are improved by using the Hankel matrix and its transpose to obtain a symmetrical matrix which is then analysed by partial SVD.

D. HTLS

The Hankel Total Least Squares method begins with SVD of the Hankel matrix of outputs just as the ERA method but the rest of the method is different. In the HTLS method, the eigenvalues of the system are taken to be the same of the eigenvalues of a matrix Q obtained by the least-squares solution of Equation 27 where U_1 and U_2 are matrices formed by omitting the first and last rows respectively of the unitary matrix obtained from the SVD step (Van Huffel *et al.*, 1994). This method is applied to power systems in Sanchez-Gasca and Chow (1997).

$$U_1 Q = U_2 \quad \text{Equation 27}$$

Frequency Domain Methods: The second group of linear methods for transient analysis presented in the hierarchical tree is *frequency-domain methods*. These methods fit a linear model to data by analysing the frequency spectra of the data. There are two methods presented under this heading in

the hierarchical tree: frequency domain identification (fID) and z-transform identification (zID). fID is introduced in Poon and Lee (1990) and uses the FFT of a sliding window of data to obtain the relative amplitude of modes in the signal. This relative amplitude corresponds to the damping ratio of the mode. zID on the other hand performs the search for system poles in the z-domain using estimations obtained from the FFT of the signal. This is carried out by searching special z-plane contours for positions where the evaluated frequency spectrum from the estimations match that obtained from the measurements via conditions of magnitude maximality and phase reversal. This method is due to Corinthios (1985) and is applied to power systems in Bonou *et al.* (1992).

Non-linear Methods: The second group of transient methods in the hierarchical tree in Figure 22 comprises non-linear methods. Non-linear methods recognise that power systems are inherently non-linear to an extent and assume that the post-fault or post-disturbance response is mainly non-linear. In this case, non-linearity refers to interactions between the frequency components in the transient response. This interaction can be observed using Higher Order Spectral (HOS) analysis, for example in Messina and Vittal (2005). Therefore, non-linear methods aim to track the evolution of frequency and damping over short intervals of time. The non-linear methods that have been reviewed in the literature can be classified further into parametric and non-parametric methods. In this context, parametric methods provide specific values for the damping of modes while non-parametric methods do not.

Non-parametric methods: The methods presented under non-parametric methods in the hierarchical tree in Figure 22 are frequency domain pattern recognition (FDPR) and the Short Time Fourier Transform (STFT). The FDPR and STFT methods are based on the observation that undamped oscillations are related to excess kinetic energy in the power system which in turn can be related to the peaks in the power spectral densities (PSD) obtained from the output measurements. The peak in the PSD becomes sharper as the oscillation becomes less damped. These methods are applied to power systems in Ostojic and Heydt (1991) and Ostojic (1993) respectively. The FDPR method in Ostojic and Heydt (1991) used Artificial Neural Networks (ANNs) to track the movement of the peaks in the frequency spectra. In the STFT method in Ostojic (1993), the peaks are tracked by

measuring the rate of change of the maximum peak over time and by using a threshold to determine whether the level of damping has gone below a critical value. However, in both these methods, an exact value of damping is not obtained.

Parametric methods: The final group of methods in this part of the hierarchical tree is parametric methods. These methods determine instantaneous values of frequency and damping within the analyzed window of data. Two main types of such methods have been implemented in power systems: wavelets and Hilbert Analysis. These methods are reviewed and compared in Ruiz-Vega *et al.* (2005).

A. Wavelets

Wavelet methods decompose signals as a function of a mother wavelet which is chosen prior to application of the method, and can provide good time-frequency resolution. The mother wavelet can be described as an oscillating sinusoid that exists in a small finite time period, from which a family of self-similar wavelets with a range of durations and frequencies can be generated. This instantaneous time-localization property implies that it can be used to represent non-stationary and nonlinear signals. Wavelet analysis works by comparing a wavelet with the signal being analyzed and then defining a coefficient which is high if the wavelet looks like the signal or low otherwise. By comparing the signal with various wavelets in the family over different time intervals, the signal can be decomposed as a weighted sum of the damped wavelets over different time periods. This leads to the concept of instantaneous frequency and damping.

B. Hilbert Analysis

Hilbert Analysis or the Hilbert Huang Transform (HHT) is a two-step procedure for the evaluation of the instantaneous time-frequency characteristics of signals. In the first step, the measured signal is decomposed into intrinsic mode functions (IMFs) by a process known as empirical mode decomposition (EMD). Each IMF represents a simple oscillatory source that is both amplitude and frequency modulated. The second step involves determining the analytic form of each IMF via the Hilbert transform. The Hilbert transform describes the extracted IMFs in terms of instantaneous amplitude, frequency and phase functions (Ruiz-Vega *et al.*, 2005). There have been various improvements made on the HHT, mainly to improve the IMF extraction via EMD and applications

of these variants to power systems are described in Messina and Vittal (2006), Messina *et al.* (2006), Senroy *et al.* (2007) and Laila *et al.* (2009).

Observations and Comments: Methods for transient analysis are applied to analyse the post-fault or post-disturbance response of a system. The steps involved in the application of these methods are:

- Assumption that the post-fault or post-disturbance response represents the true system frequency and damping.
- Choice of a linear or non-linear method for analysis.
- Estimation of frequency and damping.

There is clearly a gap in this field of research in terms of *detecting* transient behaviour. Transient behaviour is easily observable by visual inspection but harder to detect automatically. The methods that have been reviewed assume that transient behaviour has already been inferred and therefore the data that is analysed represents transient behaviour of the system. There is therefore a requirement for methods that can determine the onset of transient behaviour.

2.1.4. Summary

This section has presented an in-depth review of methods for determination of power system stability available in electrical power system literature. The methods were divided into methods applicable to ambient operation and transient operation respectively. Methods for ambient operation can be methods that require probing and those that do not. Furthermore, if probing is applied, the system stability can be determined by first identifying the system model using standard system input-output relationships. In the case that probing is not applied, mode-meter or non-parametric methods can be used to assess the frequencies of the modes present in the data but they do not provide meaningful information about the damping of these modes.

Conversely, parametric methods assume a functional form of the system structure and a stochastic nature of the system excitations hence determine the system model from which the system stability is inferred. On the other hand, methods applicable to transient operation assume that the measured outputs represent the free decay response of the system and hence determine the system stability using a choice of linear or non-linear methods. For this project, mode-meter methods will therefore

be useful in determining system modes. However, in order to obtain the mode hence system stability, ring-down methods are also required.

2.2. Methods for Stability Estimation in Vibration Analysis

This section presents a review of methods used in vibration analysis and structural engineering for the purpose of determining the stability of structures. Similar to the review in the previous section, this review has been published in Thambirajah *et al.* (2010). The review groups the methods in literature in a hierarchical tree that is initially divided into stationary and non-stationary methods. The aim of this review is to establish similarities between the approaches in vibration analysis that have also been applied in power systems analysis, and also therefore identify other novel approaches in vibration analysis that have the potential for application in power systems.

2.2.1. Overview

There are many methods in structural, mechanical and aeronautical engineering which have similar approaches to those being used for power system analysis. These methods fall under a general category labelled as vibration analysis and are listed in the classification trees of Figures 23, 24 and 26 with relevant references supplied in the diagram.

The main analogies between vibration analysis and power systems analysis are:

- Vibrating structures are continuously excited by random inputs just as power networks are continuously loaded.
- The input signal cannot be measured in most cases.
- Model structures chosen for identification are similar.
- Damping information is very important in order to predict failure.

There is also a fundamental difference:

- The concept of transient operation is usually not defined because excitations to structures rarely take the form of large disturbances.

Instead, a distinction is made between stationary and non-stationary methods. Stationary methods are used to analyse stationary signals which are the outputs from a stationary process. A *stationary process* is a stochastic process whose probability density function does not vary over time and

therefore has a constant mean and variance. Figure 25 demonstrates an example of a system response under stationary and non-stationary vibration analysis. The figure shows measurements at the onset of an earthquake where the response is initially stationary but becomes non-stationary. *Stationary* methods are those that assume that the system is linear and time-invariant (stationary) whereas *non-stationary* methods are those that assume that the system is time-variant and hence whose measurements have a time-varying mean and variance. This section describes a brief selection of the methods from vibration analysis that may have potential for application in power systems analysis. This section also speculates about the problems in electrical power systems which the described methods may be able to solve and explains why they might be useful. The first of the following subsections describes the classification of stationary methods while the second describes the classification for non-stationary methods.

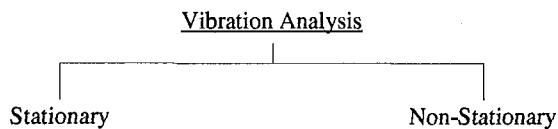


Figure 23: Hierarchical tree showing classification of methods for vibration analysis

2.2.2. Stationary methods

Stationary methods for vibration analysis can be broadly split into methods that use both excitations and responses and those that use responses only (Peeters and De Roeck, 2001).

Excitation and Response Methods: These methods are similar to the methods discussed for ambient operation of power systems that require probing. However in practice, it can be difficult to measure the excitations on the structure unless the excitation is known and quantifiable, for example tidal impact on the bases of bridges that can be measured using sensors. For such cases, standard input-output methods of system identification can be applied. These methods are available in Ljung (1987) and have previously reviewed in the review of methods for power system stability estimation as methods for system identification with known input.

Response-Only Methods: A review of response-only methods that have been applied to system identification of vibrating structures is presented in Peeters and De Roeck (2001). In Peeters and De

Roeck (2001), the initial classification of methods is between time-domain and frequency domain methods; we will however make an initial classification similar to the one presented for methods that do not require probing under ambient operations in electrical power systems. The hierarchical classification tree shown in Figure 24 is hence split into parametric and non-parametric methods.

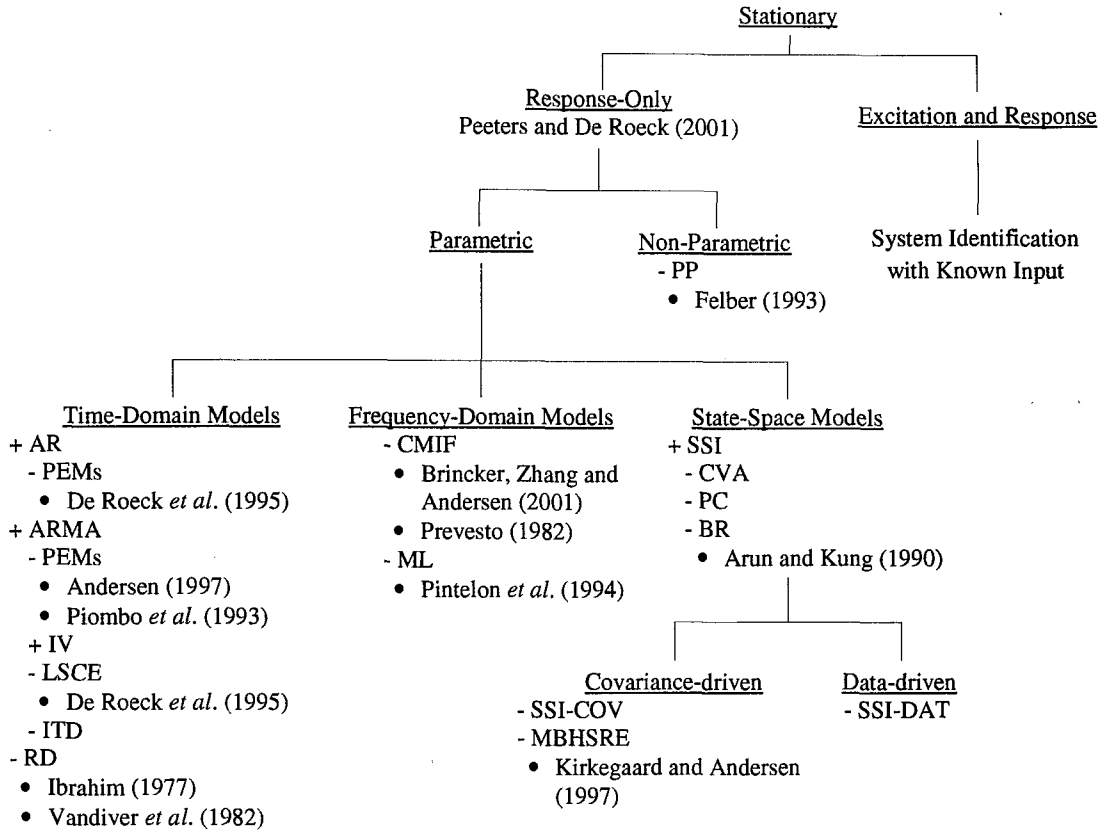


Figure 24: Hierarchical tree showing classification of stationary methods for vibration analysis

Non-parametric methods: The main non-parametric method that has been applied for mode frequency estimation is the Peak Picking (PP) method. In the PP method, the eigenfrequencies of the system are obtained by identifying the peaks in the spectra of the measured outputs (Felber, 1993). This is very similar to the Welch Periodogram method since the main algorithm is the FFT. It is reported in Peeters and De Roeck (2001) that the half-power bandwidth method is commonly used to obtain the mode damping in the PP method. However, it is recognised that this extension of the PP method into a parametric approach does not yield reliable estimates. The PP method also has limitations that the system modes should be lightly damped and well separated in the spectral plots.

Its accuracy is also diminished in the presence of noise. Variants of the PP method are also reported such as methods that use coherence functions. Such methods perform better under low signal-to-noise ratios and are similar to higher order spectral methods presented in the electrical power systems classification tree.

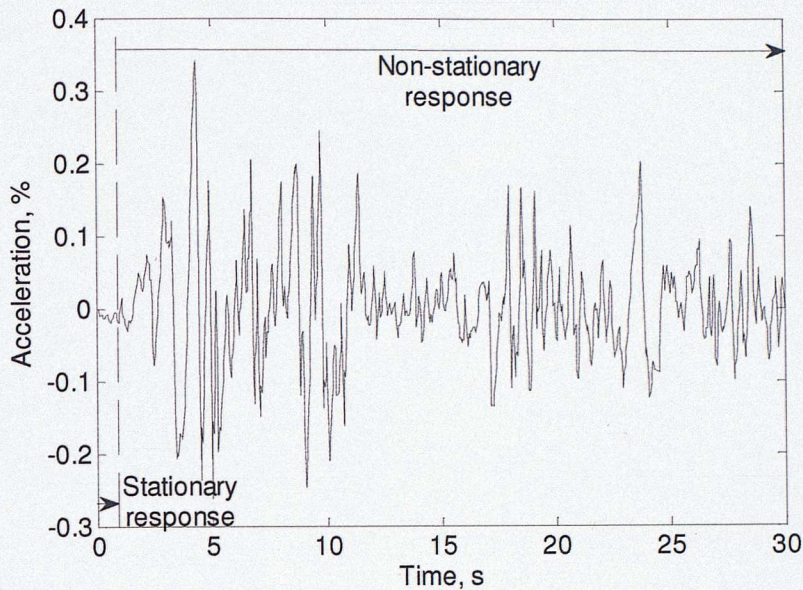


Figure 25: Stationary and non-stationary response in vibration analysis. After <http://www.owlnet.rice.edu/~elec532/PROJECTS00/earthquake/earthquakes.htm>, accessed December 2009

Parametric methods: The other branch in the hierarchical tree (Figure 24) under response-only methods contains parametric methods. Parametric methods aim to fit a model onto measurements of outputs by making assumptions about the inputs of the models. It is difficult to estimate the inputs or excitations applied to a structure and hence it is usually assumed that the excitations during normal use of a structure are random and realisations of a stochastic process. Based on this assumption, a system model can be identified. Parametric methods can be classified with reference to the type of model that is chosen to represent the system. The hierarchical tree shows that there is further branching into time-domain models, state-space models and frequency-domain models. The classification refers to the domain in which the system parameters are identified. Time-domain models represent the system as a realisation of present and past inputs, and past outputs. Frequency-domain models identify system parameters from the spectral representation of the system outputs. Finally, state-space models identify the system parameters by computing the state-space

representation of an equivalent system with the measured signals as its outputs.

A. Time-Domain Methods

Three methods are presented in the hierarchical tree in Figure 24 under time-domain models. These methods are the Autoregressive (AR), Autoregressive Moving Average (ARMA) and Random Decrement (RD) methods.

▪ AR and ARMA models

AR and ARMA models have already been described as Yule-Walker (YW) methods for time-domain non-recursive implementations of parametric methods that do not require probing in ambient analysis of electrical power systems. The AR and ARMA model parameters can similarly be estimated using Prediction Error Methods (PEMs). The AR model is easily solved using such methods and has been applied in De Roeck *et al.* (1995). However, in the case of ARMA models, this procedure leads to a non-linear optimisation problem due to the MA parameters. The method is additionally not robust when using real-life data because of the adverse effect of noise on the selection of the order of the model. Despite these drawbacks, ARMA methods using PEMs have found extensive application in civil engineering, for example in Piombo *et al.* (1993) and Andersen (1997). ARMA models have alternatively been solved for vibrating structures using a group of methods known as Instrumental Variable (IV) methods. A general explanation of IV methods was presented earlier in this chapter as a parametric correlation approach for power system stability estimation. The basic principle is that the model parameters are obtained by minimizing the correlation between past data and the errors between the model and measured outputs which follows from the hypothesis that the errors should be completely uncorrelated with past data if the model parameters perfectly describe the system. Imposing such conditions effectively reduces the ARMA model into an AR model. Examples of IV methods that have been applied to vibration analysis are the Ibrahim Time Domain (ITD) and the Least Squares Complex Exponential (LSCE) methods (De Roeck *et al.*, 1995).

▪ Random Decrement

The final method presented in this part of the hierarchical tree is the Random Decrement (RD)

method. The RD method assumes that the system input can be decomposed into a series of steps, impulses and a random component. The measured system output is therefore composed of the responses due to each of the components. By averaging the mean-centred measured outputs subject to a threshold condition, the responses due to the random and step components average to zero leaving an estimate of the impulse response (Ibrahim, 1977). One drawback of this method is that this decomposition is only strictly valid in the case of a stochastic input. However mathematical proof in Vandiver *et al.* (1982) shows that the RD can be used to estimate correlation functions when the input is not strictly stochastic. The RD method is explored in detail in Chapter 6 of the thesis.

B. Frequency-Domain Methods

The middle branch in the hierarchical classification tree in Figure 24 shows two parametric response-only frequency-domain methods. The first of these methods is the Complex Mode Identification Function (CMIF). The CMIF is a parametric extension of the non-parametric PP method. This is achieved by diagonalisation of the spectral density matrix from the PP method by SVD (Prevesto, 1982). In Peeters and De Roeck (2001), this decomposition is interpreted as separation of the system response into equivalent single-degree-of-freedom (SDOF) systems which can be analysed using modal techniques to yield the system eigenfrequencies and corresponding damping. In Brincker, Zhang and Andersen (2001), the method was reintroduced as the Frequency-Domain Decomposition (FDD) method. This FDD method has recently been applied to electrical power systems in Guoping and Venkatasubramanian (2008). The advantages and disadvantages of the method have also been discussed in the text describing the FDD approach that was applied to electrical power systems.

The second frequency-domain method in the hierarchical tree is the Maximum Likelihood (ML) method. The ML method is an optimization technique that aims to optimize the parameters of a model by minimizing the error norm between the output of the model and measurements made from the system. It is therefore a realization of a Prediction Error Method (PEM). It has been applied in structural engineering in the frequency domain in Pintelon *et al.* (1994) in order to make it applicable to the problem of output-only identification. In Pintelon *et al.* (1994), the method is used to identify the parameters of a model that is a function of the ratio between the output and unknown

input spectra. Similar to the ARMA time-domain model method, the ML method leads to a set of nonlinear equations which require an iterative solution and can hence be computationally demanding. It however has been shown to be a robust method for identification of modal parameters from large noisy data sets, unlike the ARMA model.

C. State-Space Models

The final branch of parametric methods in the hierarchical tree shows state-space models. State-space models have been introduced in the review of methods for ambient operation in electrical power systems. One technique that can be used to obtain state-space models is Subspace Identification (SSI). Publications in vibration analysis have used singular value decomposition (SVD) of Hankel or Toeplitz matrices of outputs followed by truncation to a defined number of modes. Using the SVD representation, the parameters of the state-space model are estimated (Peeters and De Roeck, 2001). In vibration analysis, SSI methods can be further divided based on the nature of the approach taken to solve the parameters of the model.

The hierarchical tree in Figure 24 hence branches into covariance-driven and data-driven approaches. Data-driven approaches work directly on output data to estimate the state-space model while covariance-driven approaches first estimate the output covariances before the derivation of the state-space model. The data-driven SSI-DAT method uses the measured outputs in the matrices while the covariance-driven SSI-COV uses estimations of the output covariances in the matrices. An alternative name for SSI-COV presented in literature is the Matrix Block Hankel Stochastic Realization Algorithm (MBHSRA) (Kirkegaard and Andersen, 1997). There are also variants of the SSI-DAT and SSI-COV methods which are realized by weighting the matrices prior to SVD. Examples of such variants are Canonical Variate Analysis (CVA), Principal Components (PC) and Balanced Realization (BR) (Arun and Kung, 1990). These methods are applicable to both the data- and covariance- driven approaches and are hence placed directly under methods for state-space models in the hierarchical tree in Figure 24.

The main shortcoming of SSI methods is that it is assumed that the outputs are realizations of a stochastic process and hence if this is not truly the case, an error is introduced in the estimation of the state-space model. The methods of SSI that have been used for ambient analysis of power

systems are all data-driven, providing future opportunities for the application of some covariance-driven SSI methods.

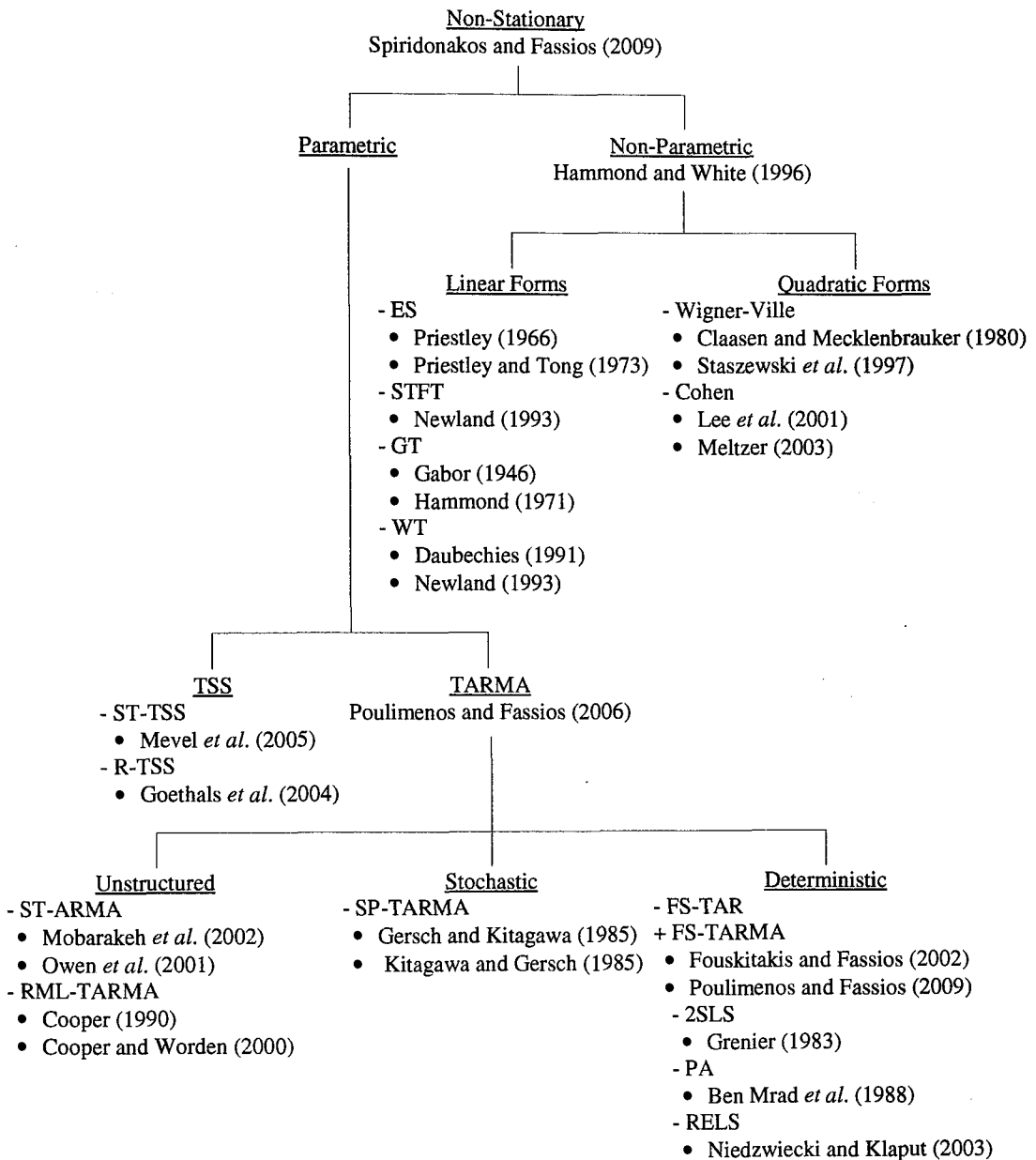


Figure 26: Hierarchical tree showing classification of non-stationary methods for vibration analysis

Observations and Comments: The key steps in applying stationary response-only methods for system identification are:

- Assumption of stochastic excitation of a linear time-invariant system.
- Choice of a suitable input-output model.

- Finding a stochastic output-only realization of model.
- Estimation of system model parameters.
- Inferring the system eigenvalues hence mode frequencies and damping.

It can be noted that the key steps taken in the application of response-only stationary methods are similar to those presented for the application of parametric methods of analysis of power systems under ambient conditions without probing. In fact, many of the methods that have been reviewed in this section have previously been reviewed. However, this review highlights some promising approaches that have not yet been applied to power systems including ARMA models solved using IV methods, the RD method and variants of the SSI method using Principal Components (PCs). They are simple and robust approaches which can be applied in real-time: ARMA models solved using IV methods lead to a linear solution compared to those solved using PEMs, the RD method is very easy to apply because it only requires the operation of averaging, and SSI based on PCs can help in screening measured signals to determine the best measurements for model identification.

2.2.3. Non-Stationary methods

Non-stationary methods are those that assume that the system is time-variant which can result from non-linearity. This can be the case in rotating machinery or during earthquake vibration analysis, as well as non-linearity due to non-stationary stochastic excitation on structures. Hence, the statistical properties of the measured signal, for example mean and variance, vary with time. Thus, these methods aim to identify time-varying parameters of models. The reason for presenting a review of non-stationary methods of vibration analysis is so as to identify methods that can be used to differentiate between ambient and transient operation in electrical power systems. Since these methods identify time-varying parameters of models, they can effectively differentiate between behaviour when deviations in measured variables are small (ambient behaviour) and behaviour when deviations are large (transient behaviour).

In literature, non-stationary methods are generally divided into parametric and non-parametric methods (Spiridonakos and Fassios, 2009), whose definitions are similar to the ones described previously in this chapter. The hierarchical tree in Figure 26 therefore branches into these two groups of methods.

Non-Parametric Methods: Non-stationary non-parametric methods decompose a measured response into a representation localized in frequency and/or time. A review of these methods is presented in great detail in Hammond and White (1996) therefore only a brief introduction is presented in this section. Following Hammond and White (1996), the branch of non-parametric methods in the hierarchical tree can be further divided into linear and quadratic forms. This classification refers to the nature of the decomposition of the signal.

Linear Forms: Linear forms decompose a signal into a series of components that can be summed to yield the original form. Examples of such methods are Evolutionary Spectra (ES) (Priestley, 1966, Priestley and Tong, 1973), the Short Time Fourier Transform (STFT) (Newland, 1993), the Gabor Transform (GT) (Gabor, 1946, Hammond, 1971) and the Wavelet Transform (WT) (Newland, 1993, Daubechies, 1991). The STFT is a time-varying periodogram obtained by sliding a window across a time record and performing a Fourier transform where the magnitude of the periodogram is plotted as a function of frequency and time. ES and the GT extend this idea to time-varying processes: ES decompose a signal as a function of time-modulated sines and cosines, while the GT decomposes a signal as a function of Gaussian pulse modulated sines and cosines (Hammond and White, 1996). However these representations do not provide good localizing properties in the time and frequency domain; this is instead provided by the WT (Daubechies, 1991). Wavelet methods have been previously described in the context of parametric non-linear methods for transient analysis of power systems.

Quadratic Forms: Quadratic forms decompose the energy function of the signal rather than the signal itself. The decomposition involves a time-dependent spectral density related to the weighted local autocorrelation function of the signal. Examples of the weighting functions are Wigner-Ville (Claasen and Mecklenbrauker, 1980, Staszewski *et al.*, 1997) and Cohen distributions (Lee *et al.*, 2001, Meltzer, 2003). The details of these methods are presented in greater detail in Hammond and White (1996).

Parametric Methods: Non-stationary non-parametric methods do not lead directly to the model parameters required for stability inference, such as system damping because they estimate the

characteristics of the measured signals which are formed by convolution of both the system inputs and the system response. Non-stationary parametric methods aim to identify the models of systems whose outputs have been measured, but unlike the stationary parametric models, the parameters of the identified model are time-varying. The methods that have therefore been applied in vibration analysis are time-varying extensions of stationary time-domain and state-space parametric models. The hierarchical tree in Figure 26 is therefore divided into Time-varying Autoregressive Moving Average (TARMA) and Time-varying State Space (TSS) models.

Time-varying Autoregressive Moving Average (TARMA) models: TARMA models generalize all time-varying time-domain models including AR, ARMA and ARMAX models. They are reviewed extensively in Poulimenos and Fassios (2006) hence only a brief summary is provided here. Following Poulimenos and Fassios (2006), they can be further divided with reference to the structure of evolution of the time-varying model parameters. The hierarchical tree in Figure 26 therefore has three further branches, as outlined in the next three sub-sub-sections.

A. Unstructured Parameter Evolution Methods

These methods do not impose a particular structure upon the evolution of the time-varying model parameters (Poulimenos and Fassios, 2006). They therefore can only track slow dynamics and have the highest complexity of the three groups of methods. Examples of these methods are the Short-Time ARMA (ST-ARMA) (Owen *et al.*, 2001, Mobarakeh *et al.*, 2002) and recursive methods such as Recursive Maximum Likelihood TARMA (RML-TARMA) (Cooper and Worden, 2000, Cooper, 1990).

B. Stochastic Parameter Evolution Methods

These methods impose a stochastic structure upon the evolution of the time-varying model parameters via stochastic smoothness constraints and are also referred to as Smoothness Priors TARMA (SP-TARMA) models (Poulimenos and Fassios, 2006). These methods have been mainly reported for the modelling of earthquake ground motions (Gersch and Kitagawa, 1985, Kitagawa and Gersch, 1985). They can track slow to medium dynamics but are similarly as complex as unstructured parameter evolution methods.

C. Deterministic Parameter Evolution Methods

This is the final group of TARMA methods; they impose a deterministic structure upon the evolution of the time-varying model parameters. Examples of these methods are Functional Series TAR (FS-TAR) and TARMA (FS-TARMA) models. These methods have been applied in various fields including modelling of bridge-like structures (Poulimenos and Fassios, 2009) and earthquake ground motions (Fouskitakis and Fassios, 2002). They can be solved via algorithms such as two-stage Least Squares (2SLS) (Grenier, 1983), Polynomial-Algebraic (PA) (Ben Mrad *et al.*, 1988) and Recursive Extended Least Squares (RELS) (Niedzwiecki and Klaput, 2003). These methods are the least complex of the TARMA models and can track slow, medium and fast dynamics of the system.

Time-varying State Space (TSS) models: The left-hand branch of non-stationary parametric methods for vibration analysis consists of time-varying State-Space models. As in the case of TARMA models, they are the counterparts of the stationary case parametric state-space models with time-varying parameters. TSS models can be further divided into the groups of methods reviewed in TARMA models; however, the research literature available for output-only methods is confined to unstructured parameter evolution methods such as Short-Time Time-varying Subspace (ST-TSS) (Mevl *et al.*, 2005) and Recursive Time-varying Subspace (R-TSS) methods (Goethals *et al.*, 2004).

Observations and Comments: Non-stationary methods for vibration analysis present a possible direction for the application to power systems. They work on the principle of estimation of time-varying parameters. The non-parametric methods decompose signals into representations localized in frequency and/or time. This approach is similar to the ones for transient operation in power systems such as the Hilbert Huang Transform (HHT) that decomposes a signal into an instantaneous amplitude and phase which can be translated into an instantaneous frequency and damping. However, non-parametric methods are only capable of providing system damping in the case when the measured output contains a transient. On the other hand, some of them can be used to identify episodes when the power system operation is not ambient because they perform differently under ambient and transient conditions. Non-stationary methods for vibration analysis may be able to fulfil this purpose because in ambient operation of a power system, the system can be assumed to be

approximately stationary. Another difference between these methods and the methods applied for ambient conditions in power systems is the assumption of linear operation in the latter group. Non-stationary methods would be more robust owing to the time-dependent parameters of models; however, care needs to be taken in ensuring that real-time identification can be achieved.

2.2.4. Summary

This section has presented the methods used for estimation of stability of structures in the fields of vibration analysis and structural engineering. The methods are broadly divided into stationary and non-stationary methods of identification where the stability is inferred as a characteristic of the identified system model. Stationary methods assume that measurements are made from a linearly time-invariant system whereas non-stationary methods assume that the system generating the measurements is time-variant. It was also identified that the key steps in applying stationary response-only methods for system identification are:

- Assumption of stochastic excitation of a linear time-invariant system.
- Choice of a suitable input-output model.
- Finding a stochastic output-only realization of model.
- Estimation of system model parameters.
- Inferring the system eigenvalues hence mode frequencies and damping.

These steps are similar to those presented for the application of parametric methods of analysis of power systems under ambient conditions without probing and therefore some of the reviewed methods can be applied to the problem of real-time stability estimation in power systems. Some examples are ARMA models solved using IV methods, the RD method and variants of the SSI method using Principal Components (PCs). Non-stationary methods on the other hand decompose signals into representations localized in frequency and/or time. This approach is also similar to the ones for transient operation in power systems and these methods are only capable of providing system damping in the case when the measured output contains a transient. However, some may be useful in identifying episodes when the power system operation is not ambient because they perform differently under ambient and transient conditions.

The methods reviewed in this section show promising prospects for application to electrical power system problems. Additionally, research in the fields of vibration analysis and structural engineering has benefitted from longer spans of research than data-based stability estimation in power systems. As a result the depth of opportunity for cross-application is great.

2.3. Methods for Process Systems Fault/Oscillation Diagnosis and Detection

This section presents a review of methods used for fault or oscillation diagnosis and detection in process systems engineering. A review of the types of methods available is first discussed, followed by a list of specifications for an optimum tool of diagnosis and detection. Following this, data-driven methods for oscillation diagnosis and detection are reviewed. The reason for reviewing these methods is that they are the ones applicable to this research project. The use of data for fault diagnosis has been established in the field of process systems engineering for a longer period than power systems engineering, and as a result methods for detection of oscillations are more widely researched in the former field. Some of these methods have the potential for application in power systems engineering, and hence the aim of this review is to identify such methods and consequently develop them to address the research problem.

2.3.1. Process Systems - Overview

Chemical plants consist of numerous connections between process flow components through which chemical reactants flow and control components that monitor the flow of these reactants such as flow, pressure and temperature indicators and controllers. When a fault or disturbance occurs in such a plant, it manifests as a deviation in the flow, pressure or temperature measured by indicators in the plant. Such a fault may be due to failure of a component in the process, such as a condenser, or even the failure of a component in the control loop, such as a valve. However, due to the complex connectivity of pipes within most plants, this/these fault/s can propagate along the direction of flow of the reactants and may be measured at various other points within the plant. Thus, a deviation at one point in the system is hard to analyze due to the fact that it might have occurred due to a fault in some other element before it (upstream).

In such a case, the use of human labour to pin-point the source of such a fault which could have many origins becomes time-consuming, difficult and expensive. Venkatasubramanian *et al.* (2003a) pointed out that statistics in 1999 estimated that the petrochemical industry in the US alone loses an average of 20 billion US dollars (Nimmo, 1995), and the British economy up to 27 billion dollars (Laser, 2000), every year due to abnormal events. Abnormal Event Management refers to the process of timely detection and deduction of the root cause of an abnormal event or failure in a plant when it occurs, and the consequent fixing or repairing process to bring the plant process(es) back to its (their) original state (Nimmo, 1995).

There has therefore been a great deal of research in the field of process systems engineering geared towards the detection of faults in chemical process plants. Venkatasubramanian *et al.* (2003a, b and c) carried out a comprehensive review of methods of fault diagnosis and detection in a three-part publication. In these papers, the methods are classified in hierarchical trees with attention being given to both methods that use models and those that use data.

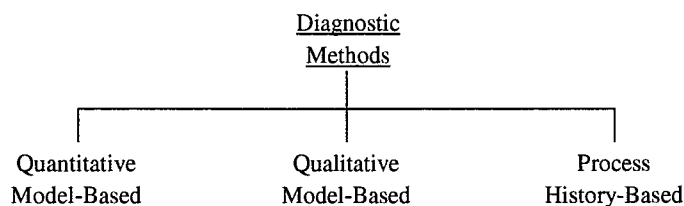


Figure 27: Classification of diagnostic algorithms. After Venkatasubramanian *et al.* (2003a)

Venkatasubramanian *et al.* (2003a) describes a fault as a “process abnormality or symptom”, while the underlying cause of the fault as the “basic event, root cause, malfunction or failure”. The concept of fault diagnosis is described as detecting and correcting failures that may cause plant variables to deviate from acceptable limits and therefore cause malfunctioning of the system. Thus, a series of methods can be developed to detect and correct such faults. This piece of literature goes on to classify these methods of fault diagnosis as quantitative model based, qualitative model based and process history based approaches. All the classes are based on some kind of understanding of the physics of the process. Quantitative based approaches are methods that express this knowledge as mathematical functions or relationships. Qualitative based approaches, on the other hand, represent

this knowledge in terms of “qualitative functions centred on different units in a process”. This requires some kind of understanding of the underlying chemical process as well (Venkatasubramanian *et al.*, 2003b). Both these methods are known as model-based approaches and are based on first-principle knowledge of the system. History-based approaches, in contrast, assume the availability of a large amount of historical process data and there are so many ways in which to extract (transfer and present) the a priori knowledge to a diagnostic system. Figure 27 shows the classification of diagnostic methods according to this piece of literature.

Whatever the method adapted for fault diagnosis, a couple of factors need to be considered when designing the system. These parameters determine the reliability of the system. A good diagnostic system should among others be:

- Capable of quickly detecting and diagnosing faults,
- Capable of differentiating between different failures,
- Robust to various uncertainties,
- Able to decide whether a process is functioning normally or not and deduce whether the reason for failure is known or not.
- Able to provide an explanation of the fault diagnosis to the user.

This represents the perfect diagnostic system but realistically, a number of trade-offs arise, for example, a robust system may not perform very well because of being too insensitive, or a system with a quick response will be prone to high frequency influences. Of the classified methods that have been described, only process history-based methods are reviewed in this section because the aim of the review is to identify data-driven methods that may be applicable to power systems analysis.

2.3.2. Process History-Based Methods

Process history-based methods require the availability of a large amount of historical data; they however do not require the need of a priori knowledge of the process. The processing of the data requires the extraction of features from the data. Venkatasubramanian *et al.* (2003c) classify the methods of data extraction broadly into two groups – qualitative and quantitative methods. *Qualitative methods* are generally expert systems (which use rule-based logic for the purpose) and

trend modelling/analysis. *Quantitative methods* of feature extraction, on the other hand, try to reformulate the problem as a pattern recognition problem, by trying to classify the data into generally pre-determined classes. The pattern recognition problem can then be solved using statistical methods such as Principal Component Analysis (PCA) or non-statistical methods such as neural networks.

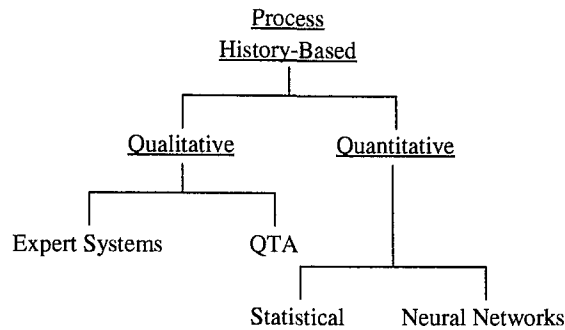


Figure 28: Classification of process history based methods. After Venkatasubramanian *et al.*

(2003c)

Figure 28 shows the classification that was proposed in Venkatasubramanian *et al.* (2003c). Venkatasubramanian *et al.* (2003c) goes on to point out the strategies involved in feature extraction using a statistical approach. Real process data measurements can be thought of as part of a statistical time series describing the underlying stochastic process. When the process is under regulatory (as opposed to set point tracking) control (ambient operation), the observations can be described by some kind of probability or statistical distribution; when there is a disturbance or fault, there will be a deviation in the distribution, and accordingly, the problem of fault diagnosis is reformulated as a problem of detecting changes in the underlying measurements.

A review of available process history-based methods for plant-wide disturbance detection and diagnosis using dynamic persistent data is presented in Thornhill and Horch (2006); this subsection follows the same classification. These methods are process history-based because they use historical data collected during operation of the processes, as would be the case for data collected from power systems. The methods perform plant-wide analysis and the reasons for taking such an approach rather than a local approach such as a single-input-single-output approach on each control loop are

the rewards: being less time-consuming and the cause of a disturbance being identified the first time in most cases.

Paulonis and Cox (2003) and Qin (1998) outline the key requirements for a plant-wide analysis to be capable of detecting the presence and locations of multiple periodic and non-periodic disturbances, including the root-cause of the disturbance. Desborough and Miller (2002) also highlight other desired properties of a plant-wide analysis, for example the clustering of measurements relating to their behaviour, and an automated model-free causal analysis. Thornhill and Horch (2007) therefore differentiate between methods that are capable of detecting disturbances and methods that are capable of diagnosing the root-cause of disturbances in a plant. In this thesis, the main concern is to detect oscillations in the power system and the frequency of the oscillation, therefore only methods for detecting disturbances in process systems are reviewed hereafter. Disturbances in process systems are typically oscillations and therefore these methods are applicable to power systems analysis. However, there is also a need to determine the strength of oscillations hence special attention will be given to certain methods that can additionally fulfil this role.

Methods for Disturbance Detection: Thornhill and Horch (2007) subdivided the available methods based on the type of disturbance being detected: stationary and non-stationary disturbances. *Stationary disturbances* are those that are assumed to be constant over the time horizon of observations whereas *non-stationary disturbances* are those that are assumed to vary over the time horizon of the observations. Figure 29 shows the classification of methods according to this criterion.

Non-Stationary Disturbances: Stationary disturbances can be detected using either time domain or frequency domain methods as discussed later on. On the other hand, non-stationary disturbances are harder to detect using these methods because the amplitude and frequency of oscillations tend to be dynamic with time. They are hence detected using methods which provided temporal localisation in frequency and time. There is not a great deal of research into non-stationary disturbance diagnosis in chemical processes because most disturbances tend to be observed over large time horizons. However non-stationary methods are best suited to detection of oscillations due to limit cycles,

which are non-linear. Two such methods are available in literature: wavelet analysis and Empirical Mode Decomposition (EMD).

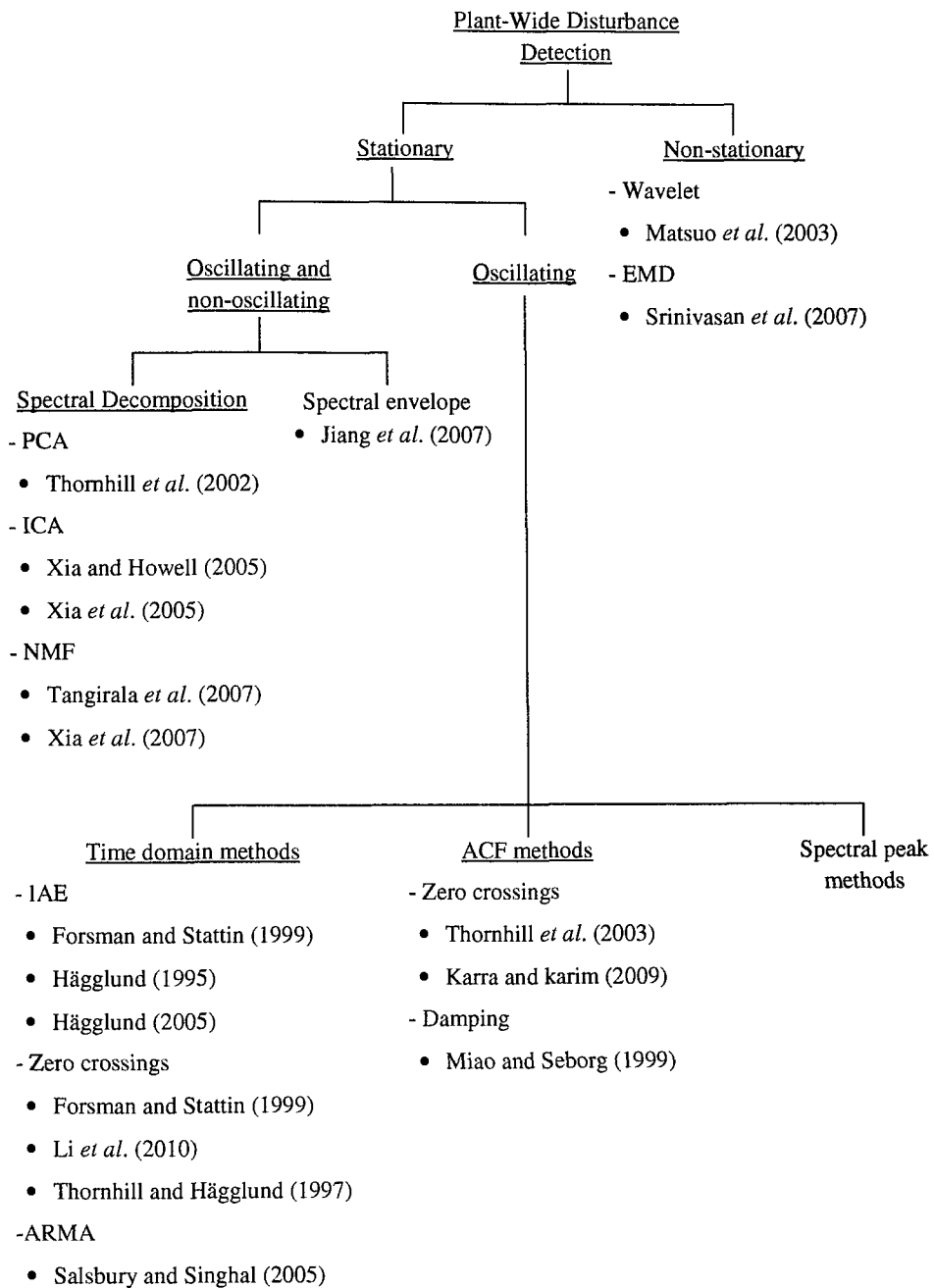


Figure 29: Data-driven methods of fault detection. After Thornhill and Horch (2007), with additions of recent work

Matsuo *et al.* (2003) demonstrated the use of wavelets to diagnose the frequency of persistent oscillations by determining the time-evolution of frequencies in the collected plant-wide measurements. Srinivasan (2005) remarked that the success of this method depends on a large

number of factors including the choice of mother wavelet, the scaling filter and the level considered for analysis. As a result it is hard to automate wavelet analysis so that it is robust in determining oscillations present in thousands of control loops that are typical in industry. Srinivasan *et al.* (2007) therefore proposed a modified EMD approach (after Huang *et al.*, 1998) for application to process data where there is a non-constant mean (non-stationary data). The first step of the algorithm is to determine and remove the non-constant mean from the measurements, after which the different frequency components in it are separated via a procedure called sifting (modified from sifting presented in Huang *et al.*, 1998) such that the original signal can be obtained by summing these components. These components are termed the Intrinsic Mode Functions (IMFs) and a cumulative sum is calculated over the time horizon of analysis for each IMF. The extrema of these cumulative sums are the zero-crossing points of the original IMFs, and these values are used to diagnose the presence of oscillations. Similar methods, for example in Turunen *et al.* (2010) and Laila *et al.* (2009), have already found application in the field of electrical power systems.

Stationary Disturbances: Relative to non-stationary disturbances, much more research has been carried out in the area of disturbance detection concerning stationary disturbances in process systems. The hierarchical tree in Figure 29 shows that Thornhill and Horch (2006) further divided the stationary methods into methods suitable for detecting oscillating disturbances only and those suitable for detecting both oscillating and non-oscillating disturbances. Oscillatory disturbances can be easily identified in the time domain and show up as a peak in the frequency domain (spectra) whereas non-oscillating disturbances may create similar looking time trends in the time domain but since they contain many frequencies, it is best to use the frequency domain to identify any characteristics (Thornhill and Horch, 2006).

A. Oscillating Disturbances

As shown in the hierarchical tree in Figure 29, methods of detecting oscillating disturbances fall within three major categories: time-domain, autocorrelation function (ACF) and spectral peak methods. As the name suggest, time-domain methods are those that work on trends in the time domain while ACF methods find relationships between future and past measurements of data and spectral peak methods work on signals in the frequency domain. The latter are standard textbook

methods whereby oscillations in the time domain appear as sharp peaks in the frequency domain. The methods available in literature fall in either of the other two categories.

- Time-Domain Methods

Examples of time-domain methods are shown in the hierarchical tree. These methods are methods based on Intergrated Absolute Error (IAE) deviations, methods based on zero-crossings and Autoregressive Moving Average (ARMA) models.

Methods based on IAE deviations aim to detect oscillations by looking at the error associated with a controller of a process. Hägglund (1995) introduced this method and applied it in an on-line implementation. In Hägglund (1995, 2005), the integral of the absolute deviations of the controller error is found and the value at each instant is compared to a threshold limit obtained by assuming a maximum level of oscillation allowed in the loop. In the case that an oscillation stronger than the maximum allowed level is encountered, the calculated IAE exceeds the previously defined IAE threshold level hence indicating the presence of a sustained oscillation. Thornhill and Hägglund (1997) extended the method to offline analysis and defined an index to reflect the regularity of the zero-crossings of the identified oscillation.

A more recent method by Li *et al.* (2010) uses the Discrete Cosine Transform (DCT) to decompose signals into real components, each of which can then be used to check for the presence of oscillations using the zero-crossings as defined in Forsman and Stattin (1999). The merit of this method is the decomposition into discrete cosines which are real and therefore physically more meaningful signals (compared to spectral methods which decompose signals into real and imaginary parts). However this method, just as the others described so far, is a single time-series approach and therefore is less efficient when applied to plants with hundreds or even thousands of measurement points.

The final method in this category available in literature is the method in Salsbury and Singhal (2005) who used autocorrelation lags to construct an ARMA model of the process. The zeros of the Moving Average (MA) part of the model are the system poles and therefore these are used to determine the detected oscillations and their respective stability.

- ACF Methods

The second group of methods for detecting oscillating disturbances are ACF methods. The advantage of ACF methods is that the ACF of an oscillatory signal is oscillatory itself and additionally, the impact of noise is reduced since the ACF of white noise, which is usually present in process systems data, appears only at zero lag, leaving a clean signal for analysis at other lags. The ACF is the inverse Fourier transform of the two-sided power spectrum (which is in turn the square of the FFT of the original signal).

Thornhill *et al.* (2003) use the zero-crossings of the ACFs of data to determine the presence of an oscillation and the regularity of the oscillation detected. Miao and Seborg (1999) on the other hand use the determined ACF functions to determine the decay ratio of an oscillation via an oscillation index computed using a ratio of the perpendicular distance of the first minima from the first two peaks to the perpendicular distance of the first maxima from the first two troughs of the ACF function. This index is used to determine whether a loop is excessively oscillatory or not. Karra and Karim (2009) combined these two methods in an algorithm called the Oscillation Detection and Characterisation (ODC) algorithm where the power spectral densities (PSDs) of measurements are used to determine the frequencies present in the data after which both the previously described methods are used to characterise the oscillation. However, as noted in Tangirala *et al.* (2007), in the presence of coloured noise (i.e. a disturbance that is not wholly random), the ACF is affected at lags other than the zero lag hence making the zero crossings less-regular.

B. Oscillating and Non-Oscillating Disturbances

The second group of stationary methods for detection of disturbances are methods that can be used to detect both oscillating and non-oscillating disturbances. The spectra of such disturbances usually have broadband features due to the presence of multiple oscillations. These methods are therefore spectral methods and the hierarchical tree in Figure 29 categorises them further as methods that use spectral decomposition and methods that use spectral envelopes.

- Spectral Decomposition Methods

Spectral decomposition methods are those that try to break down a set of spectra (of measurements from different locations) into a set of common basis functions whereby each measured spectra can be reproduced as a linear sum of the basis functions using a combination of weights. The difference between the methods lies in the method of decomposition and hence the basis functions obtained. Principal Component Analysis (PCA) decomposes spectral data into a set of orthonormal basis functions (Thornhill *et al.*, 2002). However, these basis functions (principal components – PCs) are not unique in the frequency spectrum and therefore not physically meaningful. The derived PCs can however be used to determine similarity between measurements through clustering, for example in Thornhill and Melbø (2006). Independent Component Analysis (ICA) on the other hand aims to obtain basis functions that are statistically independent (Xia and Howell, 2005). These basis functions (independent components – ICs) are therefore narrowband spectra and are hence more physically meaningful than PCs. However, they are not sign constrained in the frequency spectrum and are therefore a bit ambiguous in frequency bands other than those holding the narrowband peaks of the ICs. The last of these methods is Non-negative Matrix Factorisation (NMF) whose basis functions are a set of functions that are constrained by sign (Tangirala *et al.*, 2007). The basis functions are therefore physically meaningful because they can only take positive values and hence can be directly related to the original spectra that were decomposed.

In all these methods, the determined basis functions can be used to reconstruct the original spectra. This is done using a matrix containing how much of each basis function is in each measured spectrum. This mixing matrix can be normalised to identify the spectra that has most of a certain basis function and also the most dominant oscillation in the data (Xia *et al.*, 2005, Xia *et al.*, 2007). However, the NMF basis vectors can contain more than one peak in each basis function making this relationship ambiguous especially in relation to application to power systems. The reason for this is that the entries in the mixing matrix indicate the relative strengths of oscillations in each of the measurements. In the case that the basis functions contain unique spectral peaks in the frequency domain (represent only one oscillation in the time domain), the mixing matrix indicates the strength of that oscillation in each measured signal but in the case that the basis function contains more than one peak, the strengths represented by the entries in the mixing matrix relate to all the peaks in the

basis function. These methods, especially ICA, can be applied to power systems analysis because the aim is to find inter-area oscillations, which are usually common in many measurements from different locations. Additionally in ICA, the mixing matrix can be used to determine the strength of the oscillation at different points and hence identify areas taking part in an oscillation.

- Spectral Envelope Methods

Spectral envelope methods categorise the measured spectra into groups to which numerical values are assigned and a spectral analysis of these values carried out. The resulting spectral envelope is capable of identifying the frequencies in the signals. In Jiang *et al.* (2007), a statistical hypothesis test is carried out to identify measurements that have oscillations at the oscillatory frequencies identified by the spectral envelope. The hypothesis test is used to formulate an oscillation contribution index (OCI) for each measurement. The OCI indicates the contribution of the measurement to the oscillation and hence can be used to identify the source of an oscillation. This method outperforms ACF methods used to identify oscillating disturbances but Teck *et al.* (2007) compared it to ICA and concluded that ICA is more capable of resolving closely spaced frequencies than the spectral envelope method.

2.3.3. Summary

This section has presented a review of methods of oscillation or disturbance detection and diagnosis in process systems. Venkatasubramanian *et al.* (2003a) started with a classification of diagnostic methods in process system and divided methods into qualitative model based, quantitative model based and process-history based methods. Process-history based methods are those that require historical data from the process for diagnosis. Since this research concerns the use of measured data, only process-history based methods were considered in this review. Venkatasubramanian *et al.* (2003c) divided these methods further into qualitative and quantitative methods, and the latter was further divided into statistical approaches and neural networks. Statistical approaches are the methods applicable to this research.

Thornhill and Horch (2006) performed a review of process history based methods and classified them as methods for oscillation detection and methods for root-cause diagnosis. The latter group of

methods look at propagation of faults in process systems and since this is beyond the scope of this thesis, only methods for oscillation detection were reviewed. These methods can be either non-stationary or stationary with the latter being further subdivided into methods that can only detect oscillating disturbances and those that are capable of detecting both oscillating and non-oscillating disturbances. The methods that can detect only oscillating disturbances are further subdivided into time-domain methods, ACF methods and standard textbook methods. However due to the non-linear nature of some measurements from power systems, methods that are capable of detecting both oscillating and non-oscillating disturbances are more applicable.

Methods that can detect both oscillating and non-oscillating disturbances can be further divided into spectral envelope and spectral decomposition methods. Spectral decomposition methods use multivariate data and aim to decompose the spectra of measured signals into a set of basis functions that can be added in certain weights to recompose the original signals. The novelty of these methods is that they can relate the basis functions to oscillations in the data and also backwards to identify the strengths of the oscillations in the different sets of measured data. This would be especially useful in electrical power system analysis to enable detection of inter-area modes and to identify areas participating in the mode activity. Additionally, the methods could find application in identifying the sources of measured oscillations that are not inter-area modes.

2.4. Summary

This chapter has presented a review of methods available in literature of three different fields of engineering. The first section reviewed methods for power system stability estimation in both ambient and transient operation. The review identified the need for methods that can automate the selection of the best signals for estimation of frequencies and damping of modes during ambient operation, as well as the need for methods for automated detection of transient behaviour.

The second section reviewed methods for determination of stability of vibrating structures in structural engineering. The review showed that the problem definition is the same as power systems and the two fields of research are analogous. The review further highlighted some methods that have the potential for development towards determination of damping of modes during ambient operation

of power systems. The review also identified various methods that determine time-varying parameters of model (non-stationary methods). These methods are applicable to the problem of detection of transient behaviour in power systems because the time varying parameters are expected to differ greatly in transient operation compared to ambient operation.

The final section reviewed methods for the detection of faults/oscillations in process systems. This field has benefitted from a great deal of research, and potential methods for determination of frequencies of modes and the relative strength of modes in different measurements were identified. Such methods can fill in the gap in power systems stability estimation for methods that automate the selection of the best signals for estimation of frequencies and damping of modes, as was identified in a previous section.

The following chapter presents the methodology that was developed which incorporates expertise from all the reviewed fields of engineering to develop a solution to the research problem addressed in this thesis.

3. Overview of Proposed Solution and Case Study

This chapter presents an overview of the proposed solution to the problem of estimation of the frequency and damping of inter-area modes in electrical power transmission systems, and introduces the case study scenarios that are used to verify the suitability of the developed methods in subsequent chapters. It begins by taking into consideration all the requirements that were outlined in Chapter 1 and the methods that are applicable towards fulfilling these requirements that were reviewed in Chapter 2. The selection of methods is presented and justified, and the chapter also gives an account of how the methods were adapted and developed for use in electrical power transmission systems. A methodology for the solution is presented thereafter. This chapter concludes by presenting the case study system on which the developed methods were tested and the scenarios that were selected to demonstrate the suitability of the developed methods.

3.1. Outline of Requirements and Selected Methods

In Chapter 1, a detailed breakdown of the objectives of the research was provided. The objectives were to:

- Differentiate between ambient and transient operation.
- Detect the existence of inter-area oscillations during ambient operation using data measurements.
- Determine the frequency of the oscillations.
- Detect the areas participating in the oscillations.
- Estimate the damping factors of the oscillations.
- Alert operators to changes in damping.

Detailed reviews of methods from the fields of process systems engineering and structural and vibration engineering were presented in Chapter 2. It was identified that some of the methods that have already been applied to these fields could potentially be developed and adapted to address the objectives in this research. This section discusses these methods, identifies the methods that were ultimately applied to the research problem and the reasons why they were chosen.

3.1.1. Ambient and Transient Operation

Section 2.2 of the literature review chapter presented methods for vibration analysis. Non-stationary methods for vibration analysis are capable of identifying transient behaviour because they perform differently under ambient and transient conditions. Energy operators were identified as possible algorithms for detection of transient operation because transient events involve a high exchange of energy and this exchange is reflected in the measured signals. An example in particular of such a method is the Teager operator. It is preferred over other methods because it consists of two simple operations: multiplication and subtraction. Additionally, the energy at an instant is calculated using only three measured values hence the method is computationally inexpensive as well as rapid. The latter characteristic serves the purpose of transient detection well because transient events in power systems occur over short periods of time in most cases and therefore need to be detected almost instantaneously.

A potential drawback of the method is the false detection of transient operation for example due to a measurement error which will affect the calculated energy change; an algorithm is therefore required to ensure that the method is robust to false detections. The work on this algorithm was done mainly by the post-doctoral researcher on the project, Dr. Emilio Barocio, through discussions with the rest of the people involved in the project. The method is presented in this thesis because it is the first step of the overall approach and forms an integral part of the tool for damping estimation during ambient operation. The method of Barocio demonstrated the use of Teager operator, but did not give a clean decision of transient operation because of the nature of the scheme for detection of transients which was based on a threshold that is at times not exceeded during transient operation. Further development carried out towards this thesis has reduced the problem of spurious detections by integrating the output of the TO and estimating the rate of change of the integral over short periods of time; the rate of change is significantly different for ambient and transient operation.

3.1.2. Detection of Modes and Sources (Modal Observability)

As discussed in section 2.3 of the literature review chapter, methods for oscillation detection that are capable of determining the most probable source or the location at which an oscillation is strongest, have great potential for application to power systems engineering. The main group of methods that

was identified to fulfil this purpose is the group of methods consisting spectral decomposition techniques.

These methods are applied to the spectra of measurements and they decompose the spectra into a set of basis functions that can be used to reconstruct the original spectra. Examples of these methods that were reviewed are Principal Component Analysis (PCA), Independent Component Analysis (ICA) and Non-negative Matrix Factorisation (NMF). ICA was identified as the best method to fulfil the purpose of oscillation detection in power systems because the basis functions contain unique spectral peaks in the frequency domain and hence each basis function represents only one oscillation in the time domain. Additionally, the mixing matrix which contains information regarding how much of each basis function is present in each measured spectrum therefore indicates the strength of each unique oscillation at each measurement location. The results of the decomposition are hence physically meaningful. In the context of power systems, this can be used to determine the locations or areas participating in a particular inter-area mode (modal observability) and signals measured in those areas can be used to get the best estimate of the damping of the mode.

The main drawback with ICA is that its performance degrades with decreasing Signal-to-Noise Ratio (SNR). In ambient operation of electrical power systems, SNRs are typically low. The method has therefore been adapted and developed by adding some pre-processing steps to the data to effectively increase the SNR at the desired frequency. This ensures that the frequencies of oscillations and their relative strengths are diagnosed correctly.

3.1.3. Damping Estimation

Section 2.2 of the literature review chapter presented methods for stability estimation in structural engineering and vibration analysis. It was observed that the key steps taken in the application of response-only stationary methods in vibration analysis are similar to those taken for the application of parametric methods of analysis of power systems under ambient conditions without probing. Furthermore, many of the reviewed methods had already found application in power systems analysis. The chapter therefore highlighted some promising approaches that have not yet been applied to power systems including ARMA models solved using IV methods, the RD method and variants of the SSI method using Principal Components (PCs).

The RD method has been identified to be the most suitable approach for this research because it is very easy to apply since it only requires the operations of addition and averaging. It however is univariate and requires a signal in which the mode in question is readily observable. It has been adapted and developed by combining it with ICA in order to automate the selection of the best signals for analysis and has accordingly been extended to a multivariate implementation that can use measurements of more than one quantity from more than one location to determine a weighted system-wide estimate for the damping of an inter-area mode.

3.1.4. Alerting System Operators

Information about the frequencies and damping ratios of detected inter-area modes then need to be passed on to system operators. This needs to be done via a graphical display. Chapter 7 discusses the requirements of such a display; it should hide the complexities of the developed algorithms and provide simple information to the system operators in the form of metrics that can be tracked over time. Moore (2006) presented an industrial perspective on the importance of visualisation techniques in a control centre, a view that was reinforced during technical discussions with operators at the National Grid UK Electricity National Control Centre. They both called for decision support tools that give clear indications of the state of the system in a transmission grid control room such as traffic lights or analogue metres. These requirements were taken into consideration in developing the graphical display for alerting operators in this thesis.

3.2. Structure of Solution

Selection of methods to fulfil each of the objectives leads into a structural approach for applying the methods to data measured from power systems in order to determine the stability of the system. In this context, structural refers to the sequence of application of the methods. The steps involved in this structural approach can be summarised as below:

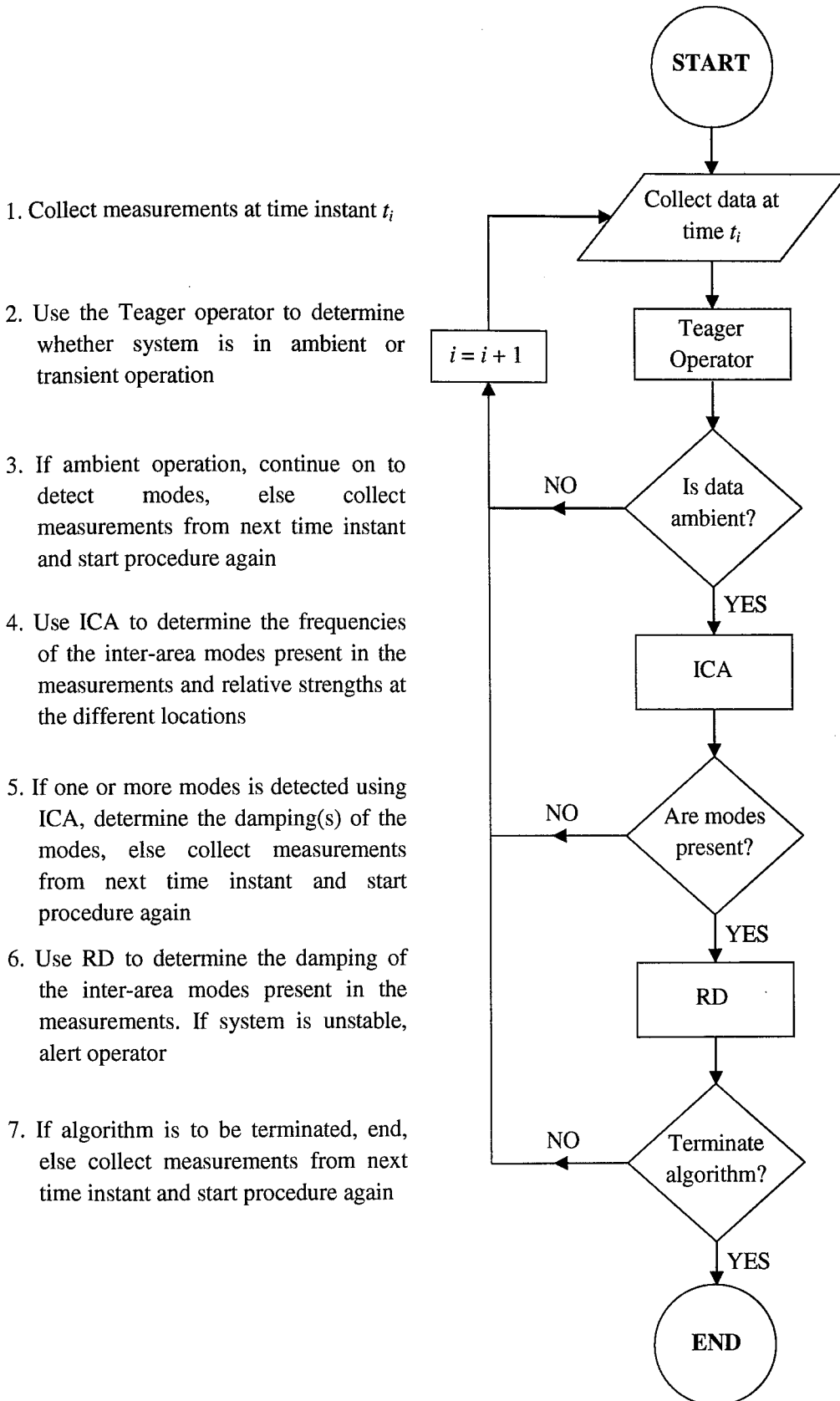


Figure 30: Structural methodology for determining power system stability

- Since this research is concerned with ambient operation, the first step involves determining whether the system is under ambient or transient operation. This can be done using the Teager operator.
- Having established that the system is under ambient operation, the data can be processed in order to detect any inter-area modes present in it. This is done using Independent Component Analysis.
- If there are inter-area modes present in the data, the frequencies of these modes can be obtained and the strengths at the various locations where measurements were made.
- The data is finally analysed by the random decrement method to identify the damping ratios of the detected inter-area modes.

Figure 30 presents a flowchart that summarises the structural methodology discussed in this section. Various data processing steps are required in between application of these methods, and these steps are discussed under the respective chapters describing these methods in detail.

3.3. Case Study System – The Nordic Power System

This section describes case studies from the Nordic Power System which is used to illustrate the ideas in subsequent chapters. The methods were similarly applied to measurements from the English transmission network; however, due to data protection agreements, the results from the studies are not presented in this thesis. The Nordic system has previously been introduced in Chapter 1. As previously described, the prominent mode in the Finnish part of the system, where data used in this project has been measured, is a 0.3 Hz inter-area oscillation between generators in Southern Sweden and Norway and those in Southern Finland. In order to demonstrate the effectiveness of the chosen methods that are presented in subsequent sections, two scenarios have been chosen so that the methods can be tested against standardised scenarios. The first scenario uses data that was measured from the actual system while the second scenario was simulated using a full Nordic system model in collaboration with Jukka Turunen at the Aalto University School of Science and Technology.

3.3.1. Scenario Matching

In order to standardise results, the conditions of the simulated scenario were chosen to match a measured scenario. This was done by selecting the real-life measured ambient scenario first, and then using the average power transferred across the Sweden-Finland boundary over the time duration of measurement to determine the steady-state power transfer condition for the simulation.

The full-system model was then manipulated by altering the loads and generation at either side of the boundary to ensure that the power transferred across the Sweden-Finland boundary matched the real-life steady-state power transfer condition. In order to simulate ambient operation whereby the loads on the system are assumed to vary randomly, the loads on either end of the power transfer boundary were varied by $\pm 1\%$ of their nominal value at randomly chosen locations and this was done for the entire duration of the simulation (20 minutes). The data produced by the simulation hence consisted of random variations about the determined steady-state power transfer condition.

The reason for using both measured and simulated data is to ensure that the results from both cases are similar. Given that the expected result for the simulated case is known, the methods can be checked to ensure that they perform the analysis correctly in the simulated scenario, and to determine how different the results from the actual system are, if at all, from the simulated system model.

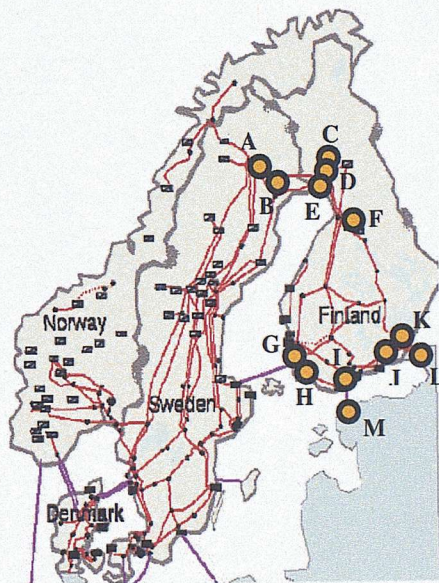


Figure 31: Map of the Nordic power system showing locations of points where measurements were made in the measured and simulated scenarios.

3.3.2. Measured Scenario

Data was measured during ambient operation (with some power fluctuations) of the Finnish system for a period of four hours on 05th November 2008, between 0300 hrs and 0700 hrs. This data was provided by Fingrid Oyj, the Finnish transmission system operator, and has been kindly approved for use in this thesis.

The data was measured at or between seven primary locations in Finland. These locations are Petäjäsoski, Keminmaa and Sallee in North-West Finland towards the border with Sweden, Olkiluoto and Rauma in South-West Finland near the HVDC interconnection with Southern Sweden, and Kymi and Yliskälä in South-East Finland. The approximate locations of these places are indicated as C, D, E, G, H, J and K on the map in Figure 31. The quantities that were measured are current flows, active power flows, voltage angle differences and the frequency derivations. From the active power flow measurements made at the locations in Northern Finland, the average power transfer to Sweden was deduced to be approximately 1050 MW (export).

3.3.3. Simulated Scenario

A non-linear simulation of the Nordic system, the procedure of which was discussed previously, was carried out by researchers at the Aalto University School of Science and Technology (J. Turunen, personal communication).

Simulated data was collected at or between the following stations: Letsi and Svartbyn in Sweden, Petäjäsoski, Keminmaa, Sallee, Pikkarala, Olkiluoto, Rauma, Espoo, Kymi and Yliskälä in Finland, Vyborg in Russia, and Harku in Estonia. These locations are marked by A, B, C, D, E, F, G, H, I, J, K, L and M respectively in the map in Figure 31. The simulation was carried out such that the steady-state power export from Finland in the simulation matched as closely as possible the average power export of 1050 MW across the Finland-Sweden boundary (D-B and C-A) from the measured scenario. The loads in Southern Sweden and Southern Finland were then varied as described previously to get ambient driven data around this operating point. Noise was additionally added to the data to simulate real-life scenarios where the SNR is typically low. The following simulated outputs were sampled from the model at 10 Hz:

- machine speed deviations.

- machine rotor angles.
- bus voltages (magnitude and phase).
- bus frequency deviations.

Using linear analysis of the simulation model, the critical inter-area mode is known to be 0.3 Hz with a small-signal damping ratio of 7 %. In subsequent chapters, the implemented algorithms are tested to check whether they can provide the same conclusion. In this way, the developed methods can be checked to see if they can be applied to power system data.

3.4. Summary

This chapter has presented the methods chosen for the research solution, the objectives each method addressed, the reasons why they were chosen, potential drawbacks in this specific application that need to be addressed and a structure for implementation of the methods.

The Teager energy operator (from the field of vibration analysis) was chosen to determine whether data measured from the power system represents ambient or transient operation. Independent Component Analysis (from the field of process systems engineering) was chosen to determine the frequencies of inter-area modes present in the ambient data and the modal observabilities of the modes at the locations of the measurements. Finally the random decrement method (from the field of structural engineering) was chosen to determine the damping of the detected inter-area modes. It was also commented that these methods need to be masked behind a graphical display that presents the results of analysis to a system operator in the form of simple metrics that can be tracked over time.

This chapter also presented the case study scenarios to which the selected methods will be applied to in subsequent chapters. The aim is to use the same data for all methods to ensure that they are tested to the same standard conditions. Both measured and simulated scenarios are used to ensure that the results from both cases are similar. Given that the expected result for the simulated case is known, the methods can be checked to ensure that they perform the analysis correctly in the simulated scenario, and to determine how different the results from the actual system are, if at all, from the simulated system model. The following chapters discuss the methods chosen in this chapter in greater detail.

4. Ambient and Transient Detection

This chapter presents the method that was selected for the purpose of determining the nature of power system operation, the Teager operator. The method is used to determine whether the power system and each of the measurements from the system represent episodes from ambient or transient operation. Barocio *et al.* (2010) discusses the Teager operator as a tool to detect transient behaviour in power systems and for characterising oscillations during transient operation. The research in this PhD thesis concerns ambient operation, and the Teager Operator is being used to distinguish between episodes of transient and ambient operation.

The chapter starts with a description of the Teager operator including some of the special features of the operator after which its use in determining the state of power systems is presented using the threshold detection method developed by Barocio *et al.* (2010). The method developed by Barocio is presented in this thesis because it is the first step of the overall approach and forms an integral part of the tool for damping estimation during ambient operation. The method of Barocio demonstrated the use of Teager operator, but did not give a clean decision of transient operation because of the nature of the scheme for detection of transients which was based on a threshold that is at times not exceeded during transient operation. Further development carried out towards this thesis to improve the decision made using the Teager operator is therefore presented in this chapter. Both algorithms are demonstrated to work using a separate case study system, introduced later in this chapter, containing both ambient and transient data. A separate case study system is used because the simulated and measured data from the Nordic case study system only contains ambient data and is therefore unsuitable for the demonstration of this method. Nevertheless, the proven method is then applied to the Nordic case study system to show that the system is in ambient operation as is required for the methods in the following chapters.

4.1. Overview

The Teager Operator or the Teager-Keiser Energy Operator (TKEO), as the non-linear operator is referred to in Barocio *et al.* (2010), was developed to track the instantaneous energy in speech

measurements (Kaiser, 1999). It takes the theory of simple harmonic motion and applies it to measurements. A simple mass-spring system can be described by Equation 28, where c_i is the displacement, \dot{c}_i the velocity, \ddot{c}_i the acceleration, b the damping coefficient, m the mass, g the spring constant and F the driving force.

$$\ddot{c}_i + \frac{b}{m}\dot{c}_i + \frac{g}{m}c_i + \frac{F}{m} = 0 \quad \text{Equation 28}$$

When the driving force is zero and taking the initial displacement to be zero, the solution to this equation describes by an exponentially decaying sinusoid which is in the form of the Equation 29, where A_i is the amplitude of the response, σ_i is the decay rate of the sinusoid, ω_i the angular frequency of the sinusoid and θ_i the phase delay. Event-induced transients in an a.c. transmission system are conventionally described by second order dynamics analogous to the expressions above as shown previously in Chapter 1.

$$c_i(t) = A_i e^{-\sigma_i t} \cos(\omega_i t + \theta_i) \quad \text{Equation 29}$$

The mass-normalised energy in the system at any instant in time can be obtained via the sum of the potential and kinetic energy, as shown in Equation 30. It can then be simplified by substitution to give Equation 31 where the RHS of the equation is known as the TKEO, $\Psi(c_i(t))$.

$$E_T(t) = \frac{1}{2} \omega_i^2 c_i^2(t) + \frac{1}{2} \dot{c}_i^2(t) \quad \text{Equation 30}$$

$$E_T(t) \approx \omega_i^2 \left(A_i e^{-\sigma_i t} \right)^2 = \dot{c}_i^2(t) - c_i(t) \ddot{c}_i(t) \quad \text{Equation 31}$$

This equation can be discretised to give the discrete TKEO, $\Psi(c_i(k))$, for a discrete temporal signal $c_i(k)$ as shown in Equation 32.

$$\Psi(c_i(k)) = c_i^2(k) - c_i(k-1)c_i(k+1) \quad \text{Equation 32}$$

The calculation of the Teager energy at an instant only requires three measurements: the measurements at the present, previous and next instants. This calculation is easily implemented in an offline analysis but is not feasible in real-time operation where the measurement at the next instant is not available. However, this can be mitigated by delaying the estimation by one sampling period which is negligible for high rate sampling periods. The estimated Teager signal is therefore shifted

one sample. The concept of using Teager operator for transient detection of wide area oscillations therefore applies Equation 32 to measurements from electrical power transmission systems.

Having calculated the energy of the signal, the next step is to determine whether the calculated energy represents ambient or transient operation. Two schemes were investigated; they are presented in section 4.4. However, since the available data from the case study system represents *ambient* operation of the Nordic System, it is not suitable for demonstration of the application of the Teager operator. An alternative is used in this chapter from the Mexican interconnected network. This case study signal is presented later in the chapter, but first the question of the best signal for analysis is addressed in the next section.

4.2. Signal Selection

Since various signals measurements are usually available from PMUs, an important consideration for any transient detection scheme is the selection of the best signal for detection. Since the Teager operator uses a measure of the energy change in the signal, the ideal signal should contain large deviations only when a transient event occurs. Line current and power, and bus voltage measurements usually contain steps when power flow conditions are changed. On the other hand, the system frequency is regulated to ensure that it does not fall below or exceed tight margins around the nominal frequency. The frequency is only disturbed by transient events in the system and is therefore suitable for transient detection. The bus frequency deviations would similarly be suitable because they are the frequency measurements shifted by the nominal system frequency.

4.3. Mexican Case Study Signal

The case study signal comes from the Mexican interconnected grid which has a nominal system frequency of 60 Hz. The measured signal (for a time duration of 20 s) is shown in Figure 32 and represents the time before, during and after a system event in which two areas of the grid that were initially unconnected were joined at about 1.27 s resulting in a transient. Due to failure of the system to stabilise, the areas were disconnected causing the system frequency to drop at about 2.44 s, after which it recovered slowly (Messina *et al.*, 2006). There are therefore five major regions of operation represented in the signal:

- Ambient operation up to 1.27 s.
- Transient operation from 1.27 s to about 1.89 s.
- A brief return to ambient operation after the first transient ring-down between 1.89 s and 2.44 s.
- A small transient at 2.44 s.
- A slow return to ambient operation thereafter.

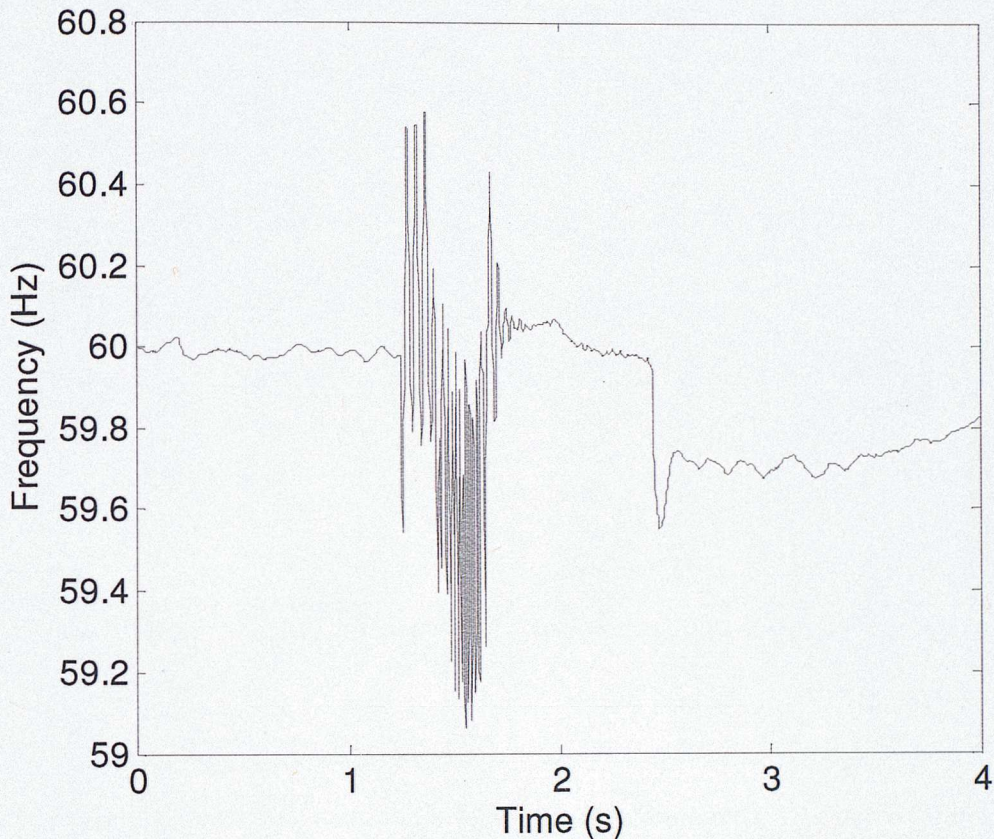


Figure 32: Case study Mexican frequency signal for the demonstration of the Teager Operator

The signal is therefore ideal for demonstration of the Teager operator for transient detection because it contains both ambient and transient regimes which can be distinguished by simple observation. The aim of the analysis in the next section is to demonstrate different schemes that can correctly identify these regimes.

4.4. Schemes for Detection of Transient Behaviour using Teager operator

This section presents the methods that were investigated for the detection of transient behaviour using the Teager operator. Two different methods were considered. The first (from Barocio *et al.*) concerns the use of a threshold detection scheme while the second, which is novel work of this thesis, uses an integrated energy measure. The methods are discussed in greater detail in the following subsections. Both methods calculate the Teager energy; however they differ in the way in which they treat the results to determine episodes of transient operation. Figure 33 shows the Teager energy signal calculated using the Teager operator for the case study signal. It can be observed that the Teager energy stays very close to zero during the expected regions of ambient operation and then becomes higher during the transient events.

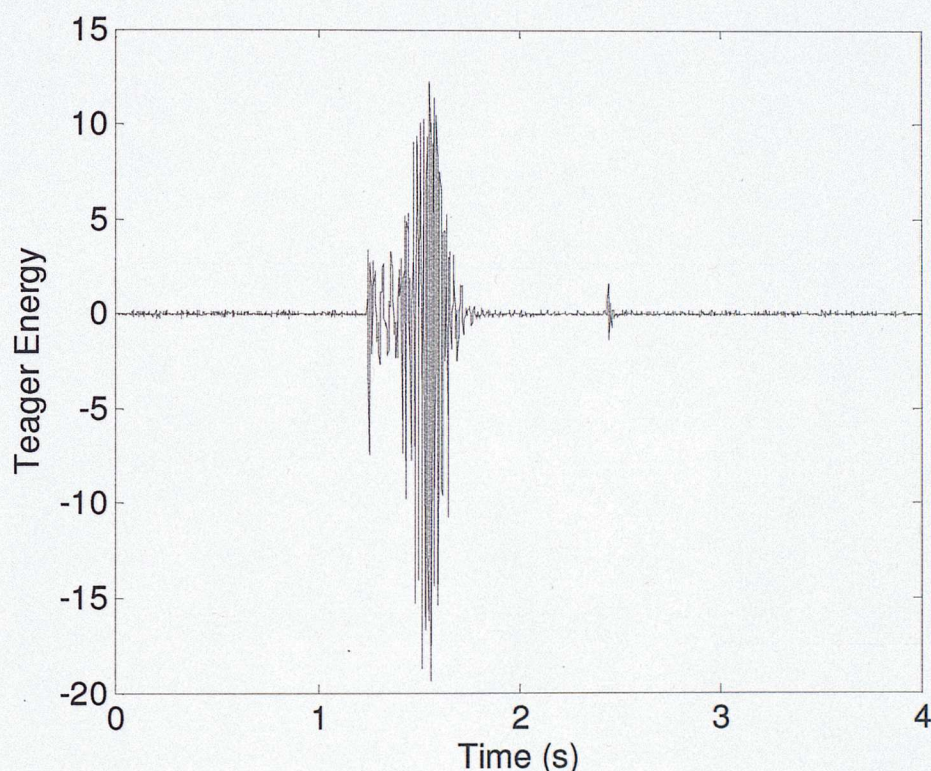


Figure 33: Teager energy signal of Mexican frequency signal calculated using the Teager Operator

4.4.1. Threshold Detection

The simplest scheme for transient detection would rely on a threshold region for the Teager energy between which the system operation can be taken to be ambient. This method is presented here after

Barocio *et al.* (2010) where the method was initially presented. If the absolute value of the estimated Teager energy is used, a single threshold can be used below which the signal or system behaviour is inferred to be ambient and above which it is taken to be transient.

This threshold is selected from historical calculations of the Teager energy whereby the maximum value of the Teager energy during ambient operation of the system is used as the optimum threshold.

This is indicated by the red dotted line in Figure 34.

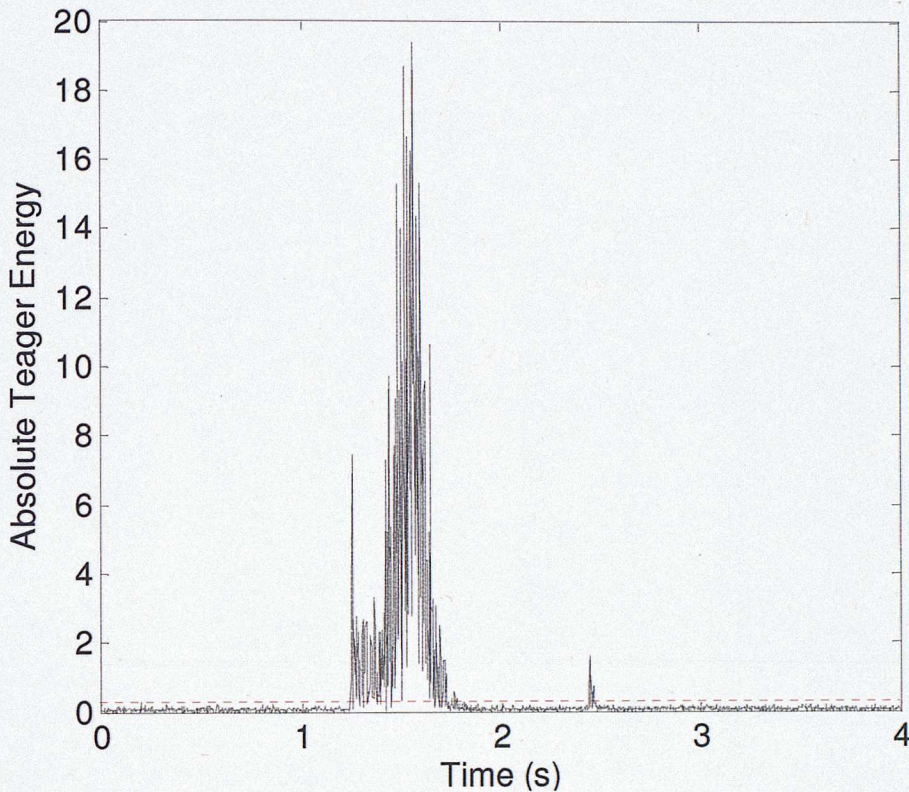


Figure 34: Absolute Teager energy signal of Mexican frequency signal

For periods of time when the Teager energy is below the red line, the system operation is ambient and for periods of time when the Teager energy is above the red line, the operation is taken to be transient. Figure 35 demonstrates the ambient and transient regions obtained using this method. The regions of ambient and transient operation are as expected though the binary status signal drops to the ambient level during the transient region a couple of times. This drop corresponds to small changes in the Teager energy when the energy level is near the ambient level during transitions of the Teager energy between positive and negative values. This is a problem because it leads to confusion regarding the state of operation of the power system; further information would be required by an operator to determine whether the system is in ambient or transient operation during

such episodes. A more robust method for detecting transient operation was therefore explored. This is presented in the next subsection.

4.4.2. Integrated Absolute Teager Energy (IATE)

The Integrated Absolute Teager Energy (IATE) refers to the integral of the absolute values of the calculated Teager energy using the Teager operator over time. The idea for the IATE was derived from the Integrated Absolute Error (IAE) method from process systems engineering which is used to detect sustained oscillations in control loops (Hägglund, 1995).

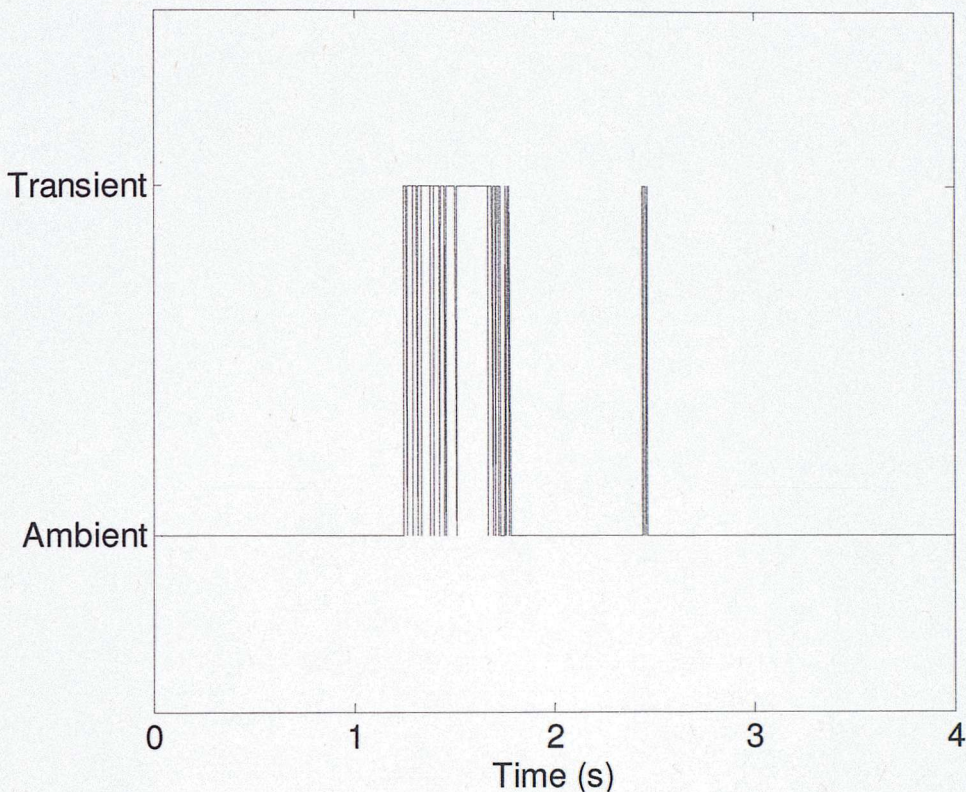


Figure 35: Ambient and transient operation using Absolute Teager energy signal for Mexican frequency signal

The IAE method was previously reviewed in Chapter 2 and is used to determine the presence of sustained oscillations in process control loops using the error in the control signal of the loop which is the difference between the actual output of the control loop and the set-point. It determines the absolute value of the integral of the error in a control loop. Under normal operation of the loop, the error is small and therefore the integral is small too. In the presence of a sustained oscillation, the integral increases above normal. Hence a threshold can be set to detect when this integral exceeds

levels observable during normal operation of the loop. This minimum allowed IAE is used as a threshold and when the IAE exceeds this value continuously, a sustained oscillation is inferred. In this thesis, the IATE, is proposed where the integral of the absolute values of the Teager energy is used. The discrete representation of this integral is shown in Equation 33 and it can be interpreted as the sum of the discrete Teager energy values for all time instants of measurement up to the n th instant.

$$IATE_n = \sum_{k=1}^n \Psi(c_i(k)) \quad \text{Equation 33}$$

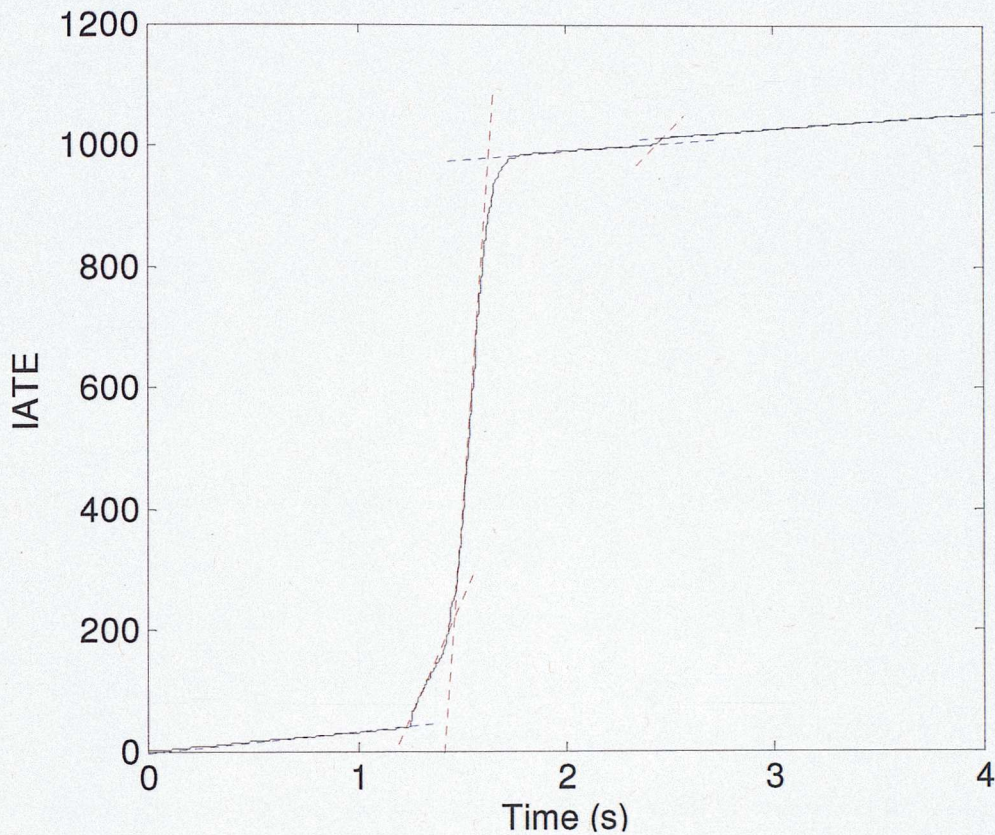


Figure 36: Integrated Absolute Teager Energy (IATE) signal of Mexican frequency signal

The basis for using this measure is that the Teager energy can be observed to increase greatly during transient disturbances in Figure 33 and hence the rate of change of energy during transient events is expected to be high. Therefore the integral of the absolute values of the Teager energy is expected to increase rapidly during a transient event than during ambient operation. This is clearly demonstrated in Figure 36 which shows the IATE calculated using Equation 33. The blue dotted lines indicate the regions of ambient operation while the red dotted lines indicate the regions of transient operation. As

expected, the gradients of the red lines are greater than the gradients of the blue lines indicating a higher rate of change or transfer of energy.

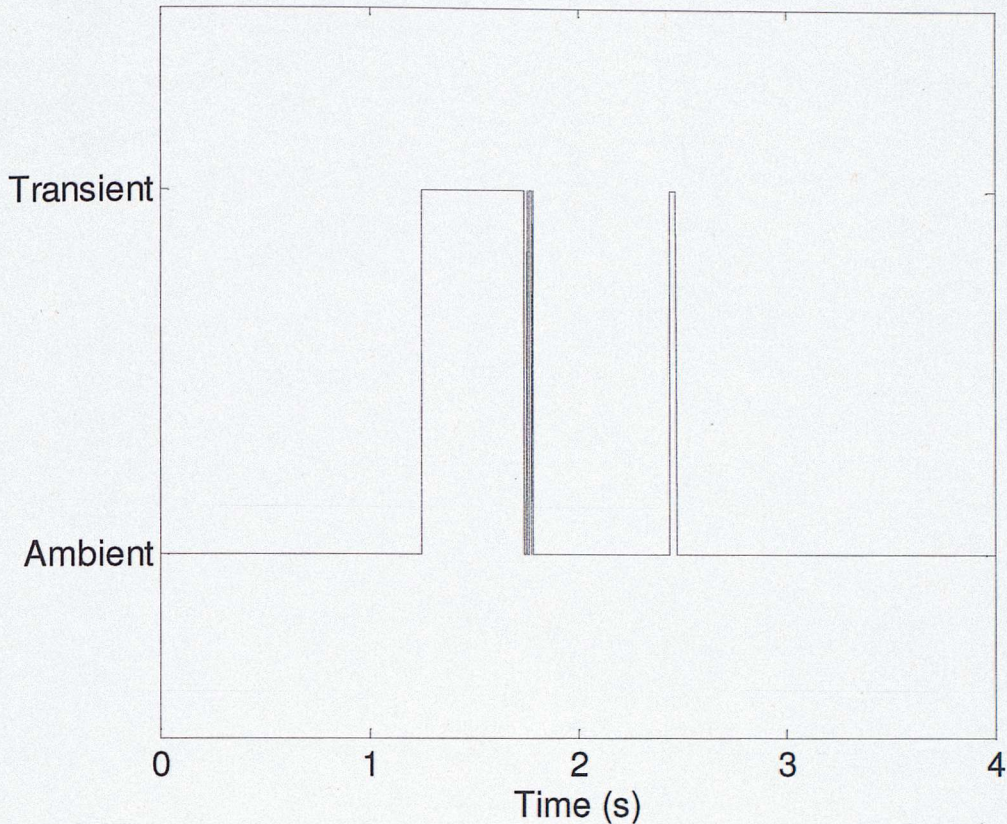


Figure 37: Ambient and transient operation using Integrated Absolute Teager Energy (IATE)

signal for Mexican frequency signal

This change in the rate of transfer of energy can be exploited to display a binary status indicator of ambient or transient operation, just as in the case of the threshold detection that was described by Barocio *et al.* (2010). Historical calculations of the IATE can be used to determine the maximum instantaneous rate of change of the IATE during ambient operation and this value can be used as a threshold above which transient operation is inferred.

However, due to the discrete nature of the signal, a four-point gradient computation is used for calculation of the instantaneous change of the IATE in order to mitigate the effect of an approximate step change in the IATE from one instant to another. The four-point gradient was chosen by trial and error. It was computed using a least-squares fitting algorithm as shown in equations 34 and 35 where the IATE values between $k-4$ and $k-1$ constitute the y vector while the x vector is taken to be linear from 1 to 4. The last point in the series occurs at time instant $k-1$ because the Teager energy is

computed one step backwards as previously discussed. Therefore the most recent IATE value is the one at time instant $k-1$. Figure 38 shows how the IATE is calculated (labelled as I measurements) directly from the Teager energy calculations and indirectly from the output measurements. It can be observed that the Teager energy calculation determines the Teager energy at the time instant immediately previous to the current time instant and hence the IATE calculation has a lag of one measurement.

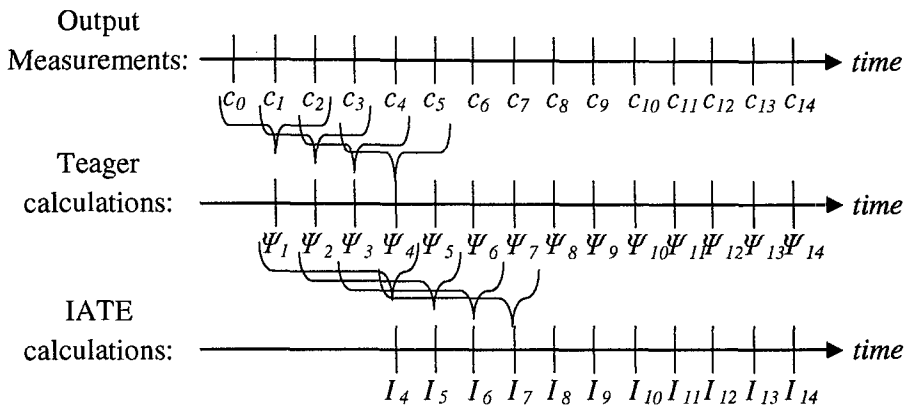


Figure 38: Demonstration of calculation of IATE directly from Teager energy calculations and indirectly from output measurements

The gradient of the least-squares fit, m_{k-1} , is the four-point gradient. The threshold condition is therefore applied to the four-point gradient computations as shown in Equation 36 where t is the chosen threshold from historical four-point gradient computations during ambient operation.

$$y = IATE_{k-4:k-1}; x = 1:4 \quad \text{Equation 34}$$

$$y = m_{k-1}x + c_{k-1} \quad \text{Equation 35}$$

$$\text{if } (m_{k-1} \leq t) \{ \text{Ambient Operation} \} \text{ else } \{ \text{Transient Opeartion} \} \quad \text{Equation 36}$$

Figure 37 shows the ambient and transient regions obtained using this method. It can be observed that there is an improvement in the continuous detection of transient behaviour especially at the onset of the transient compared to the threshold detection method. This is expected because the four-point gradient computation corresponds to smoothing the original Teager energy signal in order to eliminate some spurious detection. Figure 39 presents a flowchart that demonstrates the steps involved in the transient detection algorithm using the Teager operator and the improved IATE measure for transient detection, named the TO-IATE method. The integrated value can eventually be

set back to zero after a sustained period of ambient operation in order to ensure that there are no numerical overflows encountered in the integration.

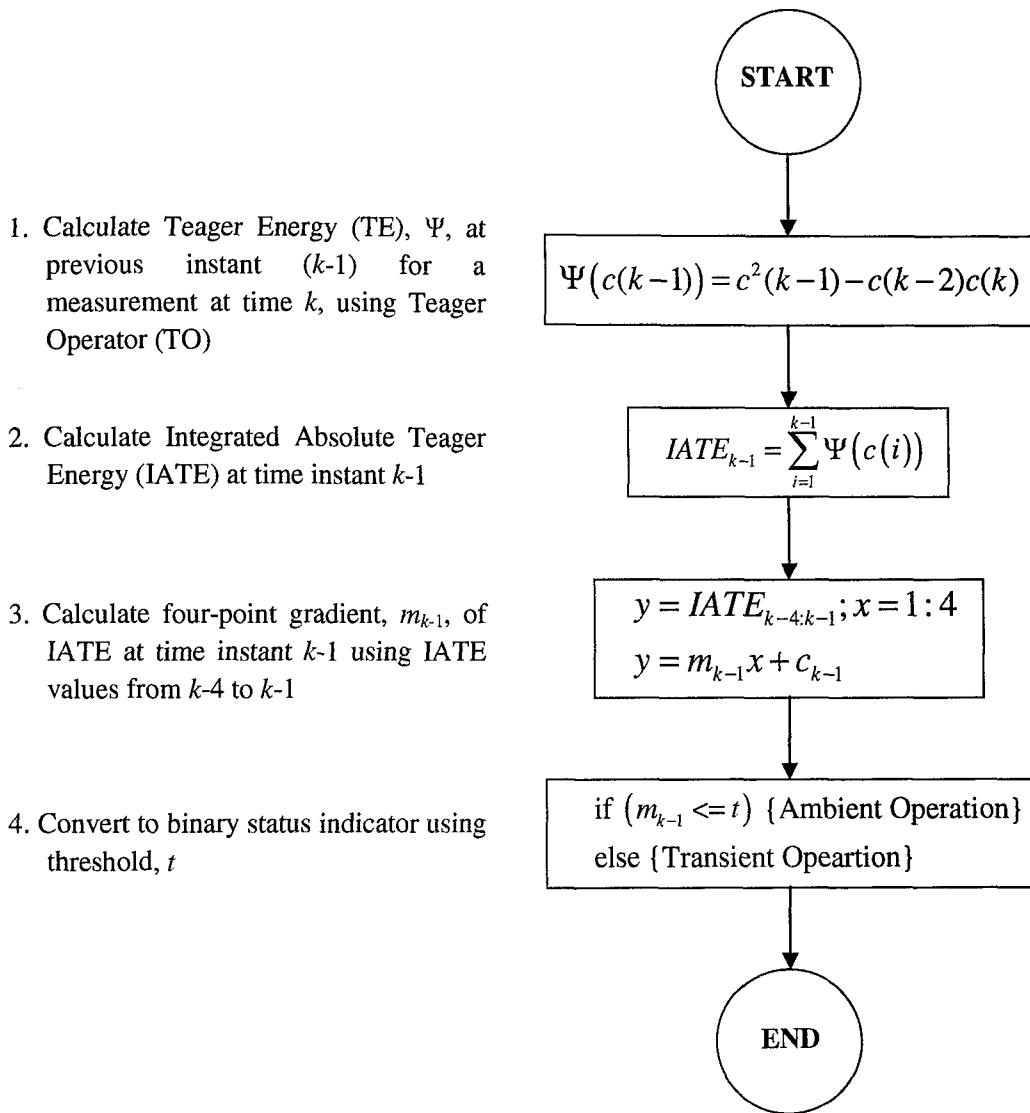


Figure 39: Flowchart demonstrating the use of the TO-IATE method

4.5. Results from Case Study System

The data available from the Nordic System case study was collected during ambient operation of the system. It is therefore not expected to yield any transients. Nevertheless, the Teager operator method combined with the IATE detection scheme can be used to verify this. The following sections therefore present the IATE signals over the whole time duration of the signal measurement and the corresponding binary status signals indicating ambient or transient behaviour.

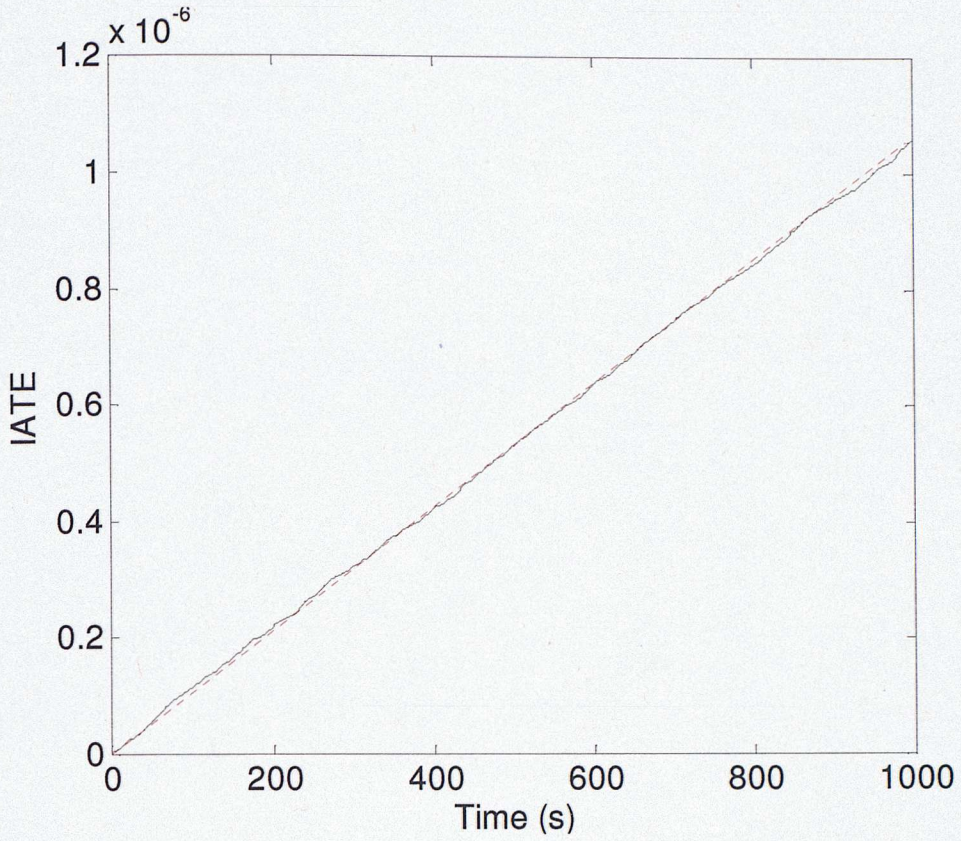


Figure 40: Integrated Absolute Teager Energy (IATE) signal of simulated case study

frequency deviation signal

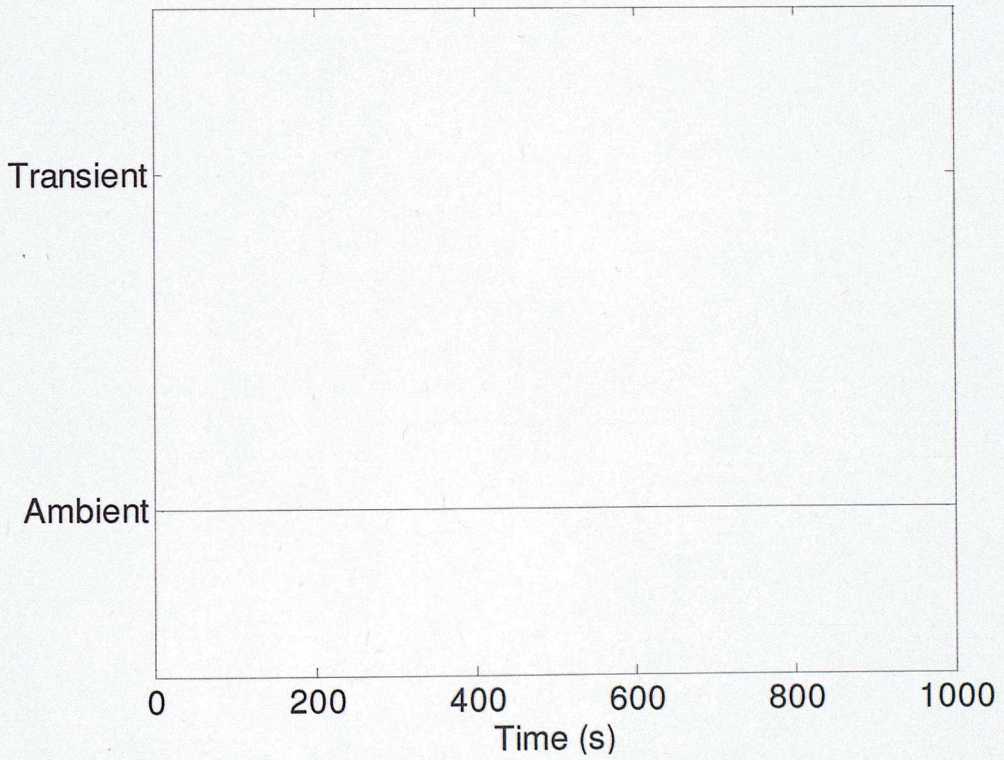


Figure 41: Ambient and transient operation using Integrated Absolute Teager Energy (IATE)

signal for simulated case study frequency deviation signal

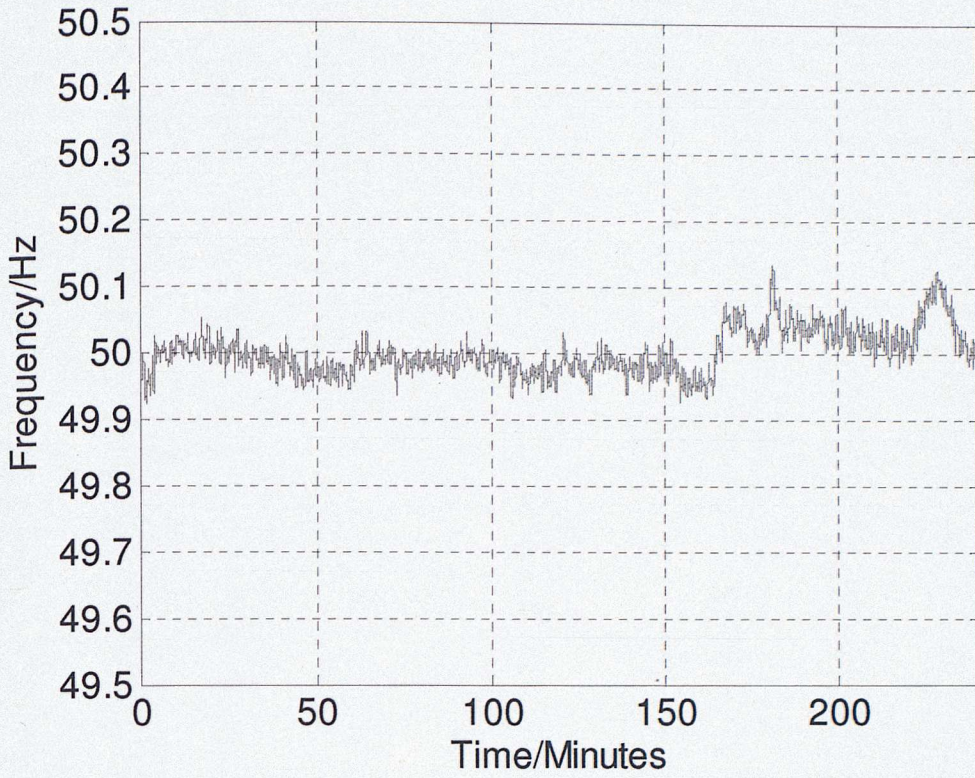


Figure 42: Plot of frequency measurements for measured scenario

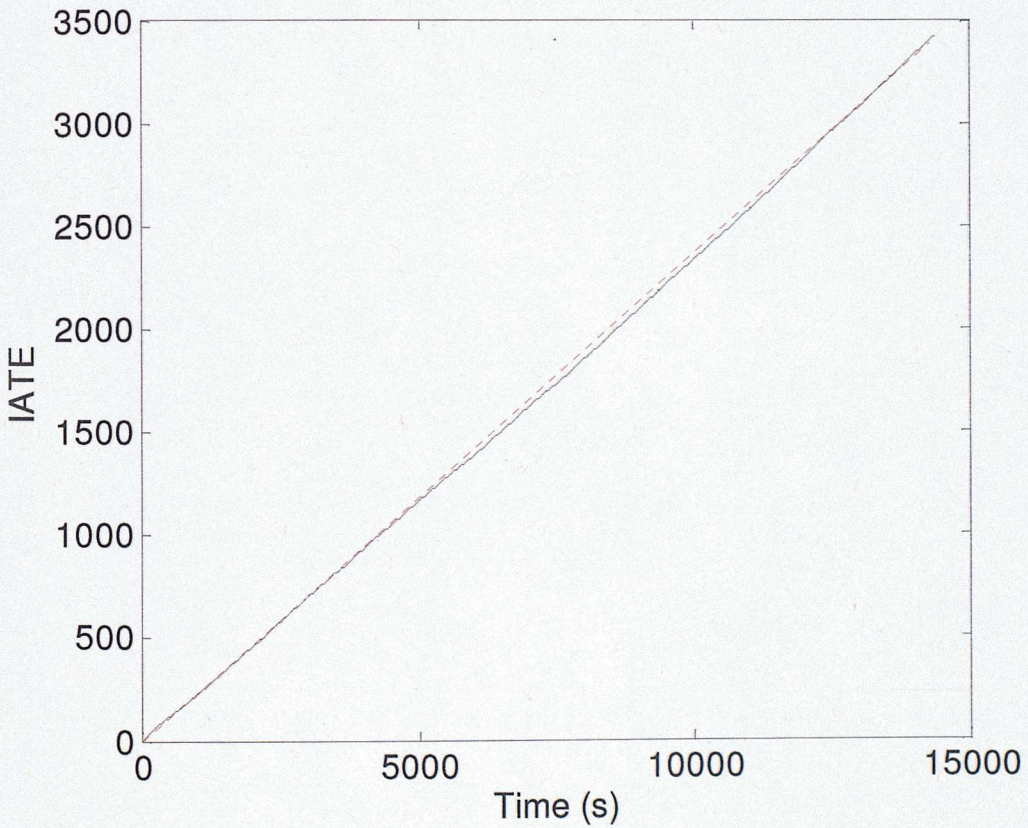


Figure 43: Integrated Absolute Teager Energy (IATE) signal of measured case study

frequency signal

4.5.1. Simulated Scenario

The TO-IATE method was applied to one of the simulated measurements of the bus frequency deviations. Figure 40 shows the IATE over the horizon of the simulation. The values of the IATE are small because the level of noise is very low. As expected the IATE increases at an approximately constant rate for the whole horizon of the simulation indicating one type of system behaviour. This is indicated by the red dotted line. The IATE tracks this line at most points. When a four-point gradient threshold is set using the first few seconds as the historical benchmark, the binary status signal in Figure 41 is obtained. As expected, the system is in ambient operation.

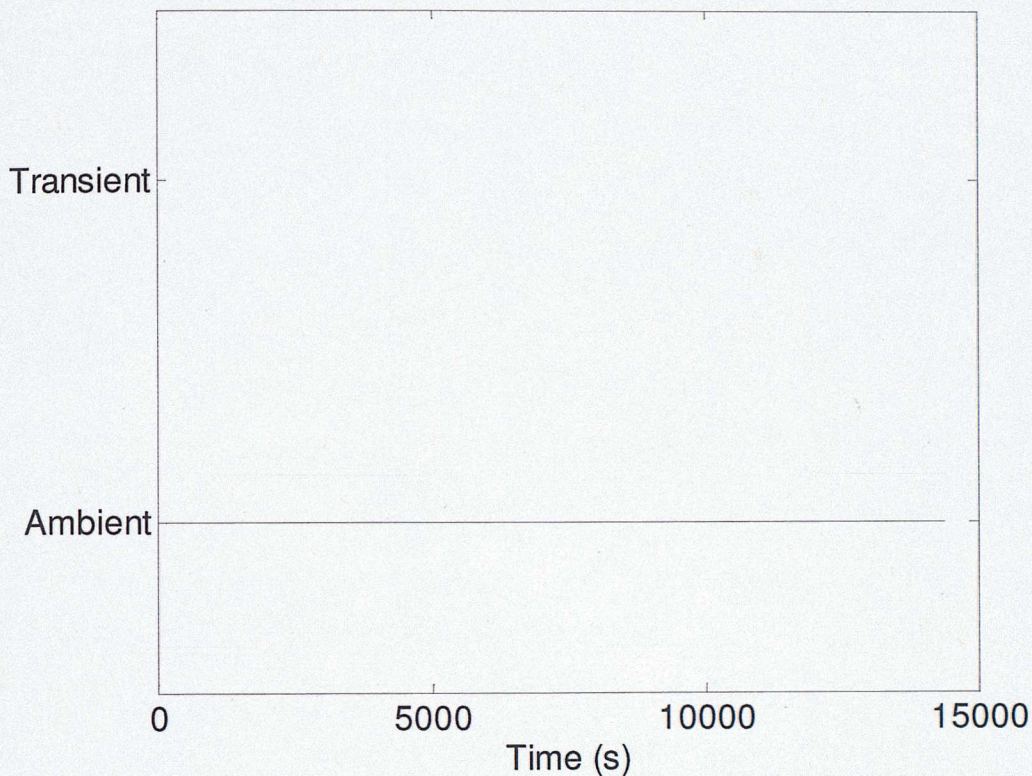


Figure 44: Ambient and transient operation detection using Integrated Absolute Teager Energy (IATE) signal for measured case study frequency signal

4.5.2. Measured Scenario

Similar to the case of the simulated scenario, the TO-IATE method was applied to one of the measurements of the bus frequency from the real Nordic system. Figure 42 shows a plot of the measurements while Figure 43 the IATE over the horizon of the measurement. Once again, as expected, the IATE increases at an approximately constant rate for the whole time horizon indicating

one type of system behaviour as indicated by the red dotted line. The IATE tracks this line at most points. When a four-point gradient threshold is set using the first few seconds as the historical benchmark, the binary status signal in Figure 44 is obtained. Again, as expected, the system is in ambient operation.

4.6. Summary

This chapter has presented a method for detection of transient operation in an a.c. transmission system. It is needed so as to ascertain that the power system is under ambient operation. This is required in order to ensure that the methods discussed in the following chapters can be applied. The chosen method, the Teager operator, estimates the energy in the signal using only three measurements at a time. Having obtained the Teager energy, a further algorithm is required to translate the Teager energy into a binary status signal representation of ambient or transient operation. A novel scheme that calculates the Integrated Absolute Teager Energy (IATE) was introduced as a solution to this problem. It was shown to be better than a simple threshold scheme that has been published in literature because it gets rid of spurious detections of transients. The method was demonstrated using frequency measurements from the Mexican interconnected network that contained regions of both ambient and transient operation. The combined method, TO-IATE, was then applied to data from the simulated and measured scenarios of the Nordic case study that was introduced in Chapter 1 in order to demonstrate that the Nordic data is from ambient operation of the system. The following chapter discusses the use of the ambient data for the detection of inter-area modes and the determination of their sources or areas of participation.

5. Mode Detection and Source Identification

This chapter presents the method that was selected for mode detection and source identification, which is Independent Component Analysis (ICA). The chapter begins with an explanation of ICA and the mathematical basis that leads to the detection of modes and determination of sources, demonstrated with an example. It continues to present the results of ICA on both the simulated and measured data from the case study system presented in Chapter 1, showing that the method is suitable for mode detection and source identification in power systems. The methods and results presented in this chapter have been accepted for publication by the IEEE Transactions on Power Systems in a journal paper titled, “A Multivariate Approach towards Inter-Area Oscillation Damping Estimation under Ambient Conditions via Independent Component Analysis and Random Decrement.”

5.1. Overview

The aim of this chapter is to present methods that are:

- Capable of detecting inter-area modes in the data.
- Identifying the frequencies of the inter-area modes.
- Determining the sources of modes or signals in which the modes are strongest.

This section presents an overview of the methods. It starts with a description of the method for mode detection and then continues to present the method for source identification.

Mode Detection: Independent Component Analysis (ICA) is a multivariate analysis technique. It is one of the methods that can be applied to a Blind Source Separation problem. Blind source separation refers to any technique that aims to reconstruct the original sources of a set of data, without any prior information about either the sources or the mixing parameters of the system that has the data as its output (Tan and Wang, 2001). ICA seeks to estimate the sources by assuming that the outputs are dominated by a set of hidden oscillatory sources which are statistically independent of each other and which contribute to each of the outputs (Xia and Howell, 2005). Spectral ICA, which is one type of ICA, uses the normalized power spectra of the measured time trends in the

analysis such that each of the resulting estimated sources or independent components (ICs), as they are known, is a narrowband spectrum with one sharp peak in the frequency domain corresponding to the frequency of the estimated oscillatory source. The main reason for using the power spectra is that they are invariant to time lags and outliers. The aim of spectral ICA is therefore to determine independent sources of similar spectral signatures and the mixing ratios in which they appear in each signal.

The formulation of Spectral ICA used in this thesis follows that of Xia and Howell (2005) and Xia *et al.* (2005). Spectral ICA is performed by entering the normalised power spectra of the measured (time-domain) signals into a matrix \mathbf{X} where each row contains the power spectrum of the data from one measurement point. Each element in the row corresponds to the signal power present at one frequency in the spectrum. The number of rows in \mathbf{X} is the same as the number of measurement points, and the number of columns is the same as the number of frequencies present in the spectrum. \mathbf{X} can be decomposed as a mixture of n independent non-Gaussian sources (\mathbf{S}) where \mathbf{A} is the mixing matrix such that $\mathbf{X} = \mathbf{AS}$. The rows of \mathbf{S} can be interpreted as the power spectra of the sources that mix to create the observed power spectra in \mathbf{X} . The task of ICA therefore is to find the unknown \mathbf{A} and \mathbf{S} matrices given \mathbf{X} . As outlined in Hyvärinen and Oja (2000), the ICs can be estimated by finding the vectors that maximize the non-Gaussianity index, the cumulant-based kurtosis of each normalized IC. The kurtosis function is given in Equation 37, where s_i refers to the i th spectral source and $E\{\}$ is to the expectation operator. The kurtosis is chosen as a measure of non-Gaussianity because it is very small for the power spectrum of white noise and maximum for the power spectrum of a pure sinusoid (Xia *et al.*, 2005), while it decreases slowly from this maximum as other frequencies are introduced. Hence, maximizing the non-Gaussianity of each source extracts the IC that is closest to a hidden pure sinusoidal source.

$$kurt(s_i) = \frac{E\{s_i^4\} - 3(E\{s_i^2\})^2}{(E\{s_i^2\})^2} = E\{s_i^4\} \quad \text{Equation 37}$$

Having made an estimation of the sources, the next step is the estimation of the mixing matrix. In order to estimate \mathbf{A} , $\mathbf{X} = \mathbf{AS}$ can be written as $\mathbf{S} = \mathbf{WX}$ where \mathbf{W} is the separating matrix, and \mathbf{W} can be found.

$$\mathbf{S} = \begin{bmatrix} \mathbf{w}_1^T \\ \mathbf{w}_2^T \\ \dots \\ \mathbf{w}_n^T \end{bmatrix} \mathbf{X}, \text{ where } \mathbf{w}_j \text{ is the } j\text{th normalized separating vector.} \quad \text{Equation 38}$$

One way to determine \mathbf{W} is to estimate the separating vector \mathbf{w}_j that maximizes the non-Gaussianity of $\mathbf{s}_j^T = \mathbf{w}_j^T \mathbf{X}$ whilst ensuring that each source vector, \mathbf{s}_j^T , is independent¹ of all the others. Having obtained \mathbf{W} , \mathbf{A} can be found since it is the matrix inverse of \mathbf{W} . The matrix \mathbf{A} therefore contains the mixing ratios of the ICs in \mathbf{S} that can be used to reconstruct the power spectra in \mathbf{X} . However, because the results of the kurtosis constraint in Equation 38 are not unique in terms of sign and magnitude, extra constraints need to be imposed on the decomposition in order to make the results physically meaningful. Following Xia and Howell (2005), these constraints are imposed by scaling the matrix containing the determined sources, and correcting this compensation in the \mathbf{A} matrix in order to preserve the original relationships. Each source is initially normalised to unit power by dividing the power in each frequency channel by the total power in all frequency channels of the source as shown in Equation 39.

$$\mathbf{y}_j [f_0, f_1, \dots, f_r] = \frac{\mathbf{s}_j [f_0, f_1, \dots, f_r]}{\Delta_j}, j = 1, 2, 3, \dots, n,$$

$$\text{whereby } \Delta_j = \sum_{i=1}^r |\mathbf{s}_{ji}| = \sum_{i=1}^r |[f_0, f_1, \dots, f_r]_j|,$$

$$\text{such that } \mathbf{Y} = [\mathbf{y}_1, \mathbf{y}_2, \dots, \mathbf{y}_n]^T, \quad \text{Equation 39}$$

where r is the number of frequency channels and i is the sequential index of the individual, frequency channels, f , from 1 to r , whereby $|\mathbf{s}_{ji}|$ is the absolute value of the i th element of the \mathbf{s}_j vector. Similarly \mathbf{A} is adjusted as in Equation 40.

$$\mathbf{B} = \mathbf{A} \mathbf{diag} (\Delta_1, \Delta_2, \dots, \Delta_n) \quad \text{Equation 40}$$

Hence $\mathbf{X} = \mathbf{AS}$ becomes $\mathbf{X} = \mathbf{BY}$. Additionally, the signs of the determined sources are manipulated such that the dominant peak in each scaled source in the \mathbf{Y} matrix is positive. The reason for doing

¹ Statistical independence means that $p(x_1, x_2) = p(x_1)p(x_2)$. Here $p(x_1, x_2)$ is the joint probability of the combination of values x_1 and x_2 , while $p(x_1)$ and $p(x_2)$ are the independent probabilities.

this is because the amplitude of a physical oscillation source is positive by definition and hence it must have a positive magnitude in the frequency domain. The signs of the other channels are not of concern because their magnitudes are negligible. Similarly, the \mathbf{B} matrix is adjusted to counteract this change in the \mathbf{Y} matrix.

Source Identification: Having identified the frequencies present in the data via the ICs, the next step is to determine the relative ratios in which they exist in the measured signals. The mixing matrix \mathbf{B} provides this information; however, it would be more meaningful to compare the mixing ratio of one signal relative to that of the other signals for each spectral source. This is possible because the determined ICs are scaled to unit power and therefore the mixing ratios in \mathbf{B} are a measure of how much of each normalised IC is present in each measured signal. For example, the result of the decomposition can be written as shown in Equation 41, whereby \mathbf{Y}_1 to \mathbf{Y}_n are the identified ICs such that $\mathbf{X}_i = B_{i1}\mathbf{Y}_1 + B_{i2}\mathbf{Y}_2 + \dots + B_{in}\mathbf{Y}_n$ for $i = 1, 2, \dots, n$. The i th spectrum in \mathbf{X} can be reconstructed by multiplying each of the values in the i th row of the mixing matrix with the respective IC in the \mathbf{Y} matrix and summing them up.

$$\begin{pmatrix} \mathbf{X}_1 \\ \mathbf{X}_2 \\ \vdots \\ \mathbf{X}_n \end{pmatrix} = \begin{pmatrix} B_{11} & B_{12} & \cdots & B_{1n} \\ B_{21} & B_{22} & \cdots & B_{2n} \\ \vdots & \vdots & \vdots & \vdots \\ B_{n1} & B_{n2} & \cdots & B_{nn} \end{pmatrix} \begin{pmatrix} \mathbf{Y}_1 \\ \mathbf{Y}_2 \\ \vdots \\ \mathbf{Y}_n \end{pmatrix}$$

Equation 41

It therefore follows that the j th column of the mixing matrix contains the relative amounts of the j th IC in each of the measured signals. For instance, if B_{11} is much larger than B_{21} it means that \mathbf{X}_1 contains a greater amount of the source \mathbf{Y}_1 than \mathbf{X}_2 . In the context of the power systems measurements, the relative ratios in each column of \mathbf{B} represent the relative strength of each source or oscillation in the measured outputs, for example, for the case that B_{11} is much larger than B_{21} , it means that the oscillation represented by the spectral source \mathbf{Y}_1 is stronger at the location of the measurement of \mathbf{X}_1 than \mathbf{X}_2 . Xia *et al.* (2005) introduced a concept known as the significance index which is formed by scaling each column of \mathbf{B} by the maximum value in each column so that the values in the column have a magnitude less or equal to 1 as demonstrated in Equation 42. Similarly the \mathbf{Y} matrix is scaled to account for this compensation as demonstrated in Equation 43.

$$\mathbf{C} = \mathbf{B} \text{diag} (\alpha_1^{-1}, \alpha_2^{-1}, \dots, \alpha_n^{-1}), j = 1 \dots n; \alpha_j = \|\mathbf{b}_j\|_{\infty},$$

where \mathbf{b}_j is the j th column of \mathbf{B} Equation 42

$$\mathbf{D} = \text{diag} (\alpha_1, \alpha_2, \dots, \alpha_n) \mathbf{Y}, \text{ hence } \mathbf{X} = \mathbf{CD} \quad \text{Equation 43}$$

The highest value in each column of \mathbf{B} now takes a value of 1 in \mathbf{C} . The new mixing ratio is referred to as a matrix of significance indices (SI s) such that:

$$\begin{pmatrix} \mathbf{X}_1 \\ \mathbf{X}_2 \\ \vdots \\ \mathbf{X}_n \end{pmatrix} = \begin{pmatrix} SI_{11} & SI_{12} & \dots & SI_{1n} \\ SI_{21} & SI_{22} & \dots & SI_{2n} \\ \vdots & \vdots & \vdots & \vdots \\ SI_{n1} & SI_{n2} & \dots & SI_{nn} \end{pmatrix} \begin{pmatrix} \mathbf{D}_1 \\ \mathbf{D}_2 \\ \vdots \\ \mathbf{D}_n \end{pmatrix} \quad \text{Equation 44}$$

The significance of this manipulation is that if $SI_{jk} = 1$, \mathbf{X}_j has the greatest amount of source \mathbf{D}_k relative to all the other measured outputs. In the context of power systems, the k th mode is strongest at the location of the j th measurement and is therefore closest to the source of the oscillation. In the case of inter-area modes, the locations with the highest SI s indicate the areas participating in the inter-area oscillation. Figure 45 presents a flowchart that demonstrates the process of mode detection and source identification using ICA.

Most Significant Mode: Xia *et al.* (2005) also introduced another term known as the dominance ratio (DR), which is a measure of the significance of each source calculated by ICA. It is a measure of the percentage of energy from all the spectra that can be attributed to a particular source. Though not directly related to the objectives of the research, it can be used to determine which modes are most critical to monitor in terms of having greater impact on operation because modes with higher DR s are the most observable modes. The total energy of all the spectra can be estimated by $\|\mathbf{CD}\|_{\text{sum}}$ which represents the sum of the absolute values of all its elements. The total energy related to the j th IC can then be represented as $\|\mathbf{c}_j \mathbf{d}_j^T\|_{\text{sum}}$ where \mathbf{c}_j represents the j th column of the \mathbf{C} matrix while \mathbf{d}_j^T represents the j th column of the transpose of the \mathbf{D} matrix. The DR s can hence be calculated using Equation 45.

$$DR(j) = 100 \left\{ \frac{\|\mathbf{c}_j \mathbf{d}_j^T\|_{\text{sum}}}{\|\mathbf{CD}\|_{\text{sum}}} \right\} \% \quad \text{Equation 45}$$

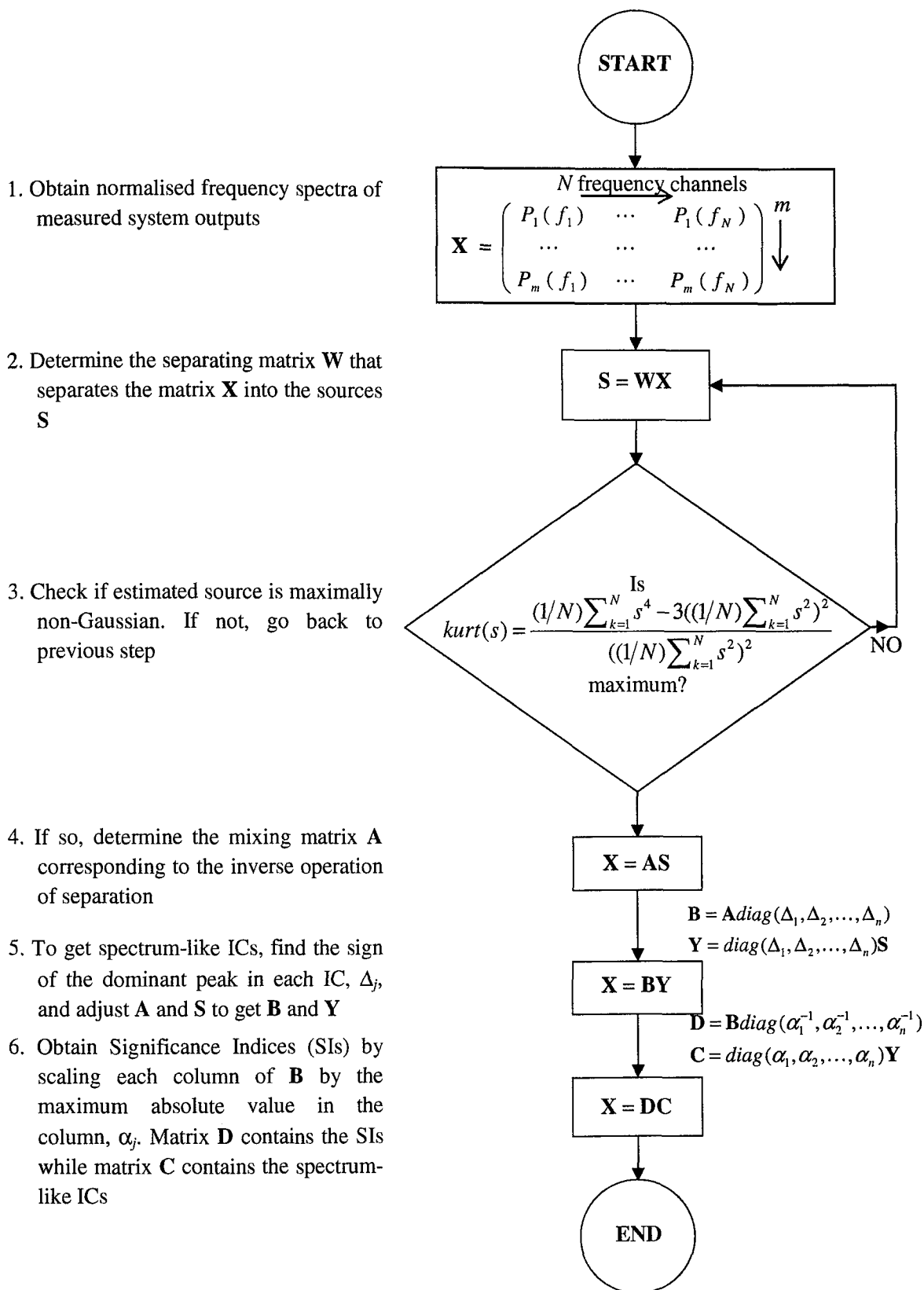


Figure 45: Flowchart demonstrating Independent Component Analysis (ICA)

The IC with the greatest dominance ratio is the most dominant oscillation in all the calculated ICs, hence the higher the dominance ratio, the more dominant the IC. An additional use of the *DRs* is that they can be used to screen oscillations that have no impact on operation of the power system: a threshold *DR* can be set, below which the IC can be ignored because it represents an oscillation that has no impact on operation.

Example: The aim of this example is to demonstrate the use of ICA to detect modes and the use of the *SIs* obtained from the decomposition to determine the signal in which a given mode is strongest. The Fast-ICA algorithm by Hyvärinen and Oja (1997) is used. The algorithm, which can be downloaded from <http://www.cis.hut.fi/projects/ica/fastica/>, is based on a neural network learning rule that is translated into a simple fixed-point iteration scheme for finding the local extrema of the kurtosis function mentioned previously. The algorithm is initialized using the outputs of a similar spectral decomposition method known as Principal Component Analysis (PCA). As a result, it has a fast convergence rate making it suitable for the application of on-line monitoring.

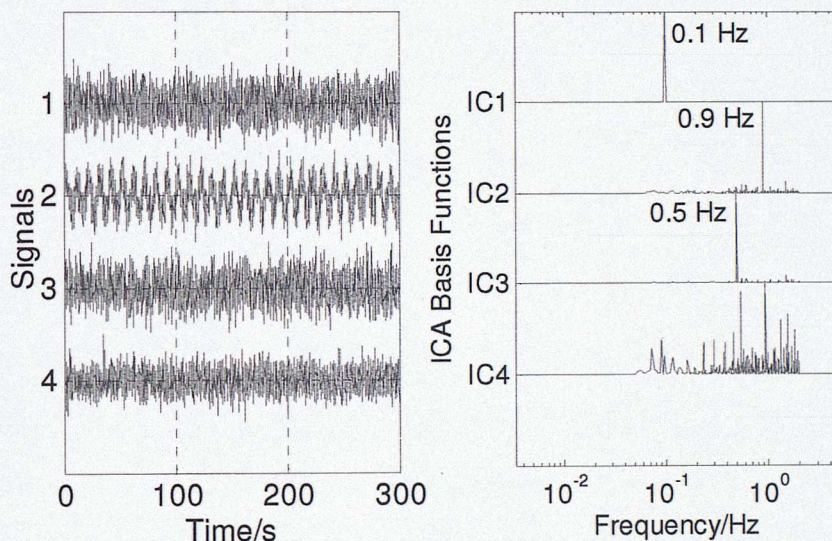


Figure 46: A - Synthetic signals, B - Independent components from application of ICA on synthesized signals.

Figure 46A shows the synthetic signals in equations 46-19 sampled at 10 Hz (inter-sampling time: 0.1 s) for a duration of 300 s with noise added such that the SNRs are 2, 10, 4 and 2.5 respectively:

$$y_1 = 0.5 \sin(2\pi f_1 t) + 0.3 \sin(2\pi f_2 t) + 0.2 \sin(2\pi f_3 t) \quad \text{Equation 46}$$

$$y_2 = 0.7 \sin(2\pi f_1 t) + 0.2 \sin(2\pi f_2 t) + 0.1 \sin(2\pi f_3 t) \quad \text{Equation 47}$$

$$y_3 = 0.4 \sin(2\pi f_1 t) + 0.3 \sin(2\pi f_2 t) + 0.3 \sin(2\pi f_3 t) \quad \text{Equation 48}$$

$$y_4 = 0.2 \sin(2\pi f_1 t) + 0.4 \sin(2\pi f_2 t) + 0.4 \sin(2\pi f_3 t) \quad \text{Equation 49}$$

where $f_1 = 0.1$ Hz, $f_2 = 0.5$ Hz and $f_3 = 0.9$ Hz represent three independent sources. The motivation for using multi-sine data contaminated with varying levels of noise is to demonstrate the application of ICA to ambient data from power systems. Assuming that a power system's dynamics are linear during ambient operation, the data collected over a short time duration (for example 10 minutes) can be expected to be relatively stationary. When filtered to the inter-area mode range (high and very low frequency components removed), the data is expected to contain only the system output response to the narrow-band excitation in the inter-area mode frequency range, and noise in the same frequency range. The results of filtering can thus be expected to be similar to multi-sine data corrupted with noise. In addition, the filtered data is also expected to contain different relative amounts of each mode depending on the location of the measurement, and this is reflected in this example by using different mixing ratios to generate the multi-sine data.

Figure 46B shows the results of ICA when applied to the frequency spectra of the signals. It is not possible to observe any oscillations by visual inspection of the plot of the time trends of the signals (except signal 2); however, ICA is capable of extracting the sources of the signals. The estimates of the frequencies are 0.1 Hz, 0.5 Hz and 0.9 Hz, all of which are the original frequencies that were used to construct the synthesized signals. The last IC contains the broadband noise added to the signal; visual inspection shows that it is not narrowband and can hence be discarded for the purpose of mode detection. Additionally, the *SIs* obtained from the decomposition are shown in Table 1. ICA is able to identify that the 0.1 Hz mode is strongest in signal 2 and that the 0.5 Hz and 0.9 Hz modes are strongest in signal 4. These results can be validated by observing the relative quantities of the sources in the original signal equations.

Signal	Significance Indices for each IC			
	IC ₃	IC ₁	IC ₂	IC ₄
1	0.4009	0.0850	0.4217	1.0000
2	1.0000	0.0001	0.0240	0.0000
3	0.5713	0.3976	0.9531	-0.0032
4	0.0001	1.0000	1.0000	0.2962

Table 1: Significance indices for each IC

5.2. Method Development

The previous section has provided an overview of the methods that were proposed for detection of the inter-area modes from the measurements and the determination of the relative strengths of the mode in the measured signals. However, two issues that need to be addressed are:

- Parameter selection of the window duration over which ICA is applied: The window duration refers to the length of data used to obtain one estimate of the inter-area mode frequency and the duration of the data window (number of samples used) determines the resolution of the spectra obtained. This is because the frequency resolution of a fast fourier transform is dependent on the number of samples taken and the sampling frequency.
- The effect of noise on the estimation of frequency: Real-life measurements from electrical power systems have a large amount of noise. This is an important factor because the greater the amount of noise in a signal, the harder it is to separate the inter-area modes from the noise spectra. The methods therefore need to be robust to different degrees of noise.

5.2.1. Parameter Selection

As previously explained, the window duration determines the resolution of the spectra used in ICA. A longer duration implies that a finer resolution is achieved hence the frequency estimate is more accurate while a shorter duration implies a coarser resolution hence less accurate frequency estimate. However, conversely from an operation perspective, the duration of data window used affects the response time for detection of changes in mode frequency (and damping) because ambient operation assumes that the data is reasonably stationary over long periods of time. If there were to be a change in the operation scenario, this change can only be detected once the new scenario dominates the data window. Hence in the case of a long data window, an event will take longer to be detected and in the case of a short data window, an event will be detected more quickly. There is therefore a trade-off between the speed of response of the detection and the accuracy of the estimation.

Window duration over which ICA is applied: The minimum window duration for the application of ICA was determined by using the data from the simulated Nordic case study scenario to determine the expected value of the frequency of the critical inter-area mode in Finland.

In order to determine a robust value for the data window duration, a sliding window was used to assess the estimated mode frequency over the period of the simulation. The duration of the window was initially set and then used to obtain a first estimate of the frequency. The window was then slid 30 s forward, another estimate obtained and so on until the whole simulated data set was used. This technique is demonstrated in Figure 47.

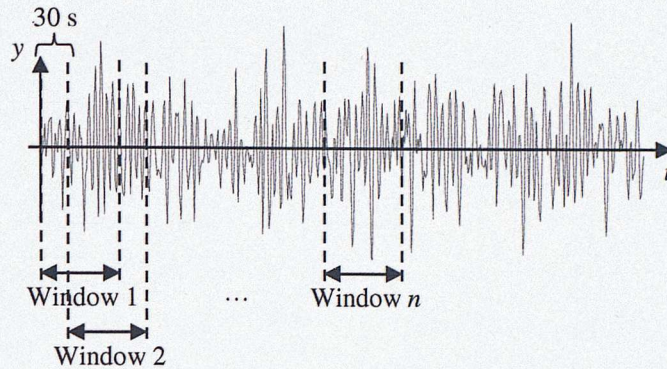


Figure 47: Demonstration of sliding window

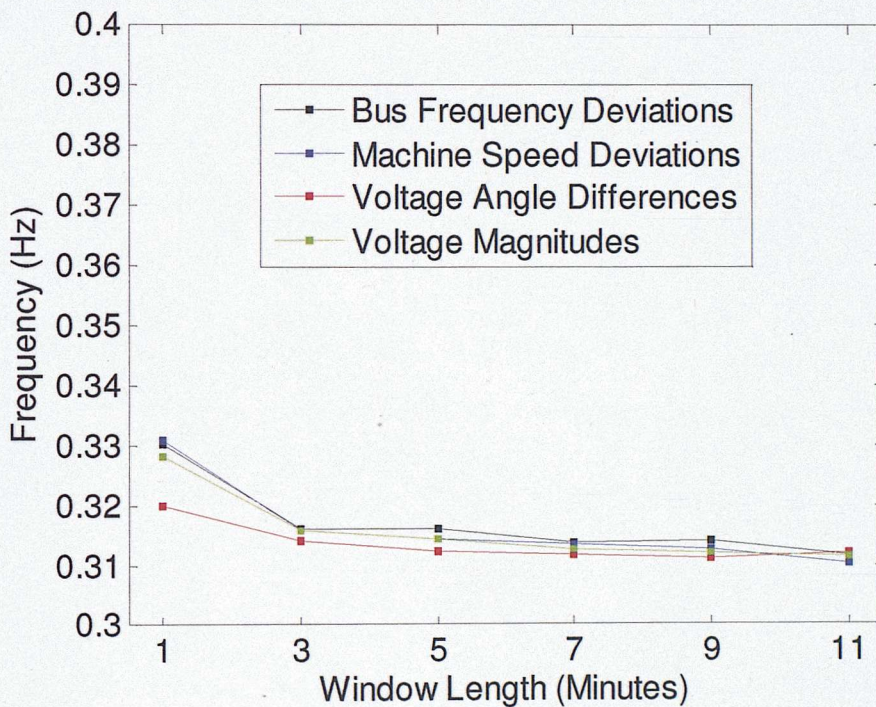


Figure 48: Variation of mean of frequency estimate with window length

The window durations that were used are 1, 3, 5, 7, 9 and 11 minutes. Having obtained various estimates of the mode frequency, the mean frequency and its standard deviation was obtained using the MATLAB normfit toolbox. This toolbox fits a normal distribution to the frequency estimates to determine the mean and standard deviation of the estimates. The standard deviation is a measure of

the spread of the estimates and it represents the bound above and below of the mean where 67 % of the data lies; it determines the 67 % confidence interval (CI) of the estimates (mean \pm standard deviation = 67 % CI). Similarly, the 95 % and 99 % CIs are obtained using twice and thrice the standard deviation respectively. If the mode frequency is assumed to remain constant, these statistical measures are an indication of the accuracy of the method. Ideally, the standard deviation should be a small fraction of the estimated value.

Figure 48 shows the estimated mean frequency of the mode for the different window lengths for the different quantities used while Figure 49 shows the standard deviation of the estimated mean frequency for the same window lengths and quantities. From the results, it can be seen that starting from a window duration of three minutes, the mean value of the frequency estimate is roughly constant as the duration of the window increases and the standard deviation of the estimates decreases only slightly for all quantities.

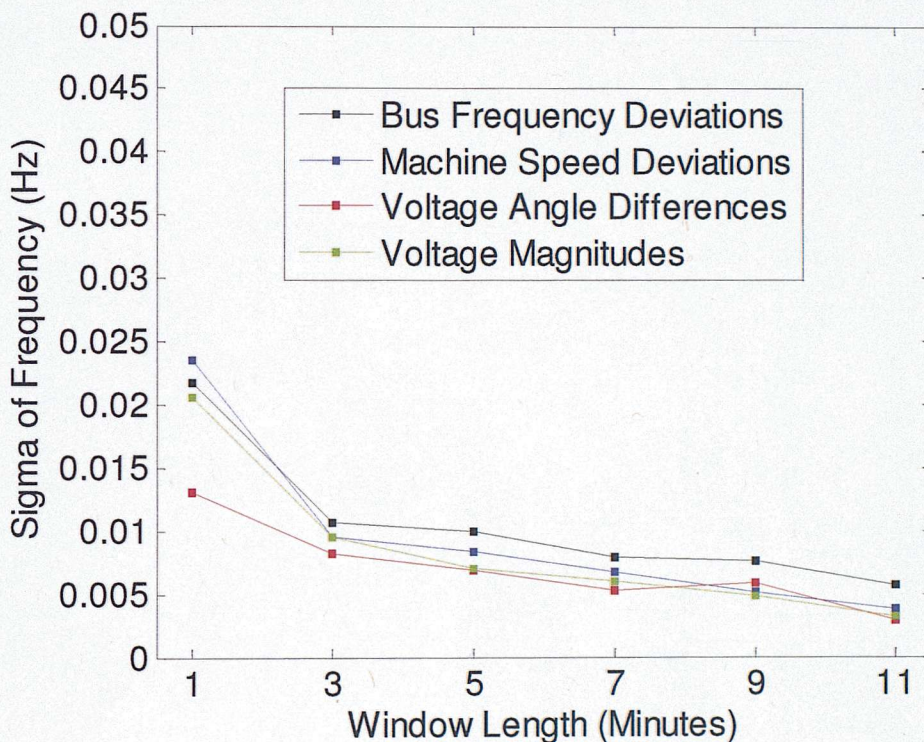


Figure 49: Variation of standard deviation of frequency estimate with window length

It can be concluded that *the duration of the data window does not affect the estimation of the inter-area mode frequency significantly if the duration of the window is greater than three minutes.*

However, for the results presented in the rest of this chapter, a window duration of 11 minutes was used because Figure 49 shows that the frequency estimate has the lowest CI for a window duration of 11 minutes.

5.2.2. Effect of Noise on Estimate

The next task is to determine the effect of noise on the estimate of frequencies using ICA. This is done by fixing the window duration of the estimate and using a fixed measured quantity. In this section, a window duration of 11 minutes is used, as was determined in the previous subsection. The reason for doing this is because measurements from ambient operation are noisy by nature and in order to make sure that the chosen method can perform adequately under noisy conditions, it has to be tested using simulated data with various amounts of added noise. Noise was therefore added to the voltage angle difference data in order to achieve signal-to-noise ratios (SNRs) of infinity, 10 and 5.

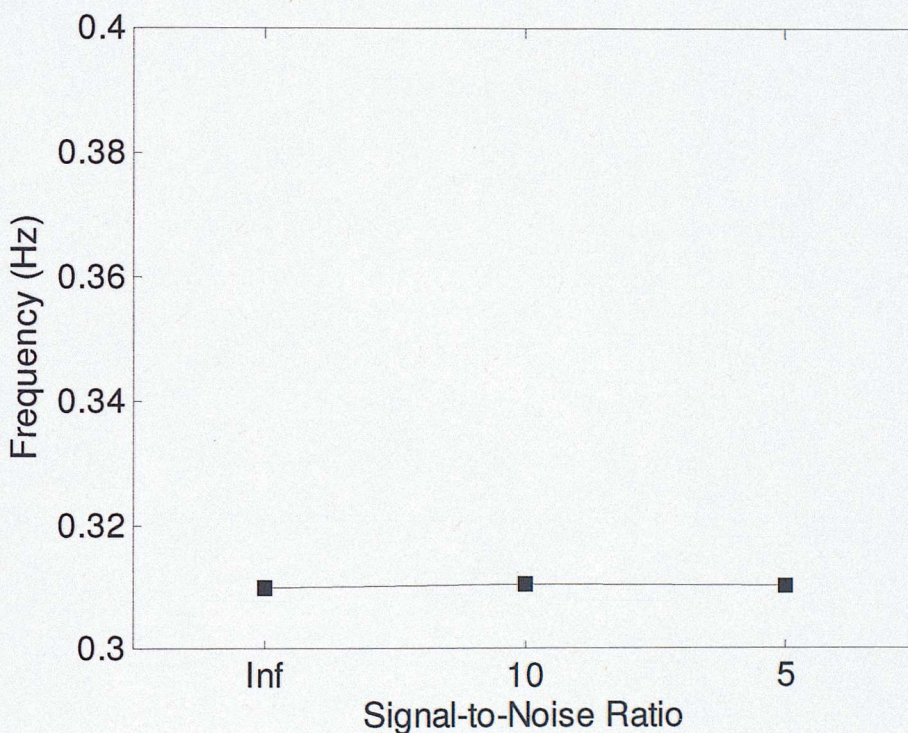


Figure 50: Variation of mean of frequency estimate with SNR using voltage angle difference data

These values of SNR range from the case of no noise to the case of a high level of noise which is expected to be greater than the amount typical in data from ambient operation. Figure 50 shows the

results of the investigation. It can be observed that the SNR of the data has negligible impact on the mean inter-area frequency estimation. This implies that ICA should be capable of detecting and correctly estimating the inter-area mode using real measured data where the SNR is not as low as 5. This is demonstrated in the next section where ICA is used to determine the damping of the 0.31 Hz inter-area mode using both the simulated and measured data from the case study system.

5.3. Results from Case Study System

The methods presented previously in the section were tested using the data presented in Chapter 3, from the Nordic case study system. In the following subsections, the simulated scenario is first used to determine the critical inter-area mode frequency in the Nordic grid. The result is then compared to the expected value of 0.3 Hz known from linearization of the full Nordic model. Finally, the method is applied to data from the measured scenario to determine the actual system frequency of the critical inter-area mode. In both cases, the window duration of 11 minutes that was determined in the previous section was used.

Quantity	Approximate Frequency, ω (Hz)
Machine Speed Deviations	0.3124±0.0076
Rotor Angle Differences	0.3135±0.0052
Voltage Angle Differences	0.3101±0.0035
Bus Frequency Deviations	0.3116±0.0067
Average	0.3119±0.0060

Table 2: Frequency estimates for different quantities in simulated scenario

5.3.1. Simulated Scenario

Table 2 shows the estimates of the frequency of the inter-area modes with the 67 % CI for all quantities using a window duration of 11 minutes and using the simulated data with an SNR of 5. By combining the estimates using the different quantities, an average inter-area mode frequency estimate of 0.3119 Hz with a 67 % CI of 0.0060 Hz is obtained. The estimated inter-area mode frequency is slightly higher than the 0.3 Hz value that was expected. This discrepancy can be explained by the fact that the frequency of oscillation is dependent on the configuration of the power transmission network and is therefore dependent on the parameters of the simulation. The frequency

of the inter-area oscillation is therefore expected to vary to a certain degree around the expected 0.3 Hz value. Additionally, the frequency estimate is roughly the same for all quantities.

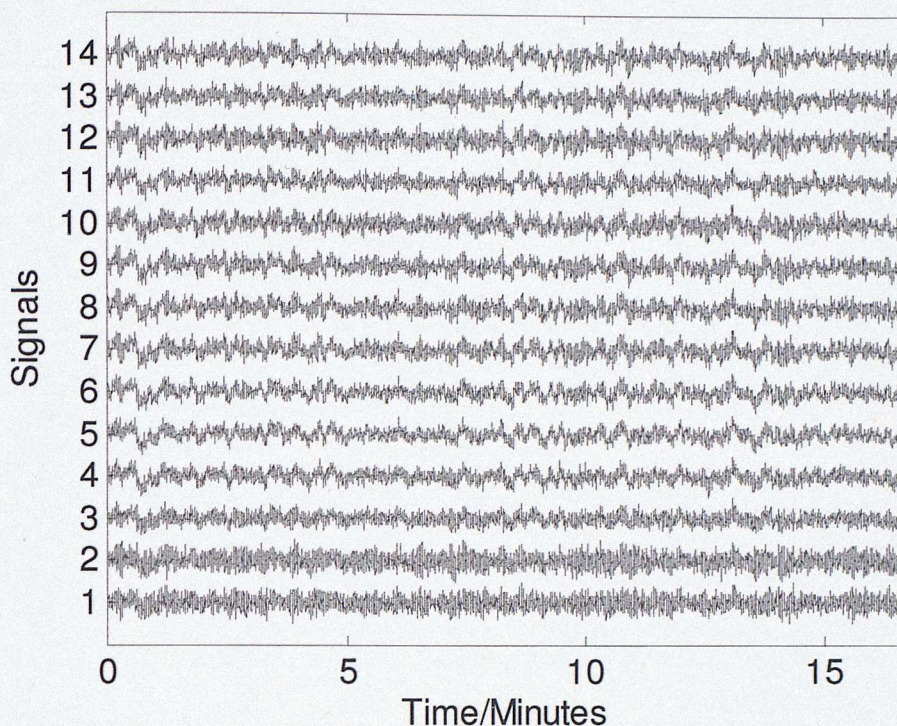


Figure 51: Plot of bus frequency deviation measurements from simulated scenario

ICA was additionally used to determine the significant indices (*SIs*) at the different locations of the bus frequency deviations measurements. 14 different bus frequency deviation measurements were available and are shown in Figure 51. The locations of these measurements are summarised in Table 3.

Since the 0.3 Hz is an oscillation between Southern Sweden and Denmark against Southern Finland, it is expected that the *SIs* of measurements at locations in these areas are higher than those at locations in other areas. A contour plot of the *SIs* at different times of the frequency estimation is shown in Figure 52. The contour plot shows the evolution of the oscillation at different measurements points (given by Location number on y-axis) at different times of the simulation (x-axis). The strength of the oscillation is given by the coloured contours at the intersection between a measurement point and a time value, with an increasing intensity describing an increasing strength of the oscillation. For example, the contour map indicates high intensity of the oscillation at measurement location 9 for the time interval of 11 to 12 minutes, and conversely a low intensity of oscillation at measurement location 10 for almost the whole duration of the simulation. Ideally, the

contour should plot the evolution of the strength of the oscillation at each measurement point over time resulting in horizontal bars of varying intensity. However, due to the discretized nature of the data on the x and y axes, the contour plot is discretized and is therefore not smooth. In the presence of more measurements as was the case in the measured scenario, this horizontal tracking is more visible. Nevertheless, distinct bands where the mode is strongest are observable. These appear as red bands over the time-scale of the estimation.

Measurement Number	Location
1	Olkiluoto (Southern Finland)
2	Loviisa (Southern Finland)
3	Pirttikoski (Northern Finland)
4	Harsprånget (Northern Sweden)
5	Stornorrfors (Northern/Central Sweden)
6	Forsmark (Central/Southern Sweden)
7	Oskarshamn (Central/Southern Sweden)
8	Ringhals (Central/Southern Sweden)
9	Karlshamn (Southern Sweden)
10	Rana (Northern Norway)
11	Aura (Central Norway)
12	Kvilldal (South Western Norway)
13	Tokke (South Eastern Norway)
14	Asnaesvaerket (Eastern Denmark)

Table 3: Locations of bus frequency measurements in simulated scenario

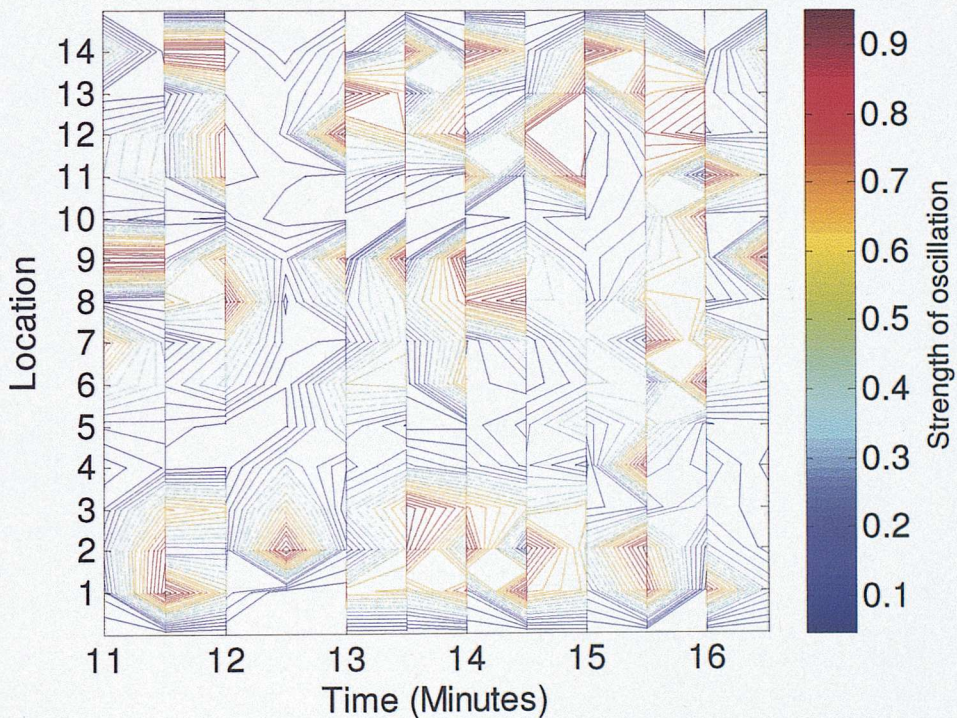


Figure 52: Contour plot of SO s for the 0.31 Hz mode at different times for bus frequency

deviations

The 0.31 Hz mode is seen to be strongest in measurements at locations 1, 2, 9, 12, 13 and 14. These locations are in Southern Finland, Southern Sweden and Southern Norway as expected. The *SIs* from ICA are therefore capable of identifying areas that participate in the inter-area oscillation as expected.

Measurement Number	Location
1	Espoo (Southern Finland)
2	Keminmaa (Northern Finland)
3	Kymi (South East Finland)
4	Petäjäsoski (Northern Finland)
5	Yllikälä (South East Finland)
6	Olkiluoto (South West Finland)
7	Rauma (South West Finland)

Table 4: Locations of bus frequency measurements in measured scenario

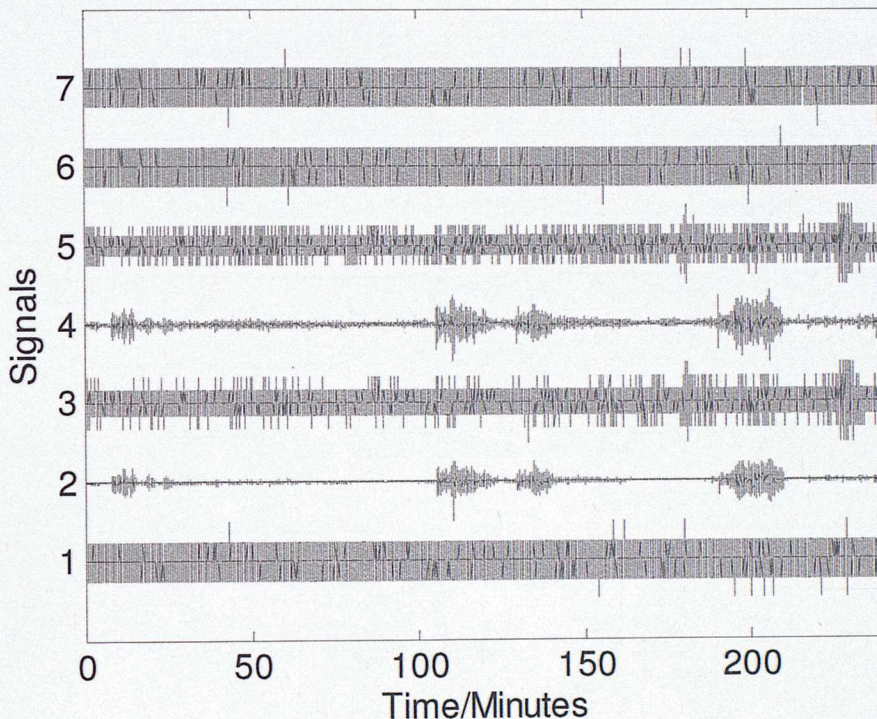


Figure 53: Plot of df/dt measurements from measured scenario

5.3.2. Measured Scenario

ICA was then applied to data from the measured scenario introduced in Chapter 3. A window duration of 11 minutes was used and this window was slid every 30 s to obtain a new estimate for the inter-area mode frequency. This was done for all measured quantities: the active power flows, current flows, derivatives of the frequency and the voltage angle differences. Figure 53 shows a plot

of the frequency deviation measurements made from eight locations in Finland. The locations of these measurements are summarised in Table 4.

Quantity	Estimated Mode Frequency (Hz)
Active Power Flows	0.352 ± 0.012
Current Flows	0.353 ± 0.010
df/dt	0.359 ± 0.009
Voltage Angle Differences	0.352 ± 0.008
Average	0.354 ± 0.010

Table 5: Frequency estimates for different quantities in measured scenario

Figure 54 shows the variation of the inter-area mode frequency estimate over the whole duration of the measurements (about 4 hours) for the frequency deviation measurements shown in Figure 53 as well as the other measured quantities. There is some variation in the frequency that can be attributed to spectral leakage in the FFT and noise in the measurements. A 20-point moving average filter was implemented to smooth-out the high frequency variation and hence produce the low frequency trend over time.

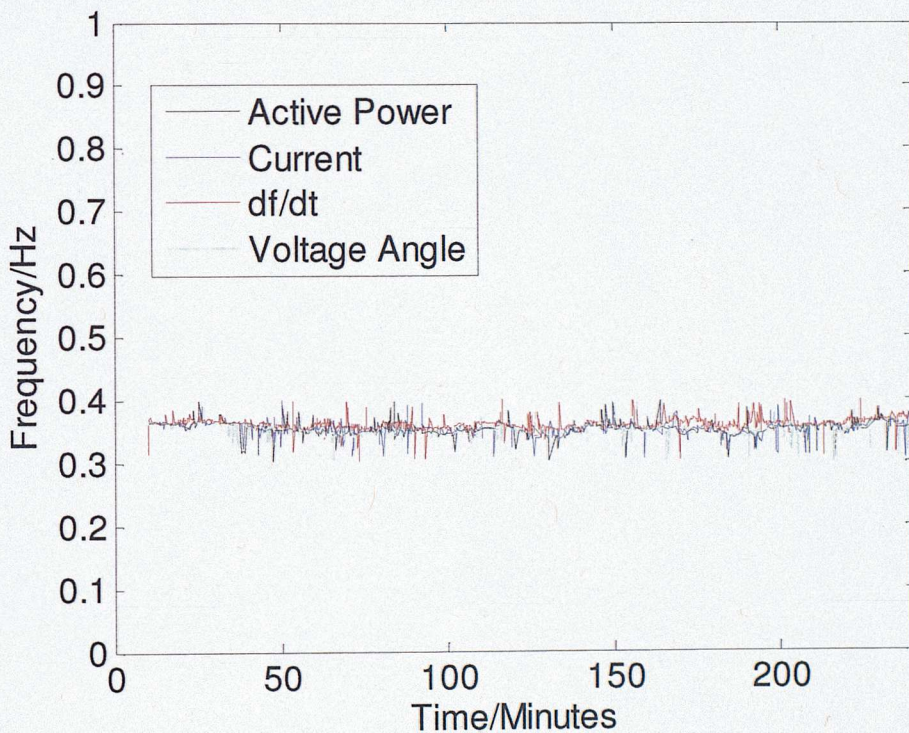


Figure 54: Unfiltered variation of frequency estimate over time

Figure 55 shows the filtered frequency estimates over time. The frequency estimates are observed to be relatively constant over the time duration of the estimation and the values obtained from the different quantities are in general conformity with one another. The MATLAB normfit toolbox was

used to determine the mean frequency and CIs of the estimates for each quantity. Table 5 summarises the results of the analysis.

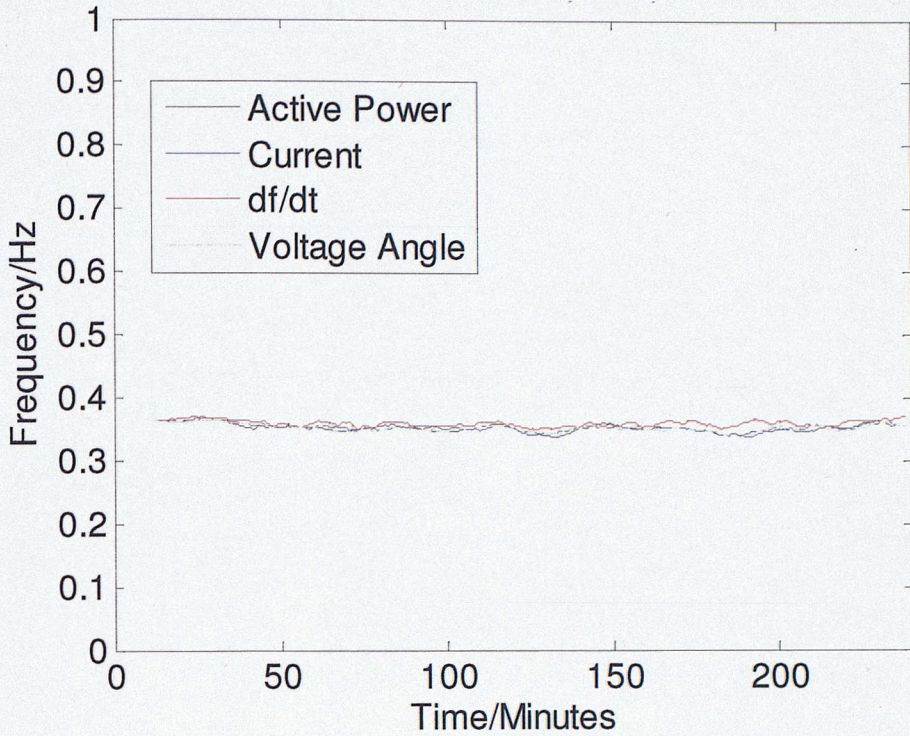


Figure 55: Filtered variation of frequency estimate over time

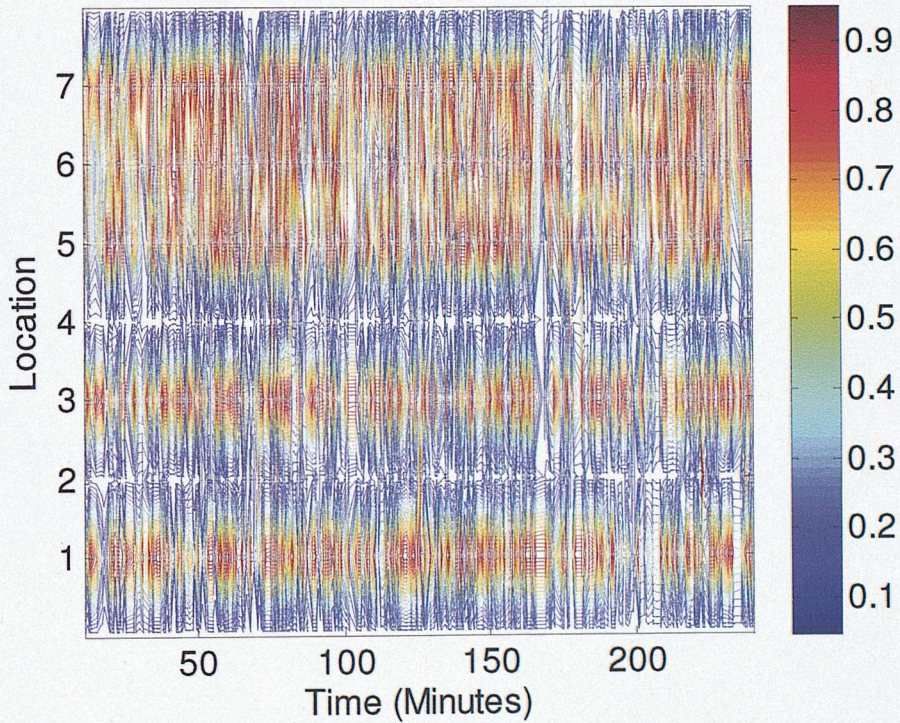


Figure 56: Contour plot of SIs for the 0.35 Hz mode at different times for frequency derivative measurements

By combining the estimates using the different quantities, an average inter-area mode frequency estimate of 0.354 Hz with a 67 % CI of 0.010 Hz is obtained.

Just as in the simulated scenario, ICA was additionally used to determine the *SIs* at the different locations of the frequency derivative measurements. The locations of the measurements that were used are summarised in Table 4, and a contour plot of the *SIs* at different times of the frequency estimation is shown in Figure 56. As expected the *SIs* at locations 1, 3, 5, 6 and 7 in South, South-East or South-West Finland are high. This is observed as red horizontal bands that appear over time in the contour plot. The *SIs* at locations 2 and 4 which are both in North Finland are on the other hand close to zero and this is demonstrated as white horizontal bands in the contour plot. This is expected because they are at the spine or fulcrum of the 0.3 Hz oscillation and therefore would not expect to take part in the oscillation as demonstrated in Figure 57.

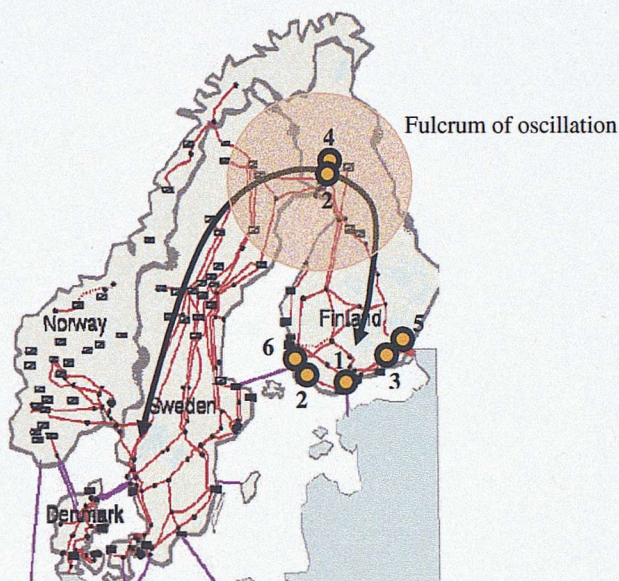


Figure 57: Fulcrum of 0.3 Hz oscillation relative to oscillation path

5.3.3. Discussion of Results

The inter-area mode frequency estimated from the measured data is about 0.04 Hz higher than that estimated from the simulated data, corresponding to an increase greater than 10 % from the model value. This difference is not negligible and therefore cannot be ignored. However, it is expected that it might be different from the model value for various reasons including:

- Uncertainties in system parameters in the model and linear approximations of component models.
- The true inter-area mode frequency of the operational system is known to vary according to the configuration of generators and loads. The results suggest it was higher than normal on the day when the measured data set was collected. This change in the inter-area mode frequency is expected to be reflected in the estimated damping of the mode too.

5.4. Summary

This chapter has presented the methods for detection of inter-area modes and identification of sources of oscillations. In the context of inter-area modes, the inferred sources of the oscillation refer to the areas participating in the oscillation.

The chosen method, Independent Component Analysis (ICA), aims to decompose a matrix of measurements from various points into a set of common sources that contribute to the measurements. ICA additionally determines a matrix relating the sources back to the measurements. This mixing matrix indicates how much of each source is present in each measurement. Mathematical manipulations that change the results of ICA into physically meaningful interpretations were also presented. These manipulations are the changing of the sources into positive-peaked narrowband functions which relate to physical frequencies present in the data, and conversion of the mixing matrix into a matrix of significance indices (*SIs*) which are normalised values indicating the relative strengths of oscillations in the measurements.

The method was then applied to data from both the simulated and measured scenarios presented in Chapter 3 to determine the critical inter-area mode frequency in Finland. The frequency was determined to be 0.3119 ± 0.0060 Hz from the simulated data while it was determined to be 0.354 ± 0.010 Hz from the measured scenario. This difference in estimates was attributed mainly to conservative choices of model parameters for the simulation and differences in the system configuration between the model and the actual operational scenario. The effect of noise and the window duration of data on each estimation were also considered. It was concluded that neither significantly affects the estimation of the frequency.

Finally, the *SIs* were used to demonstrate the ability of the ICA method to identify the measurement locations participating in an inter-area oscillation. ICA correctly identified that measurement locations in Southern Sweden, Southern Denmark and Southern Finland participated in the 0.3 Hz oscillation from the simulated scenario data, and that only measurements locations in Southern Finland participated in the oscillation from the measured scenario data. The reason for the latter inference is that measured data from Sweden or Norway were not available for analysis.

6. Damping Estimation

Having obtained the oscillatory frequencies, the next step for system identification is estimation of the damping of the modes. This chapter presents a method for estimation of mode damping, the Random Decrement (RD) method. The chapter begins with an overview of RD and an explanation of how to estimate the damping of a mode from output measurements during ambient operation of a power system. A further development to improve the accuracy of the RD method using the matrix of significance indices (*SIs*) from Independent Component Analysis (ICA) is also presented. The chapter then continues to present the reasons for selection of various parameters of the RD method based on simulations and then presents the results of RD on both the simulated and measured data from the Nordic case study system introduced in Chapter 3, showing that the method is suitable for damping estimation. The results presented in this chapter have been accepted for publication by the IEEE Transactions on Power Systems in a journal paper titled, “A Multivariate Approach towards Inter-Area Oscillation Damping Estimation under Ambient Conditions via Independent Component Analysis and Random Decrement.”

6.1. Overview

The aim of this chapter is to present a method that is capable of determining the impulse response of the system to a particular mode from ambient data. This is clearly demonstrated in Figure 58 which shows an example of ambient data on the left and a corresponding second order decay function on the right. The second order decay function represents a linear approximation of the impulse response of an electrical power system to a mode exciting it (Kundur, 1994).

The stability of the system is inferred from the damping of the exciting mode. This damping measure, ζ , can be obtained from the frequency of the mode, ω , and the rate of decay of the impulse response, σ , as shown in Equation 50. This value can be converted to a percentage by multiplying by 100.

$$\zeta = \frac{-\sigma}{\sqrt{\sigma^2 + \omega^2}} \quad \text{Equation 50}$$

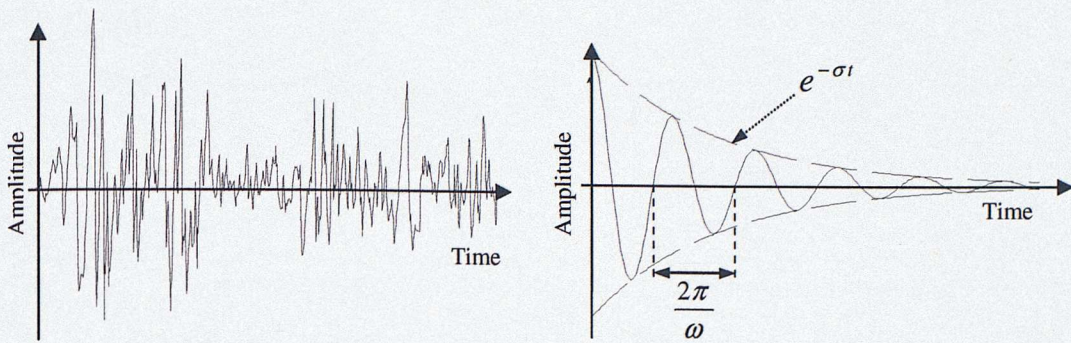


Figure 58: A - Example of an ambient response, B - Example of a second order decay function

6.1.1. Estimation of Impulse Response

As previously discussed in Chapter 1, the determination of system impulse response, and hence damping, is a challenge in ambient operation because the system measurements are a convolution of the system response and unknown load variation. This problem of system identification from outputs-only has been investigated extensively in the fields of structural and mechanical engineering, especially in the determination of the stability of structures that are in daily use and are excited by external factors such as wind on bridges. A method known as the Random Decrement (RD) technique, which was initially developed by Henry Cole and his fellow colleagues for application to space structures and aeroelastic systems (Chang, 1975, and Cole, 1973), can be applied to the problem of damping estimation in power systems. Since its original application, it has been applied to other engineering fields such as system identification of large structures (Ibrahim, 1977) and damping measurements of soil (Al-Sanad *et al.*, 1986).

The RD method is an averaging technique in the time domain. It is described in Brincker (1992) as “a fast technique for estimation of correlation functions for Gaussian processes.” The resulting average is known as the RD autocorrelation signature and it is obtained by averaging various segments, $y(t_r : t_r + \tau)$ of length τ , of a mean-centered signal collected every time the signal passes through a threshold, a , (either above or below at times t_r - triggering condition), where N represents the total number of segments that fulfil the threshold condition, as shown in Equation 51.

$$\hat{D}_{YY}(\tau) = \frac{1}{N} \sum_{r=1}^N y(t_r : t_r + \tau) \quad \text{Equation 51}$$

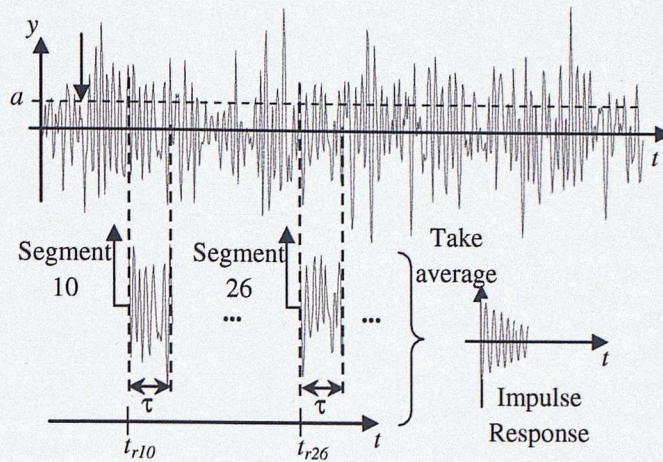


Figure 59: Demonstration of triggering mechanism of the Random Decrement method

This process is demonstrated in Figure 59. It shows a threshold, a , which is exceeded from time to time by the signal. Segment 10 and Segment 26 shown in the figure are examples of the signal segments following the 10th and 26th excursion. It is these (and other segments) that are averaged to find the RD signature. Brincker (1992) further clarifies that this RD autocorrelation signature is proportional to the free decay response of the system under the assumption of white noise loading. Papoulis (1991) defines white noise as a process in which the values of the process at any two given times are uncorrelated. During the ambient operation of power systems, the excitation to the system can be assumed to be Gaussian and uncorrelated (white noise). Hence the RD signatures obtained from output measurements from the system can be assumed to be estimates of the free decay response of the system, hence making the RD technique applicable to estimation of system damping of modes.

This concept is more easily explained by considering the nature of the response of a system to ambient excitation. Cole (1971) suggested that under ambient excitation, the measured response of a linear system $y(t)$ can be decomposed into three distinct responses: a step response, $y_{step}(t)$, an impulse response, $y_{imp}(t)$ and a random response, $y_{rand}(t)$ as shown in Equation 52.

$$y(t) = y_{step}(t) + y_{imp}(t) + y_{rand}(t) \quad \text{Equation 52}$$

Mean-centring the signal prior to application of the RD method ensures that the average of the step responses over many segments is zero. Similarly, the random components average to zero because the signal excursions are expected to move equally above and below the mean of the signal. The

impulse response does not average to zero because of the procedure of choosing segments following thresholds which selects the sampled segments which contain the response of the system to random impulsive events which are just a little larger than usual. The selection of a suitable triggering threshold is discussed in section 6.2.2. The average of the sum of responses would hence be an impulse response function. The estimation of the system free decay response using the RD method is therefore simple because only detection of triggering points and averaging is performed.

In other cases when ambient operation cannot be assumed, the RD signatures are estimates of correlation functions and thus require the use of correlation based approaches for estimation of system properties.

6.1.2. Estimation of Damping

Having obtained the impulse response of the system to the exciting mode using the RD method, the next step is to determine the damping of the mode from the impulse response. The impulse response is in the form of the example on the right hand of Figure 58, and resembles a transient response of the system. There is a wide range of methods available in literature for analyzing transient responses, for example the Prony method, the Hilbert-Huang Transform (HHT) (Laila *et al.*, 2009) and wavelets. These methods have their own characteristic advantages, for example, the Prony method can identify multiple modes that are closely spaced while HHT and wavelet methods work better in the presence of non-linearity. The simplest available method that can be applied to this problem is the exponential-fit method. This method aims to fit a second order decay function to the RD signature.

The RD signature can be assumed to be in the form of an exponentially decaying sinusoid (Kijewski and Kareem, 2000). It can therefore be described by the equations 53 and 54, where σ is the damping coefficient, ζ is the damping ratio of the system, ω_n is the natural frequency of the oscillation, ω_t is the observed frequency of the oscillation and ϕ is a phase (Seborg *et al.*, 2004).

$$z = Ae^{-\sigma t} \cos(\omega_t t + \phi) \text{ where } \omega_t = \omega_n \sqrt{1 - \zeta^2} \quad \text{Equation 53}$$

$$\sigma = \omega_n \zeta \quad \text{Equation 54}$$

The parameters of the second order decay function can be estimated using a least squares fitting

algorithm. Figure 60 presents a flowchart that demonstrates the process of damping estimation using the RD method.

1. Using filtered PMU measurements, containing only one inter-area mode, from ambient operation of power system, set a threshold level and every time the signal crosses the threshold, collect a signal segment of defined length.
2. Average the segments to obtain the correlation estimate, which corresponds to the free decay response under the assumption of stochastic excitation.
3. Fit an exponentially decaying sinusoid to the obtained free decay response to determine the decay rate. Hence determine the damping ratio using the estimated parameters of the exponentially decaying sinusoid.

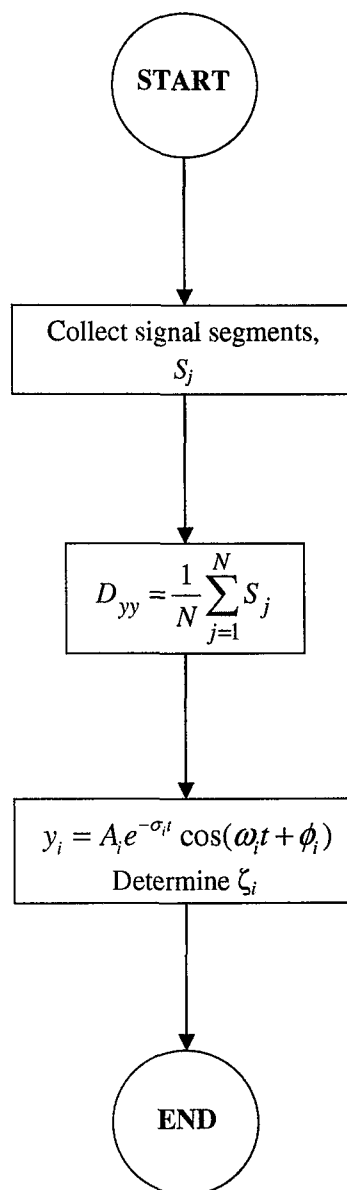


Figure 60: Flowchart demonstrating the Random Decrement method

6.2. Method Development

The previous section has provided an overview of the methods that were proposed for determination of the damping of a detected mode. However, further adjustments were made for the following reasons; this section presents how the methods were developed in order to address these issues.

- Most damping estimation methods including the RD method require the careful selection of a signal in which the modes of interest participate greatly in order to correctly estimate the

damping ratio of a mode. In order to automate the estimation when various measurements are present, a multivariate implementation of the methods is necessary.

- There are various parameters that need to be chosen for the RD method as was discussed in the previous section, for example the triggering threshold for averaging. These parameters depend on the application of the method and hence need to be carefully selected.

6.2.1. Multivariate Damping Estimation

The RD method is a univariate technique, yet the data-set available for analysis is multivariate because each PMU at each location generates measurements of several quantities. Assuming that the power system dynamics are linear, the system damping of a mode is expected to be the same regardless of the quantity analyzed. However, the estimation of damping might be affected by the location of the device measuring the output because a good estimate of damping can only be obtained using a signal in which the mode of interest has a high participation; inter-area modes are most observable in areas participating in the oscillation while in all other areas, the observability is less.

It is proposed that a robust value of the damping can be obtained by utilizing all the measured outputs whilst mitigating the effect of an output with a low modal participation by using the matrix of significance indices (*SI*s) obtained using Independent Component Analysis (ICA) to weight the damping estimates obtained for each output. The reason for this is that the *SI*s represent the levels of participation of the mode in each output hence outputs with higher participation will have higher *SI*s. Using the individual damping estimates from each measurement and the *SI*s from ICA, the estimated system damping of the *s*th mode, ζ_s , can therefore be expressed by the following equation, where *m* represents the number of measured outputs and ζ_i and *SI*_{*i*} represent the damping estimate from and significance index of the particular (*s*th) mode in the *i*th measured output:

$$\zeta_s = \frac{\sum_{i=1}^m \zeta_i SI_i}{\sum_{i=1}^m SI_i} \quad \text{Equation 55}$$

This simple algorithm works most efficiently when there is only one mode present in the signal because the S_i s correspond to only one mode as estimated by ICA. The Prony method would be a better tool for obtaining the damping ratios if many modes are present because the Prony method fits to the data a model which accounts for the presence of different modes rather than only one as implemented in this thesis. However, the use of the Prony method would require the choice of a signal in which all the modes have a high participation – this can be very tricky.

In order to ensure that only one mode is present in the data, a pre-filtering stage based on the results of ICA was introduced prior to the application of RD so as to obtain the output response band-limited to each detected mode. This ensures that the RD signature contains only one mode prior to application of the algorithm described in this section. Figure 61 demonstrates how this filter was implemented with relation to the outputs from ICA and the developed method. The new algorithm is referred to as RD-ICA from here on.

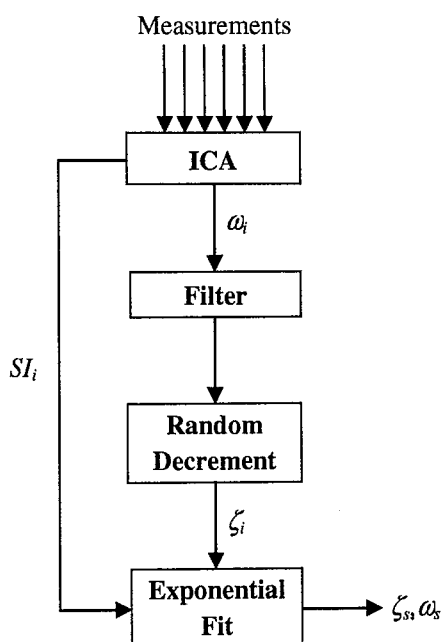


Figure 61: Implementation of RD-ICA

6.2.2. Parameter Selection for RD method

As previously discussed in the overview of the RD method, there are some parameters that need to be chosen. These parameters are:

- **Threshold for triggering:** The threshold for triggering needs to be sufficiently high such that the sampled segments contain the response of the system to random impulsive events which are just a little larger than usual. This ensures that the average of the segments represents the system impulse response to the exciting mode.
- **Window duration over which triggering is applied:** The window duration determines how many segments are collected before averaging is applied.
- **Length of the RD signature:** The MATLAB optimization toolbox was used to fit an exponential decay function to the absolute values of the mean-centred impulse response (to both the maxima and minima of the function) obtained using the RD method. Due to the sensitivity of the parameters from the exponential fit to the number of cycles of the oscillation captured, a robust value was required.

The choice of these parameters is also dependent on the application of the method and therefore they need to be chosen such that the damping estimates obtained using the method for electrical power systems are reliable. The first of these parameters was chosen using a linear model of a system with a pair of complex conjugate poles while the other two parameters were chosen using data from the simulated scenario introduced in Chapter 3 because the expected damping value is known.

Threshold for Triggering: Electromechanical modes are typically less than 20 % damped. When the damping of modes is greater than 20 %, oscillations in the data die out quicker than they can be detected. A robust threshold value for triggering which produces good quality of results for data with damping up to 20% therefore needs to be selected. The aim of doing this is so that the method can be confidently used with PMU data where the damping value is unknown but can be expected not to exceed 20 %.

In order to select this value, simulations were carried out in SIMULINK using a linear system consisting of a pair of complex conjugate poles. By selecting the values of the poles, the actual mode frequency and damping value was varied to simulate damping values up to 20% for frequencies between 0.2 Hz and 1 Hz (the inter-area mode range). The system was then excited using a random input in order to generate an output that resembles ambient operation of a power system. The aim was to use the RD technique to estimate the damping of the mode from the simulated output using

various thresholds for triggering. By comparing the estimated value with the actual value used to create the output measurements, the robust threshold value could be determined.

There are different triggering conditions that have been implemented in literature, for example:

- using a level triggering where only one threshold level is used (Cole, 1973)
- using range triggering where various values above a defined threshold level are used
- using a vector triggering scheme (Asmussen *et al.*, 1999)

The different triggering conditions can also be used with other constraints such as derivative constraints as demonstrated in Brincker *et al.* (1992). The triggering condition that has been adopted in this research is range-triggering with a derivative constraint as shown in Equation 56: a segment is collected once the signal level goes higher than the threshold a , and reaches a maximum or minimum (hence the derivative is 0). This condition was selected in order to ensure that the sampled segments contain the response of the system to random impulsive events which are larger than usual.

Figure 62 shows the structure of the model that was used.

$$y > a \text{ and } \frac{dy}{dt} = 0 \quad \text{Equation 56}$$

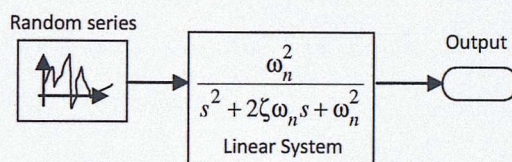


Figure 62: SIMULINK model used to obtain robust threshold value. ω_n is the natural frequency and ζ is the damping value

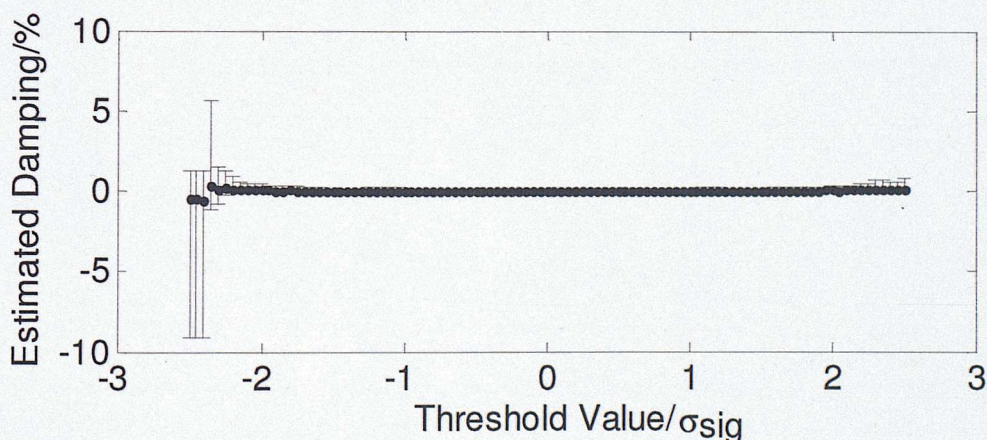


Figure 63: RD damping estimates using different threshold values for 0% actual damping

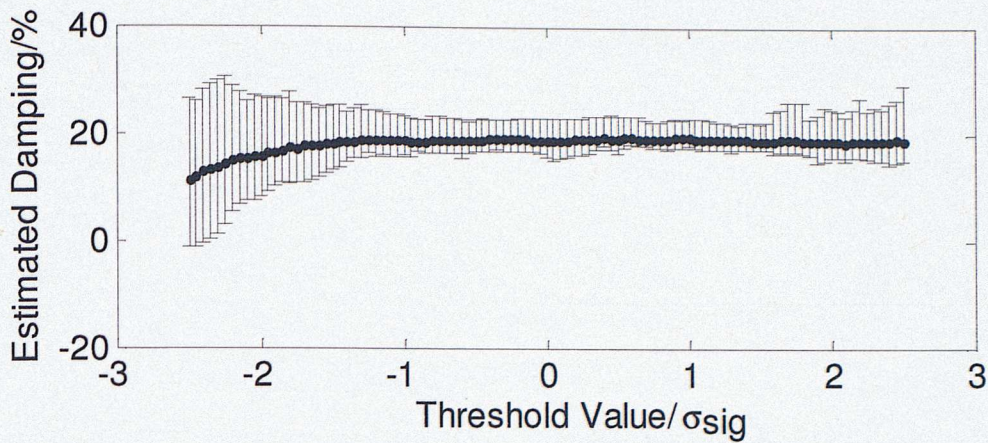


Figure 64: RD damping estimates using different threshold values for 20% actual damping

Figures 63 and 64 show the resulting estimates of the damping ratio obtained for different thresholds where the actual damping values are known to be 0% and 20% respectively (from the system pole selection). Each graph was obtained by fixing the RD threshold value, a , as a fraction of the output signal standard deviation (σ_{sig}), and varying the mode frequency (system poles) using the SIMULINK model parameters, ω_n and ζ . The estimated damping value for each case was stored; this procedure was repeated for different threshold values. The error-bars indicate the maximum and minimum estimates for each threshold value, for all frequencies in the inter-area mode range. The plots in Figures 63 and 64 suggest that a threshold value of $-0.25\sigma_{sig}$ is suitable because the variance of the damping estimate is both low and does not change considerably around this threshold.

Therefore, a threshold of $-0.25\sigma_{sig}$ was used in the work of the thesis.

Window Duration over which Triggering is Applied: The window duration refers to the total time duration over which averaging is applied in order to obtain one estimate of the impulse response function and hence damping of the mode.

The selection of a window duration for application of triggering is important because the longer the window, the more the number of segments that can be collected and averaged and hence the more accurate the impulse response estimation. However, as previously discussed in the previous chapter, the window duration for each frequency or damping estimation affects the speed of response of the method.

In order to determine the optimum window duration over which triggering should be applied, the window duration was varied from 1 to 11 minutes in steps of 2 minutes to determine the effect on the estimate of damping made using the RD-ICA method. This time window was slid forward every 30 s in order to get a new damping estimate. The MATLAB normfit toolbox was then used to determine the mean estimate of damping and its confidence interval over the whole duration of the simulation. Data from the simulated scenario in Chapter 3 was used because the expected damping value was known to be about 7 %.

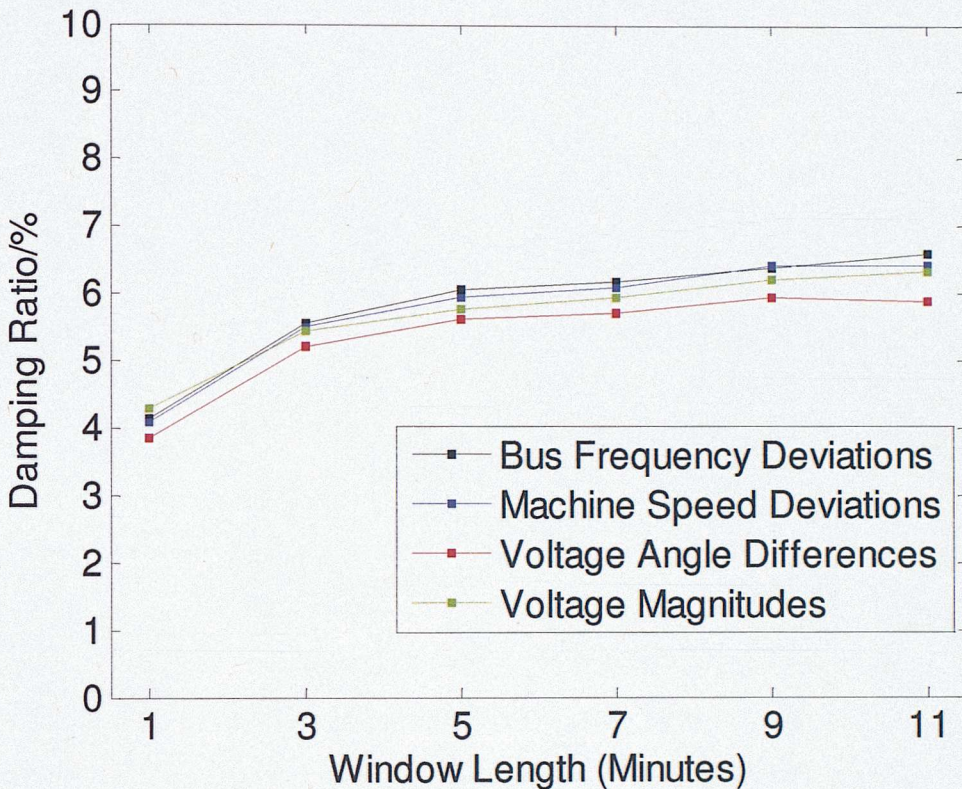


Figure 65: Variation of mean of damping estimate with window length

Figure 65 shows the estimated mean damping of the mode for the different window durations and for the different quantities while Figure 66 shows the standard deviation of the estimated mean damping for the same window lengths and quantities. From the results, it can be seen that the mean values of the damping estimate increase as the duration of the window increases, tending towards the true damping value. Also, the standard deviations of the estimates decrease significantly for all quantities as the window duration increases. Both these observations are expected because the longer the window duration, the more segments collected and averaged, the more accurate each damping

estimate is and hence the less the spread in the estimates over time. Additionally, the estimates using the different quantities are in general conformity with one another.

It can be concluded that the duration of the data window should be kept greater than 9 minutes for a 0.3 Hz oscillation. This window duration, l_w , can be generalised to any inter-area mode frequency, f , using the number of oscillation cycles present in the time window to give the optimum window length that is dependent on frequency, $l_{w,f}$, as shown in equations 57 and 58.

$$l_w \geq \frac{9 \times 60}{0.3} \text{ cycles} \quad \text{Equation 57}$$

$$l_{w,f} \geq 1800f \text{ seconds} \quad \text{Equation 58}$$

Therefore, a window duration of $2200f$ seconds, where f is the inter-area mode frequency, was used in the work of this thesis (corresponding to 11 minutes for a 0.3 Hz oscillation).

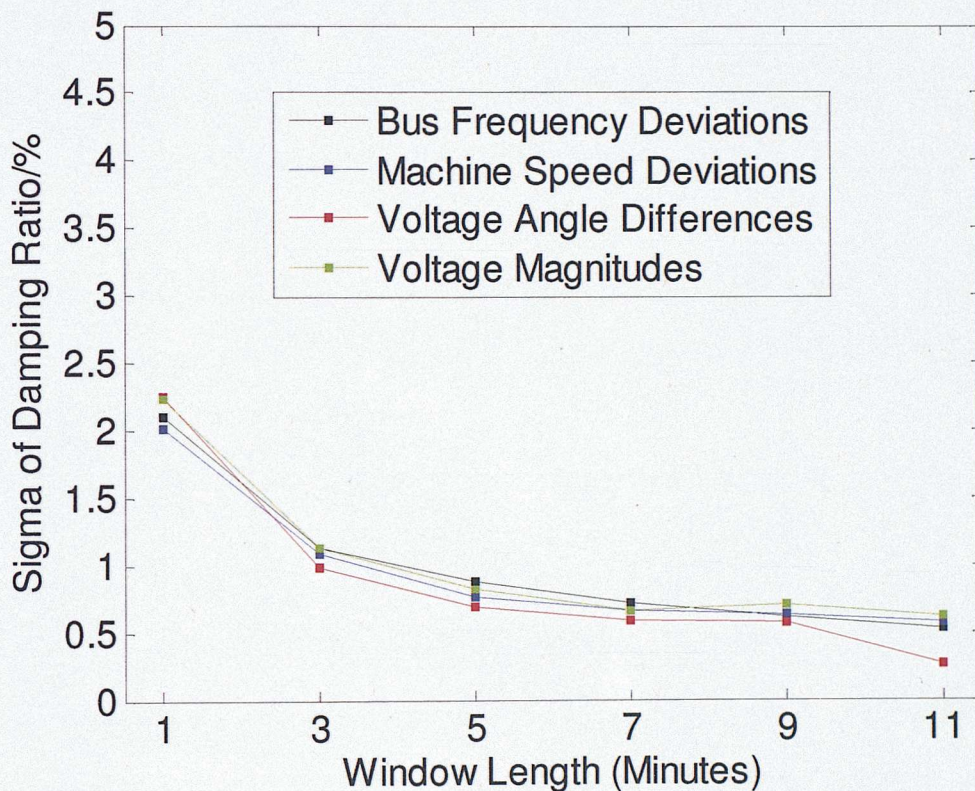


Figure 66: Variation of standard deviation of damping estimate with window length

Length of RD Signature: The final parameter that needs to be chosen is the length of each segment collected when the trigger threshold condition is achieved. This segment length is equivalent to the length of the RD signature because the latter is obtained by averaging the different segments. This

length can be expressed as a number of oscillation cycles. The choice of a robust length is necessary because the curve-fitting technique implemented to estimate the damping is sensitive to the number of oscillation cycles captured.

In order to determine this value, the outputs from the simulated scenario were analysed using a window duration of 11 minutes and the damping was estimated using the curve-fitting technique. The time window was slid after 30 s to obtain a new damping estimate and so on until the end of the simulation data. The means and standard deviations of the damping estimates were then plotted as a function of the number of cycles used in the RD technique. The cycles were increased from 1 to 8 in steps of 0.5.

Figure 67 shows the results from the analysis where the error bars indicate the standard deviation of the mean estimates for each number of RD cycles. It can be observed from the figure that the mean damping increases towards the true value as the number of cycles used is increased from 1 to 4.5, after which the estimates do not vary much. A segment length of six oscillation cycles is a robust value for the segment length because it lies in the area of the graph where the damping estimate does not change much. This corresponds to a time duration of 20 s for a 0.3 Hz oscillation. Figure 68 shows the estimated RD signature for the 0.3 Hz mode using six cycles in the RD (* points) and the second order decay curve that was fitted using the MATLAB optimization toolbox (solid line). The curve matches the estimated signature well.

A value of six oscillation cycles was therefore used consistently in the work of the thesis.

6.3. Results from Case Study System

Having determined robust values for the parameters of the RD method, it was tested using the data presented in Chapter 3, from the Nordic case study system. In the following subsections, the simulated scenario is first used to demonstrate the effectiveness of the multivariate RD-ICA method that was proposed in a previous section of this chapter. The simulated scenario is then used to estimate the damping ratio of the critical 0.31 Hz inter-area mode that was detected using ICA, and the result is compared to the expected value of 7 % known from linearization of the full Nordic model. Finally, the performance of the method for different levels of added noise is evaluated after

which the method is applied to data from the measured scenario to determine the actual system damping of the critical 0.35 Hz mode.

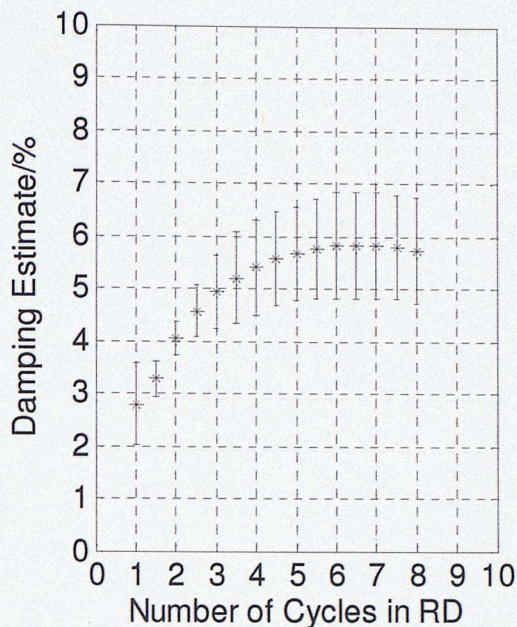


Figure 67: Mode damping estimates using different number of cycles in RD for 0.3 Hz

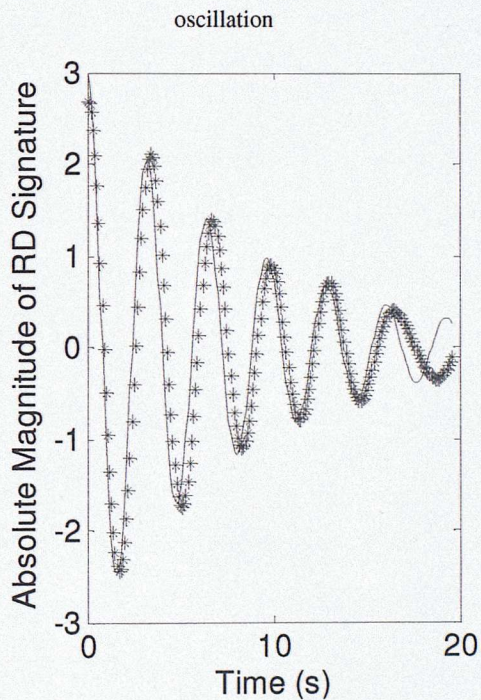


Figure 68: Estimated RD signature for the 0.3 Hz oscillation obtained using 6 cycles (* points) and second order decay curve fitted using MATLAB optimization toolbox (solid line)

6.3.1. Simulated Scenario

The RD method was applied to the voltage angle difference data using a sliding time window to determine the damping at different locations. The voltage angle differences were obtained by finding the relative angles between the measurements at the locations in Table 33 (Chapter 5) relative to the measurements at Loviisa (Southern Finland). Voltage angle differences are theoretically expected to have a greater visibility of inter-area modes due to the fact that they determine the relative flow of electric power between two generators and are therefore directly related to the eigenvalues of the power system which are the inter-area modes (Kundur, 1994). The voltage angle differences can thus be used to identify the areas participating in an inter-area oscillation because locations within the same area will have negligible angle differences hence these differences will have a low observability of the oscillation. Additionally, taking the angle differences removes a low frequency trend that is typical of voltage angle measurements. The voltage angle differences that were used in the analysis are summarised in Table 6. The aims of the analysis were to:

- Determine the effectiveness of the developed multivariate damping algorithm
- Determine the effect of noise on the estimates of damping
- Investigate the effect of choice of measurement quantity for analysis on the estimate of damping

Difference Number	Voltage Angle Difference
1	Olkiluoto (Southern Finland) - Loviisa (Southern Finland)
2	Pirttikoski (Northern Finland) - Loviisa (Southern Finland)
3	Harsprånget (Northern Sweden) - Loviisa (Southern Finland)
4	Stornorrfors (Northern/Central Sweden) - Loviisa (Southern Finland)
5	Forsmark (Central/Southern Sweden) - Loviisa (Southern Finland)
6	Oskarshamn (Central/Southern Sweden) - Loviisa (Southern Finland)
7	Ringhals (Central/Southern Sweden) - Loviisa (Southern Finland)
8	Karlshamn (Southern Sweden) - Loviisa (Southern Finland)
9	Rana (Northern Norway) - Loviisa (Southern Finland)
10	Aura (Central Norway) - Loviisa (Southern Finland)
11	Kvilldal (South Western Norway) - Loviisa (Southern Finland)
12	Tokke (South Eastern Norway) - Loviisa (Southern Finland)
13	Asnaesvaerket (Eastern Denmark) - Loviisa (Southern Finland)

Table 6: Voltage angle differences in simulated scenario

Effectiveness of Multivariate Damping Algorithm: The RD technique was applied to each of the voltage angle difference measurements estimates in order to determine the mean damping of the

mode and its confidence interval (CI) at each of the different locations. The developed RD-ICA algorithm was then used to make an estimate of the system-wide damping of the mode utilising the *S*/s from ICA. Figure 69 shows a plot of the estimated mode frequency versus the damping for the estimates at each individual location together with the CIs as indicated by the error bars (x points). The \diamond point in the figure indicates the mean system-wide damping of the mode and the CI of the estimate made using RD-ICA.

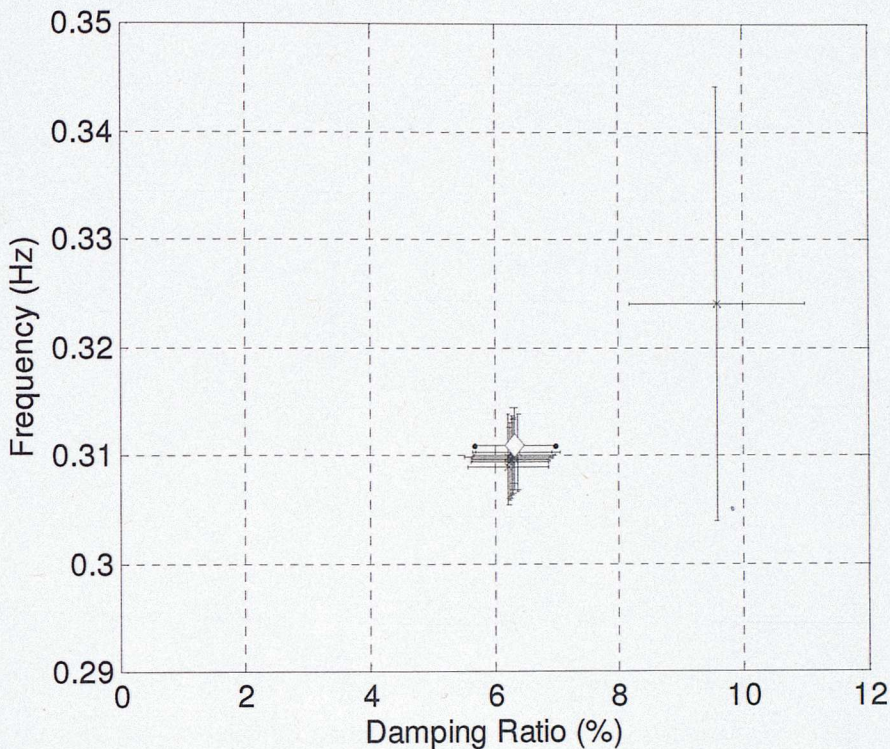


Figure 69: 0.31 Hz critical mode damping estimates using voltage angle differences

It can be observed that the damping estimate using RD-ICA mitigates the effect of the outlier in the plots. The outlier has a higher damping estimate than the average as shown in Table 7 because of the absence of the 0.31 Hz mode in this angle difference (difference number 1: Olkiluoto – Loviisa). This is expected because Olkiluoto and Loviisa are both in the same area of Southern Finland and therefore are not expected to have a relative oscillation at the frequency of the inter-area mode. This can be verified by observing the contour map of the *S*/s shown in Figure 70: there is no 0.31 Hz activity in difference number 1 throughout the whole time duration. On the other hand, the rest of the angle differences relative to Loviisa are from locations that are not in the same area as Loviisa and

therefore the 0.31 Hz oscillation is visible in them with varying levels of significance as indicated by the intensity of the contour plot in Figure 70.

Difference Number	Damping estimate
1	9.58 ± 1.41
2	6.23 ± 0.65
3	6.25 ± 0.63
4	6.26 ± 0.62
5	6.25 ± 0.62
6	6.29 ± 0.64
7	6.30 ± 0.63
8	6.29 ± 0.65
9	6.22 ± 0.69
10	6.32 ± 0.65
11	6.38 ± 0.68
12	6.38 ± 0.67
13	6.28 ± 0.63
Average using RD-ICA	6.32 ± 0.65

Table 7: Damping estimates using voltage angle differences in simulated scenario

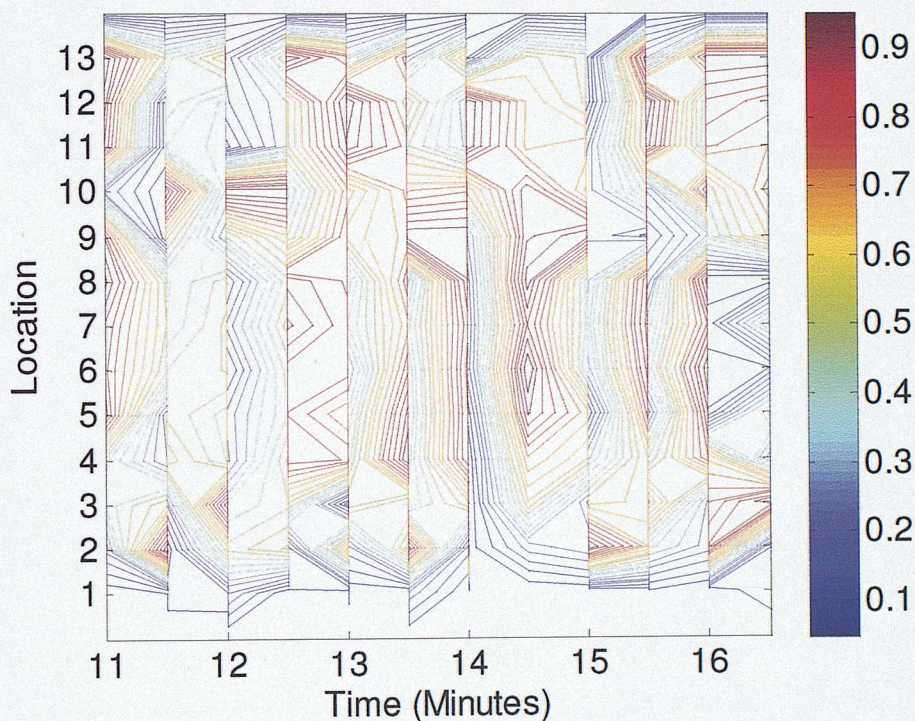


Figure 70: Contour plot of SIs at different times for voltage angle differences

The use of the SIs therefore mitigates the effect of the use of a signal with a low observability of the inter-area mode. Hence, it allows the use of a wide number of measurements without the need of manual selection of a suitable signal for analysis.

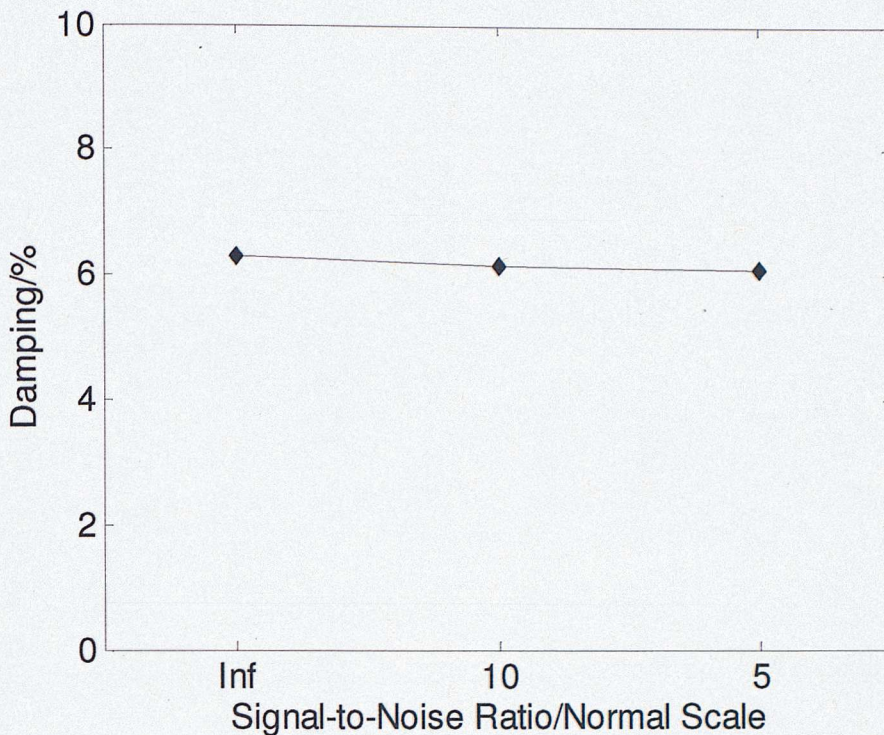


Figure 71: Variation of mean of damping estimate with SNR using voltage angle difference data

Effect of Noise on Estimation: RD-ICA was then used to determine the effect of noise on the estimation of the mode damping for a fixed quantity and window duration, as was done for the frequency estimation. Just as before, noise was added to the voltage angle difference data in order to achieve signal-to-noise ratios (SNRs) of infinity, ten and five respectively. A window duration of 11 minutes was used for each estimation. Figure 71 shows the results of the investigation. It can be observed that the SNR of the data has negligible impact on the mean damping ratio estimation.

This therefore implies that the RD method can be used on real measurements, and the results of the estimation using real data are presented in the next sub-section.

Effect of Use of Different Quantities: RD-ICA was applied to the different signal quantities that were available in order to investigate whether the selection of a particular quantity has an effect on the estimate of the system-wide damping of a mode.

Table 8 shows the estimates of the damping ratio of the 0.31 Hz inter-area mode with the CI for all available quantities using a window duration of 11 minutes and using the data with an SNR of five.

Quantity	Approximate Damping Ratio, ζ (%)
Machine Speed Deviations	6.51±0.49
Rotor Angle Differences	6.75±0.64
Voltage Angle Differences	6.32±0.65
Bus Frequency Deviations	6.48±0.59
Average	6.52±0.60

Table 8: Damping estimates for different quantities in simulated scenario

The table shows that the mean estimates from different quantities are consistent and lie within the error estimates of one another. This indicates that the specific quantity used in the estimation does not have a significant effect on the estimate of the damping of an inter-area mode. The results can hence be combined by finding the mean of all the estimates. This gives an average inter-area mode damping ratio estimate of 6.52 % with a CI of ± 0.6 %.

6.3.2. Measured Scenario

Having demonstrated that the RD-ICA method can be used to estimate the damping ratio of an inter-area mode using simulated data, it was then applied to data from the measured scenario. A window duration of 11 minutes was used and this window was slid every 30 s to obtain a new estimate for the damping ratio of the 0.35 Hz inter-area oscillation detected using ICA. This was done for all measured quantities: the active power flows, current flows, derivatives of the frequency and the voltage angle differences. The aims of the analysis were:

- Observe the typical variation of the estimate of damping for extended periods during ambient operation
- Investigate the effect of choice of measurement quantity for analysis on the estimate of damping
- Demonstrate the effectiveness of the developed multivariate damping algorithm on real measured data

Typical variation of damping estimate: The variation of the damping estimate over the whole duration of the measurements (about four hours) was plotted; it is shown in Figure 72. It can be observed that there is a great deal of variation from one instant to the next. This is expected because the generation and loads are expected to change rapidly in a power system resulting in small changes

in damping of modes. However, this behaviour is not desirable from the view point of operation because it distracts the operator from the main focus - the trend in the damping over time.

The variation was therefore smoothed-out using the 20-point moving average filter that was introduced to smooth-out the frequency estimates in the previous chapter. Figure 73 shows the filtered damping estimates over time. There are generally changes in the smoother-damping values over time. This is expected due to changes in the power flows over the four-hour time duration.

Effect of Use of Different Quantities: The estimates of damping obtained from the different quantities follow one another in general as shown in Figure 73. This is expected because all the quantities are either directly or indirectly related to the flow of power in the system. The estimates made using the active power flows and the current flows are roughly the same because they are directly related to each other (since power = voltage \times current). The derivatives of frequency is indirectly dependent on the active power flow because the latter affects the frequency of the grid. However, it can be observed that the estimate made using the voltage angle differences is slightly and consistently lower than the estimates from the other quantities throughout the duration of the estimation. This can be confirmed by comparing the average estimates of damping for the different quantities over the whole time duration of estimation which shows that the average of the estimates of the damping ratio and its CI using voltage angle difference is lower than the estimates from the other quantities (the MATLAB normfit toolbox was used to determine the mean damping ratios and CIs of the estimates for each quantity). Table 9 summarises the results of the analysis.

Quantity	Estimated Damping Ratio, ζ (%)
Current Flows	7.05 \pm 0.75
Active Power Flows	7.16 \pm 0.80
Voltage Angle Differences	6.22 \pm 0.63
$d/f/dt$	7.23 \pm 0.96
Average	6.92 \pm 0.79

Table 9: Frequency estimates for different quantities in measured scenario

Also, Figure 73 shows that the estimate of the damping made using the voltage angle difference has more pronounced oscillations over time compared to the other quantities despite having a lower CI of the damping estimate. A possible explanation for these differences is the dependence of the voltage angle on the reactive power in the system. Reactive power refers to the power flow through

reactive or power storage elements of a circuit (capacitors and inductors). Power networks are typically designed to contain high-reactance equipment that compensate for the change in reactive power in different parts of the network. Reactive power affects the voltage at different points in the grid and therefore these compensators have a greater effect on the voltage angles than on the other quantities. Hence, the estimate of damping made using the voltage angle differences will be affected more than the other quantities in highly-compensated networks. The Nordic grid has a high degree of reactive power compensations due to the high level of wind generation (Zobaa and Jovanovic, 2006). Nevertheless, the mean estimates of damping obtained using the different quantities lie within the CIs of one another. They are therefore consistent with one another; this is generally expected to be the case in less compensated networks. The estimates from the different quantities can therefore be combined by taking the mean to give an average damping ratio of 6.92 % with a CI of ± 0.79 % for the 0.35 Hz inter-area mode.

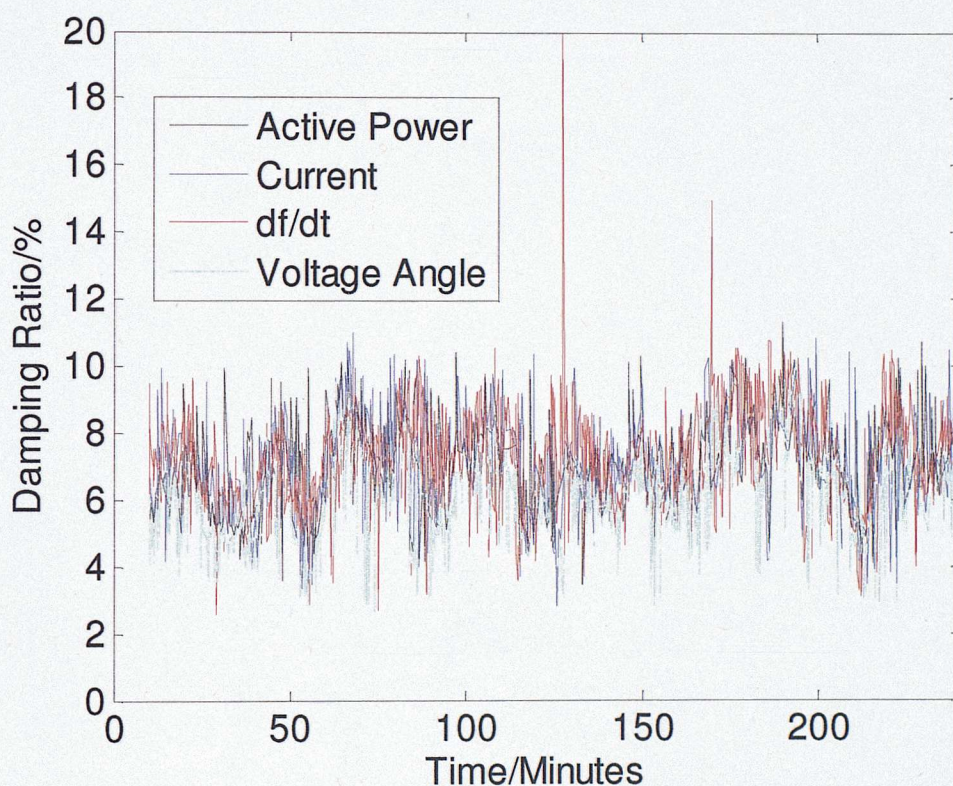


Figure 72: Unfiltered variation of damping estimate over time

Effectiveness of Multivariate Damping Estimation: Figure 74 demonstrates the effectiveness of using the *S*'s from ICA when the frequency derivative measurements in are used to estimate the

damping ratio of the 0.35 Hz inter-area mode. The locations of the measurements of the frequency derivatives are the same as those shown in Table 4 in the previous chapter.

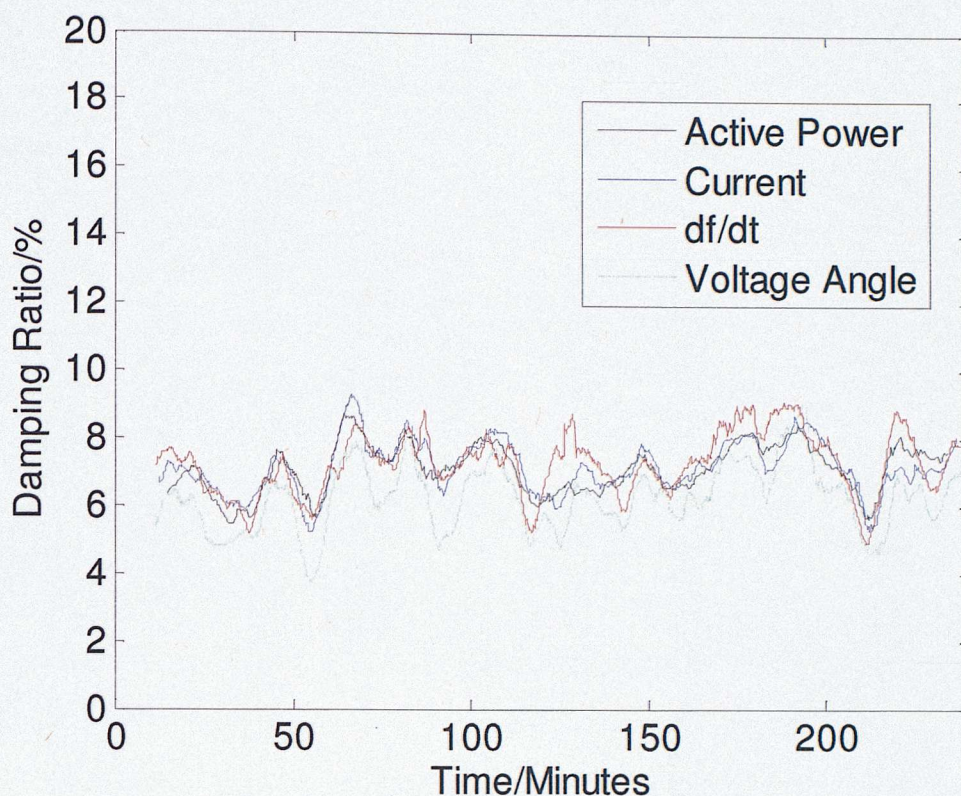


Figure 73: Filtered variation of damping estimate over time

As can be observed in Figure 74 and Table 10, RD-ICA mitigates the effect of two outliers in the estimates. These estimates are higher than the rest because the signals analysed were signals at locations where the 0.35 Hz mode has a low participation. These locations are 2 and 4; Figure 56 in the previous chapter showed the activity of the 0.35 Hz mode at all the locations of the measurements and it was concluded that the activity at locations 2 and 4 was negligible.

RD-ICA is therefore capable of automatically mitigating the effect of signals with low observabilities of modes without any manual selection of an optimum signal.

Measurement Number	Damping estimate
1	7.22±1.08
2	8.84±0.93
3	7.10±0.96
4	8.51±0.88
5	7.06±0.95
6	7.51±0.92
7	7.35±0.92
Average using RD-ICA	7.23±0.96

Table 10: Damping estimates using voltage angle differences in simulated scenario

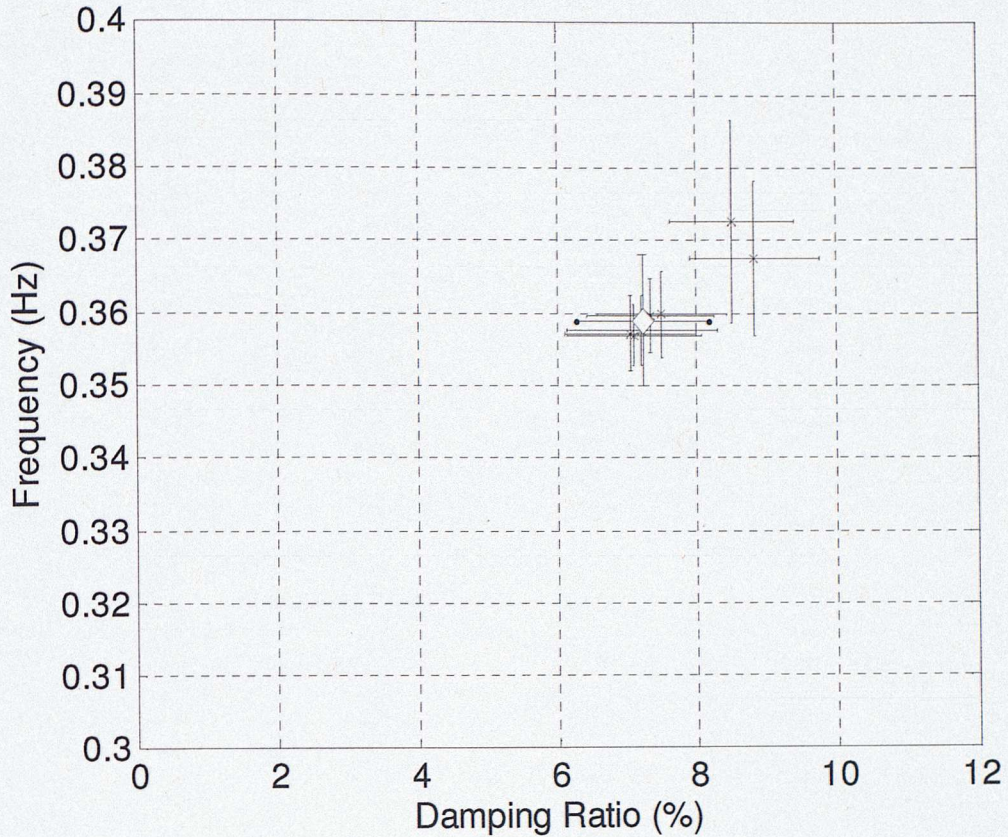


Figure 74: 0.35 Hz critical mode damping estimates using derivatives of frequency measurements

6.3.3. Discussion of Average Damping Results

The estimated inter-area mode damping ratio from the simulated scenario of 6.52% is slightly lower than the 7% value that was expected from the linearization of the system model. However, the CI of the estimate is $\pm 0.6\%$ which implies that there is a 67% probability that the damping of the mode is between 5.92% and 7.12%, in whose bounds the 7% value lies. A possible explanation why the mean value obtained using the RD-ICA technique is less than the value expected is the nature of the perturbation that was applied to produce the ambient data in the simulation. As previously explained, the theoretical basis of the RD method assumes that the excitation applied to a system is random and Gaussian. However, in the simulation, the points chosen to receive an increase or decrease in load were not chosen randomly and the excitation sequence applied may not be classed as being Gaussian. As a result, it is expected that the RD method would underperform in such circumstances;

the estimated value is expected to have a bias because the RD signature is not a true estimate of the impulse response of the system to the exciting inter-area mode.

The damping estimate obtained from the measured scenario (6.92 %) was however very close to the expected value. The CI of the estimate however is quite high (± 0.79 %); this can be explained by the great changes in damping over time that can be observed in Figure 73. There were episodes of time where the mode damping dipped or jumped in big steps. The most credible explanation for these changes is changes in the operation of the system in terms of variations in the power transferred; the 1050 MW export value that was used to create the simulation scenario was chosen from the measured scenario but reflects the average power that was transferred. This does not imply that the power transfer was constant over the 4 hr time duration of the measurements. Additionally, changes in loads and generation could easily cause changes in the damping levels.

6.4. Summary

This chapter has presented the method identified and used for determination of damping of inter-area modes in power systems. The chosen method, the Random Decrement (RD) method, is a method that estimates the correlation function of a system by the simple step of averaging segments of the measured signal, collected using an appropriate triggering technique. Under the assumption of white noise loading, this estimate is the same as the free decay response of the system. The free decay response can then be used to obtain the system damping of a mode.

The method requires the choice of robust parameters and these parameters were appropriately chosen. The following were recommended:

- A window duration of at least $1800f$ seconds where f is the frequency of the inter-area mode whose damping is required
- A RD signature or segment length of 6 oscillation cycles of the inter-area mode whose damping is required
- A triggering threshold of $-0.25\sigma_{sig}$ where σ_{sig} is the standard deviation of the mean centred signal in each window of estimation
- A multivariate implementation using the SIs from ICA

The method was then applied to simulated and measured data from the case study system in order to determine the damping of the critical inter-area mode in Finland. By linearizing the system model, it was determined that a value of 7 % was expected. The data from the simulated scenario gave a result of 6.52 ± 0.6 % while the data from the measured scenario gave a value of 6.92 ± 0.79 % hence illustrating the accuracy of the approach. It was also shown that the *S*'s from ICA are capable of selecting the best signals for estimation of damping without any knowledge of the physical structure of the system itself. This is useful especially when measurements are available without knowledge of the frequencies present or their sources.

Finally, the results showed that any measured quantity may be used to estimate the damping of an inter-area mode but the voltage angle differences may have a bias in a highly-compensated network.

7. Integrated Tool

This chapter presents the software tool created using C# .NET that integrates the three algorithms presented in chapters 4, 5 and 6 for detection of ambient operation, mode detection and source identification, and damping estimation respectively. It starts with a description of the requirements for the tool followed by a description of the implemented algorithm, how the implemented algorithm fulfils some of the requirements and some of the restrictions it presents on the design. The design of the tool is then presented starting with a description of the computer language in which it was developed, followed by the design of the key components of the tool. The user interface of the tool is presented thereafter, detailing how some of the functional requirements and non-functional requirements were addressed. Finally some results obtained using a test data set are presented.

7.1. Requirements

The requirements for the tool were compiled through discussions with the end users of the tool – the system operators at National Grid. They can be sub-divided into *functional* and *non-functional* requirements. Functional requirements refer to aspects of the functions of the tool and therefore technical aspects related to the operation of the tool whereas non-functional requirements are those aspects that relate to quality of the tool or requirements that impose constraints on the design or implementation such as performance requirements, security or reliability (Wikipedia, 2010).

7.1.1. Functional Requirements

The functional requirements for the tool are the same as the requirements presented in Chapter 1. They are the technical outputs expected from the tool. They are re-stated here:

- Capable of differentiating between ambient and transient operation.
- Able to detect the existence of inter-area oscillations during ambient operation using data measurements.
- Able to detect the frequency of the oscillations.
- Capable of detecting the areas participating in the oscillations.
- Able to estimate the damping factors of the oscillations.

- Will provide alerts to operators regarding critical changes in damping.

7.1.2. Non-functional Requirements

The main non-functional requirements obtained from the users of the tool are:

- Configurable update time
- Ease of use of tool
- Storage of settings
- Storage of results

The first non-functional requirement is the update time which refers to how long it takes for a new estimation to be carried out once one estimate has already been made. It is considered a non-functional requirement because it is flexible as control room decisions regarding inter-area oscillations can take more than five minutes to implement. The second non-functional requirement is the ease of use of the tool which refers to how easily information is presented to the user of the tool; this relates to the user interface of the tool. The third requirement is the storage of settings. Ideally, once the settings for the tool have been stored, it would be beneficial to be able to recall them whenever the tool is opened. The final requirement is the storage of results. For the tool to be effective, the operators need to be able to observe historical trends of modes detected and their damping ratios, but since a new independent estimation is made every time a new set of data becomes available, there should be a way to store and display historical results. A storage time of one hour is sufficient because it shows long term trends in the damping that are operation-critical; any changes that take place in a longer period are not operation-critical.

7.2. Implemented Algorithm

The three methods that have been chosen for the tool, the Teager Operator for the detection of transient operation, Independent Component Analysis (ICA) for the detection of modes and identification of sources or participating areas, and the Random Decrement (RD) method for the determination of system damping of modes, fulfil the first five functional requirements specified by the system operators. These methods are applied to a block of data obtained by placing a window on the data, where a window captures voltage, current flow, power flow and system frequency data for

a period of time, typically for the last few minutes of operation (for instance, from five minutes ago until the present time).

The three methods are proposed to be implemented in a block processing algorithm. A block processing algorithm uses a block of data to make an estimation of the state of operation, the modes present, their sources and damping. The window used to obtain the block of data is then moved forward as new data comes in order to get a new block of data which is used to get a new estimation and so on. The proposed implementation is presented in Figure 75. When a new block of data arrives, the Teager Operator is used to determine whether the power system is in ambient or transient operation. If the system is in ambient operation, ICA is used to determine the modes present in the data and the significance indices (*SIs*) of the modes. If a mode is detected, the RD method is used to determine the system damping of the mode using the *SIs* from ICA. This information is passed on to the system operator and then the algorithm waits until a new set of data is presented to it.

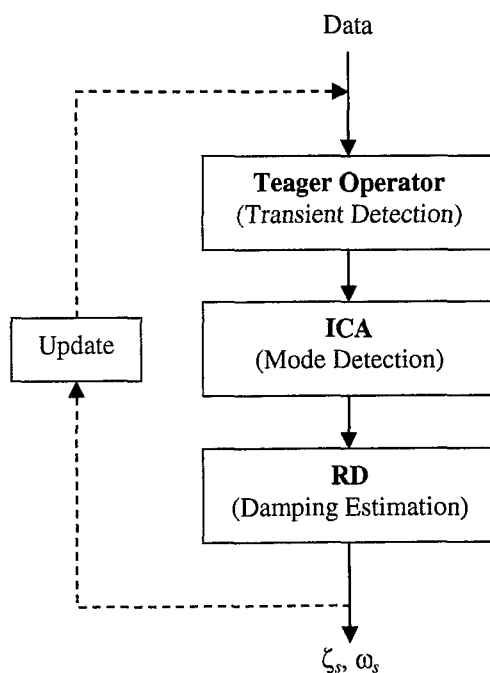


Figure 75: Implemented algorithm – sequential processing

The final functional requirement is the ability to alert operators to critical changes in damping. Since the damping of inter-area modes changes relatively slowly to other system dynamics, a threshold can be set for the damping level or for the damping level relative to the amplitude of the oscillation. This is discussed further in section 7.4.

7.3. Constraints Imposed by Implemented Algorithm

The Teager Operator is shown in Chapter 4 to require only three samples of the PMU-sampled bus frequency or bus frequency deviation to make an inference about the nature of system operation. However, in order to mitigate the effect of false detections, a longer time window is required. Chapter 5 showed that the detection of modes using ICA can use a window as small as 1 minute (for a 0.3 Hz oscillation, or $200f$ s in general where f is the frequency of the mode being detected). However the variance of the frequency estimate is quite high and therefore the longer the window length, the more accurate the estimation. However, Chapter 6 showed that the damping estimation using the RD method requires a window of data of at least 9 minutes (for a 0.3 Hz oscillation, or $1800f$ s in general) so that the number of oscillations captured is sufficient enough for the damping estimate to be accurate. Therefore the window duration for the damping estimation is the constraint on window duration of the block processing algorithm.

Similarly, the update time is mainly constrained by the time it takes for each method to make an estimation because the estimates are made sequentially hence the steps with the longest estimation time dictate the estimation time of the whole sequence. Since the Teager Operator only performs multiplication and subtraction, it is not time-intensive. However, since the RD method is inherently univariate, the time taken to obtain a system-wide damping estimate using all the measurements depends on the number of measurements available. Additionally, ICA uses a recursive optimisation algorithm to estimate the sources and the number of sources estimated depends on the number of modes present in the data and the number of measurements available. Therefore the ICA-RD algorithm update time is the constraint on the update time of the block processing algorithm. This addresses the first non-functional requirement presented in section 7.1.2.

7.4. System Design

The rest of the non-functional requirements that have not been addressed can be translated into a set of specifications for the system in development. This section presents the computer language in which the system was designed, C# .NET, and describes firstly how the implemented algorithms were linked to or integrated into the tool. The design of the rest of the tool to address the remaining

non-functional requirements is then presented.

7.4.1. C# .NET

C# .NET refers to the C# programming language in the Microsoft .NET platform that runs on the .NET framework. The following subsections describe each of these technologies.

7.4.1.1. Microsoft .NET

Microsoft .NET refers to a package that encompasses a wide range of products and technologies from Microsoft, most of which have a common dependence of the Microsoft .NET framework (Wikipedia, 2007b), a component of the Windows operating system which was developed so as to provide “pre-coded solutions for common program requirements” to facilitate their execution (Wikipedia, 2007c). “.NET is the Microsoft Web services strategy to connect information, people, systems, and devices through software.” (Microsoft, 2007) .NET technology was created so as mainly to provide developers with a way to manage and execute connected web services. However, the main and foremost attraction towards .NET comes due to the fact that it was developed to allow the interoperability of different languages. In the past, many applications were built to use different programming languages, but when a new function needed to be embedded using a different language, the whole process of development had to be repeated. The .NET framework was designed to be a work-around solution to this problem, to specialise in interoperability (SriSamp, 2003).

7.4.1.2. .NET Framework

The .NET framework is a component of the Windows operating system that simplifies and facilitates the execution of programs developed using the .NET platform. The two main components of the .NET framework are the Framework Class Library (FCL) and the Common Language Runtime (CLR) (SriSamp, 2003). The FCL is a class library that provides various programming capabilities and is used to enforce the securities of applications and web services. The CLR, on the other hand, executes .NET programs. Programs are compiled in the .NET platform in two stages: the first step is the compilation into the Microsoft Intermediate Language (MSIL), which helps to define the instructions for the CLR to execute. The CLR is capable of interpreting the MSIL of code written in different languages and this is the feature that allows for language interoperability in .NET. The executable file (assembly) of the application contains the MSIL of the different components

comprising the application. On execution of the application, a compiler in the CLR known as the Just-in-Time (JIT) compiler converts the MSIL into machine-language code which is specific for a given platform. The machine code then executes on that platform (Deitel and Deitel, 2006b). Therefore if the .NET framework has been installed for a particular platform, the platform can then be used to run any .NET program (which requires the .NET framework to execute). Thus, code that has been written on one computer can be run on another without the need to modify it. This feature is known as “platform independence” (Deitel and Deitel, 2006b) and is another reason why the .NET platform is very desirable to developers. In this project, the programming language that was chosen for the purpose of developing the integrated tool was C#.

7.4.1.3. C#

C# is a language that was developed by a team led by Anders Hejlsberg and Scott Wiltamuth at Microsoft as the inherent language of the .NET platform. The development of C# was a direct result of the boom in consumer electronic devices like Personal Digital Assistants and hence the need to produce a software tool that could be used to develop web-based applications that could be accessed by anyone at any time, on computers or even on hand-held gadgets (Deitel and Deitel, 2006a). C# is a procedural, object-oriented language that was derived from and based on syntax and aspects of C++, JAVA and Delphi. C# was designed to take advantage of the features of the underlying Common Language Infrastructure (CLI) (Wikipedia, 2007a). It is a “visual programming language in which programs can be created using an Integrated Development Environment (IDE)” (Deitel and Deitel, 2006a). An IDE allows a programmer or developer to easily create, run, test and debug code thus making it an easily implemented approach. The combination of these two factors was the main reason why C# was adopted for this purpose: it is inherent to .NET and it is easy to debug and program. An additional advantage of using C# is that code from MATLAB, in which the algorithms were developed, can be integrated. The following section discusses the aspects of integration of MATLAB into C#.

7.4.2. Integration of MATLAB Algorithms

MathWorks provides an add-on product for MATLAB known as the MATLAB compiler. The MATLAB compiler lets users compile code written in MATLAB into either executable modules or

shared libraries (known as Dynamic-Link Libraries, DLLs) that can then be used in other development environments (MathWorks, 2010). The compiled code allows the user to port the functionality of the algorithms created in MATLAB to the .NET platform by making the methods written in MATLAB available in classes. However, the compiled code requires a runtime engine called the MATLAB Compiler Runtime (MCR) to execute; the MCR is provided along with the compiler for free distribution with the compiled modules (MathWorks, 2010). The MCR was used to compile the implemented algorithm into a DLL that was then linked into .NET. Once the DLL has been created using the Matlab compiler, it still needs to be used in the .NET IDE. MATLAB provides an interface class for implementation of DLLs in .NET known as the MWArray class. The MWArray class allows the input and output of information into the DLLs.

7.4.3. Settings

Having established how to work with the MATLAB code, the next step is to create a way to allow the user to specify settings for the algorithms such as the inter-area mode range for the data filter, the duration of the sliding window and the update time among others. As mentioned in the list of non-functional requirements, it would be beneficial if user-defined settings could be stored so that they do not have to be re-entered every time the tool is opened. This can be done by storing the settings in a file. The reason this is required is that a user-defined setting is usually stored in the short-term memory of the computer during runtime. Once the application is closed, the short-term memory is cleared and therefore the settings are lost.

The Windows Operating System allows users to store settings as items in the computer's memory known as registry keys. These keys can be called during runtime to obtain pre-defined settings. However, it is recommended not to alter registry keys once they have been created in order to ensure that a wrong key is not altered leading to misbehaviour of the application to which it belongs. Additionally, registry keys might fail to be created if an application is installed on a machine using a profile that does not have administration rights. An option that is therefore more suitable is the use of INI files which are essentially initialisation files that contain values attached to certain unique keys. INI files are usually small in size, and additionally C# provides methods to read from and write to such files. An INI file was therefore used to store the user defined settings.

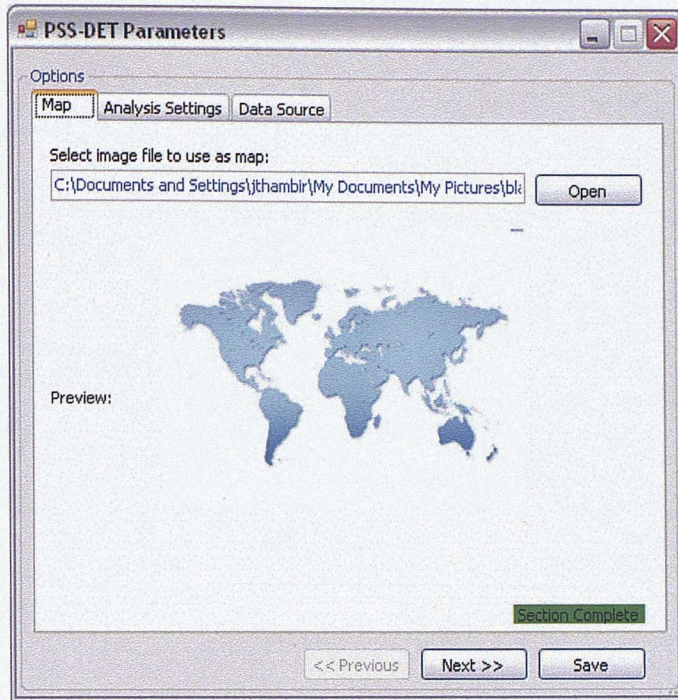


Figure 76: Map settings tab

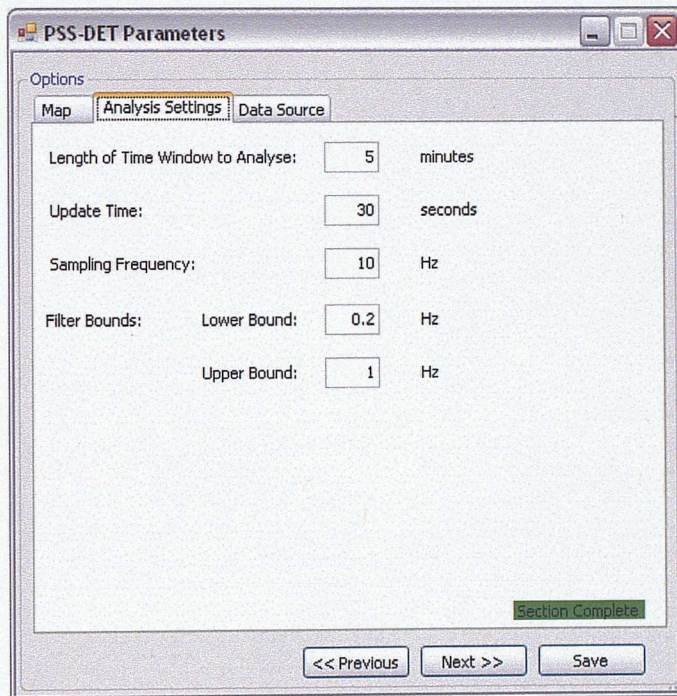


Figure 77: Parameters settings tab

There are three main settings that need to be user specified:

- The map of the area of interest.
- The parameters of the algorithms.

- The source of data to be analyzed.

The map of the area of interest needs to be loaded into the tool whereas the parameters require the user to type in certain values. The source of data requires a connection to a server. A customised settings Graphical User Interface (GUI) was therefore implemented with three tabs, where each tab allowed the user to change one of the above settings. Figures 76, 77 and 78 show screen shots of these tabs.

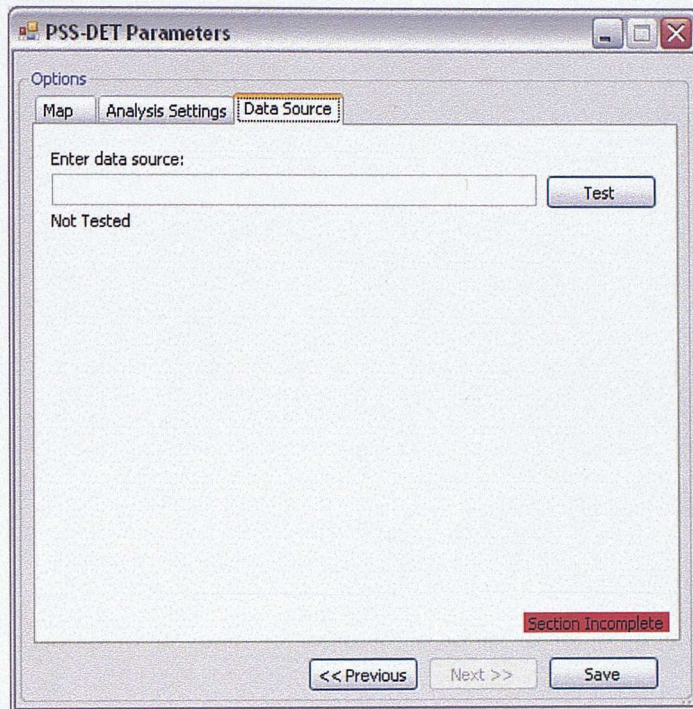


Figure 78: Data source settings tab

7.4.4. Implementation of sliding window

The next step is to implement the sliding window which captures a block of data from the data connection in the time of the update as specified by the user. In order to implement this, it is important to understand that the update algorithm is separate from the algorithm processing the data itself, though they have to run synchronously and are hence not independent.

The main algorithms that have to be coordinated are the data processing algorithm and the update algorithm. The data processing algorithm can only run once data has been made available. The latter is the function of the update algorithm: to query for data at the right time. However, once the data has been queried and passed on to the data processing algorithm, the update algorithm has to wait for

the duration of the specified update time (counted from the beginning of the last update) before it queries the data connection for new data.

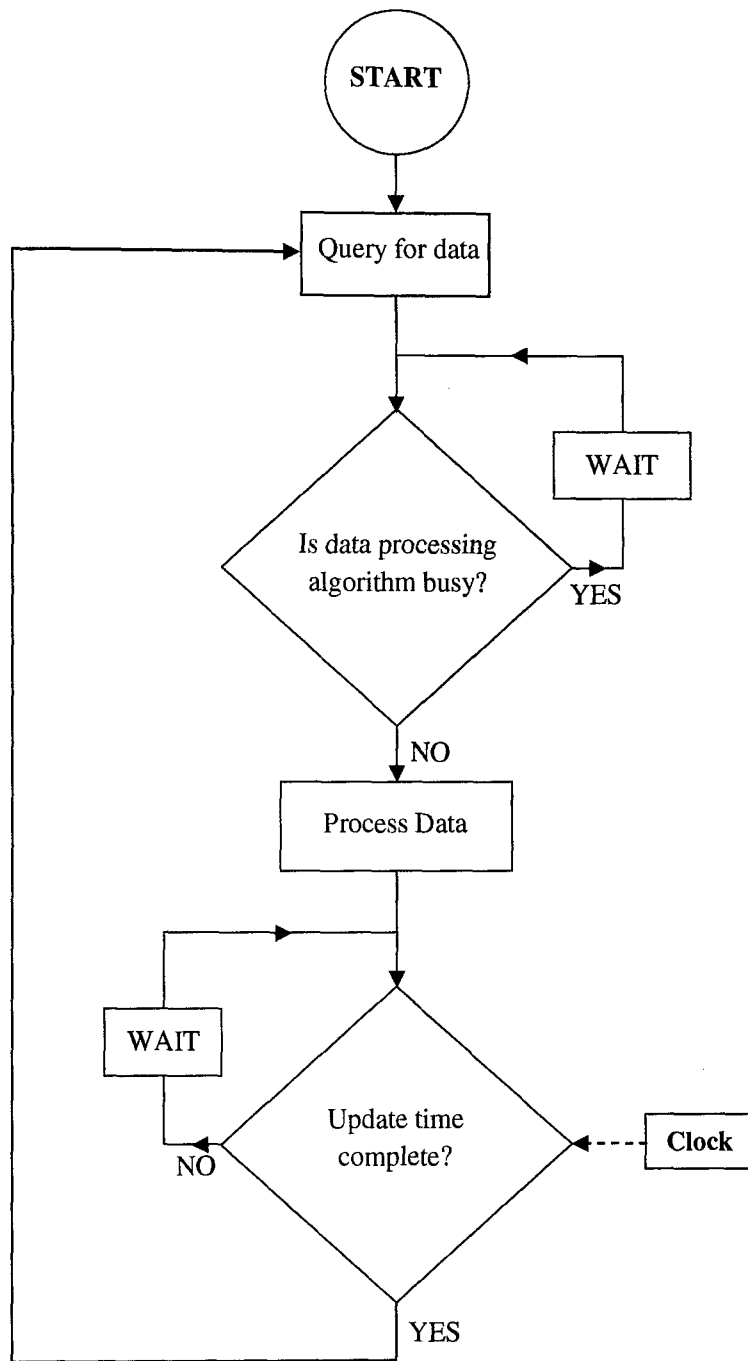


Figure 79: Flowchart showing implementation of sliding window

If new data is queried before the data processing algorithm returns a result, the system waits for that operation to finish before passing on the new data to the processing algorithm. This is achieved by the use of threads in C#. Threading, which is the process of using threads, allows programmers to ensure that blocks of code execute in a certain order when they run concurrently. This time delay is

known as polling. Figure 79 shows a flowchart that demonstrates the implementation of the sliding window for data querying or updating.

7.4.5. Storage of Results

After implementation of the sliding window, the next non-functional requirement is the storage of results. As previously discussed, the storage of results is necessary so that the operators can observe trends especially in the damping over time. A time duration of one hour of results was deemed to be sufficient. This storage can be implemented in one of two ways. The first way uses a file store to write results to, and this would be placed on the hard drive. The plotting algorithms would then read the results from the file and create the necessary plots. The second way uses the computer's short-term memory to keep the results. This would then be passed directly to the plotting algorithm for the creation of the graphs. Given that the size of results obtained from one-hour duration of analysis is pretty small, that computer cache memory is usually high and that the alternative write and read from a file would be more computationally intensive, the second option was chosen. It was then implemented using a data table. A data table is a table that can be created in C# where results from one estimation are entered into one row of the table with different columns representing different quantities for example time of estimation, frequency values and damping ratios. This data table was updated every time the sliding window was moved so that it stored one hour of results at any single moment in time. The outcome of this implementation is shown in the next subsection which shows some screenshots of the demo-tool. The demo-tool showcases the functionality offered by the algorithms that were developed in the research of this thesis. It lacks a connection to a server from which real-time data would be available. A connection to a server was not implemented because there was no access to such a server during the research.

7.4.6. Display

Finally, having obtained all the necessary inputs and outputs from the tool, the final step is to provide all the information gathered to the users. The display or main GUI presents this information in simple and easily interpretable forms. These were determined taking into consideration the functional requirements of the tool.

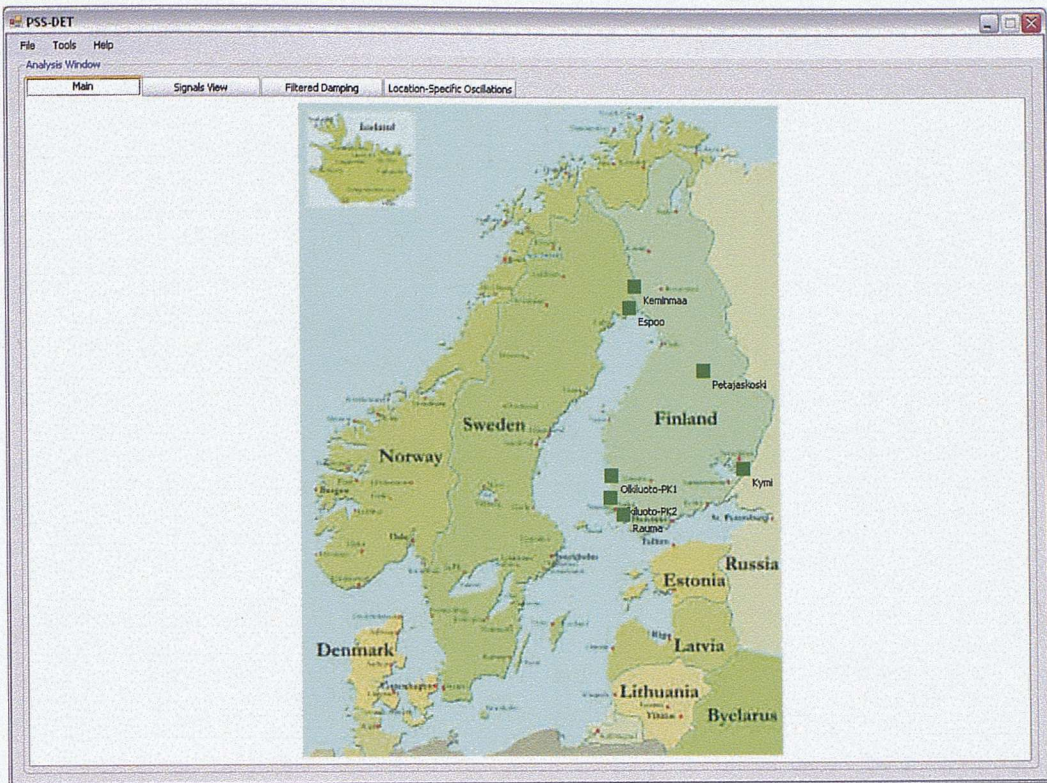


Figure 80: Main window of GUI showing system overview and dynamic markers

The most crucial information that was determined to be necessary for the operators was:

- A map showing locations of measurements.
- A one-hour time horizon of measurements from the system.
- The mode frequencies detected over this time horizon.
- The changes in damping over the time horizon.
- A graph of the mode frequencies versus damping for the same time horizon.

These requirements were then translated into three different tabs of the tool. The aim of the tab structure is to provide the operator with increasing levels of information from the first to the last tab, starting with the minimal information at the beginning. The main tab of the GUI was therefore designed to show the system overview and therefore displays a map of the system. The user can place measurement points and labels on this map as shown in Figure 80. The markers of these points are designed to have dynamic colours starting from green when there is no operational problem which would progress to red if a problem was detected in the damping of a specific mode. This type of display is known as *traffic lights* and is widely used in control rooms. The idea is that a red light indicates the need for urgent action, a yellow light indicates a less severe event that does not require

immediate action while a green light indicates that there is no problem and that the system is under normal operation (ETSI, 1994). A physical implementation of a traffic light is currently used by the UK transmission operator for the purpose of alerting operators to significant events in the system. The software implementation proposed in this thesis however localizes the traffic light implementation to each location where measurements are available.

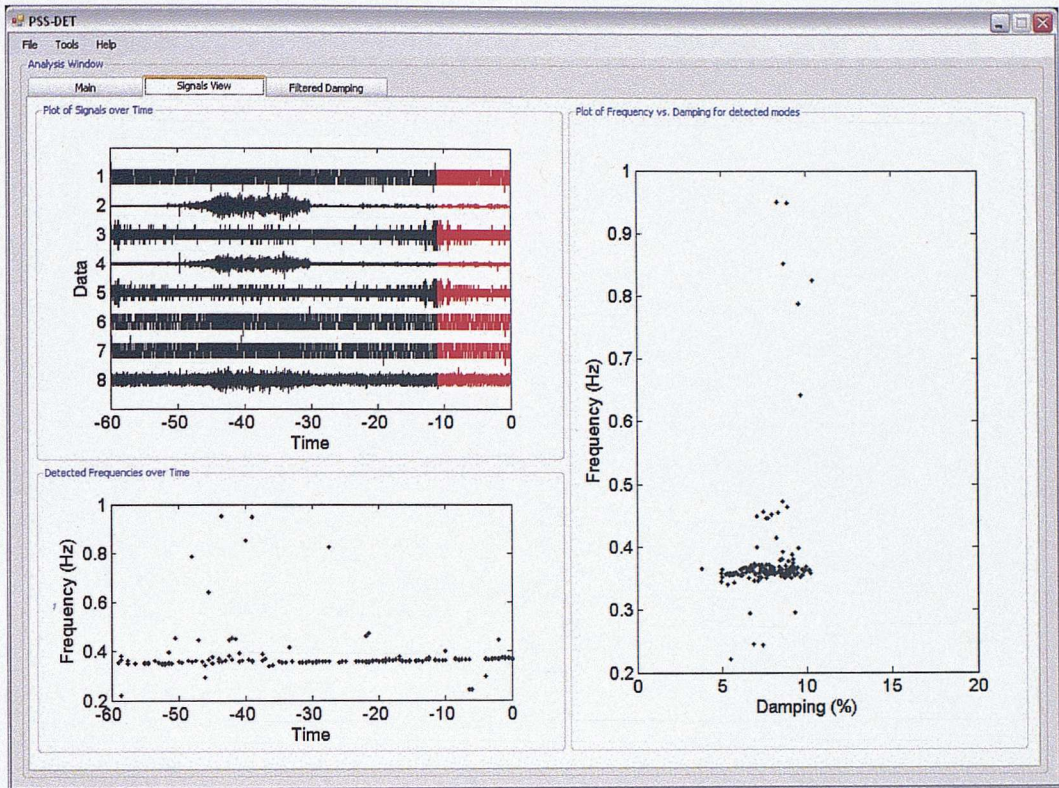


Figure 81: Signals view window of GUI showing measurements, modes and frequency vs. damping over 1 hr time horizon

The second tab progresses in detail to show various metrics over the one-hour time horizon as shown in Figure 81. One area shows the signals over the time horizon with the data that is being analysed being plotted in red. The graph right under it shows the modes that have been detected and the graph to the right of these two shows the mode frequencies versus the damping for the time horizon. If the operator sees a problem in one of the latter two graphs discussed above, he/she progresses to the third tab which allows him/her to narrow down the results to a particular frequency range as shown in Figure 82. Therefore, the operator is able to progress from the minimal level of information to the most critical level.

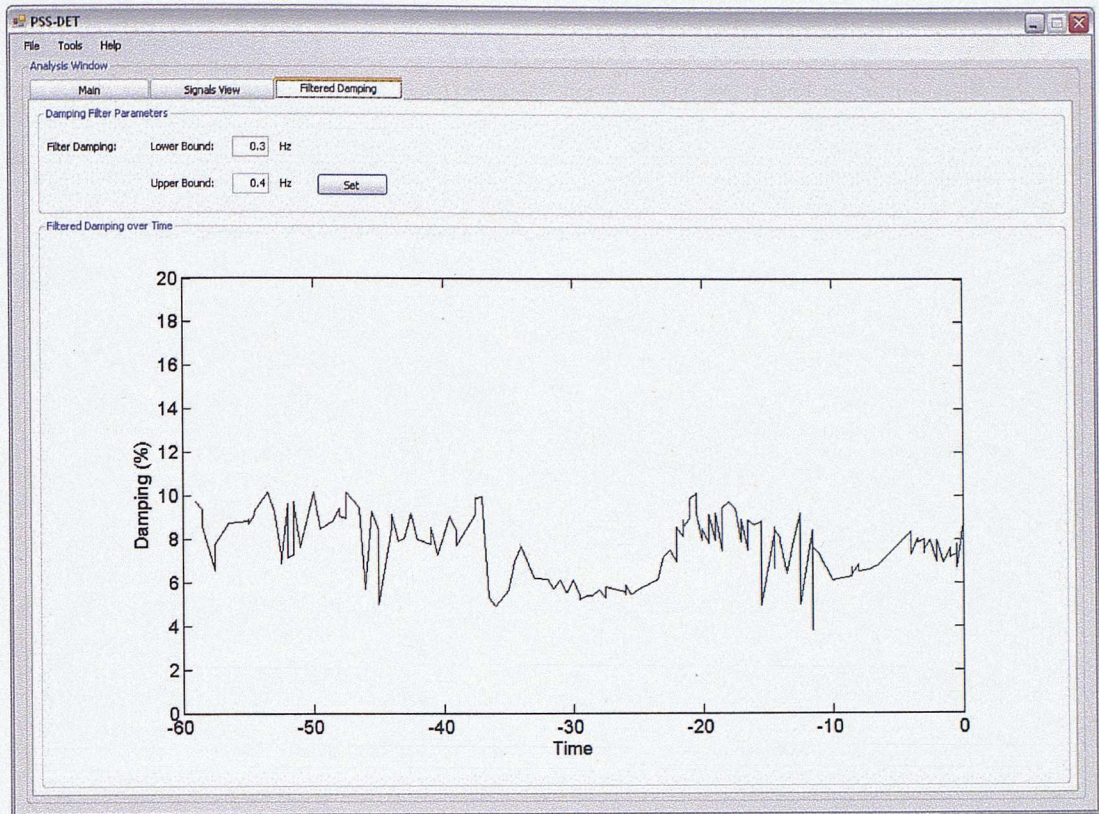


Figure 82: Filtered damping window of GUI allowing operators to focus on damping of modes in a customisable frequency range over 1 hr time horizon

7.5. Summary

This chapter has presented the design of a demo system operator tool integrating the functionality provided by each of the algorithms presented in the previous chapters. The functional and non-functional requirements of the tool were obtained through discussions with operators at National Grid's national electricity control centre.

The main functional requirements were the determination of transient operation, detection of modes and diagnosis of sources, and determination of system damping of the detected modes. The main non-functional requirements were the ease of use of the tool, the implementation of a sliding window, the storage of results and display of the stability metrics. The implemented algorithm was then presented to demonstrate how the selected methods fulfil the functional requirements.

The design of the GUI using C# .NET was then presented, taking into account the non-functional requirements. It was discussed that .NET provides the best environment for development of the demo tool because it provides a platform for integration of code written in different programming

languages and is also capable of integrating MATLAB code, in which all the data processing algorithms were written. C# was chosen as the programming language of choice because it is the inherent language of the .NET framework. The storage of settings non-functional requirement was addressed using implementation of an INI (initialisation) file with the use of a GUI to allow users to enter the user-defined settings. An INI file is a way for applications to store start-up settings using the long-term memory of the computer. The implementation of the sliding window was addressed using the threading capability of C# which allows two synchronous processes to run in a defined order.

The storage of results non-functional requirement was then addressed using the short-term memory cache of the computer with the use of a data table which is updated every time the window of data is slid. Finally the design of the main window of the tool was presented showing the tabbed approach that was taken, with the delivery of information to the operator in increasing detail from one tab to the other.

8. Summary & Future Research Opportunities

This chapter presents the summary of the work and possible future work that can be carried out regarding the research presented in this thesis. The summary section reiterates the aim of the thesis, the objectives of the research and the methods that have been used to address the aim and the objectives. A brief summary of each of the methods that has been presented in this thesis is also provided. The future work section comments on improvements that can be made on the algorithms that were presented and other possible avenues of research that can complement this research.

8.1. Summary

This section presents a summary of all the chapters in this thesis. It starts with a description of the motivation for the project followed by the aim of the research. The selection of the methods that address the aim of the research is then presented followed by the methodology for the application of the methods in real-time. The case study system that was used is then summarised followed by brief descriptions of each of the selected methods and the results that were obtained from the application of the methods to the case study scenarios. The summary is concluded with a statement of the conclusion of the research.

8.1.1. Motivation and Aim

Inter-area oscillations are inherent in large interconnected power systems and are typically created when groups of synchronous machines in one part of the system oscillate with respect to groups in another part of the system at a frequency ranging between 0.2 to 1.0 Hz. These oscillations, or modes as they are more commonly referred to, are usually stable but typically have small damping ratios. Even though oscillations are characteristic of the post-fault response of a system, they can also be excited by random events such as the normal variation of load demand. These poorly damped oscillations can pose various problems such as limiting transfer capacities and in more severe cases can lead to system instability causing a wide-scale power system blackout.

Historical wide-spread blackouts prior to 2003 opened the eyes of the power industry to the risks posed by these oscillations resulting in a drive for research into development of tools towards

improving awareness of operators. It is envisioned that in the future, as the generation capacity of power systems increase and become skewed towards intermittent renewable energy such as wind, power flows within the system are expected to become more varied and less predictable making inter-area oscillations less predictable and hence a greater risk. These reasons highlight the need for oscillation monitoring in power systems with the aim to provide system operators with a real-time view of the system.

Measurement equipment such as Phasor Measurement Units (PMUs) have become more widely deployed in power systems recently; they provide real-time GPS-stamped data to operators. The availability of large amounts of data has opened research avenues into the use of the data to increase situational awareness of transmission network operators. One specific research problem is the determination of the stability of inter-area modes when the power system is operating normally, that is, during ambient operation. This is a challenge because the oscillations are excited by random load perturbations that cannot be measured, the strength of oscillations varies according to the location of the measurements and the measurements are heavily corrupted by noise. Additionally, the topology of the power system is assumed to be unknown. The problem of stability inference is therefore difficult because both the system structure and system input are unknown; it is required to determine the approximate system response from only noise-corrupted system output measurements.

The research presented in this thesis tackles this research problem with the additional aim of creating novel tools that can be used by power system operators to increase situational awareness. The thesis has presented a novel approach to the monitoring of inter-area oscillation frequency and damping during ambient operation of electrical power transmission networks using multivariate analysis techniques by pooling knowledge and resources from different engineering fields, being chemical process systems engineering, structural engineering, vibration analysis and power systems engineering.

8.1.2. Selection of Methods

The research aim was divided into a number of objectives. These objectives were to:

- Create algorithms that can detect the on-set of transient events.
- Detect inter-area modes in ambient operation.

- Determine the participating areas in the oscillations.
- Determine the damping of the oscillations.
- Present the results of the analysis to an operator via an interactive tool.

A review of literature was then carried out in the field of power systems engineering in order to identify methods that addressed the research aim and hence identify their strengths and weaknesses. Keeping the research objectives in mind, literature from the fields of chemical process systems engineering, structural engineering and vibration analysis was reviewed to identify possibilities for application of methods to address the research objectives. A set of methods were therefore identified to address each of the first four research objectives listed above.

The Teager energy operator (from the field of vibration analysis) was chosen to determine ambient or transient operation. Independent Component Analysis (from the field of process systems engineering) was chosen to determine the frequencies of inter-area modes present in the ambient data and the modal observabilities of the modes at the locations of the measurements. Finally the random decrement method (from the field of structural engineering) was chosen to determine the damping of the detected inter-area modes.

A fifth research objective required the design of a Graphical User Interface (GUI) oriented tool and this was carried out as a separate task.

8.1.3. Structural Methodology

A structural methodology for the application of the methods in real-time was also developed. Figure 83 shows the methodology. The Teager energy operator is used to determine if a set of data collected from the power system represents ambient or transient operation. If the operation is ambient, independent component analysis is used to detect any inter-area modes, determine the frequencies of the modes and the relative strengths of the modes at the different measurement locations in the power system. The random decrement method is then used to calculate the damping of the modes and this information is passed to the operator indicating whether the system is stable or not.

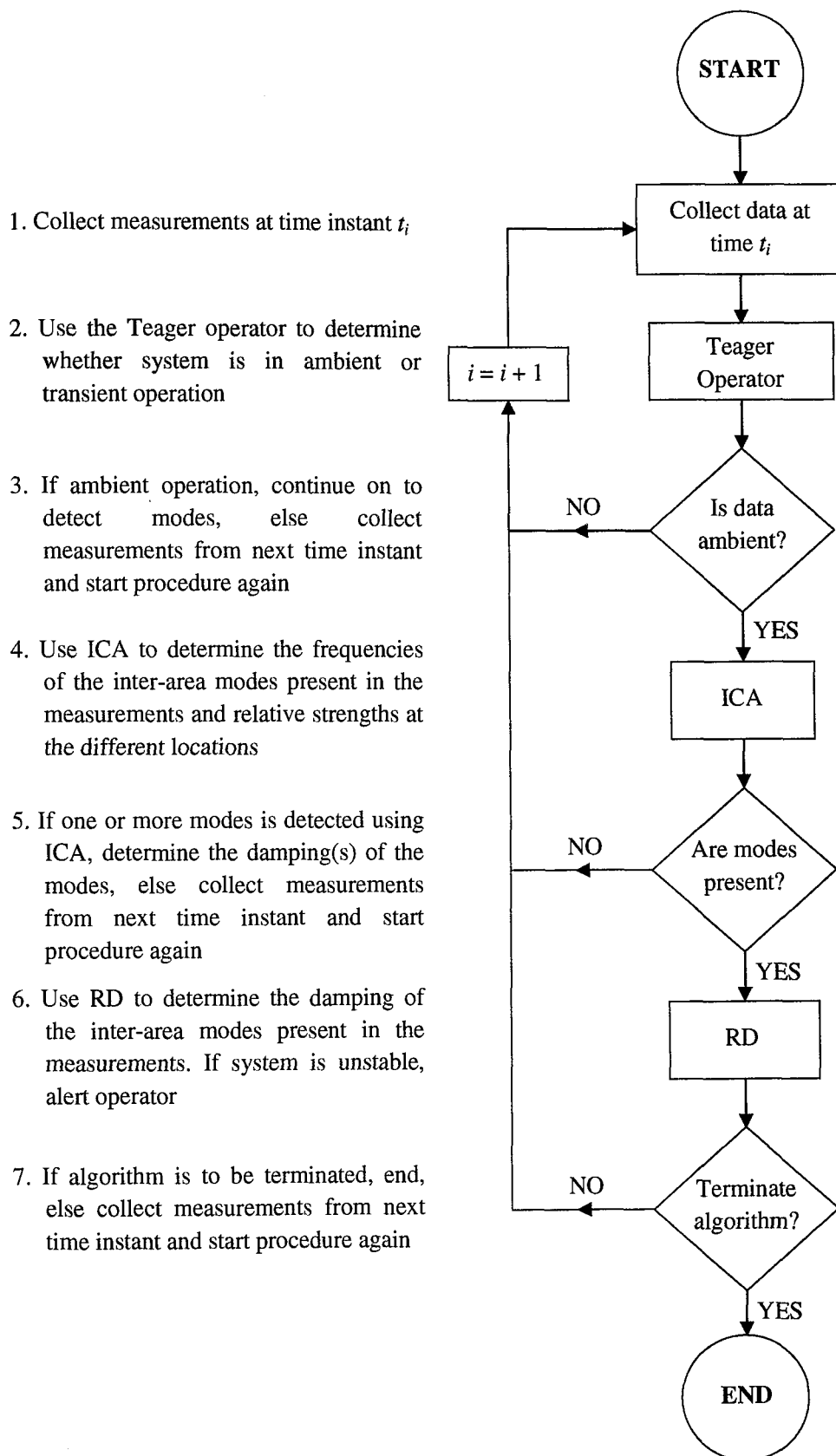


Figure 83: Structural methodology for determining power system stability

8.1.4. Case Study System

The purpose of the case study was to benchmark the performance of the methods. The Nordic system was chosen as the case study system and a measured operational scenario that comprised ambient operation was selected. By measuring the power flow from Finland to Sweden (both in the Nordic system), a simulated scenario with approximately the same power flows was created by randomly exciting loads and generators using a full Nordic system model. These two scenarios were used to benchmark the identified methods. Both measured and simulated scenarios were used to ensure that the results from both cases were similar. Given that the expected result for the simulated case was known, the methods were checked to ensure that they performed the analysis correctly in the simulated scenario, and to determine how different the results from the actual system were, if at all, from the simulated system model.

8.1.5. Transient Detection Algorithm

The transient detection algorithm is required to determine when the system enters transient operation because the methods that have been developed for detection of inter-area modes and determination of their frequencies and damping perform optimally under ambient conditions. The transient detection algorithm therefore ascertains when the system is not in transient operation and hence is in ambient operation. The chosen method, the Teager operator, estimates the energy or Teager Energy (TE) in the signal using only three measurements at a time. Having obtained the TE, a further algorithm is required to translate the TE into a metric indicating ambient or transient operation. This was done by converting the TE into a binary status signal which is zero or “off” when the system is in ambient operation and equal to 1 or “on” when the system is in transient operation.

A novel scheme that calculates the Integrated Absolute Teager Energy (IATE) was introduced as a means of converting the TE signal to a binary status signal. The IATE computes the integral of the TE over time and makes use of the fact that energy transfer takes place at a higher rate during transients than ambient operation to determine the region of operation. This is done by calculating the gradient of the IATE at every time instant using a four-point least-square computation which mitigates the effect of step changes in the TE hence IATE from one time instant to another. It was shown to be better than a simple threshold scheme that has been published in literature because it

removes spurious detections of transients. The method was demonstrated using a frequency trace from the Mexican interconnected network that contained regions of both ambient and transient operation. The combined method, was then applied to data from the simulated and measured scenarios of the Nordic case study in order to demonstrate that the data is from ambient operation of the system.

8.1.6. Mode Detection and Source Identification

The chosen algorithm, Independent Component Analysis (ICA), was demonstrated to be capable of detecting inter-area modes in multivariate data, identifying the frequencies of the modes and the sources of the modes. In the context of inter-area modes, the areas participating in the oscillation constitute the source of the oscillation.

ICA is a method that aims to decompose a matrix of measurements from various points into a set of common sources that contribute to the measurements. ICA additionally determines a matrix relating the sources back to the measurements. This mixing matrix indicates how much of each source is present in each measurement. The results of ICA are mathematically manipulated to change the sources into positive-peaked narrowband functions which relate to physical frequencies present in the data, and convert the mixing matrix into a matrix of significance indices (*SIs*) which are normalised values indicating the relative strengths of oscillations in the measurements.

The method was applied to data from both the simulated and measured scenarios of the case study system to determine the critical inter-area mode frequency in Finland. The frequency was determined to be 0.3119 ± 0.0060 Hz from the simulated data while it was determined to be 0.354 ± 0.010 Hz from the measured scenario. This difference in estimates was attributed mainly to conservative choices of model parameters for the simulation and differences in the system configuration between the model and the actual operational scenario.

The effect of noise and the window duration of data on each estimation was also considered. It was concluded that neither significantly affects the estimation of the frequency. Finally, the *SIs* were used to demonstrate the ability of ICA to identify the measurement locations participating in an inter-area oscillation. ICA correctly identified which measurement locations in Southern Sweden, Southern Denmark and Southern Finland participated in the 0.3 Hz oscillation from the simulated

scenario data. It also showed that only measurements locations in Southern Finland participated in the oscillation from the measured scenario data. The reason for the latter inference is that measured data from Sweden or Norway were not available for analysis.

8.1.7. Damping Estimation

Having obtained the frequencies of the inter-area modes in the data, the final step for stability inference is the estimation of the damping of the modes. The method chosen for damping estimation, the Random Decrement (RD) method, is a method that estimates the correlation function of a system by the averaging of segments of the measured signal collected using an appropriate triggering technique. Under the assumption of random (white noise) loading, this estimate is the same as the free decay response of the system. The free decay response can then be used to obtain the system damping of a mode.

The method requires the choice of robust parameters and these parameters were appropriately chosen. The following parameters were selected: a segment length of 6 oscillation cycles, a triggering threshold of -0.25 times the standard deviation of the mean centred signal in each window of estimation, and a window duration of at least 1800 times the inter-area mode frequency whose damping is required. The RD method is inherently univariate but was developed to take advantage of a multivariate approach using the *SIs* from ICA. The multivariate method was then applied to simulated and measured data from the case study system in order to determine the damping of the critical inter-area mode in Finland. By linearizing the system model, it was determined that a value of 7 % was expected. The data from the simulated scenario gave a result of 6.52 ± 0.6 % while the data from the measured scenario gave a value of 6.92 ± 0.79 % hence illustrating the accuracy of the approach. It was also shown that the *SIs* from ICA are capable of selecting the best signals for estimation of damping without any knowledge of the physical structure of the system itself. This is useful especially when measurements are available without knowledge of the frequencies present or their sources.

8.1.8. Integrated Tool

The methods were all finally packaged in a demonstration system operator tool integrating the functionality provided by each of the previously described algorithms. It is a demonstration tool because it shows how the results from the analysis will look like but has not implemented a server connection because at the moment there are different data servers used by different operators and there is none available at the university.

The functional and non-functional requirements of the tool were obtained through discussions with operators at National Grid's national electricity control centre during a three-month industrial placement in 2009. The main functional requirements were the determination of transient operation, detection of modes and diagnosis of sources, and determination of system damping of the detected modes. The main non-functional requirements were the ease of use of the tool, the implementation of a sliding window, the storage of results and display of the stability metrics.

A Graphical User Interface (GUI) for the tool was designed taking into account the non-functional requirements, using C# .NET. .NET provides the best environment for development of the demo tool because it provides a platform for integration of code written in different programming languages and is also capable of integrating MATLAB code, in which all the data processing algorithms were written. C# was chosen as the programming language of choice because it is the inherent language of the .NET framework. The storage of settings non-functional requirement was addressed using implementation of an INI (initialisation) file with the use of a GUI to allow users to enter the user-defined settings. An INI file is a way for applications to store start-up settings using the long-term memory of the computer.

The implementation of the sliding window was addressed using the threading capability of C# which allows two synchronous processes to run in a defined order. The storage of results non-functional requirement was then addressed using the short-term memory cache of the computer with the use of a data table which is updated every time the window of data is slid. Finally the main window of the tool was designed using a tabbed approach, where situational information is delivered to the operator in increasing detail from one tab to the other.

8.1.9. Conclusion

This thesis has described a novel approach to the problem of determination of power system stability during ambient operation of power transmission networks. This approach has made use of multivariate techniques adapted and developed from various different fields of engineering to provide an integrated solution addressing the research aim. The main research problem of the detection and determination of frequency and damping of inter-area oscillations during ambient operation of electrical power systems has been successfully addressed. This conclusion is substantiated by two research papers that have been published as a result of this research, one paper in review and one further paper being worked on which compares the method developed here to two other methods developed by collaborating researchers. The research papers that have currently been accepted or submitted for publication are:

- Thambirajah, J., Barocio, E., and Thornhill, N.F., “A Comparative Review of Methods for Stability Monitoring in Electrical Power Systems and Vibrating Structures,” Special Issue on Wide Area Monitoring and Control, IET Journal on Generation, Transmission and Distribution, doi: 10.1049/iet-gtd.2009.0485, 2010.
- Thambirajah, J., Thornhill, N.F., and Pal, B.C., “A Multivariate Approach Towards Inter-Area Oscillation Damping Estimation Under Ambient Conditions Via Independent Component Analysis and Random Decrement,” IEEE Transactions on Power Systems, 2010, doi: 10.1109/TPWRS.2010.2050607.
- Turunen, J., Liisa, H., Tuomas, R., and Thambirajah, J., “A Wavelet-Based Method for Oscillation Damping Estimation Under Ambient Conditions,” Submitted to IEEE Transactions on Power Systems, 2010.

8.2. Future Research Opportunities

This section presents ideas for opportunities for future research that can be carried out following the work that has been presented in this thesis. The research opportunities are classified into opportunities to follow the strand of research carried out in this thesis and opportunities for future strategic research in this field. The former concerns the different objectives that were described in

the previous section, for example opportunities to improve mode detection and source identification, and so on, whereas the latter concerns the general direction of research in the field of data-driven monitoring in electrical power systems.

8.2.1. Opportunities to Build This Strand of Research

Quality of Simulated Case Study Scenario: The damping estimate that was obtained using the developed algorithm from the simulated case study scenario was lower than the expected value whereas the value obtained from the measured scenario was closer to the expected value. One reason that was given for this discrepancy was the nature of the perturbations that were applied to the power system model in order to generate the simulated outputs that were then analysed. The main theoretical assumption for ambient operation of electrical power systems is that the normal load variation is random and Gaussian. The application of perturbations to the system model was done in a way that cannot be taken to be random and Gaussian because the choices of the locations to apply the perturbations were chosen by the user. Additionally, the excitation sequence applied may not be classed as being Gaussian.

In order to get true random and Gaussian data, a true random automated scheme would need to be applied to the model. This scheme would automate the selection of points to apply perturbations to and additionally select random perturbation values to apply. For such a case, the simulated outputs are more likely to approximate to real measured ambient data, and hence guarantee better performance of the damping estimation method.

Detection of Modes: The method of Independent Component Analysis (ICA) that was presented for the detection of modes and determination of sources required a pre-filtering stage in order to band limit the analysed signals to the frequency range of 0.2 – 1 Hz. This limits the application of this method to only inter-area oscillations. However, a more complete tool for power system monitoring during ambient operation would be capable of analysing frequency ranges outside the inter-area range. An important consideration in such a case would be the selection of narrow frequency bands for analysis since wide frequency bands would invalidate the ability of the mode detection method to correctly identify relatively weak modes.

A possible solution to this problem is the use of multi-resolution ICA which looks at different frequency bands independently and then combines the results to produce one output. Taking such an approach would however complicate all other tasks such as damping estimation because modes in different frequency ranges would require different durations of data to obtain reliable damping estimates. This would require an adaptive windowing technique.

Damping Estimation: The Random Decrement (RD) method was used for the purpose of damping estimation. It was shown to obtain the correlation estimates of system outputs. These correlation estimates are the same as the free-decay response of the system under the assumption of random and Gaussian excitation, as is the case with ambient operation of power systems. However, despite the wide use of this assumption, it was discussed previously in this thesis that there is no theoretical basis for it in literature. A more robust approach to damping estimation would be the use the RD outputs as correlation estimates and the subsequent use of correlation-based methods of system identification for stability estimation. Examples of such methods have already been presented in the literature reviews presented in this thesis. However, caution would need to be taken to ensure that results of such analyses are interpreted correctly.

Integrated Tool: A final avenue for future research is the integrated tool that was presented in the previous chapter. The use of Graphical User Interfaces (GUIs) for the presentation of data is a wide area of research in itself, for example research into the optimal ways of presenting results, abstraction of results and even display of graphs. However, considering the basic functionality required of such a tool, some ideas can be generated for improvement of the tool. These ideas were not implemented because the tool was created to demonstrate the concept of technology transfer from academic research to industry. A more industry-oriented tool would require fine-tuning of the GUI. Some functionality that may be included includes:

- The display of dominant oscillations at different locations and the amplitudes of the oscillations.
- Integration of methods for transient analysis of data (when transients occur).
- Functionality to allow offline analysis of data sets in order to confirm results post-event.

- Demonstration of the capability of connecting the GUI to a real PMU data concentrator for real-time operation.

8.2.2. Opportunities for Strategic Research

Production and Commercialization of Research: The work of this thesis directly addresses the requirement for the development of tools and techniques for operation of new network features that result from a greener and smarter grid, for example as highlighted in the “Operating the Electricity Transmission Networks in 2020” report published by National Grid plc in February 2010 [4]. However, the majority of this research, such as this, is being carried out in universities where the theme is innovation rather than commercialization. In order to push these solutions to industry, there is scope for research that commercializes the developed tools by providing industry-targeted software solutions. An FP7 follow-on research project with ten partners (REAL-SMART) which is coordinated by Imperial College may provide a means of achieving this recommendation.

Wide Area Control: Data-driven methods are becoming more widely used because of PMU technologies. The research in this thesis has only scratched the surface for the scope of use of advanced data-driven methods in electrical power systems. The direction investigated in this thesis regards the monitoring of electrical power systems for determination of the stability of the system with respect to inter-area oscillations. This can be extended to deal with dynamics at other frequencies and hence cross into the area of power system protection based on intelligent wide area methods. A more advanced application of data-driven methods concerns the automated control of power systems with the use of results of monitoring, known as wide area control. At the moment, the power system operator needs to make control decisions based on the result of monitoring. Many times, such control decisions require the operator to assimilate a wealth of data from different sources and to intelligently assess the implication of control decisions. This area of research has previously been limited due to the unavailability of suitable data or system-wide monitoring tools. However, with the deployment of PMUs in power systems, there is a large amount of data available which facilitates investigation of intelligent algorithms that can mimic such human reasoning and hence be used to automate previously manual operations for control of power systems.

9. References

- [1] Retrieved from <http://mahi.ucsd.edu/cathy/Classes/SIO223/Part1/sio223.chap8.pdf>, accessed August 2009.
- [2] Retrieved from <http://www.statistics.com/resources/glossary/a/armamodel.php>, accessed August 2009.
- [3] Retrieved from <http://www.puffinwarellc.com/index.php/news-and-articles/articles/30-singular-value-decomposition-tutorial.html>, accessed August 2009.
- [4] Retrieved from <http://www.nationalgrid.com/uk/Electricity/Operating+in+2020/> on 27th November 2010.
- Al-Sanad, A.A., Aggour, M.S., and Amer, M.I., "Use of Random Loading in Soil Testing," *Indian Geotechnical Journal*, vol. 16, no. 2, pp. 126-135, 1986.
- Anaparthi, K. K., Chaudhuri, B., Thornhill, N.F., and Pal, B. C. "Coherency Identification in Power Systems through Principal Component Analysis," *IEEE Transactions on Power Systems*, 2005, 20 (3), pp. 1658-1660.
- Andersen, P., "Identification of Civil Engineering Structures Using Vector ARMA Models," PhD Thesis, Department of Building Technology and Structural Engineering, Aalborg University, Denmark, 1997.
- Arun, K. S., and Kung, S. Y., "Balanced Approximation of Stochastic Systems," *SIAM Journal on Matrix Analysis and Applications*, 1990, 11 (1), pp. 42-68.
- Asmussen, J.C., Brincker, R., and Ibrahim, S.R., "Statistical Theory of the Vector Random Decrement Technique," *Journal of Sound and Vibration*, vol. 226, no. 2, pp. 329-344, 1999.
- Barocio, E., Pal, B.C., and Messina, A.R., "Online Detection and Characterization of Power System Oscillations Using an EMD-Based Teager-Kaiser Algorithm," Submitted to the *IEEE Transactions on Power Systems*, April 2010.
- BBC, "New UK Offshore Wind Farm Licences are Announced," Retrieved from <http://news.bbc.co.uk/1/hi/business/8448203.stm>, November 2010.
- Ben Mrad, R., Fassois, S. D., and Levitt, J. A., "A Polynomial-Algebraic Method for Non-Stationary TARMA Signal Analysis, 1, the Method," *Signal Processing*, 1988, 65, pp. 1-19.

- Betancourt, R., "Estimation of Parameters in Transient Stability Output Swings Using Autoregressive Models," IEE Proceedings, 1990, 137 (C-4), pp. 315-320.
- Bounou, M., Lefebvre, S., and Malhame, R.P., "A Spectral Algorithm for Extracting Power System Modes From Time Recordings," IEEE Transactions on Power Systems, 1992, 7 (2), pp. 665-672.
- Brincker, R., Krenk, S., Kirkegaard, P.H., and Rytter, A., "Identification of Dynamical Properties from Correlation Function Estimates," Bygningsstatistiske Meddelelser, vol. 63, no. 1, pp. 1-38, 1992.
- Brincker, R., Zhang, L., and Andersen, P., "Modal Identification of Output-Only Systems Using Frequency Domain Decomposition," Journal of Smart Materials and Structures, 2001, 10, pp. 441-445.
- Brincker, R., Ventura, C. E., and Andersen, P., "Damping Estimation by Frequency Domain Decomposition," Proceedings of the International Modal Analysis Conference (IMAC), Kissimmee, Florida, 2001, pp. 698-703.
- Carter, A., "Roadmap for PMU Deployment," Recent Trends in Power Grid Monitoring, London, 2010.
- Chang, C.S., "Study of Dynamic Characteristics of Aerodynamic Systems Utilizing Randomdec Signatures," NASA, CR-132563, 1975.
- Claasen, T. A. C. M., and Mecklenbrauker, W. F. G., "The Wigner Distribution – A Tool for Time-Frequency Analysis, Parts I, II and III," Philips Journal of Research, 1980.
- Cole, A.H., "Failure Detection of a Space Shuttle Wing Flutter by Random Decrement," NASA, TMX-62, 041, 1971.
- Cole, A.H., "On-line Failure Detection and Damping Measurement of Space Structures by Random Decrement Signatures," NASA, CR-2205, 1973.
- Cooper, J. E., and Worden, K., "On-line Physical Parameter Estimation with Adaptive Forgetting Factors," Mechanical Systems and Signal Processing, 2000, 14, pp. 705-730.
- Cooper, J. E., "Identification of Time Varying Model Parameters," The Aeronautical Journal of the Royal Aeronautical Society, 1990, pp. 271-278.
- Corinthios, M., "Cellular Arrays for Parallel/Cascaded Image/Signal Processing," Spectral Techniques and Fault Detection (Academic Press, 1985), pp. 217-290.

- Daubechies, I., "Advances in Spectrum Analysis and Array Processing," Chapter 8: The Wavelet Transform: A Method for Time-Frequency Localisation, (Englewood Cliffs: Prentice-Hall, 1, 1991), pp. 366-417.
- De, Roeck G., Claesen, W., and Van den Broeck, P., "DDS-Methodology Applied to Parameter Identification of Civil Engineering Structures," Vibration and Noise '95, Venice, Italy, 1995, pp. 341–353.
- Deitel, H.M., and Deitel, P.J., "Visual C# 2005 How to Program," Second Edition, Pearson International Edition, Pearson Education, Inc, pp. 9, 2006 (a).
- Deitel, H.M., and Deitel, P.J., "Visual C# 2005 How to Program," Second Edition, Pearson International Edition, Pearson Education, Inc, pp. 19, 2006 (b).
- Desborough, L., and Miller, R., "Increasing Customer Value of Industrial Control Performance Monitoring – Honeywell's Experience," AIChE Symposium Series No. 326, 98, 2002, 153-186.
- Fassios, S. D., and Sakellariou, J. S., "Time-Series Methods for Fault Detection and Identification in Vibrating Structures," Philosophical Transactions of the Royal Society A, 2007, 365, pp. 411-448.
- Felber, A. J., "Development of a Hybrid Bridge Evaluation System," PhD Thesis, University of British Columbia, Vancouver, Canada, 1993.
- Forsman, K., and Stattin, A., "A New Criterion for Detecting Oscillations in Control Loops," European Control Conference, Karlsruhe, Germany, August-September 1999.
- Fouskitakis, G. N., and Fassois, S. D., "Functional Series TARMA Modelling and Simulation of Earthquake Ground Motion," Earthquake Engineering and Structural Dynamics, 2002, 31, pp. 399-420.
- Gabor, D., "Theory of Communication," Journal of the IEEE, 1946, 93 (III), pp. 429-457.
- Gersch, W., and Kitagawa, G., "A Time Varying AR Coefficient Model for Modelling and Simulating Earthquake Ground Motion," Earthquake Engineering and Structural Dynamics, 1985, 13, pp. 243-254.
- Goethals, I., Mevel, L., Benveniste, A, and De Moor, B., "Recursive Output Only Subspace Identification for In-Flight Flutter Monitoring," Proceedings of the 22nd International Modal Conference (IMACXXII), Dearborn, Michigan, 2004.
- Grenier, Y., "Time-Dependent ARMA Modeling of Nonstationary Signals," IEEE Transactions on Acoustics, Speech, and Signal Processing, 1983, 31, pp. 899-911.

- Guoping, L., Venkatasubramanian, V., "Oscillation Monitoring from Ambient PMU Measurements by Frequency Domain Decomposition," Proceedings of IEEE International Symposium on Circuits and Systems, 2008, pp. 2821-2824.
- Guoping, L., Quintero, J., and Venkatasubramanian, V., "Oscillation Monitoring System Based on Wide Area Synchrophasors in Power Systems," Bulk Power System Dynamics and Control – VII. Revitalizing Operational Reliability, 2007 iREP Symposium, 2007, pp. 1-13.
- Hägglund, T., "A Control-Loop Performance Monitor," Control Engineering Practice, 3 (11), 1995, 1543-1551.
- Hägglund, T., "Industrial Implementation of On-line Performance Monitoring Tools," Control Engineering Practice, 13, 2005, 1383-1390.
- Hammond, J. K., and White, P. R., "The Analysis of Non-Stationary Signals Using Time-Frequency Methods," Journal of Sound and Vibration, 1996, 190 (3), pp. 419-447.
- Hammond, J. K., "Frequency Time Methods in Vibrations," PhD Thesis, University of Southampton, 1971.
- Hauer, J. F., Demeure, C. J., and Scharf, L. L., "Initial Results in Prony Analysis of Power System Response Signals," IEEE Transactions on Power Systems, 1990, 5 (1), pp. 80–89.
- Huang, N.E., Shen, Z., Long, S.R., Wu, M.C., Shih, E.H., Zheng, Q., Yen, N., Tung, C.C., and Liu, H.H., "The Empirical Mode Decomposition and the Hilbert Spectrum for Non-Linear and Non-Stationary Time Series," Proceedings of the Royal Society of London A, 454, 1998, 903-995.
- Ibrahim, S.R., "Random Decrement Technique for Modal Identification of Structures," Journal of Spacecrafts and Rockets, vol. 14, pp. 696-700, 1977.
- Jeffries, W.Q., Chambers, J.A., and Infield, D.G., "Experience with Bicoherence of Electrical Power for Condition Monitoring of Wind Turbine Blades," IEE Proceedings on Vision, Image and Signal Processing, 2006, 145 (3), pp. 141-148.
- Jiang, H., Choudhury, S., and Shah, S.L., "Detection and Diagnosis of Plant-Wide Oscillations from Industrial Data Using the Spectral Envelope Method," Journal of Process Control, 17, 2007, 143-155.
- Juang, J., and Pappa, R.S., "An Eigensystem Realization Algorithm for Modal Parameter Identification and Model Reduction," Journal of Guidance and Control, 1985, 8 (5), pp. 620-627.
- Kaiser, J.F., "On a Simple Algorithm to Calculate the 'Energy' of a Signal," Proceedings of the International Conference on Acoustics, Speech and Signal Processing, vol. 1, pp. 381-384, 1999.

- Kakimoto, N., Sugumi, M., Makino, T., and Tomiyama, K. "Monitoring of Interarea Oscillation Mode by Synchronized Phasor Measurement," *IEEE Transactions on Power Systems*, 2006, 21 (1), pp. 260-268.
- Kamel, A., "The Least Mean Squares Algorithm," Retrieved from <http://www.cord.edu/faculty/kamel/380/Presentations/LMS.pdf>, August 2009.
- Kamwa, I., Grondin, R., Dickinson, E. J., and Fortin, S., "A Minimal Realization Approach to Reduced-Order Modelling and Modal Analysis for Power System Response Signals," *IEEE Transactions on Power Systems*, 1993, 8 (3), pp. 1020–1029.
- Karra, S., and Karim, N., "Comprehensive Methodology for Detection and Diagnosis of Oscillatory Control Loops," *Control Engineering Practice*, 17, 2009, 939-956.
- Katayama, T., "Subspace Methods for System Identification," Springer, 2005.
- Kirkegaard, P. H., and Andersen, P., "State Space Identification of Civil Engineering Structures from Output Measurements," *Proceedings of SPIE, the International Society for Optical Engineering*, 1997, 3089 (1), pp. 889-895.
- Kitagawa, G., and Gersch, W., "A Smoothness Priors Time-Varying AR Coefficient Modeling of Nonstationary Covariance Time Series," *IEEE Transactions on Automatic Control*, 1985, 30, pp. 48-56.
- Korba, P., Larsson, M., and Rehtanz, C., "Detection of Oscillations in Power Systems Using Kalman Filtering Techniques," *Proceedings of the IEEE Conference on Control Applications*, 2003, 1, pp. 183 – 188.
- Kundur, P., "Power System Stability and Control," McGraw-Hill Professional, 1994.
- Laila, D. S., Messina, A.R., and Pal, B. C., "A Refined Hilbert-Huang transform with Applications to Inter-Area Oscillation Monitoring," *IEEE Transactions on Power Systems*, 24 (2), 2009, 610-620.
- Larsson, M., "PMU and Wide-Area Monitoring Technology," *Recent Trends in Power Grid Monitoring*, London, 2010.
- Larsson, M., and Laila, D. S., "Monitoring of Inter-Area Oscillations under Ambient Conditions using Subspace Identification," *IEEE Power and Energy Society General Meeting*, Calgary, Canada, 2009.
- Laser, M., "Recent Safety and Environmental Legislation," *TransIchemE*, 78 (B), 2000, 419-422.

- Ledwich, G., and Palmer, E., "Modal Estimates from Normal Operation of Power Systems," IEEE Power Engineering Society Winter Meeting, 2000, 2, pp. 1527-1531.
- Lee, S. U., Robb, D., and Besant, C., "The Directional Choi-Williams Distribution for the Analysis of Rotor-Vibration Signals," *Mechanical Systems and Signal Processing*, 2001, 15, pp. 789-811.
- Leuridan, J., "Some Direct Parameter Model Identification Methods Applicable for Multiple Input Modal Analysis," PhD Thesis, University of Cincinnati, Ohio, 1984.
- Li, X., Wang, J., Huang, B., and Lu, S., "The DCT-Based Oscillation Detection Method for a Single Time Series," *Journal of Process Control*, 20, 2010, 609-617.
- Ljung, L., "System Identification: Theory for the User," (Prentice-Hall, Inc., 1987).
- Lobos, T., Leonowicz, Z., Rezmer, J., and Schenger, P., "High-Resolution Spectrum-Estimation Methods for Signal Analysis in Power Systems", *IEEE Transactions on Instrumentation and Measurement*, 2006, 55 (1), pp. 219-225.
- MathWorks, "MATLAB Compiler 4.13," Retrieved from <http://www.mathworks.co.uk/products/compiler/> on 16th June 2010.
- Matsuo, T., Sasaoka, H., and Yamashita, Y., "Detection and diagnosis of oscillations in process plants," *Lecture Notes in Computer Science*, 2773, 2003, 1258-1264.
- Meltzer, G., "Fault Detection in Gear Drives with Non-Stationary Rotational Speed, 2, The Time-Frequency Approach," *Mechanical Systems and Signal Processing*, 2003, 17, pp. 273-283.
- Messina, A.R., Trudnowski, D., and Pierre, J., "Inter-area Oscillations in Power Systems – A Nonlinear and Nonstationary Perspective," Springer, 2009, pp. 1-36.
- Messina, A. R., and Vittal, V., "Assessment of Nonlinear Interaction Between Nonlinearly Coupled Modes Using Higher Order Spectra," *IEEE Transactions on Power Systems*, 2005, 20 (1), pp. 1515–1521.
- Messina, A. R., and Vittal, V., "Nonlinear, Non-Stationary Analysis of Interarea Oscillations via Hilbert Spectral Analysis," *IEEE Transactions on Power Systems*, 2006, 21, pp. 1234.1241.
- Messina, A. R., Vittal, V., Ruiz-Vega, D., and Enriquez-Harper, G., "Interpretation and Visualization of Wide-Area PMU Measurements Using Hilbert Analysis," *IEEE Transactions on Power Systems*, 2006, 21, pp. 1763-1771.
- Mevel, L., Basseville, M., and Beneviste, A., "Fast In-Flight Detection of Flutter Onset: A Statistical Approach," *Journal of Guidance, Control and Dynamics*, 2005, 28, pp. 431-438.

- Miao, T., and Seborg, D.E., "Automatic Detection of Excessively Oscillatory Feedback Control Loops," Proceedings of the 1999 IEEE International Conference on Control Applications, Hawai'i, USA, August 1999.
- Microsoft Corporation, "What is .NET?" Retrieved from <http://www.microsoft.com/net/basics.msp> on 04th March 2007.
- Mobarakeh, A. A., Rofooei, F.R., and Ahmadi, G., "Simulation of Earthquake Records Using Time-Varying ARMA(2,1) Model," Probabilistic Engineering Mechanics, 2002, 17, pp. 15-34.
- Newland, D. E., "Random Vibration and Spectrum and Wavelet Analysis," (Addison-Wesley, 1993).
- Niedzwiecki, M., and Klaput, T., "Fast Algorithms for Identification of Periodically Varying Systems," IEEE Transactions on Signal Processing, 2003, 51, pp. 3270-3279.
- Nimmo, I., "Adequately Address Abnormal Situation Operations," Chemical Engineering Progress, 91 (9), 1995, 36-45.
- Ostojic, D. R., and Heydt, G. T., "Transient Stability Assessment by Pattern Recognition in the Frequency Domain," IEEE Transactions on Power Systems, 1991, 6, pp. 231-237.
- Ostojic, D. R., "Spectral Monitoring of Power System Dynamic Performances," IEEE Transactions on Power Systems, 1993, 8, pp. 445-451.
- Owen, J. S., Eccles, B. J., Choo, B. S., and Woodings, M. A., "The Application of Auto-Regressive Time Series Modelling for the Time-Frequency Analysis of Civil Engineering Structures," Engineering Structures, 2001, 23, pp. 521-536.
- Pal, B.C., and Chaudhuri, B., "Robust Control in Power Systems (Chapter 2)," Springer, 2005.
- Papoulis, A., "Probability, Random Variables and Stochastic Processes," Third Edition, New York: WCB/McGraw-Hill, 1991.
- Paulonis, M.A., and Cox, J.W., "A Practical Approach for Large-Scale Controller Performance, Diagnosis and Improvement," Journal of Process Control, 13, 155-168.
- Peeters, B., and De Roeck, G., "Stochastic System Identification for Operational Modal Analysis: A Review," Journal of Dynamic Systems, Measurement and Control, 2001, 123, pp. 659-667.
- Peterson, L.D., "Efficient Computation of the Eigensystem Realization Algorithm," Journal of Guidance, Control, and Dynamics, 1995, 18 (3), pp. 395-403.
- Phadke, A.G., "Synchronized Phasor Measurements in Power Systems," IEEE Computer Applications in Power, April 1993.

- Pierre, J. W., Trudnowski, D. J., Donnelly, M. K., "Initial Results in Electromechanical Mode Identification from Ambient Data," *IEEE Transactions on Power Systems*, 1997, 12 (3), pp. 1245–1251.
- Pintelon, R., Guillaume, P., Rolain, Y., Schoukens, J., and Van Hamme, H., "Parametric Identification of Transfer Functions in the Frequency Domain – A Survey," *IEEE Transactions on Automated Control*, 1994, 39 (11), pp. 2245-2260.
- Piombo, B., Ciorcelli, E., Garibaldi, L., and Fasana, A., "Structures Identification Using ARMAV Models," *Proceedings of IMAC 11, the International Modal Analysis Conference, Orlando, FL*, 1993, pp. 588-592.
- Poon, K. P., and Lee, K. C., "Analysis of Transient Stability Swings in Large Interconnected Power systems by Fourier Transformation," *IEEE Transactions on Power Systems*, 1990, PWRS-3 (4), pp. 1441-1448.
- Poulimenos, A. G., and Fassios, S. D., "Parametric Time-Domain Methods for Non-Stationary Random Vibration Modelling and Analysis – A Critical Survey and Comparison," *Mechanical Systems and Signal Processing*, 2006, 20, pp. 763-816.
- Poulimenos, A.G., and Fassois, S.D., "Output-Only Stochastic Identification of a Time-Varying Structure via Functional Series TARMA Models," *Mechanical Systems and Signal Processing*, 2009, 23 (4), pp. 1180-1204.
- Prevesto, M., "Algorithmes d'Identification des Caractéristiques Vibratoires de Structures Mécaniques Complexes," PhD Thesis, Université de Rennes I, France, 1982.
- Priestley, M. B., "Design Relations for Non-stationary Processes," *Journal of the Royal Statistical Society*, 1966, B28, pp. 228.
- Priestley, M. B., and Tong, H., "On the Analysis of Bivariate Non-Stationary Processes," *Journal of the Royal Statistical Society*, 1973, B35, pp. 153-188.
- Qin, S. J., "An Overview of Subspace Identification," *Computers and Chemical Engineering*, 2006, 30, pp. 1502-1513.
- Qin, S.J., "Control Performance Monitoring – A Review and Assessment," *Computers and Chemical Engineering*, 23, 1998, 173-186.
- Ruiz-Vega, D., Messina, A. R., and Harper, G., "Analysis of Interarea Oscillations via Non-Linear Time Series Analysis Techniques," *Proceedings of the 15th Power Systems Computation Conference, Liege, Belgium*, 2005.

- Salsbury, T.I., and Singhal, A., "A New Approach for ARMA Pole Estimation Using Higher-Order Crossings," 2005 American Control Conference, Portland, Oregon, USA, June 2005.
- Sanchez-Gasca, J., and Chow, J., "Computation of Power System Low-Order Models from Time Domain Simulations Using a Hankel Matrix," *IEEE Transactions on Power Systems*, 1997, 12 (4), pp. 1461–1467.
- Sarkar, T. K., and Pereira, O., "Using the Matrix Pencil Method to Estimate the Parameters of a Sum of Complex Exponentials," *Antennas and Propagation Magazine, IEEE*, 1995, 37 (1), 48-55.
- Senroy, N., Suryanarayanan, S., and Ribeiro, P. F., "An Improved Hilbert- Huang Method for Analysis of Time-Varying Waveforms in Power Quality," *IEEE Transactions on Power Systems*, 2007, 22, pp. 1843-1850.
- Singleton, R. C., "An Algorithm For Computing the Mixed Radix Fast Fourier Transform," *IEEE Transactions on Audio Electroacoustics (Special Issue on Fast Fourier Transform)*, 1969, AU-17, pp. 93-103.
- Skok, S., "Why PMUs in A Small Country?," *Recent Trends in Power Grid Monitoring*, London, 2010.
- Smith, J. R., Hauer, J. F., and Trudnowski, D. J., "Transfer Function Identification in Power System Applications," *IEEE Transactions on Power Systems*, 1993, 8 (3), pp. 1282-1290.
- Spiridonakos, M. D., and Fassios, S. D., "Parametric Identification of a Time-Varying Structure Based on Vector Vibration Response Measurements," *Mechanical Systems and Signal Processing*, 2009, 23, pp. 2029-2048.
- Srinivasan, R., "Control Loop Performance Monitoring: Modeling, Diagnosing and Compensating Stiction Phenomenon in Process Control Valves," PhD Dissertation, Department of Chemical Engineering, Clarkson University, USA, 2005.
- Srinivasan, R., Rengaswamy, R., and Miller, R., "A Modified Empirical Mode Decomposition (EMD) Process for Oscillation Characterization in Control Loops," *Control Engineering Practice*, 15, 2007, 1135-1148.
- SriSamp, "What is .NET," Retrieved from The Code Project, <http://www.codeproject.com/dotnet/netbasics.asp>, 21st April 2003.
- Staszewski, W. J., Worden, K., and Tomlinson, G. R., "Time-Frequency Analysis in Gearbox Fault Detection Using the Wigner-Ville Distribution and Pattern Recognition," *Mechanical Systems and Signal Processing*, 1997, 11, pp. 673-692.

- Tangirala, A.K., Kanodia, J., and Shah, S.L., "Non-negative Matrix Factorization for Detection and Diagnosis of Plantwide Oscillations," *Industrial & Engineering Chemistry Research*, 46 (3), 2007, 801-817.
- Teck, T.W., Kiong, T.C., Samavedham, L., and Kariwala, V., "Comparison of Plant-Wide Oscillation Detection Methods," *16th IEEE International Conference on Control Applications*, Singapore, October 2007.
- Thambirajah, J., "Literature Review/Fist Report: Cause And Effect Analysis In Chemical Processes Utilising Plant Connectivity Information," UCL Final Year Project, October 2006.
- Thornhill, N.F., and Hägglund, T., "Detection and Diagnosis of Oscillation in Control Loops," *Control Engineering Practice*, 5 (10), 1997, 1343-1354.
- Thornhill, N.F., and Horch, A., "Advances and new directions in plant-wide disturbance detection and diagnosis," *Control Engineering Practice* 15, 2007, 1196-1206.
- Thornhill, N.F., Huang, B., and Zhang, H., "Detection of Multiple Oscillations in Control Loops," *Journal of Process Control*, 13, 2003, 91-100.
- Thornhill, N.F., and Melbø, H., "Detection of Plant-wide Disturbances Using a Spectral Classification Tree," In *Proceedings of the IFAC-ADCHEM 2006*, Gramado, Brazil, April 2006.
- Thornhill, N.F., Shah, S.L., Huang, B., and Vishnubholta, A., "Spectral Principal Component Analysis of Dynamic Process Data," *Control Engineering Practice*, 10, 2002, 833-846.
- Trudnowski, D. J., "Estimating Electromechanical Mode Shape from Synchrophasor Measurements," *IEEE Transactions on Power Systems*, 2008, 23 (3), pp. 1188-1195.
- Trudnowski, D., Pierre, J. W., Zhou, N., Hauer, J., and Parashar, M., "Performance of Three Mode Meter Block-Processing Algorithms for Automated Dynamic Stability Assessment," *IEEE Transactions on Power Systems*, 2008, 23 (2), pp. 680-690.
- Trudnowski, D. J., Smith, J. R., Short, T. A., and Pierre, D. A., "An Application of Prony Methods in PSS Design for Multimachine Systems," *IEEE Transactions on Power Systems*, 1991, 6 (1), pp. 118-126.
- Turunen, J., Larsson, M., Korba, P., Jyrinsalo, J., and Haarla, L., "Experiences and Future Plans in Monitoring Inter-Area Power Oscillation Damping," *IEEE Power and Energy Society General Meeting*, 2008.

- Turunen, J., Haarla, L., Rauhala, T., and Thambirajah, J., "A Wavelet-Based Method for Oscillation Damping Estimation under Ambient Conditions," Submitted to IEEE Transactions on Power Systems, 2010.
- Van Huffel, S., Chen, H., Decanniers, C., and Van Hecke, P., "Algorithm for Time-Domain nmr Data Fitting Based on Total Least Squares," Journal of Magnetic Resonance, 1994, A 110, pp. 228–237.
- Vandiver, J.K., Dunwoody, A.B., Campbell, R.B., and Cook, M.F., "A Mathematical Basis for the Random Decrement Vibration Signature Analysis Technique," Journal of Mechanical Design, 1982, 104.
- Venkatasubramanian, V., Rengaswamy, R., Yin, K. and Kavuri, S.N., "A review of process fault detection and diagnosis. Part I: Quantitative model-based methods," Computers and Chemical Engineering, 27, 2003, 293-311.
- Venkatasubramanian, V., Rengaswamy, R., Yin, K. and Kavuri, S.N., "A review of process fault detection and diagnosis. Part II: Qualitative models and search strategies," Computers and Chemical Engineering, 27, 2003, 313-326.
- Venkatasubramanian, V., Rengaswamy, R., Yin, K. and Kavuri, S.N., "A review of process fault detection and diagnosis. Part III: Process History based Methods," Computers and Chemical Engineering, 27, 2003, 327-346.
- Welch, G., and Bishop, G., "An Introduction to the Kalman Filter,"
http://www.cs.unc.edu/~welch/media/pdf/kalman_intro.pdf, July 2006.
- Wies, R. W., Pierre, J. W., and Trudnowski, D. J., "Use of Least-Mean Squares (LMS) Adaptive Filtering Technique for Estimating Low-Frequency Electromechanical Modes in Power Systems," Proceedings of the IEEE Power Engineering Society General Meeting, 2004, 2, pp. 1863–1870.
- Wies, R. W., Pierre, J. W., Trudnowski, D. J., "Use of ARMA Block Processing for Estimating Stationary Low-Frequency Electromechanical Modes of Power Systems," IEEE Transactions on Power Systems, 2003, 18 (1), pp. 167–173.
- Wikipedia, "C#," Retrieved from http://en.wikipedia.org/wiki/C_Sharp on 04th March 2007 (a).
- Wikipedia, "Microsoft.NET," Retrieved from http://en.wikipedia.org/wiki/Microsoft_.NET on 04th March 2007 (b).
- Wikipedia, ".NET Framework," Retrieved from
http://en.wikipedia.org/wiki/Microsoft_.NET_Framework on 04th March 2007 (c).

Wikipedia, "Functional Requirements," Retrieved from

http://en.wikipedia.org/wiki/Functional_requirement on 15th June 2010.

Wold, S., Esbensen, K., and Geladi, P., "Principal Component Analysis," *Chemometrics and Intelligent Laboratory Systems*, 1987, 2, pp. 37-52.

Xia, C., and Howell, J., "Isolating Multiple Sources of Plant-Wide Oscillations via Spectral Independent Component Analysis," *Control Engineering Practice*, 13, 2005, 1027-1035.

Xia, C., Howell, J., and Thornhill, N.F., "Detecting and Isolating Multiple Plant-wide Oscillations via Spectral Independent Component Analysis," *Automatica*, 41, 2005, 2067-2075.

Xia, C., Zheng, J., and Howell, J., "Isolation of Whole-plant Multiple Oscillations Via Non-negative Spectral Decomposition," *Chinese Journal of Chemical Engineering*, 15 (3), 2007, 353-360.

Zhou, N., Pierre, J. W., Trudnowski, D. J., and Guttromson, R. T., "Robust RLS Methods for Online Estimation of Power System Electromechanical Modes," *IEEE Transactions on Power Systems*, 2007, 22 (3), pp. 1240-1249.

Zhou, N., Pierre, J. W., and Wies, R. W., "Estimation of Low-Frequency Electromechanical Modes of Power Systems from Ambient Measurements Using a Subspace Method," *Proceedings of the North American Power Symposium*, 2003.

Zhou, N., Pierre, J. W., and Hauer, J. F., "Initial Results in Power System Identification from Injected Probing Signals Using a Subspace Method," *IEEE Transactions on Power Systems*, 2006, 21 (3), pp. 1296-1302.